MODIS Response versus Scan Angle (RVS) Status Report Part I: Reflectance Solar Bands

MODIS Calibration Support Team,

June, 2000.

Introduction

What is RVS:

For identical scene radiance at different scan angles, detector response will be different for scanning sensors like MODIS because of the change in the angle of incidence.

Factors affecting RVS:

1. Scan mirror reflectance
2. Polarization response of the fixed optics
3. Scene polarization state

No scene polarization is assumed throughout this talk.

Assuming this, we have $RVS \quad (\rho_s + \rho_p)/2 + c_{fix} \quad (\rho_s - \rho_p)/2$

The radiance/reflectance is retrieved from

$$L_{\text{scene}} = \frac{L_{\text{reference}}}{dn_{\text{reference}}} \; dn_{\text{scene}} \left[\frac{RVS_{\text{reference}}}{RVS_{\text{scene}}} \right]$$

Gain

RVS correction

Measuring Terra MODIS RVS (RSB)

RVS dn When constant source is used at different SA

SIS(100)
Three radiance levels were used
1) High radiance level for bands 1, 3, 4, 8 and 9. (14 SAs)
2) Low radiance level for bands 13-16. (13 SAs)
3) Medium radiance level for bands 2, 5-7, 10-12, 17-19, and 26.(12 SAs)
At three scan angles of 54.5, -23.0, and -54.5 degree, the measurement were repeated. (These corresponds to AOI of 65.25, 26.5 and 10.75 deg.)

Ten scans with 100 frames/scan were collected at each measurement.
Sweet spot of 50 frames were chosen for data analysis.

Data Analysis Methodology

- F-test was used to filter out non-usable detectors if any.
- Average over detector and sub-frame were carried out for each band and mirror side.
- Quadratic fitting to the averaged dn for each band and mirror side was done.
- Normalization at the SD AOI is carried out to obtain the final LUT for RVS.

The following charts show the quadratic fitting results of RVS, normalized at AOI corresponding to solar diffuser (SD) center frame AOI.
(in order of ascending center wavelength)

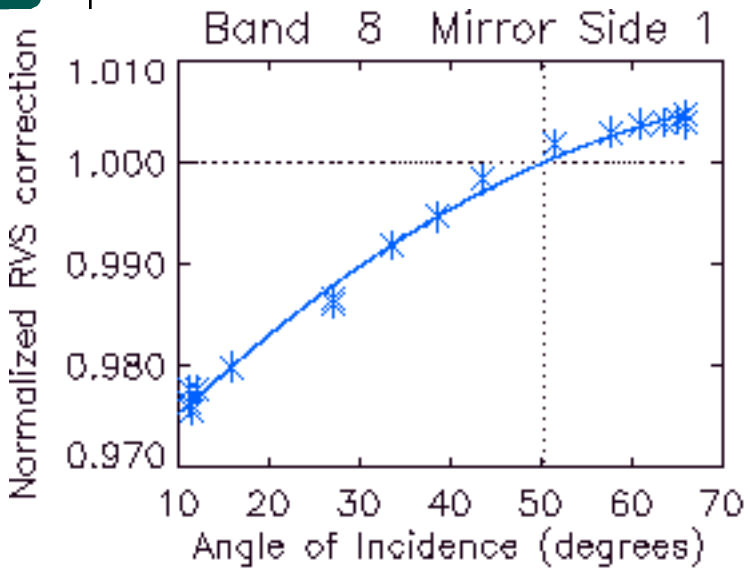
Band 8 Mirror Side 1
Normalized RVS correction
1.010
1.000
0.990
0.980
0.970
10 20 30 40 50 60 70
Angle of Incidence (degrees)

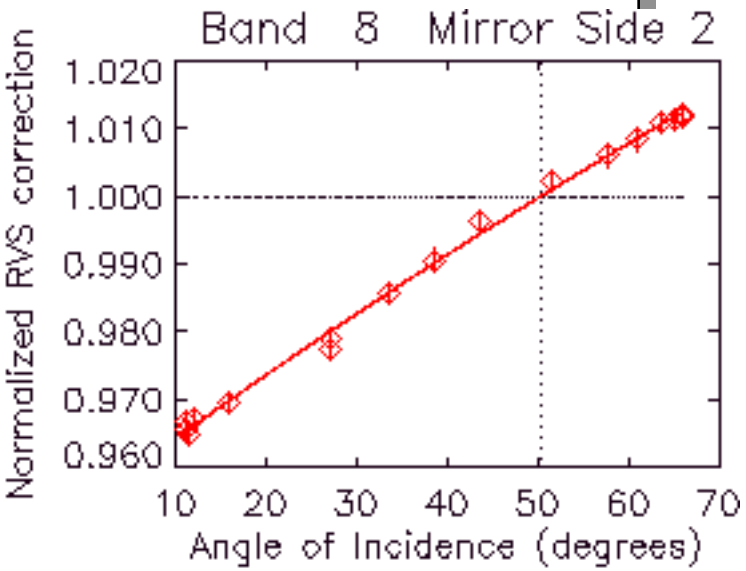
Band 8 Mirror Side 2
Normalized RVS correction
1.020
1.010
1.000
0.990
0.980
0.970
0.960
10 20 30 40 50 60 70
Angle of Incidence (degrees)

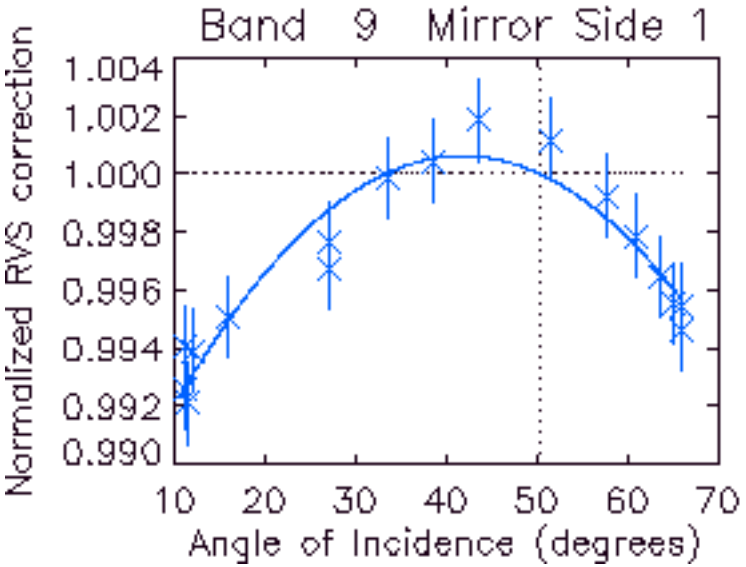
Band 9 Mirror Side 1
Normalized RVS correction
1.004
1.002
1.000
0.998
0.996
0.994
0.992
0.990
10 20 30 40 50 60 70
Angle of Incidence (degrees)

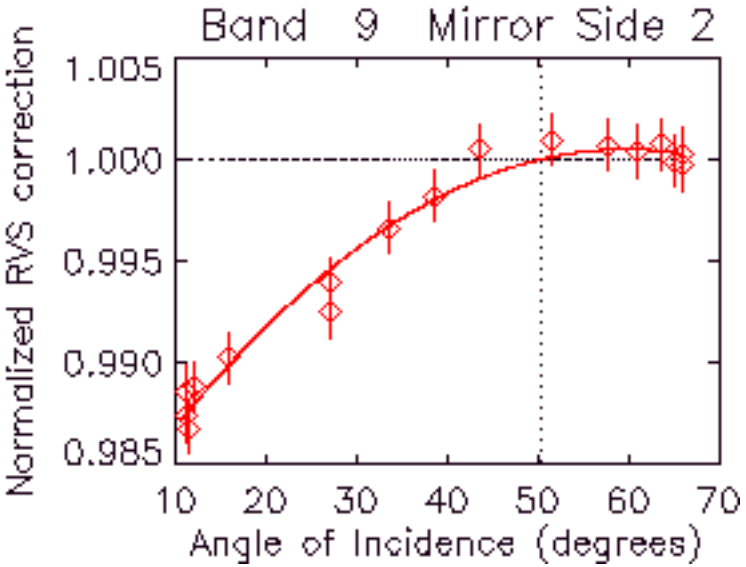
Band 9 Mirror Side 2
Normalized RVS correction
1.005
1.000
0.995
0.990
0.985
10 20 30 40 50 60 70
Angle of Incidence (degrees)

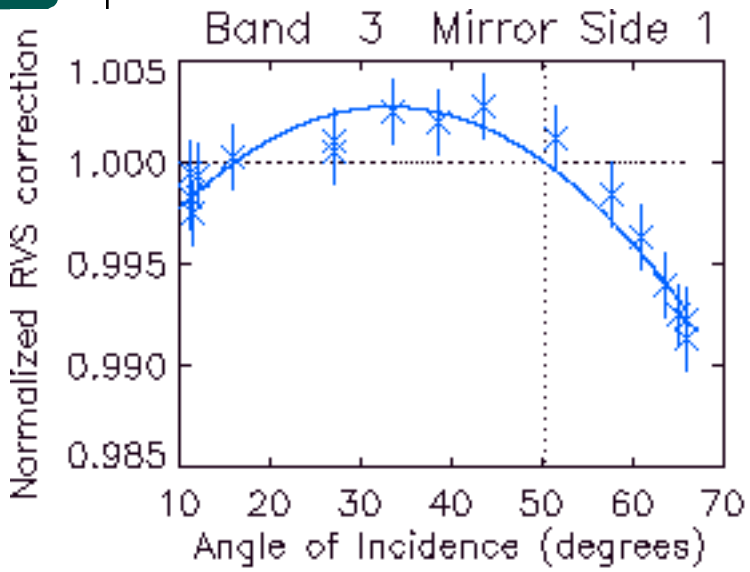
Band 3 Mirror Side 1
Normalized RVS correction
1.005
1.000
0.995
0.990
0.985
10 20 30 40 50 60 70
Angle of Incidence (degrees)

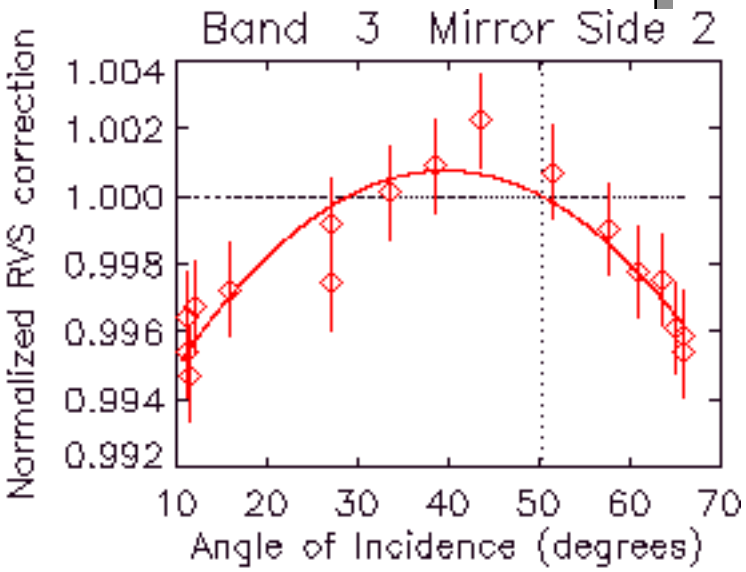
Band 3 Mirror Side 2
Normalized RVS correction
1.004
1.002
1.000
0.998
0.996
0.994
0.992
10 20 30 40 50 60 70
Angle of Incidence (degrees)

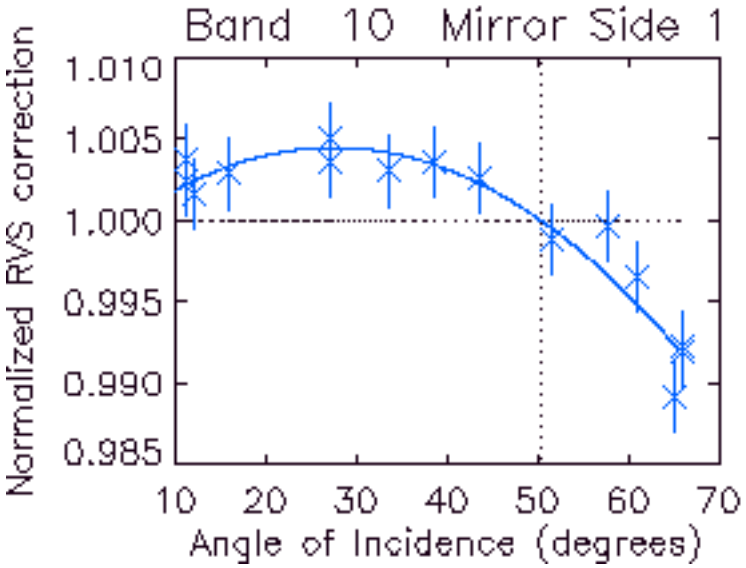
Band 10 Mirror Side 1
Normalized RVS correction
1.010
1.005
1.000
0.995
0.990
0.985
10 20 30 40 50 60 70
Angle of Incidence (degrees)

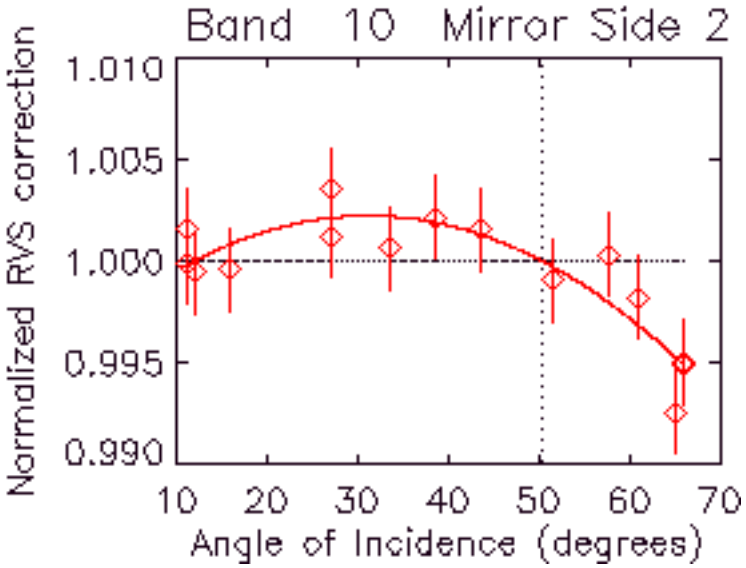
Band 10 Mirror Side 2
Normalized RVS correction
1.010
1.005
1.000
0.995
0.990
10 20 30 40 50 60 70
Angle of Incidence (degrees)

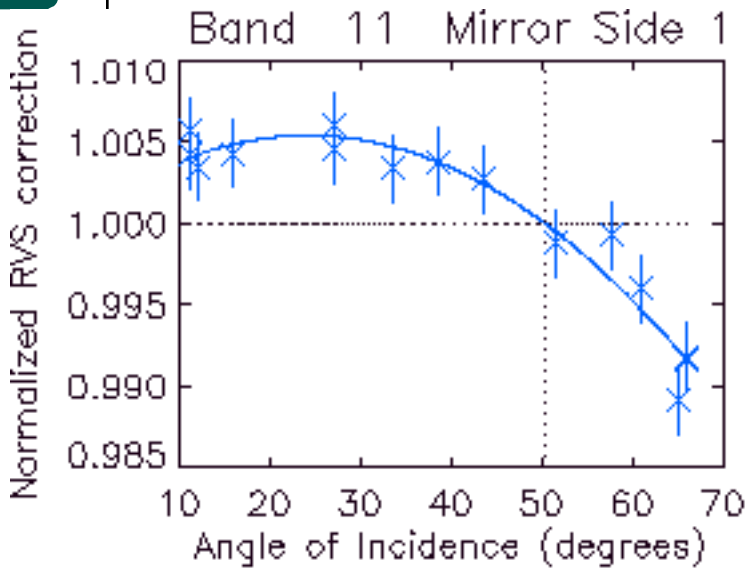
Band 11 Mirror Side 1
Normalized RVS correction
1.010
1.005
1.000
0.995
0.990
0.985
10 20 30 40 50 60 70
Angle of Incidence (degrees)

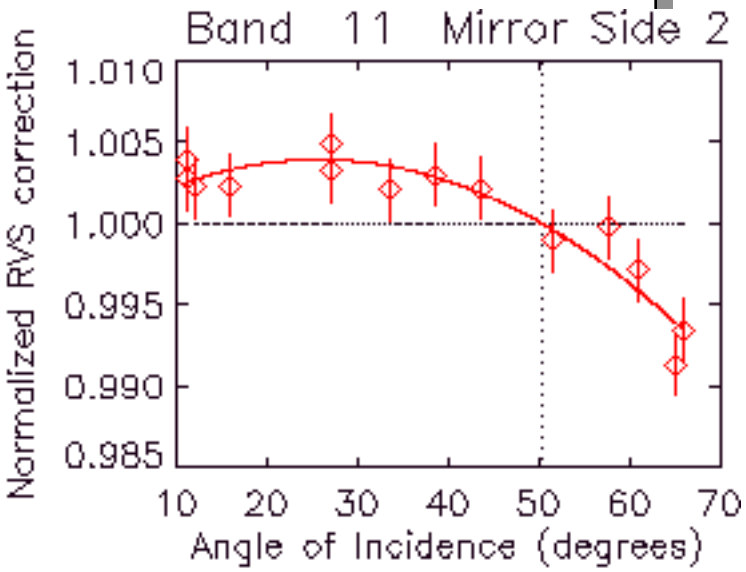
Band 11 Mirror Side 2
Normalized RVS correction
1.010
1.005
1.000
0.995
0.990
0.985
10 20 30 40 50 60 70
Angle of Incidence (degrees)

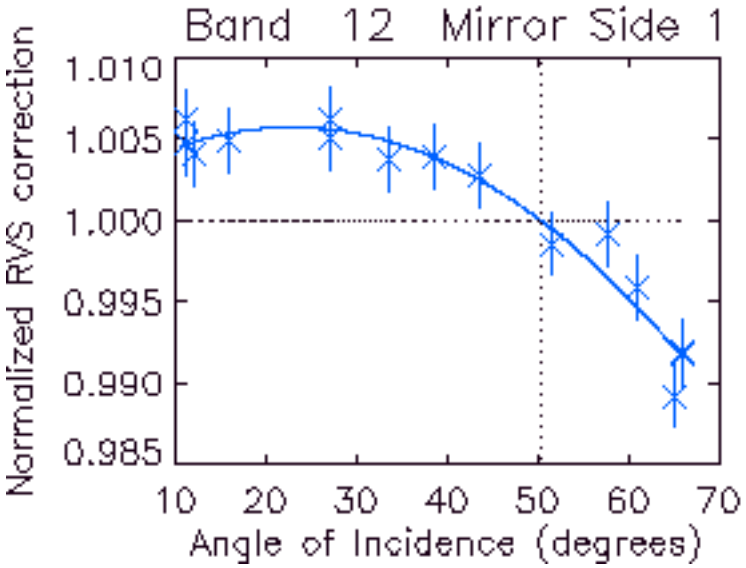
Band 12 Mirror Side 1
Normalized RVS correction
1.010
1.005
1.000
0.995
0.990
0.985
10 20 30 40 50 60 70
Angle of Incidence (degrees)

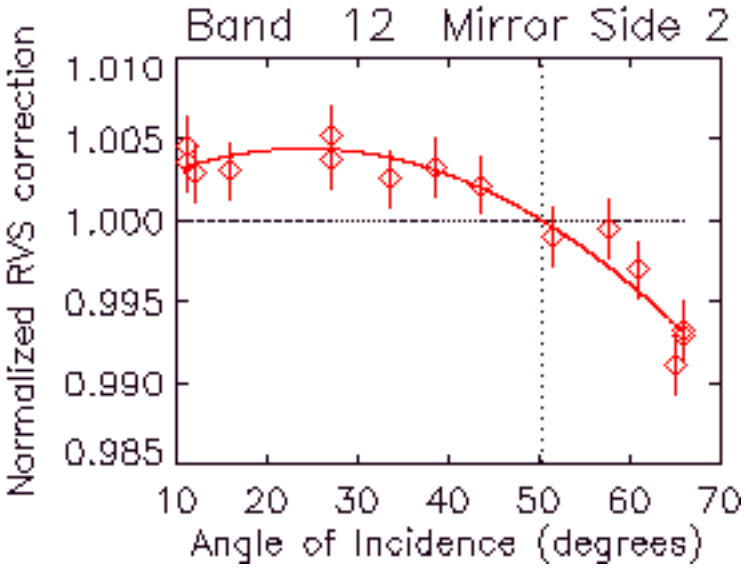
Band 12 Mirror Side 2
Normalized RVS correction
1.010
1.005
1.000
0.995
0.990
0.985
10 20 30 40 50 60 70
Angle of Incidence (degrees)

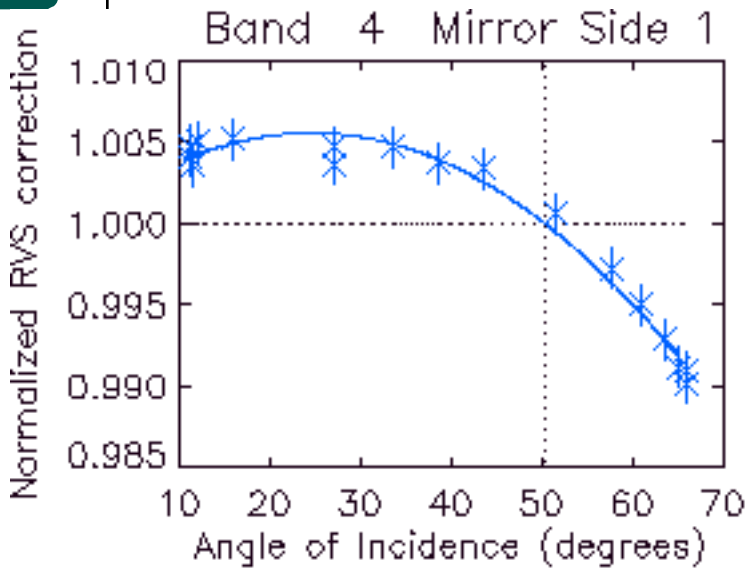
Band 4 Mirror Side 1
Normalized RVS correction
1.010
1.005
1.000
0.995
0.990
0.985
10 20 30 40 50 60 70
Angle of Incidence (degrees)

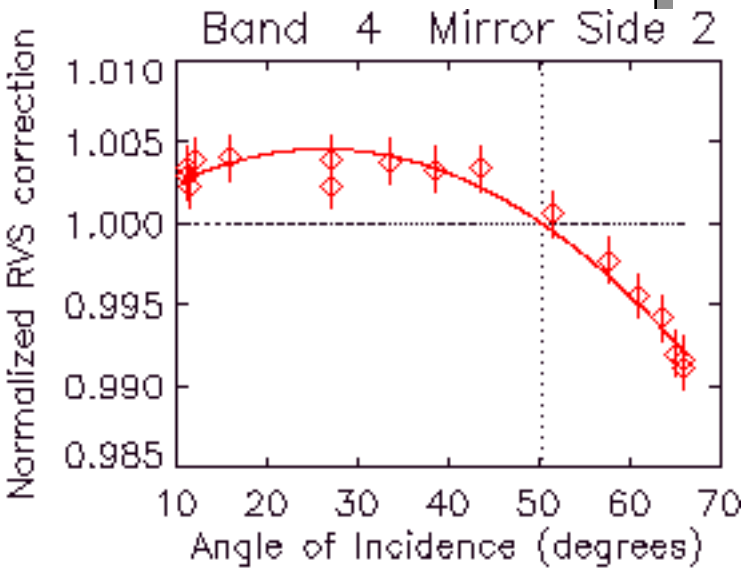
Band 4 Mirror Side 2
Normalized RVS correction
1.010
1.005
1.000
0.995
0.990
0.985
10 20 30 40 50 60 70
Angle of Incidence (degrees)

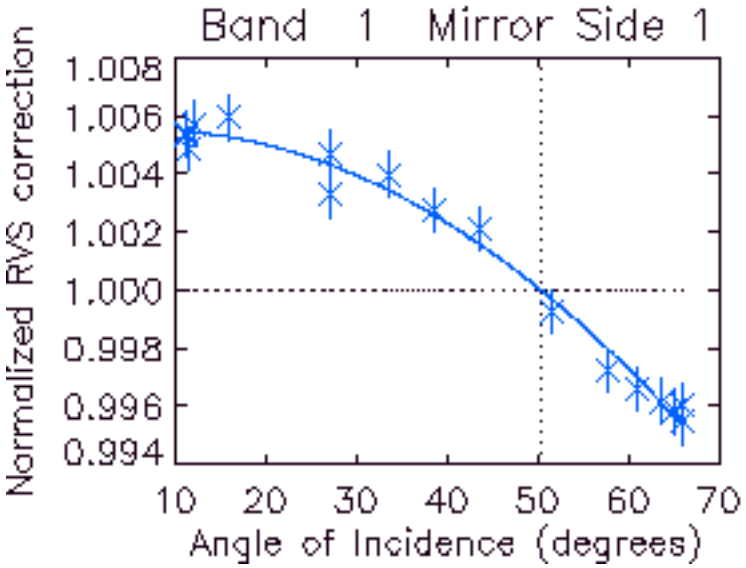
Band 1 Mirror Side 1
Normalized RVS correction
1.008
1.006
1.004
1.002
1.000
0.998
0.996
0.994
10 20 30 40 50 60 70
Angle of Incidence (degrees)

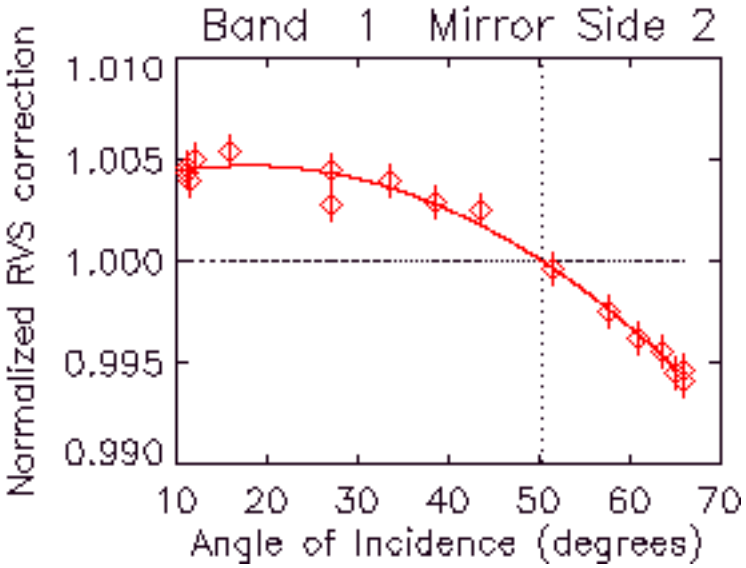
Band 1 Mirror Side 2
Normalized RVS correction
1.010
1.005
1.000
0.995
0.990
10 20 30 40 50 60 70
Angle of Incidence (degrees)

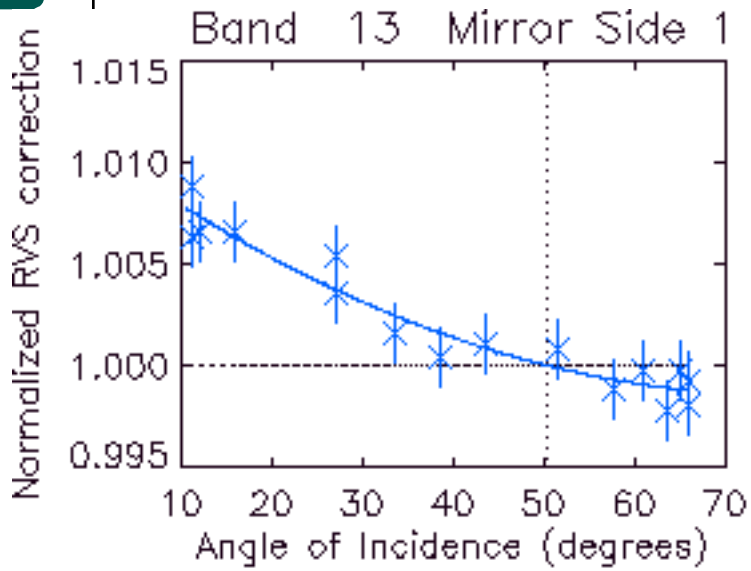
Band 13 Mirror Side 1
Normalized RVS correction
1.015
1.010
1.005
1.000
0.995
10 20 30 40 50 60 70
Angle of Incidence (degrees)

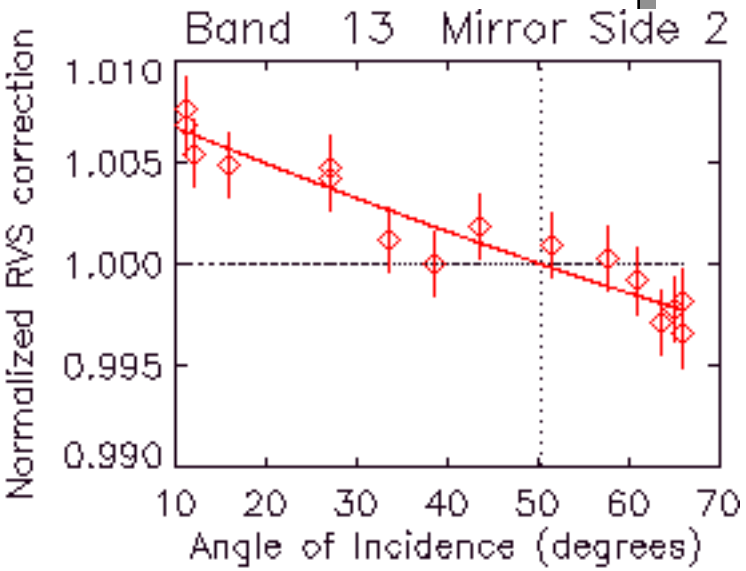
Band 13 Mirror Side 2
Normalized RVS correction
1.010
1.005
1.000
0.995
0.990
10 20 30 40 50 60 70
Angle of Incidence (degrees)

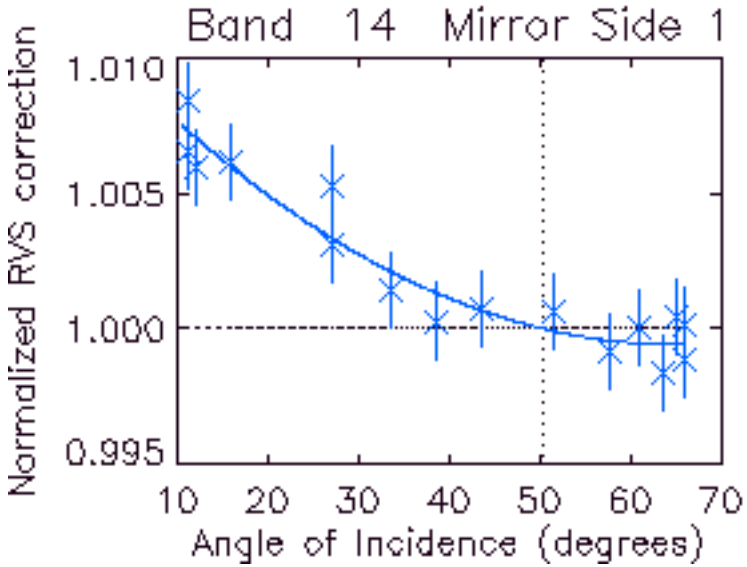
Band 14 Mirror Side 1
Normalized RVS correction
1.010
1.005
1.000
0.995
10 20 30 40 50 60 70
Angle of Incidence (degrees)

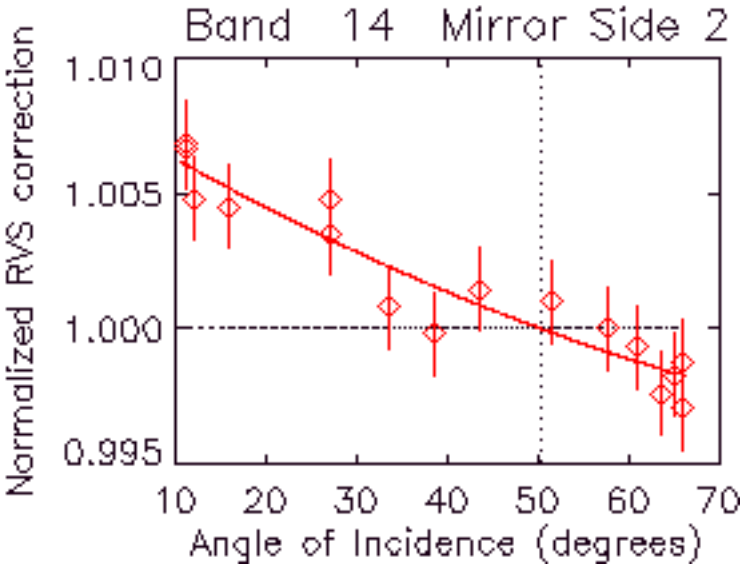
Band 14 Mirror Side 2
Normalized RVS correction
1.010
1.005
1.000
0.995
10 20 30 40 50 60 70
Angle of Incidence (degrees)

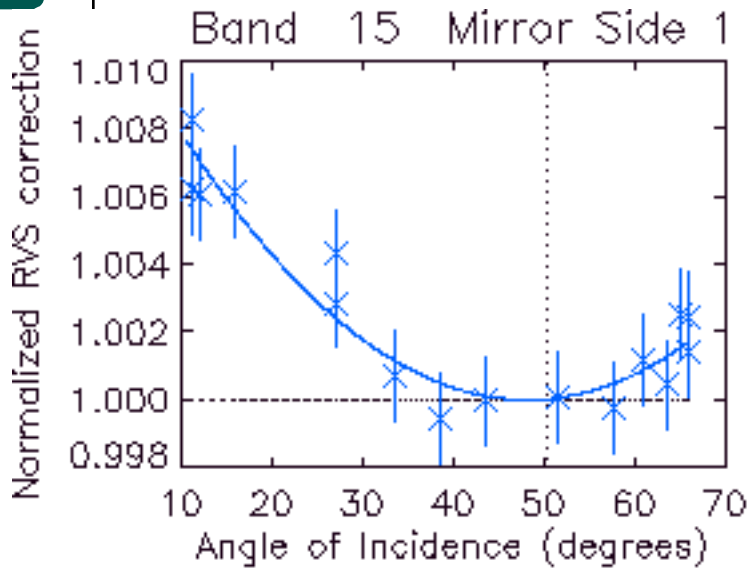
Band 15 Mirror Side 1
Normalized RVS correction
1.010
1.008
1.006
1.004
1.002
1.000
0.998
10 20 30 40 50 60 70
Angle of Incidence (degrees)

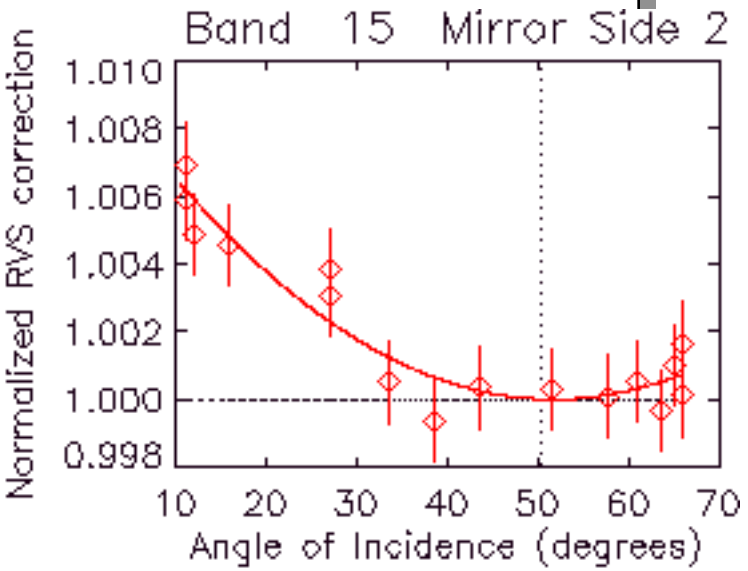
Band 15 Mirror Side 2
Normalized RVS correction
1.010
1.008
1.006
1.004
1.002
1.000
0.998
10 20 30 40 50 60 70
Angle of Incidence (degrees)

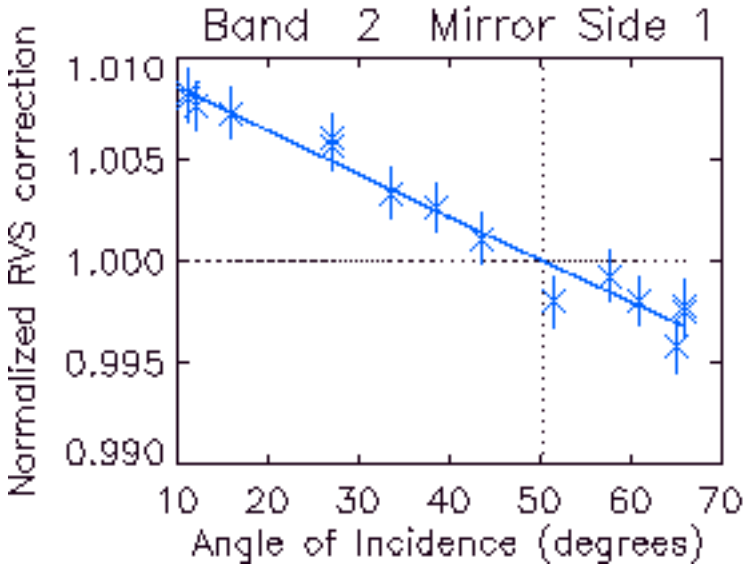
Band 2 Mirror Side 1
Normalized RVS correction
1.010
1.005
1.000
0.995
0.990
10 20 30 40 50 60 70
Angle of Incidence (degrees)

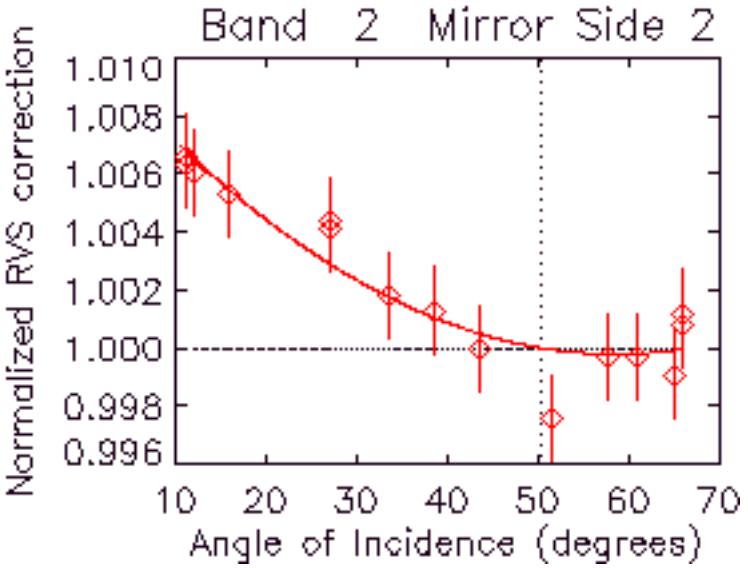
Band 2 Mirror Side 2
Normalized RVS correction
1.010
1.008
1.006
1.004
1.002
1.000
0.998
0.996
10 20 30 40 50 60 70
Angle of Incidence (degrees)

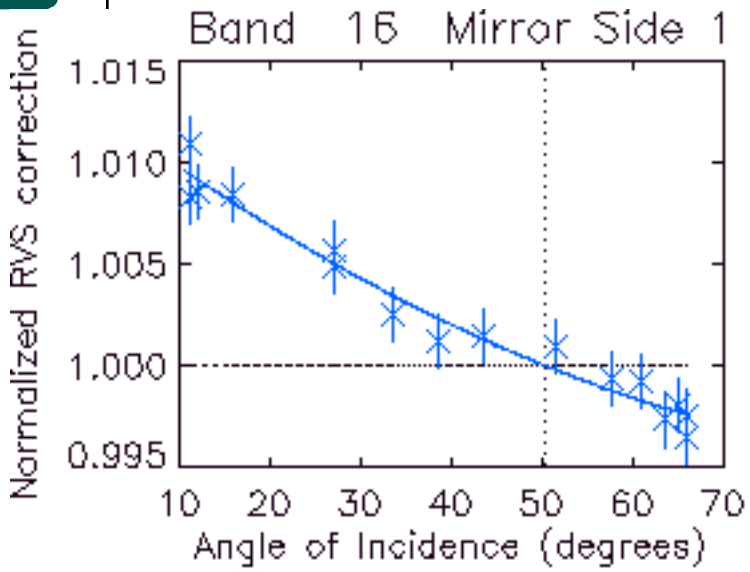
Band 16 Mirror Side 1
Normalized RVS correction
1.015
1.010
1.005
1.000
0.995
10 20 30 40 50 60 70
Angle of Incidence (degrees)

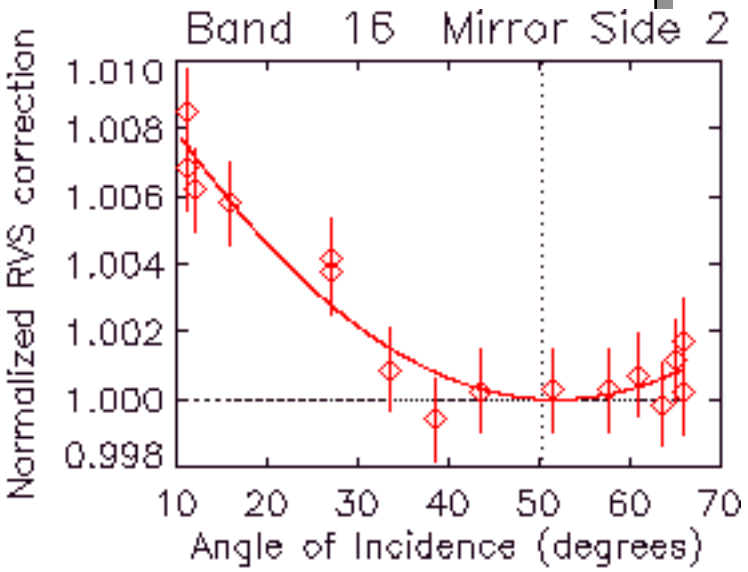
Band 16 Mirror Side 2
Normalized RVS correction
1.010
1.008
1.006
1.004
1.002
1.000
0.998
10 20 30 40 50 60 70
Angle of Incidence (degrees)

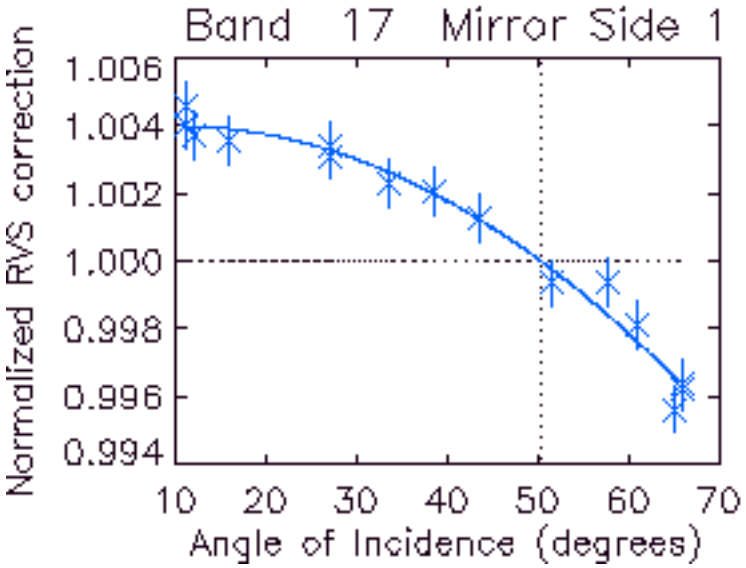
Band 17 Mirror Side 1
Normalized RVS correction
1.006
1.004
1.002
1.000
0.998
0.996
0.994
10 20 30 40 50 60 70
Angle of Incidence (degrees)

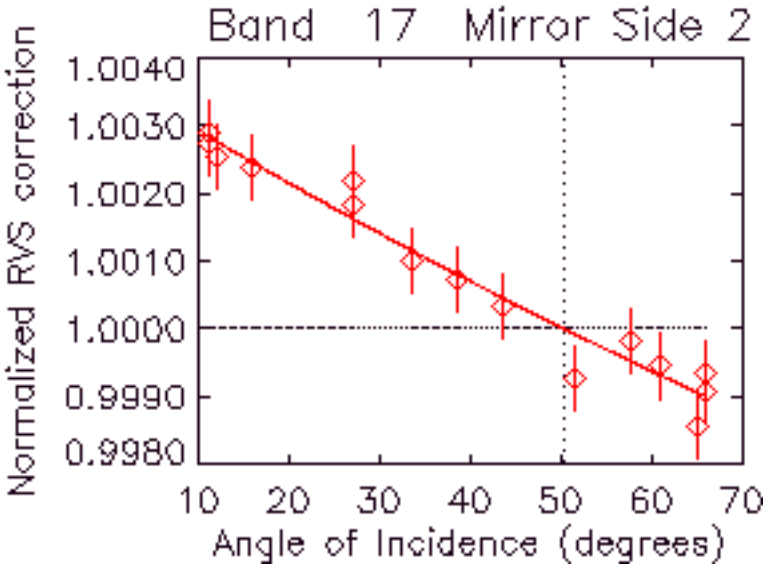
Band 17 Mirror Side 2
Normalized RVS correction
1.0040
1.0030
1.0020
1.0010
1.0000
0.9990
0.9980
10 20 30 40 50 60 70
Angle of Incidence (degrees)

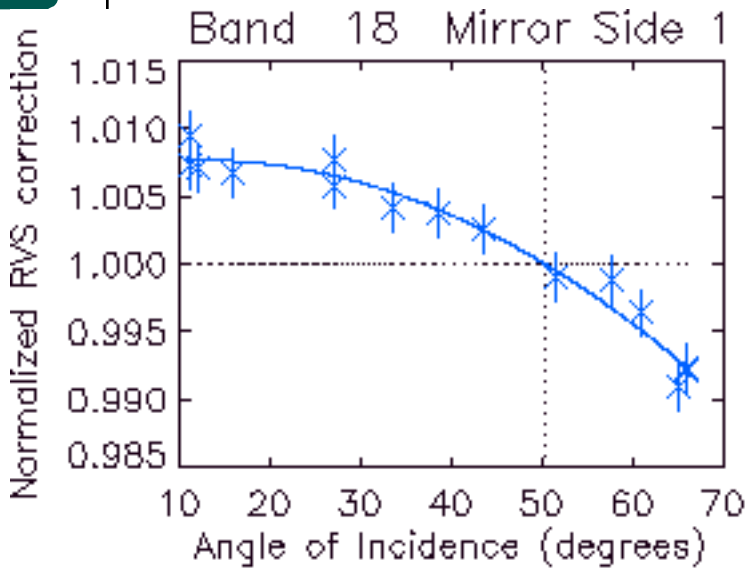
Band 18 Mirror Side 1
Normalized RVS correction
1.015
1.010
1.005
1.000
0.995
0.990
0.985
10 20 30 40 50 60 70
Angle of Incidence (degrees)

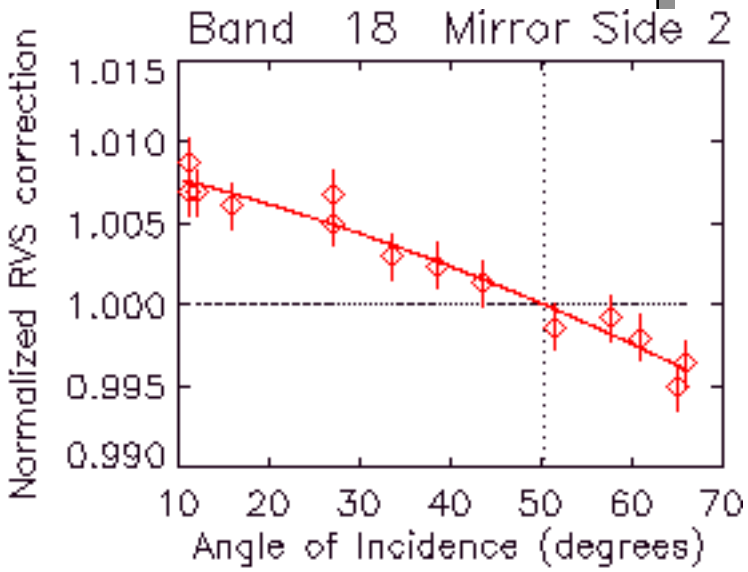
Band 18 Mirror Side 2
Normalized RVS correction
1.015
1.010
1.005
1.000
0.995
0.990
10 20 30 40 50 60 70
Angle of Incidence (degrees)

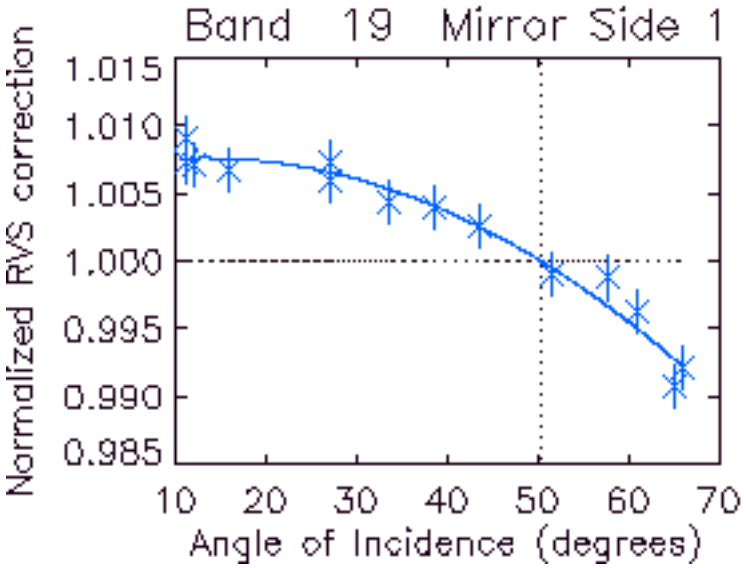
Band 19 Mirror Side 1
Normalized RVS correction
1.015
1.010
1.005
1.000
0.995
0.990
0.985
10 20 30 40 50 60 70
Angle of Incidence (degrees)

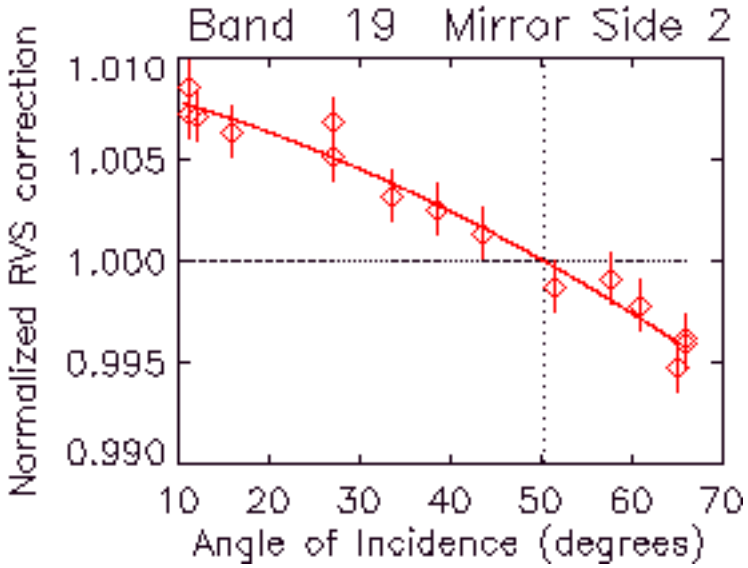
Band 19 Mirror Side 2
Normalized RVS correction
1.010
1.005
1.000
0.995
0.990
10 20 30 40 50 60 70
Angle of Incidence (degrees)

Error Analysis Methodology

- Once the optimum quadratic coefficients are obtained, the allowed range of these coefficients (which is a three dimensional ellipsoid) is estimated by enforcing the deviation of the quadratic function and the data is less than the effective 1-sigma standard deviation.
- At each AOI, the maximum and minimum value for RVS with the coefficient within the above specified range were obtained and their difference used as error bar for RVS.

The following charts show the 2-dimensional projections of the 3-d ellipsoid of the allowed parameter ranged which give less than effective 1-sigma deviation from the measured data. (in order of ascending center wavelength)

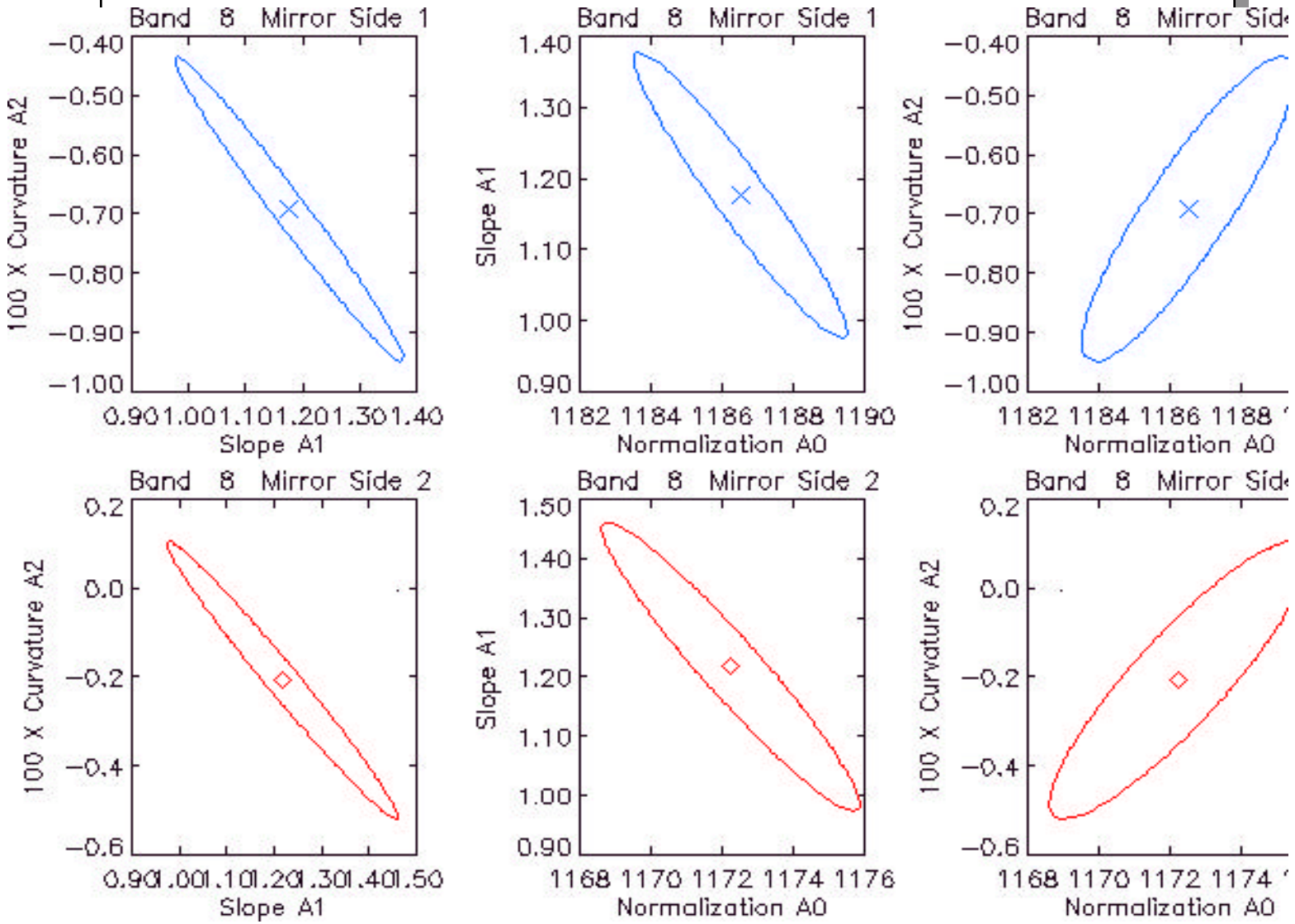
Band 8 Mirror Side 1
100 X Curvature A2
−0.40
−0.50
−0.60
−0.70
−0.80
−0.90
−1.00
0.90 1.00 1.10 1.20 1.30 1.40
Slope A1
Band 8 Mirror Side 1
Slope A1
1.40
1.30
1.20
1.10
1.00
0.90
1182 1184 1186 1188 1190
Normalization A0
Band 8 Mirror Side
100 X Curvature A2
−0.40
−0.50
−0.60
−0.70
−0.80
−0.90
−1.00
1182 1184 1186 1188
Normalization A0
Band 8 Mirror Side 2
100 X Curvature A2
0.2
0.0
−0.2
−0.4
−0.6
0.90 1.00 1.10 1.20 1.30 1.40 1.50
Slope A1
Band 8 Mirror Side 2
Slope A1
1.50
1.40
1.30
1.20
1.10
1.00
0.90
1168 1170 1172 1174 1176
Normalization A0
Band 8 Mirror Side
100 X Curvature A2
0.2
0.0
−0.2
−0.4
−0.6
1168 1170 1172 1174
Normalization A0

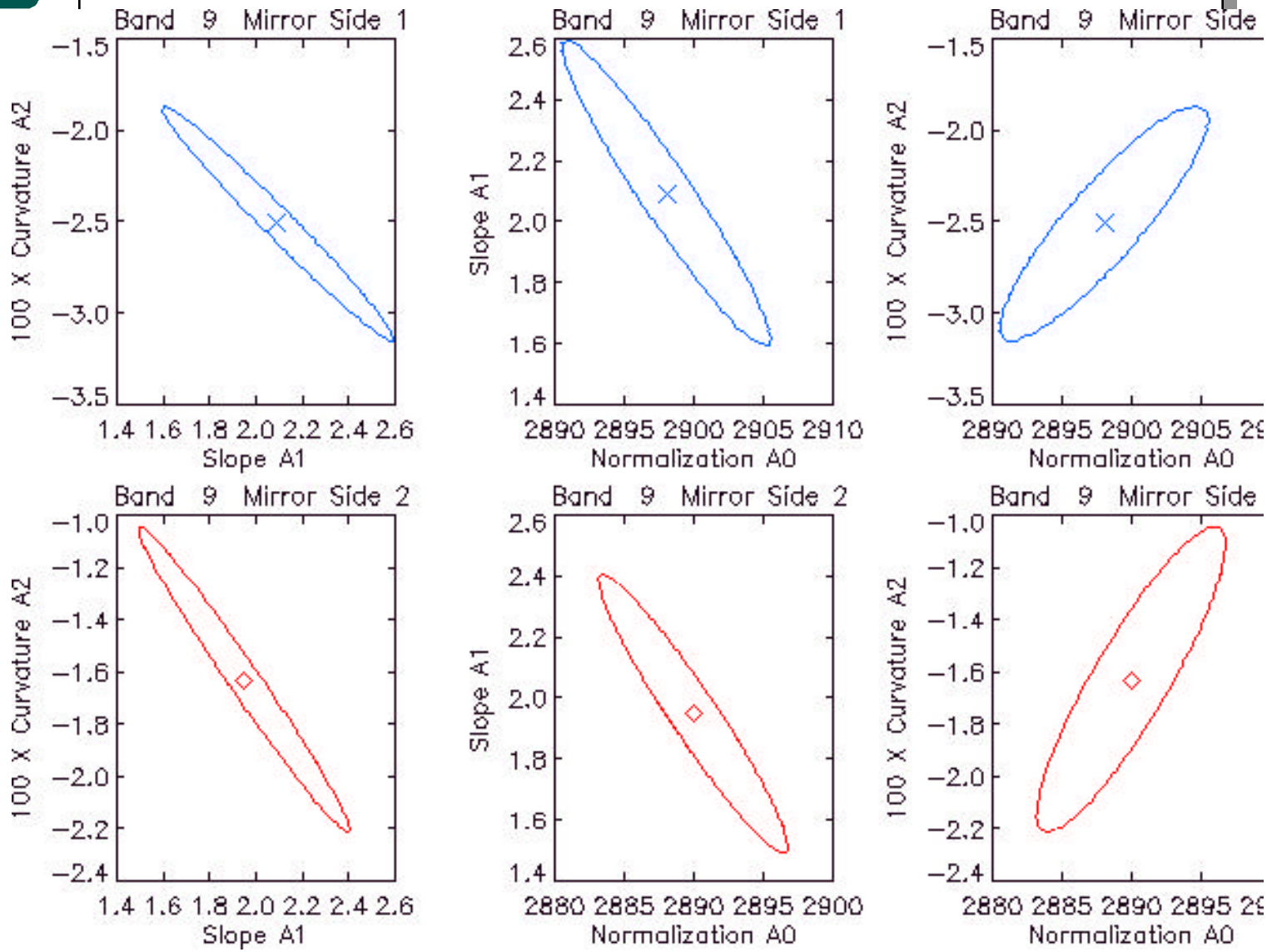
Band 9 Mirror Side 1
100 X Curvature A2
Slope A1
Band 9 Mirror Side 1
Slope A1
Normalization A0
Band 9 Mirror Side
100 X Curvature A2
Normalization A0
Band 9 Mirror Side 2
100 X Curvature A2
Slope A1
Band 9 Mirror Side 2
Slope A1
Normalization A0
Band 9 Mirror Side
100 X Curvature A2
Normalization A0

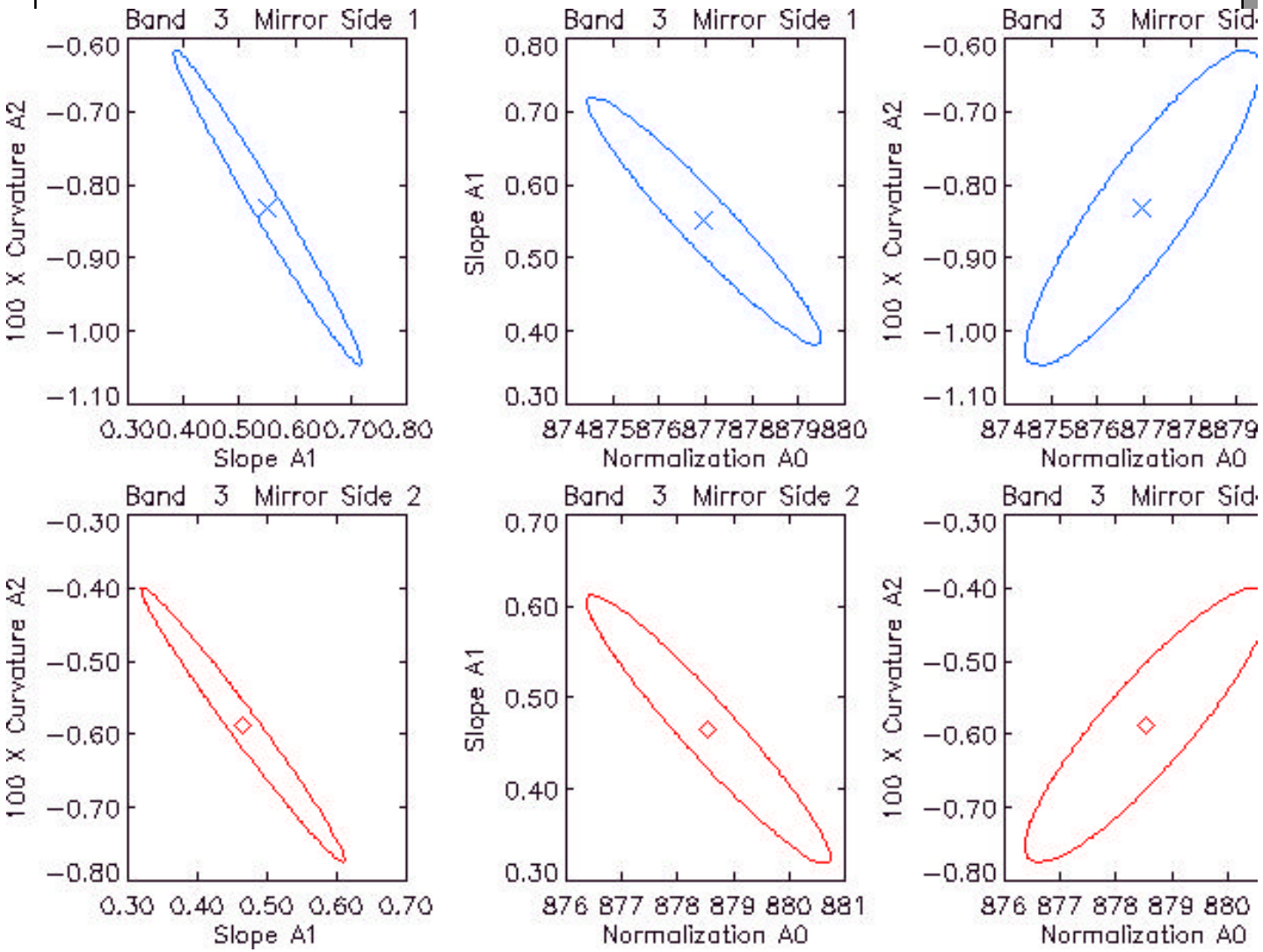
Band 3 Mirror Side 1
100 X Curvature A2
Slope A1
Band 3 Mirror Side 1
Slope A1
Normalization A0
Band 3 Mirror Side 1
100 X Curvature A2
Normalization A0
Band 3 Mirror Side 2
100 X Curvature A2
Slope A1
Band 3 Mirror Side 2
Slope A1
Normalization A0
Band 3 Mirror Side 2
100 X Curvature A2
Normalization A0

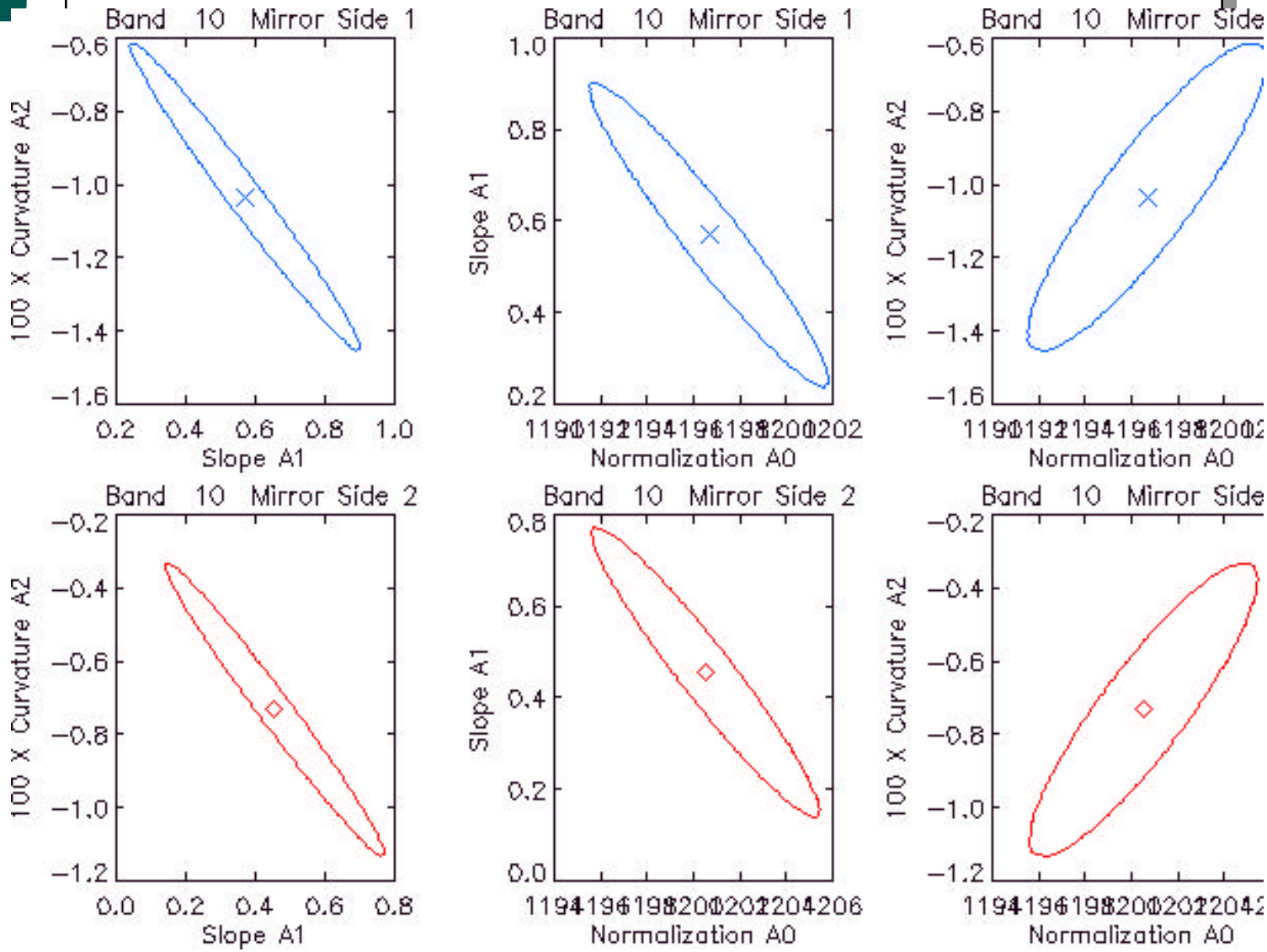
Band 10 Mirror Side 1
100 X Curvature A2
Slope A1
Band 10 Mirror Side 1
Slope A1
Normalization A0
Band 10 Mirror Side
100 X Curvature A2
Normalization A0
Band 10 Mirror Side 2
100 X Curvature A2
Slope A1
Band 10 Mirror Side 2
Slope A1
Normalization A0
Band 10 Mirror Side
100 X Curvature A2
Normalization A0

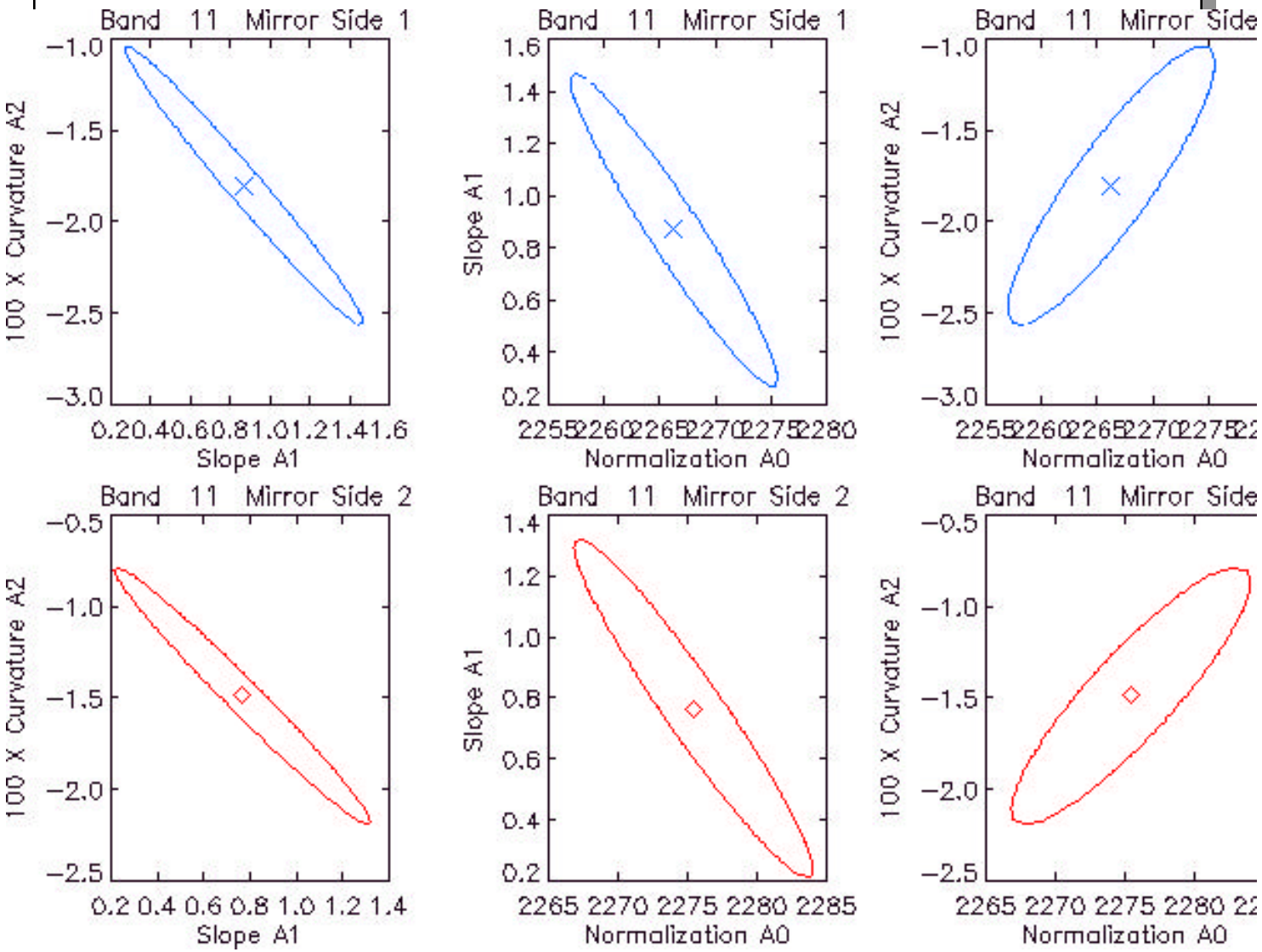
Band 11 Mirror Side 1
100 X Curvature A2
Slope A1
Band 11 Mirror Side 1
Slope A1
Normalization A0
Band 11 Mirror Side
100 X Curvature A2
Normalization A0
Band 11 Mirror Side 2
100 X Curvature A2
Slope A1
Band 11 Mirror Side 2
Slope A1
Normalization A0
Band 11 Mirror Side
100 X Curvature A2
Normalization A0

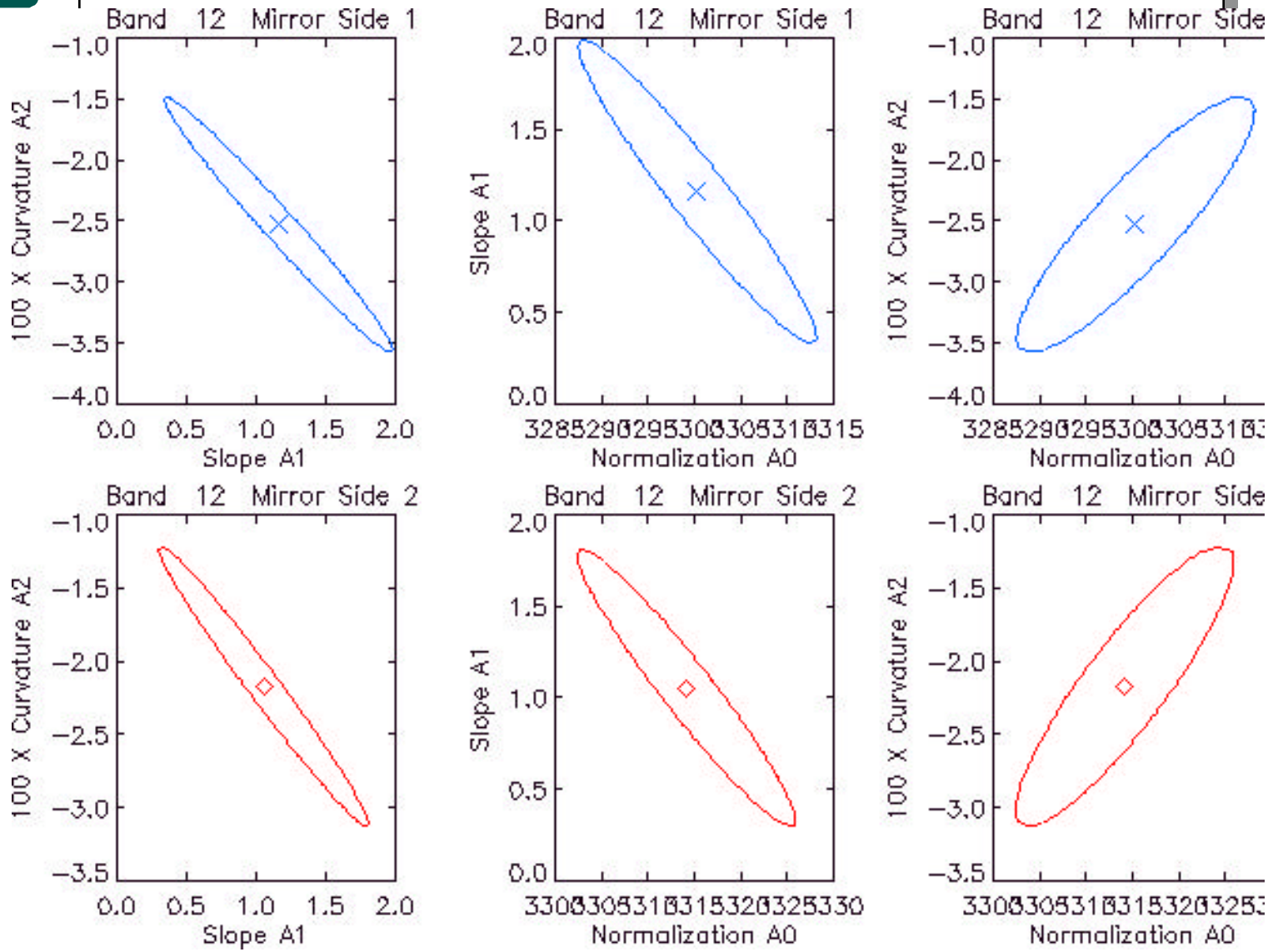
Band 12 Mirror Side 1
100 X Curvature A2
Slope A1
Band 12 Mirror Side 1
Slope A1
Normalization A0
Band 12 Mirror Side
100 X Curvature A2
Normalization A0
Band 12 Mirror Side 2
100 X Curvature A2
Slope A1
Band 12 Mirror Side 2
Slope A1
Normalization A0
Band 12 Mirror Side
100 X Curvature A2
Normalization A0

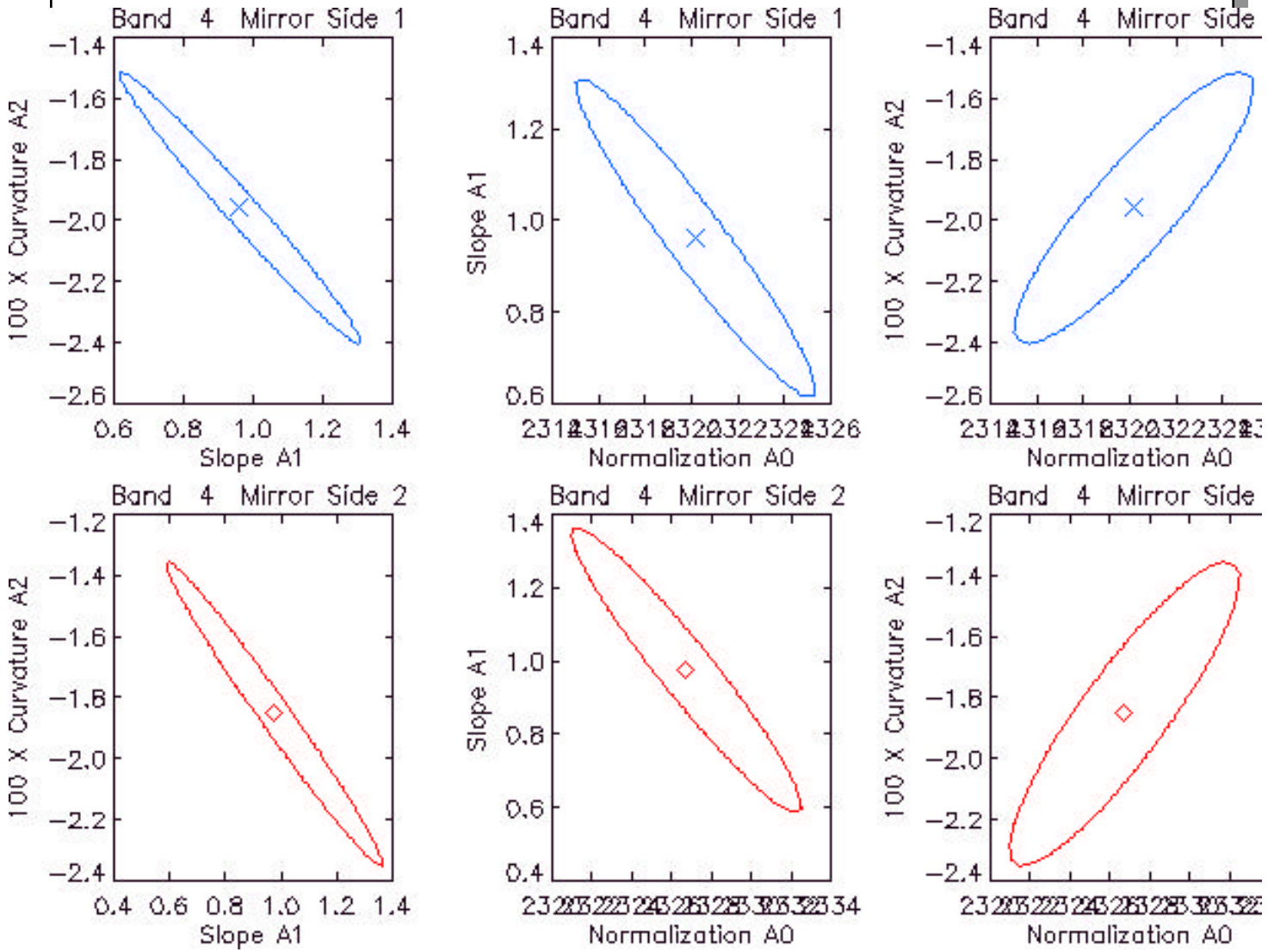
Band 4 Mirror Side 1
100 X Curvature A2
Slope A1
Band 4 Mirror Side 1
Slope A1
Normalization A0
Band 4 Mirror Side
100 X Curvature A2
Normalization A0
Band 4 Mirror Side 2
100 X Curvature A2
Slope A1
Band 4 Mirror Side 2
Slope A1
Normalization A0
Band 4 Mirror Side
100 X Curvature A2
Normalization A0

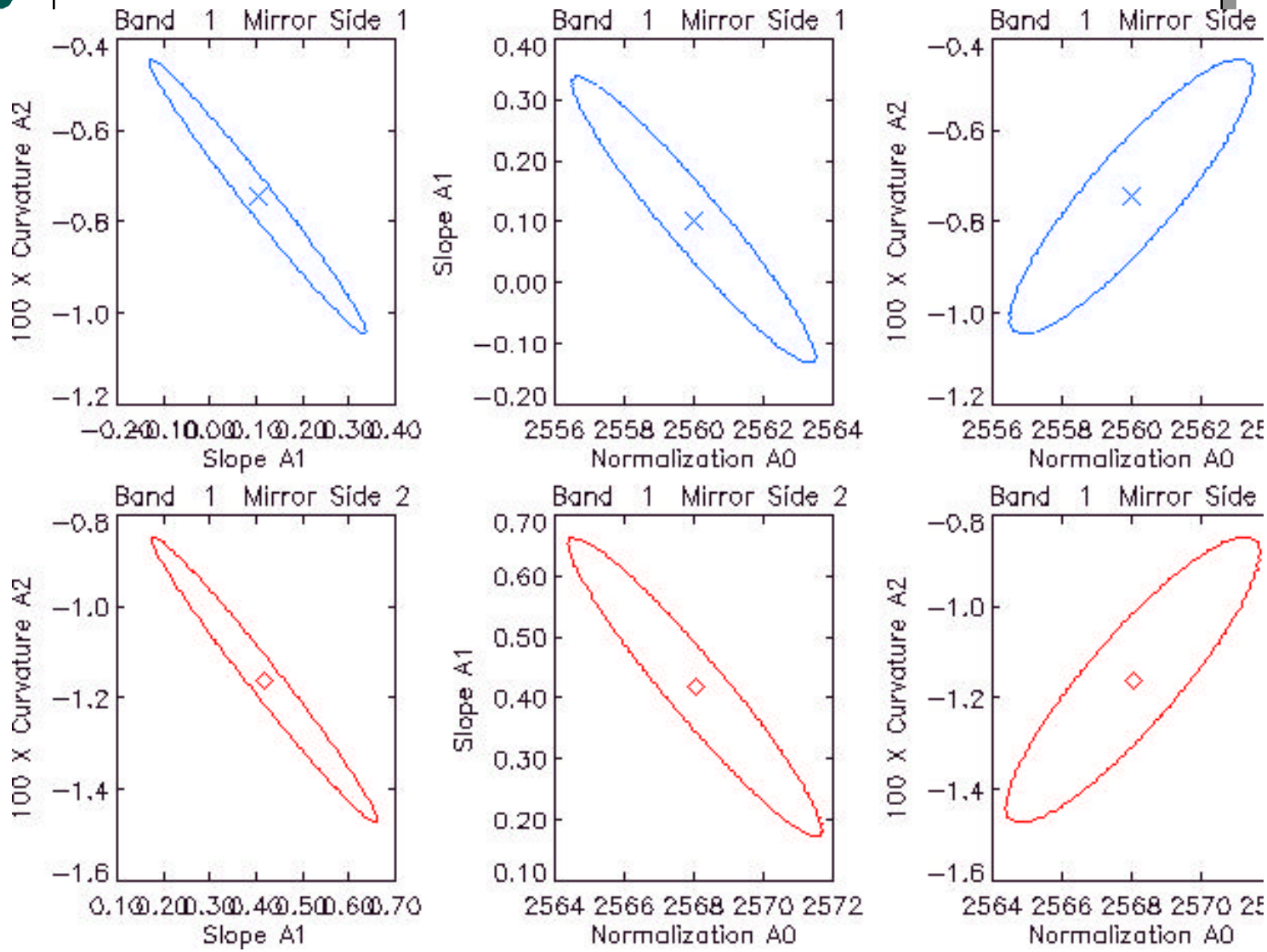
Band 1 Mirror Side 1
100 X Curvature A2
Slope A1
Band 1 Mirror Side 1
Slope A1
Normalization A0
Band 1 Mirror Side
100 X Curvature A2
Normalization A0
Band 1 Mirror Side 2
100 X Curvature A2
Slope A1
Band 1 Mirror Side 2
Slope A1
Normalization A0
Band 1 Mirror Side
100 X Curvature A2
Normalization A0

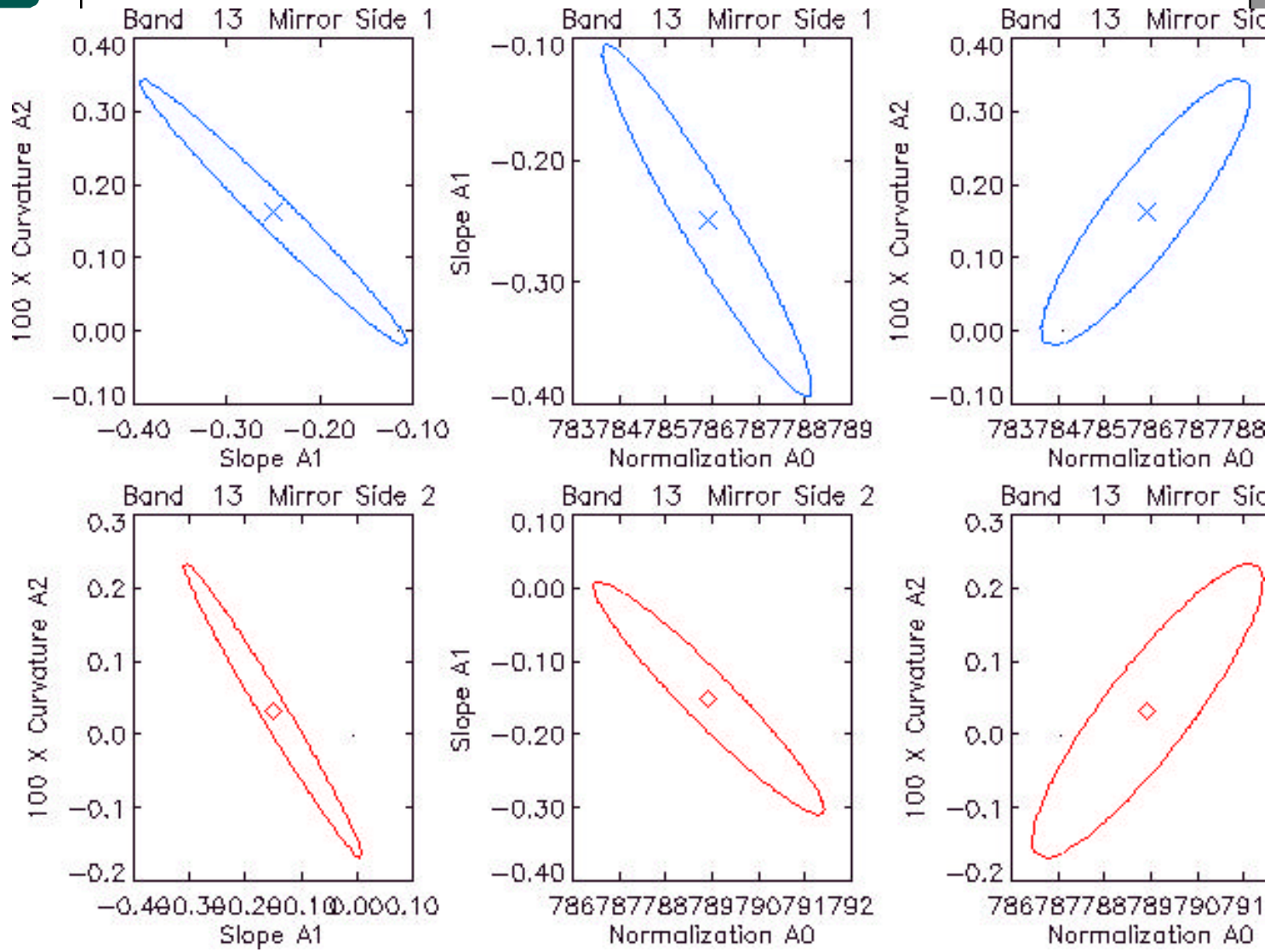
Band 13 Mirror Side 1
100 X Curvature A2
Slope A1
Band 13 Mirror Side 1
Slope A1
Normalization A0
Band 13 Mirror Side 1
100 X Curvature A2
Normalization A0
Band 13 Mirror Side 2
100 X Curvature A2
Slope A1
Band 13 Mirror Side 2
Slope A1
Normalization A0
Band 13 Mirror Side 2
100 X Curvature A2
Normalization A0

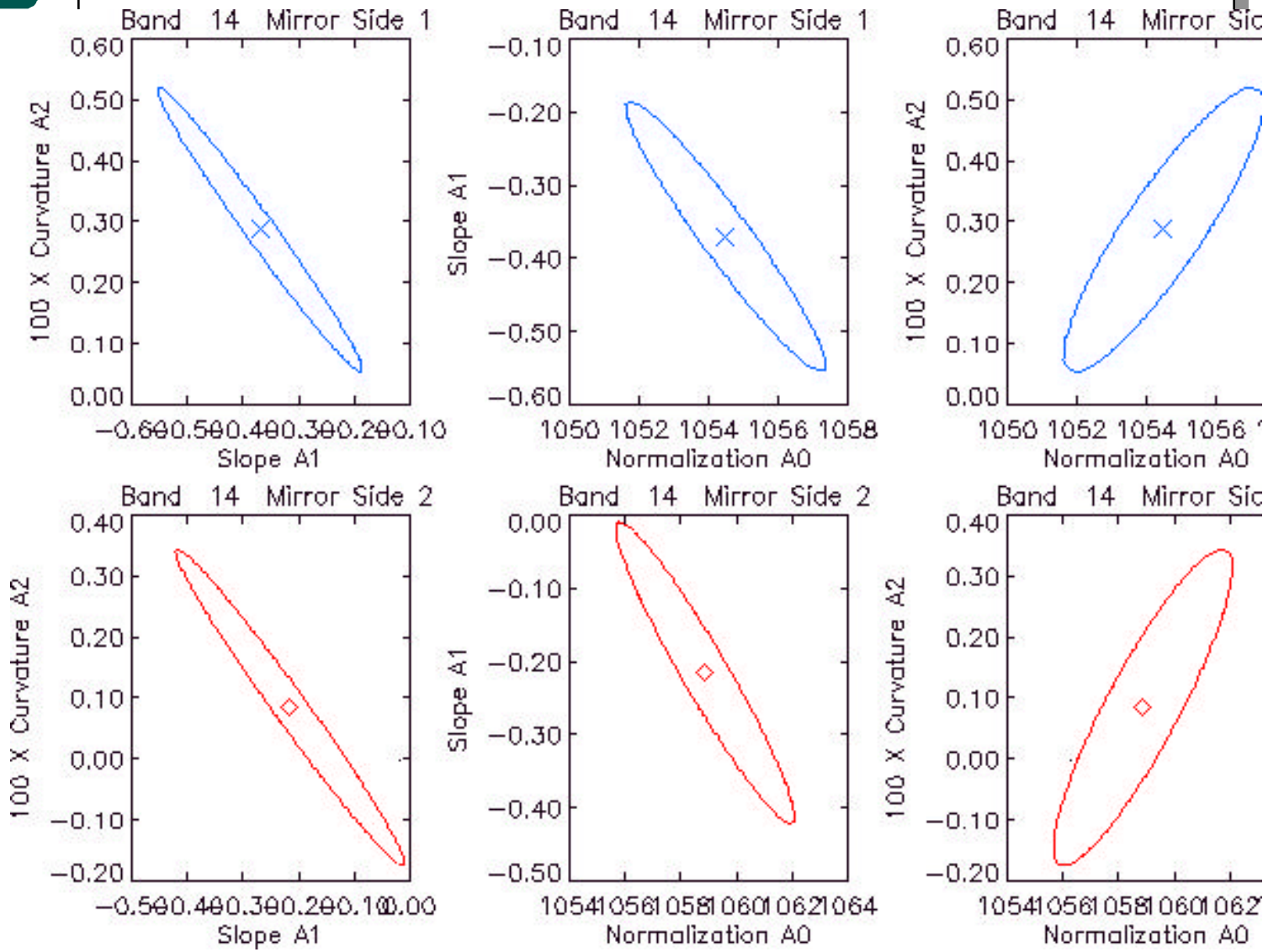
Band 14 Mirror Side 1
100 X Curvature A2
Slope A1
Band 14 Mirror Side 1
Slope A1
Normalization A0
Band 14 Mirror Sic
100 X Curvature A2
Normalization A0
Band 14 Mirror Side 2
100 X Curvature A2
Slope A1
Band 14 Mirror Side 2
Slope A1
Normalization A0
Band 14 Mirror Sic
100 X Curvature A2
Normalization A0

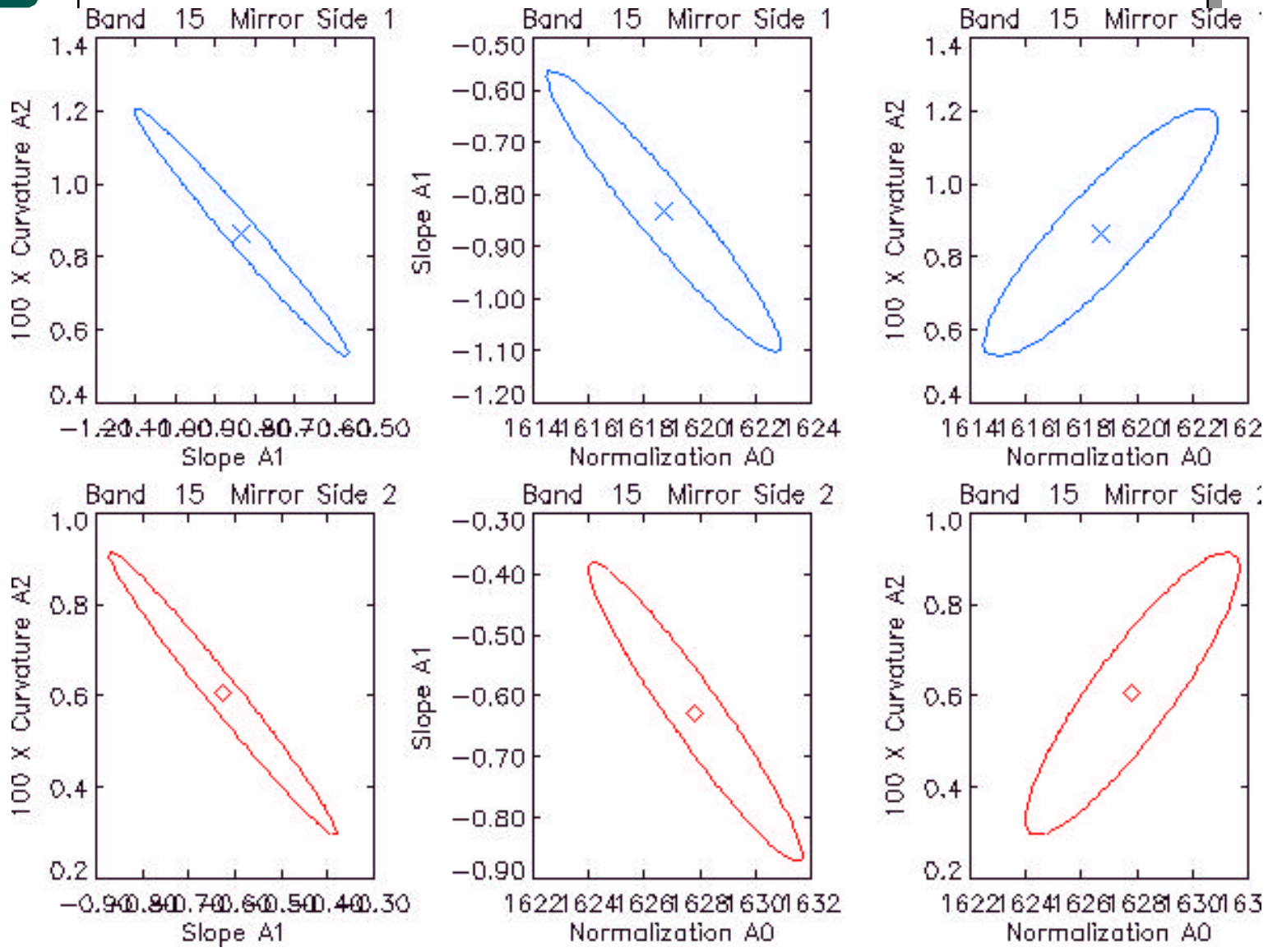
Band 15 Mirror Side 1
100 X Curvature A2
Slope A1
Band 15 Mirror Side 1
Slope A1
Normalization A0
Band 15 Mirror Side 1
100 X Curvature A2
Normalization A0
Band 15 Mirror Side 2
100 X Curvature A2
Slope A1
Band 15 Mirror Side 2
Slope A1
Normalization A0
Band 15 Mirror Side 2
100 X Curvature A2
Normalization A0

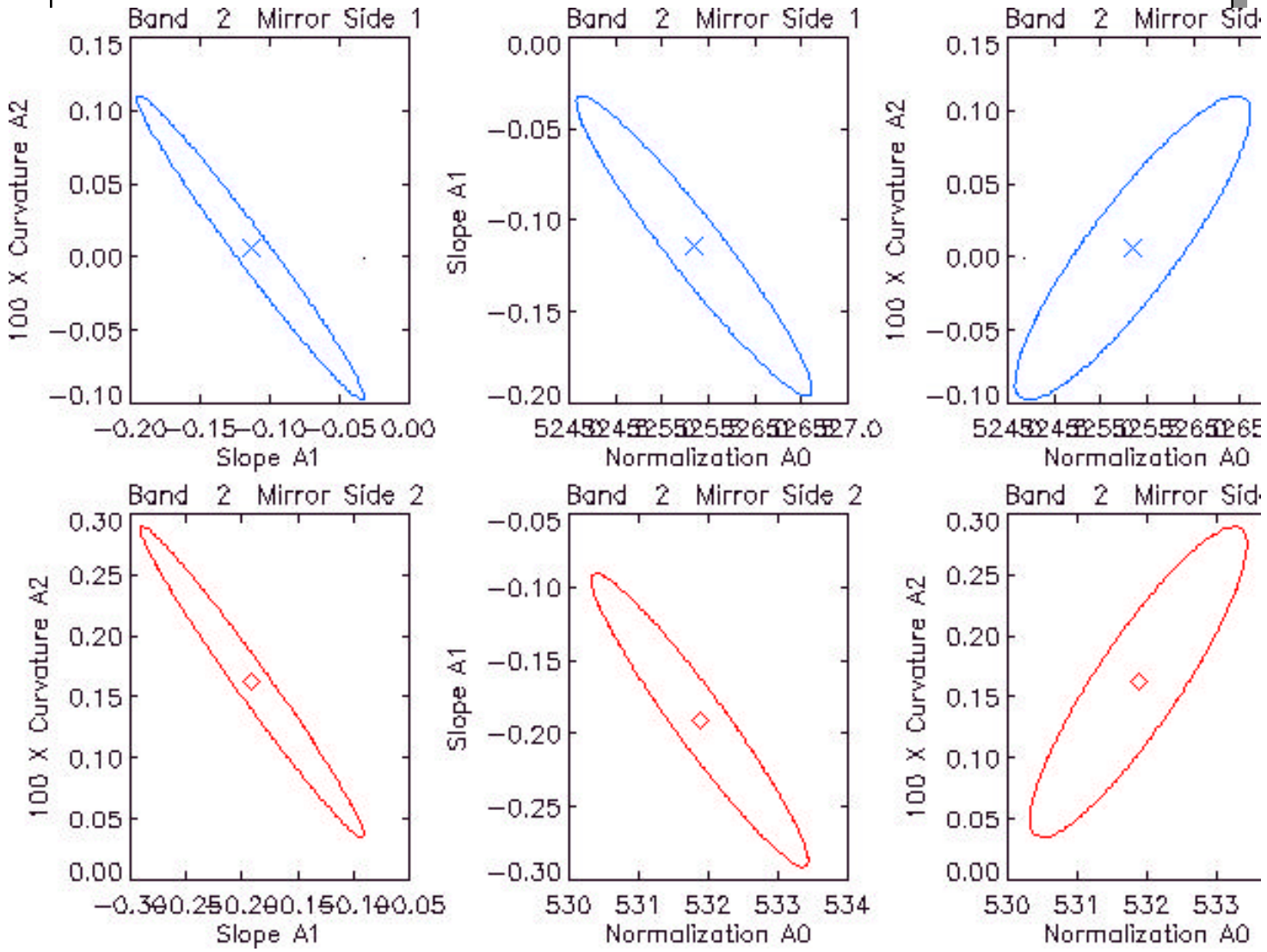
Band 2 Mirror Side 1
100 X Curvature A2
Slope A1
Band 2 Mirror Side 1
Slope A1
Normalization A0
Band 2 Mirror Side 1
100 X Curvature A2
Normalization A0
Band 2 Mirror Side 2
100 X Curvature A2
Slope A1
Band 2 Mirror Side 2
Slope A1
Normalization A0
Band 2 Mirror Side 2
100 X Curvature A2
Normalization A0

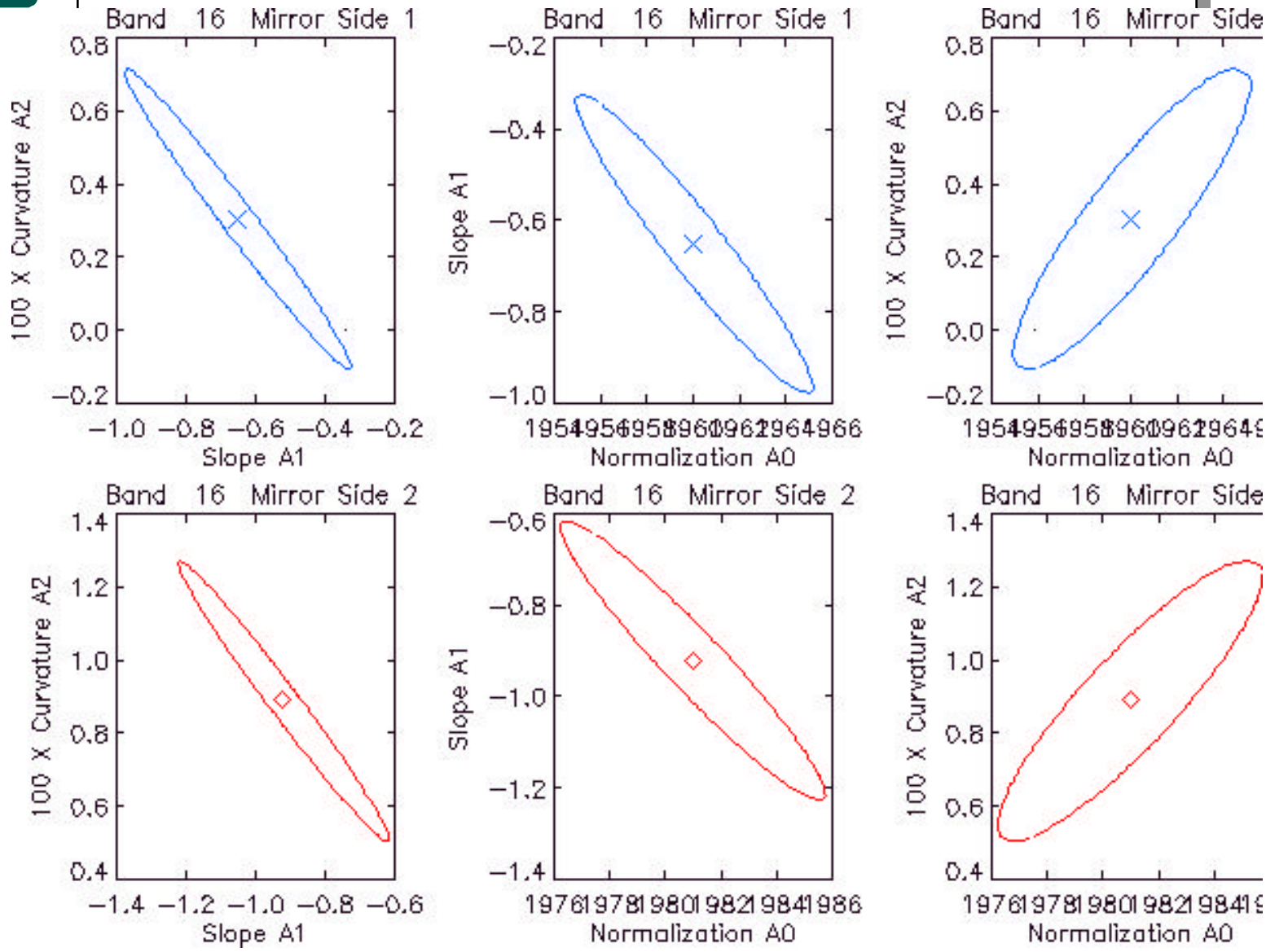
Band 16 Mirror Side 1
100 X Curvature A2
Slope A1
Band 16 Mirror Side 1
Slope A1
Normalization A0
Band 16 Mirror Side
100 X Curvature A2
Normalization A0
Band 16 Mirror Side 2
100 X Curvature A2
Slope A1
Band 16 Mirror Side 2
Slope A1
Normalization A0
Band 16 Mirror Side
100 X Curvature A2
Normalization A0

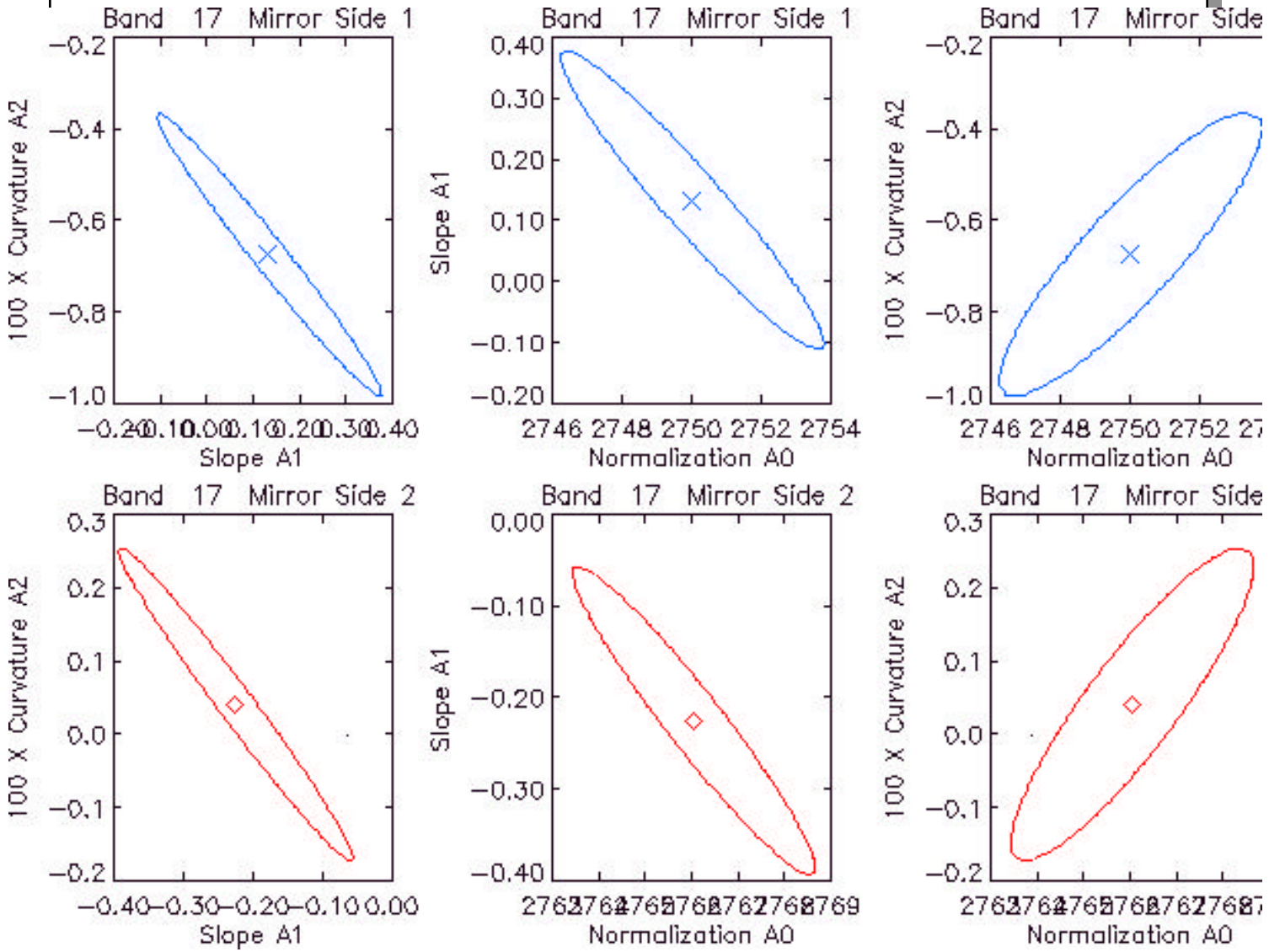
Band 17 Mirror Side 1
100 X Curvature A2
Slope A1
Band 17 Mirror Side 1
Slope A1
Normalization A0
Band 17 Mirror Side
100 X Curvature A2
Normalization A0
Band 17 Mirror Side 2
100 X Curvature A2
Slope A1
Band 17 Mirror Side 2
Slope A1
Normalization A0
Band 17 Mirror Side
100 X Curvature A2
Normalization A0

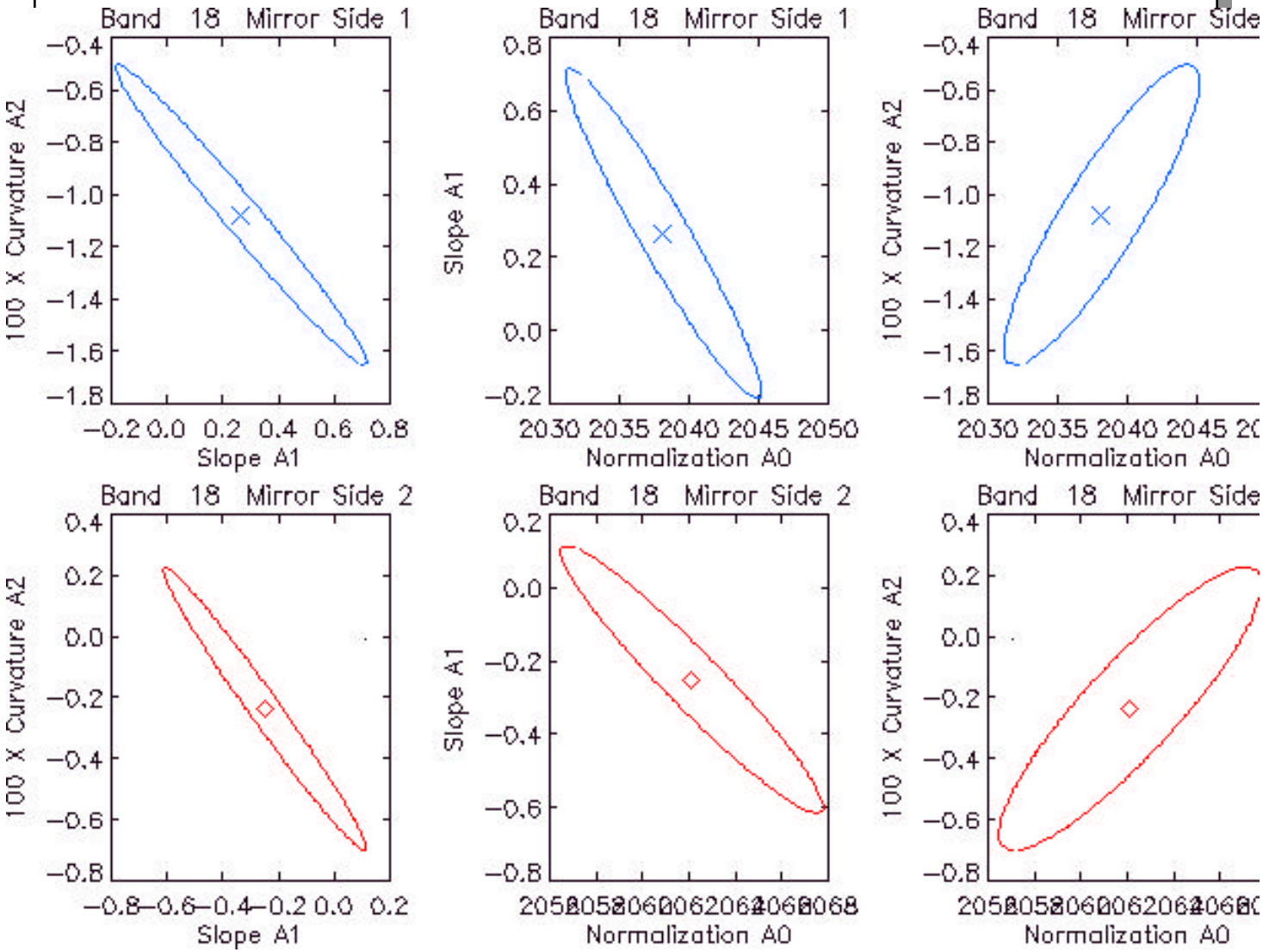
Band 18 Mirror Side 1
100 X Curvature A2
Slope A1
Band 18 Mirror Side 1
Slope A1
Normalization A0
Band 18 Mirror Side
100 X Curvature A2
Normalization A0
Band 18 Mirror Side 2
100 X Curvature A2
Slope A1
Band 18 Mirror Side 2
Slope A1
Normalization A0
Band 18 Mirror Side
100 X Curvature A2
Normalization A0

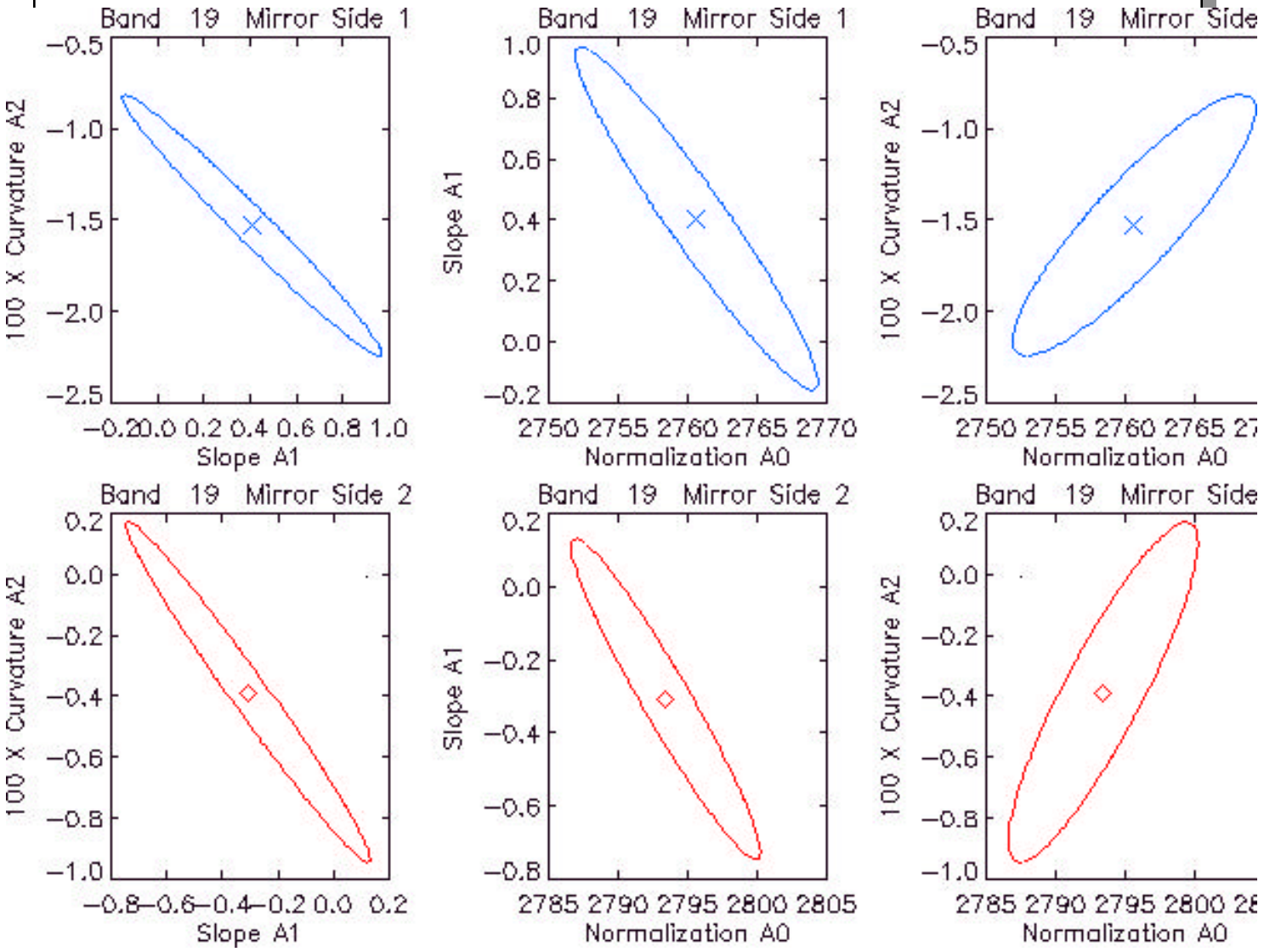
Band 19 Mirror Side 1
100 X Curvature A2
Slope A1
Band 19 Mirror Side 1
Slope A1
Normalization A0
Band 19 Mirror Side
100 X Curvature A2
Normalization A0
Band 19 Mirror Side 2
100 X Curvature A2
Slope A1
Band 19 Mirror Side 2
Slope A1
Normalization A0
Band 19 Mirror Side
100 X Curvature A2
Normalization A0

The following charts show the maximum and minimum results for RVS versus AOI calculated with the parameter range given by the ellipsoid. (in order of ascending center wavelength)

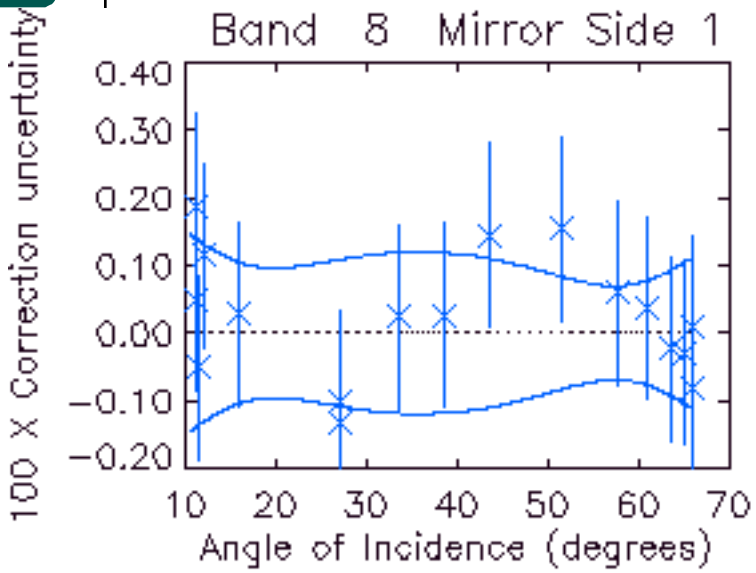
Band 8 Mirror Side 1
100 X Correction uncertainty
0.40
0.30
0.20
0.10
0.00
−0.10
−0.20
10 20 30 40 50 60 70
Angle of Incidence (degrees)

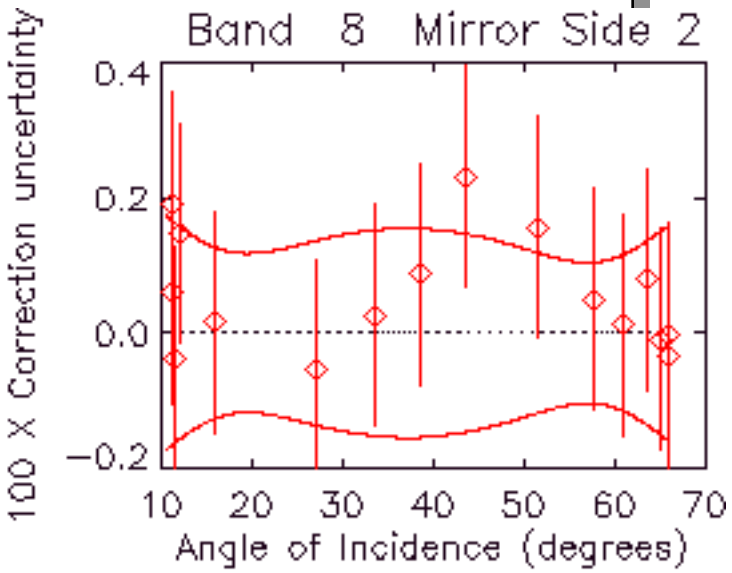
Band 8 Mirror Side 2
100 X Correction uncertainty
0.4
0.2
0.0
−0.2
10 20 30 40 50 60 70
Angle of Incidence (degrees)

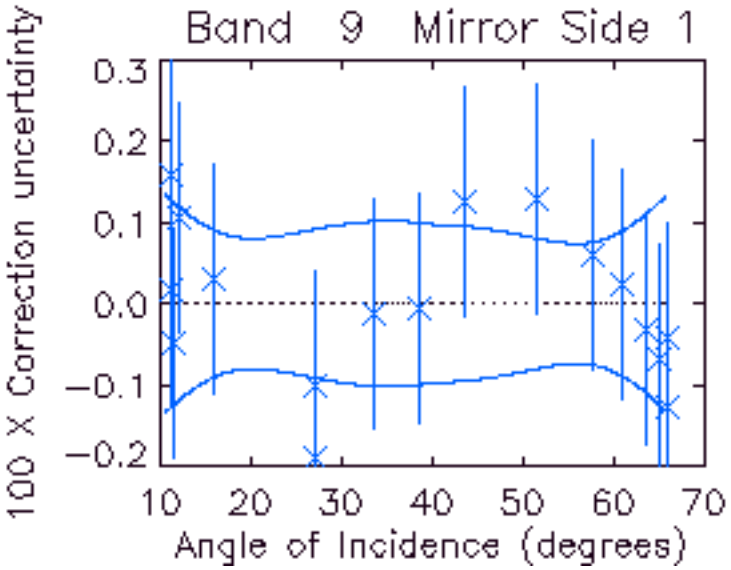
Band 9 Mirror Side 1
100 X Correction uncertainty
0.3
0.2
0.1
0.0
−0.1
−0.2
10 20 30 40 50 60 70
Angle of Incidence (degrees)

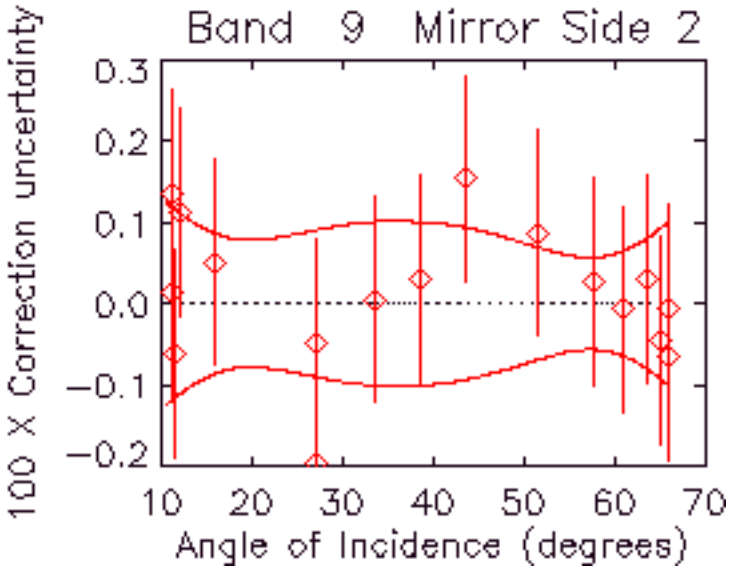
Band 9 Mirror Side 2
100 X Correction uncertainty
0.3
0.2
0.1
0.0
−0.1
−0.2
10 20 30 40 50 60 70
Angle of Incidence (degrees)

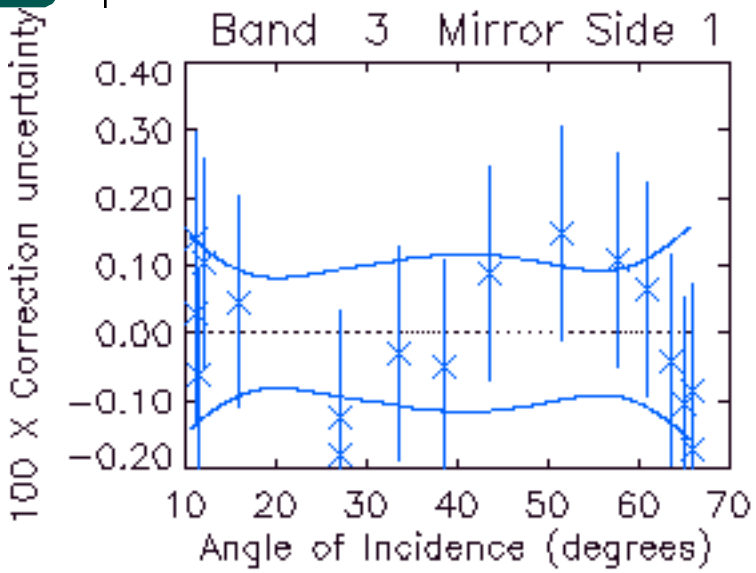
Band 3 Mirror Side 1
100 X Correction uncertainty
0.40
0.30
0.20
0.10
0.00
−0.10
−0.20
10 20 30 40 50 60 70
Angle of Incidence (degrees)

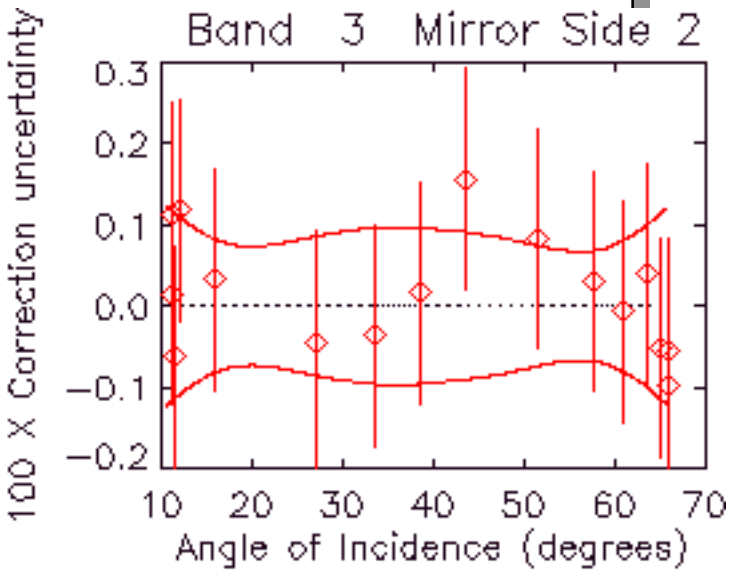
Band 3 Mirror Side 2
100 X Correction uncertainty
0.3
0.2
0.1
0.0
−0.1
−0.2
10 20 30 40 50 60 70
Angle of Incidence (degrees)

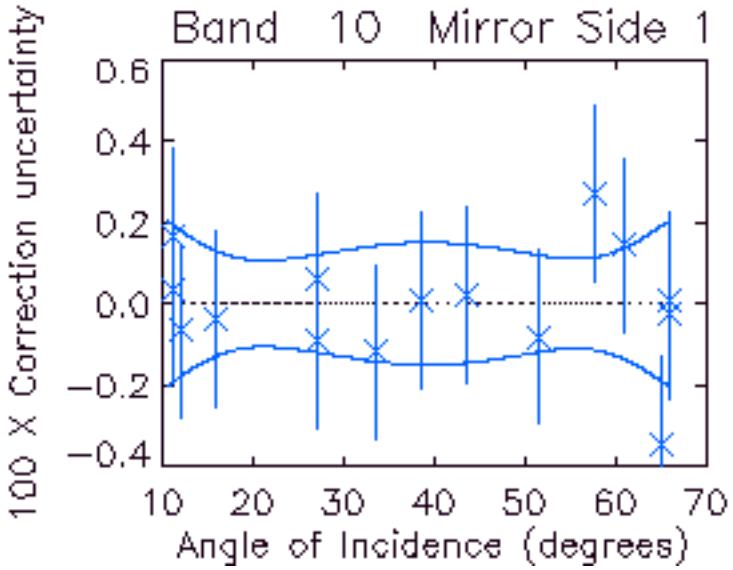
Band 10 Mirror Side 1
100 X Correction uncertainty
0.6
0.4
0.2
0.0
−0.2
−0.4
10 20 30 40 50 60 70
Angle of Incidence (degrees)

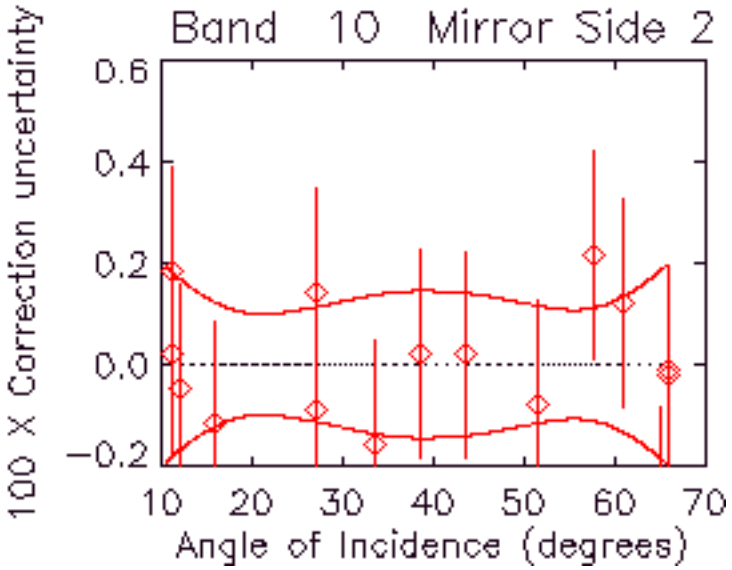
Band 10 Mirror Side 2
100 X Correction uncertainty
0.6
0.4
0.2
0.0
−0.2
10 20 30 40 50 60 70
Angle of Incidence (degrees)

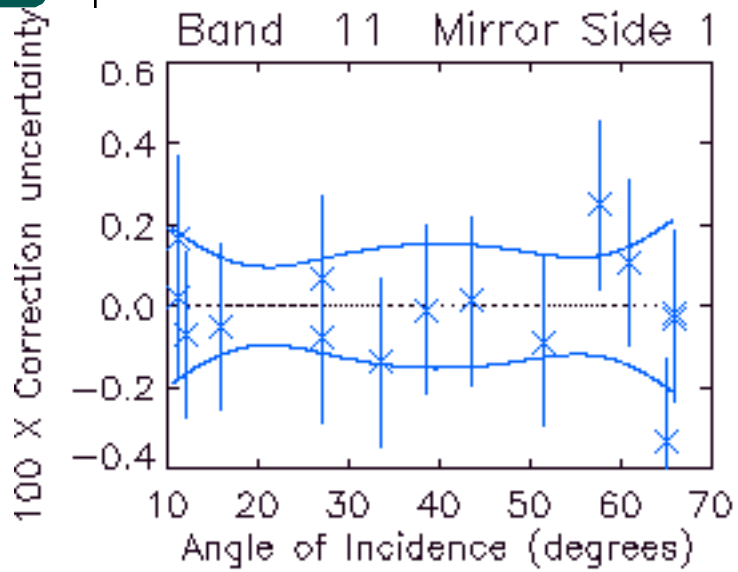
Band 11 Mirror Side 1
100 X Correction uncertainty
0.6
0.4
0.2
0.0
−0.2
−0.4
10 20 30 40 50 60 70
Angle of Incidence (degrees)

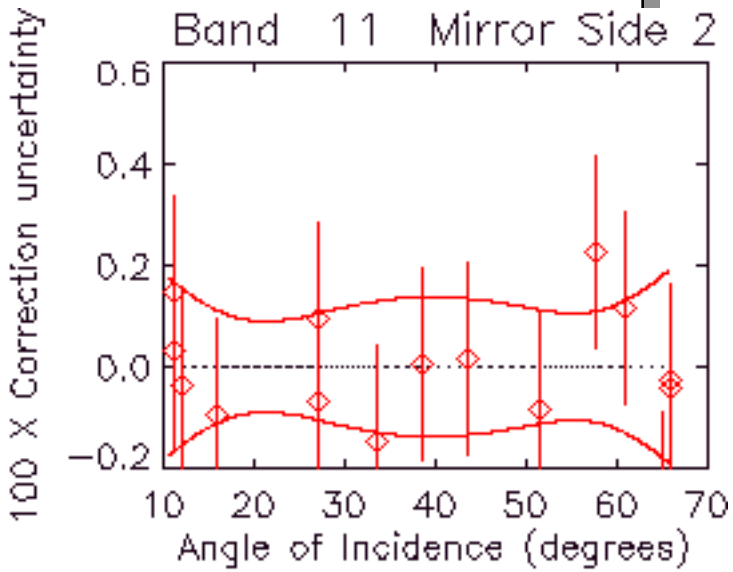
Band 11 Mirror Side 2
100 X Correction uncertainty
0.6
0.4
0.2
0.0
−0.2
10 20 30 40 50 60 70
Angle of Incidence (degrees)

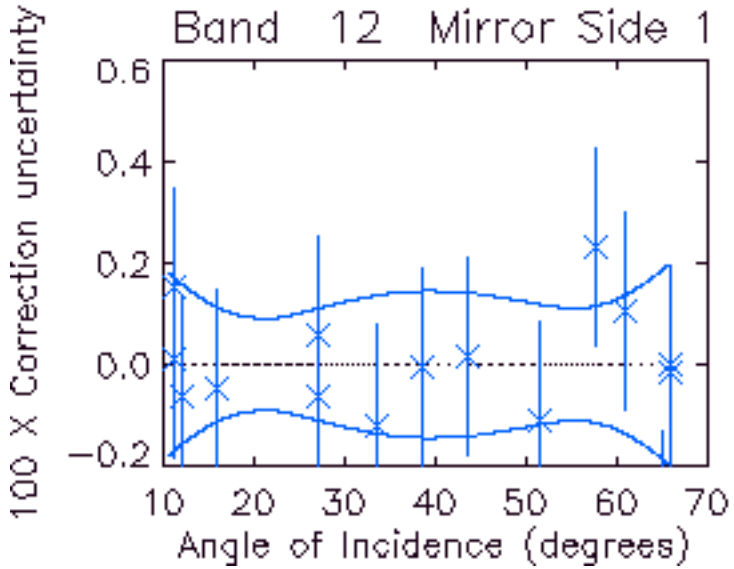
Band 12 Mirror Side 1
100 X Correction uncertainty
0.6
0.4
0.2
0.0
−0.2
10 20 30 40 50 60 70
Angle of Incidence (degrees)

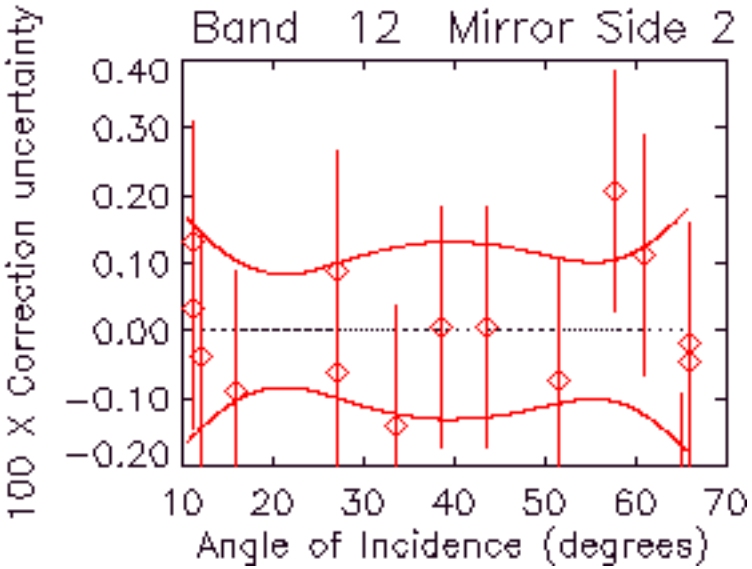
Band 12 Mirror Side 2
100 X Correction uncertainty
0.40
0.30
0.20
0.10
0.00
−0.10
−0.20
10 20 30 40 50 60 70
Angle of Incidence (degrees)

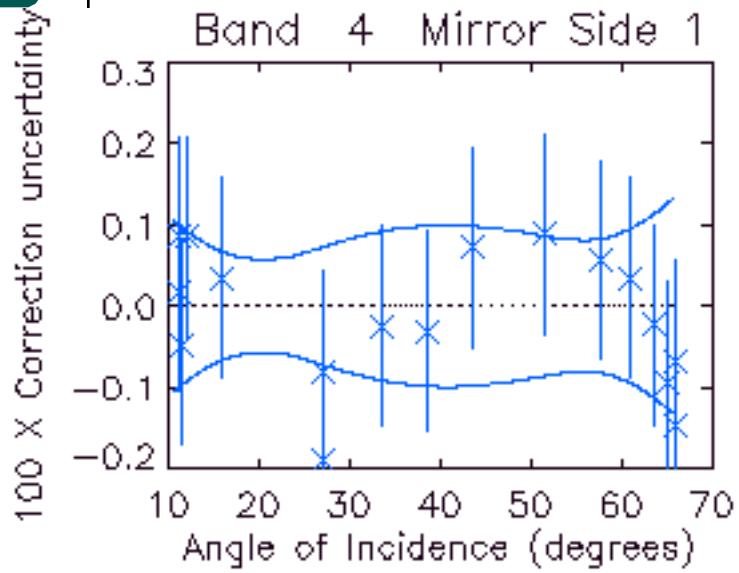
Band 4 Mirror Side 1
100 X Correction uncertainty
0.3
0.2
0.1
0.0
−0.1
−0.2
10 20 30 40 50 60 70
Angle of Incidence (degrees)

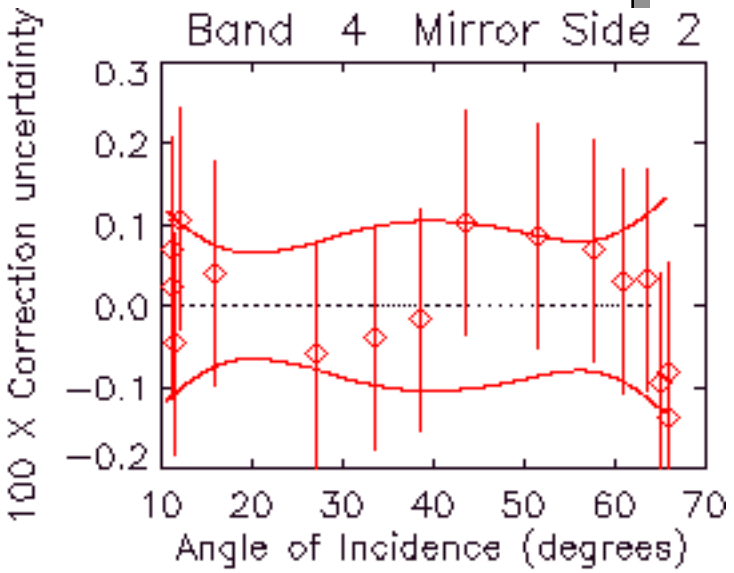
Band 4 Mirror Side 2
100 X Correction uncertainty
0.3
0.2
0.1
0.0
−0.1
−0.2
10 20 30 40 50 60 70
Angle of Incidence (degrees)

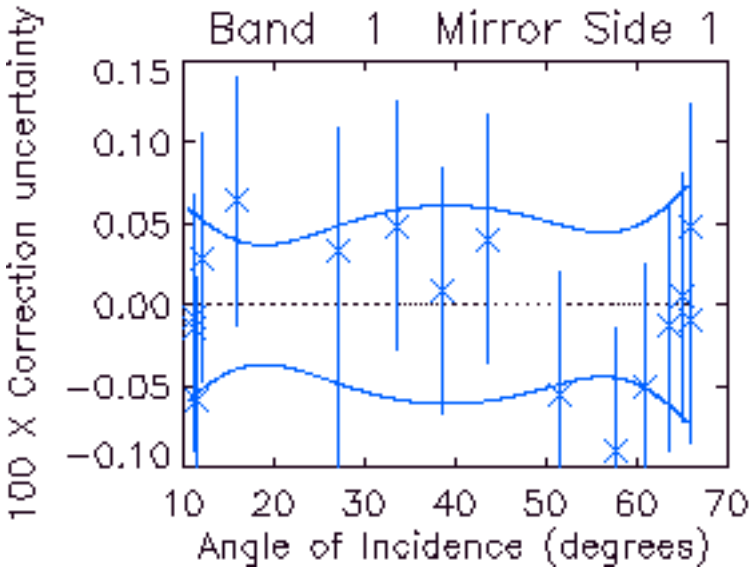
Band 1 Mirror Side 1
100 X Correction uncertainty
0.15
0.10
0.05
0.00
−0.05
−0.10
10 20 30 40 50 60 70
Angle of Incidence (degrees)

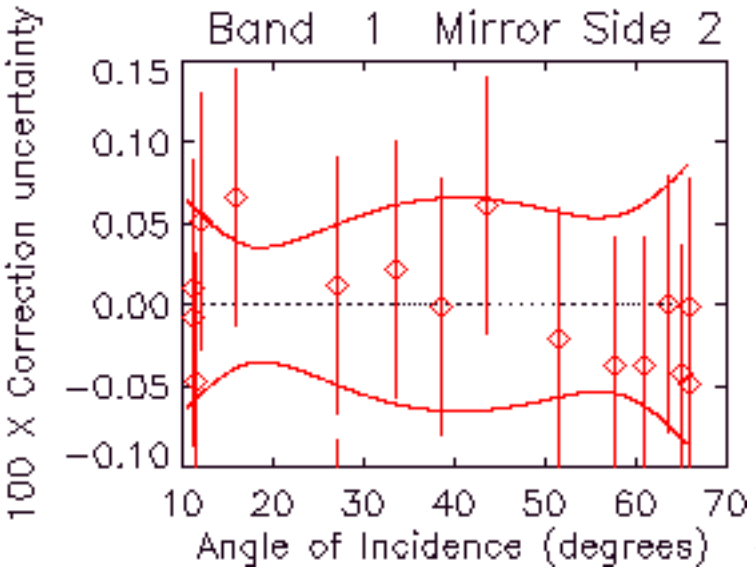
Band 1 Mirror Side 2
100 X Correction uncertainty
0.15
0.10
0.05
0.00
−0.05
−0.10
10 20 30 40 50 60 70
Angle of Incidence (degrees)

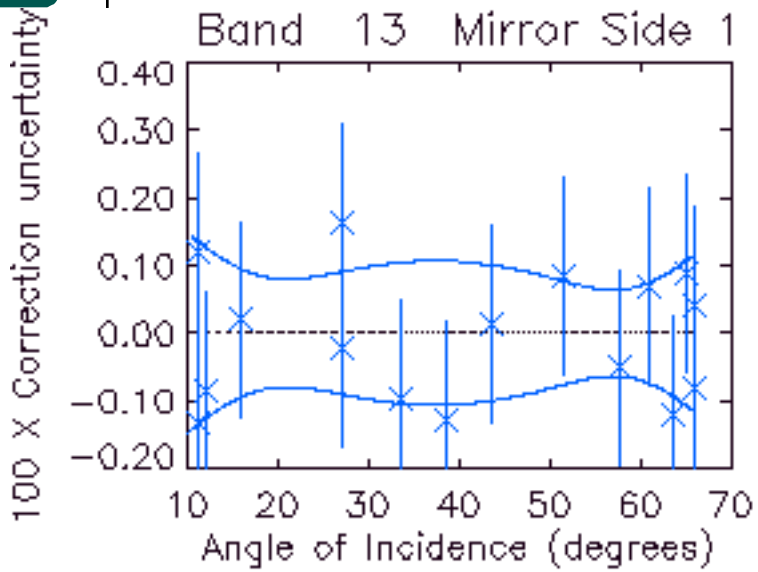
Band 13 Mirror Side 1
100 X Correction uncertainty
0.40
0.30
0.20
0.10
0.00
−0.10
−0.20
10 20 30 40 50 60 70
Angle of Incidence (degrees)

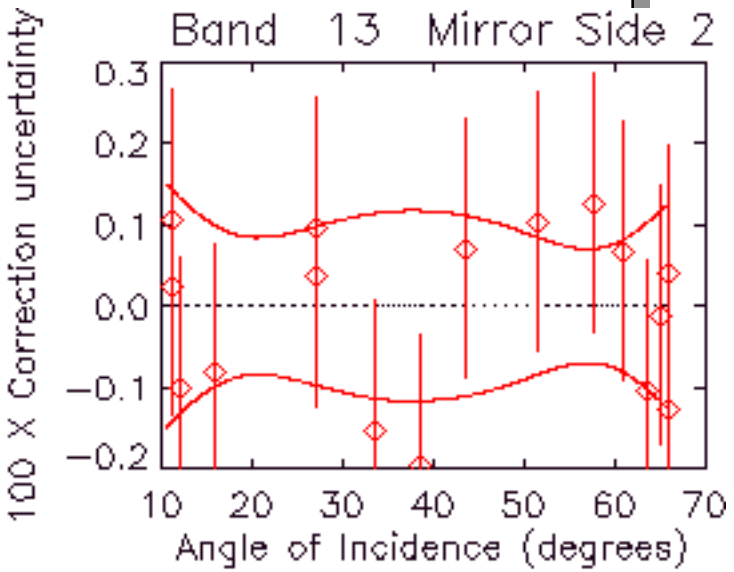
Band 13 Mirror Side 2
100 X Correction uncertainty
0.3
0.2
0.1
0.0
−0.1
−0.2
10 20 30 40 50 60 70
Angle of Incidence (degrees)

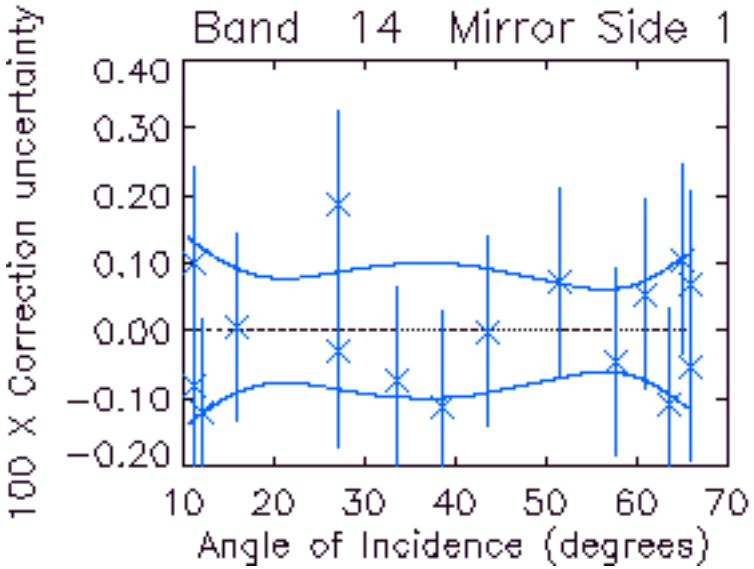
Band 14 Mirror Side 1
100 X Correction uncertainty
0.40
0.30
0.20
0.10
0.00
−0.10
−0.20
10 20 30 40 50 60 70
Angle of Incidence (degrees)

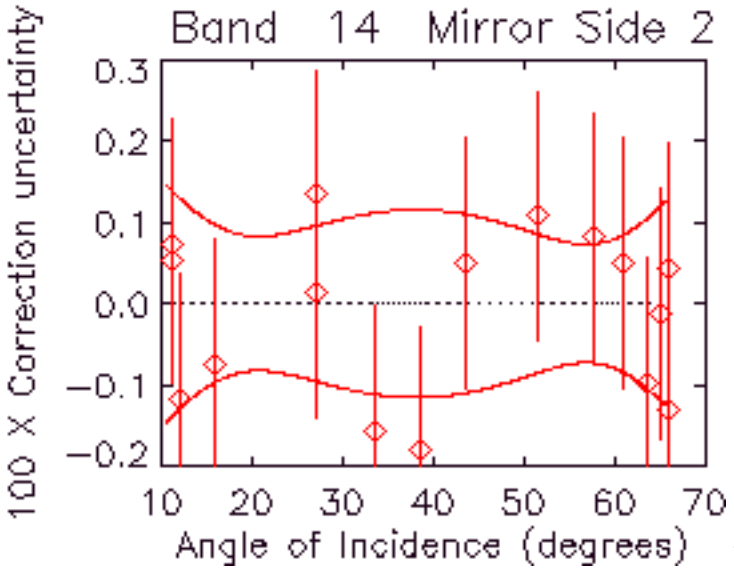
Band 14 Mirror Side 2
100 X Correction uncertainty
0.3
0.2
0.1
0.0
−0.1
−0.2
10 20 30 40 50 60 70
Angle of Incidence (degrees)

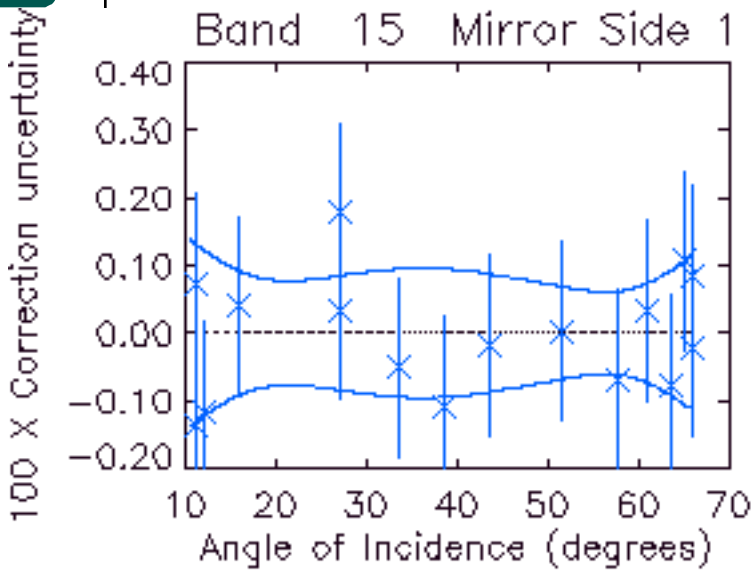
Band 15 Mirror Side 1
100 X Correction uncertainty
0.40
0.30
0.20
0.10
0.00
−0.10
−0.20
10 20 30 40 50 60 70
Angle of Incidence (degrees)

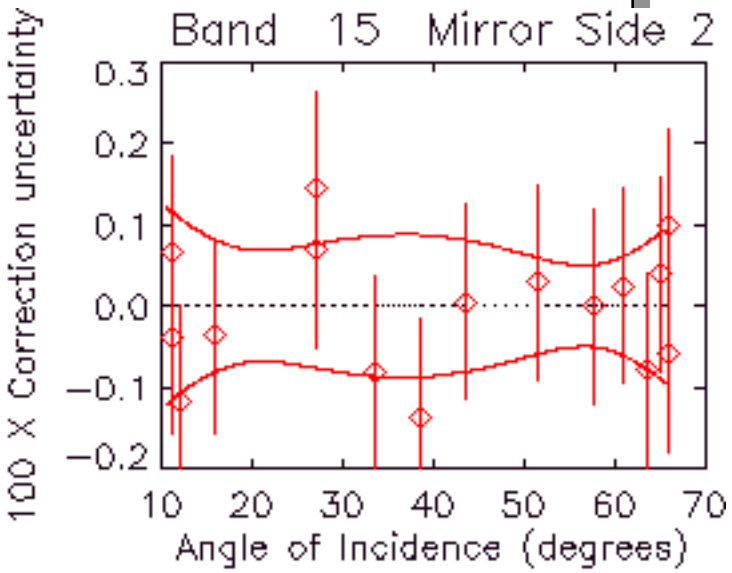
Band 15 Mirror Side 2
100 X Correction uncertainty
0.3
0.2
0.1
0.0
−0.1
−0.2
10 20 30 40 50 60 70
Angle of Incidence (degrees)

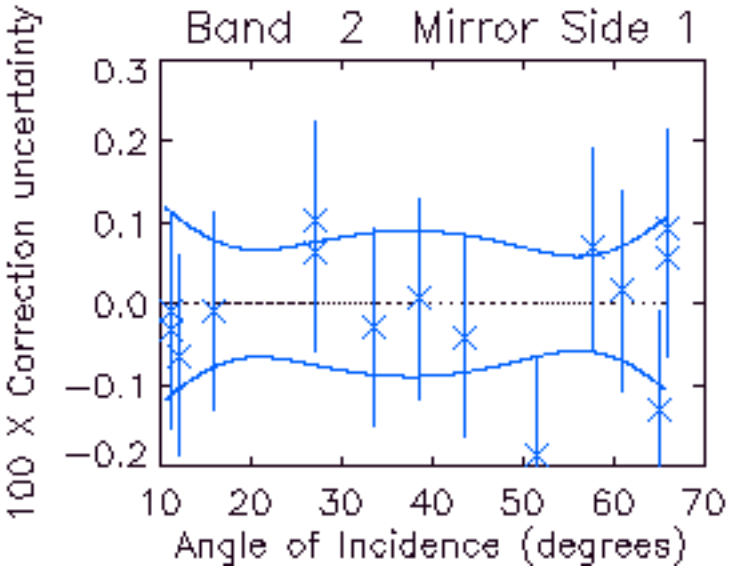
Band 2 Mirror Side 1
100 X Correction uncertainty
0.3
0.2
0.1
0.0
−0.1
−0.2
10 20 30 40 50 60 70
Angle of Incidence (degrees)

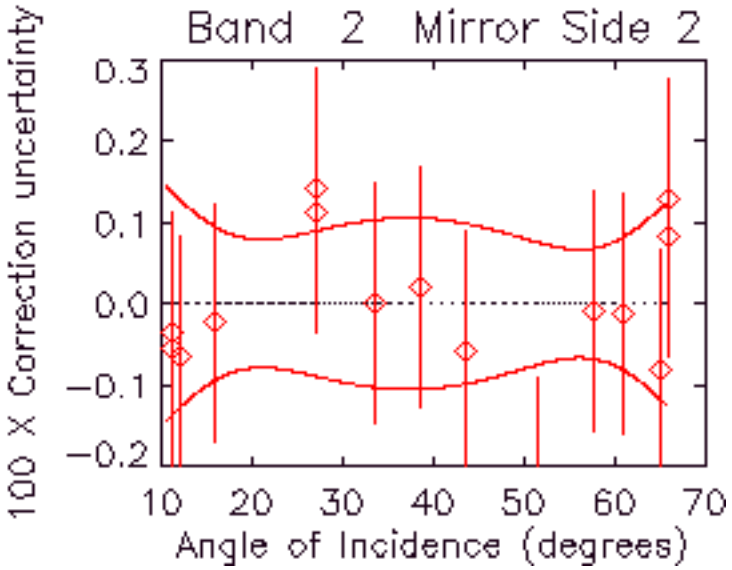
Band 2 Mirror Side 2
100 X Correction uncertainty
0.3
0.2
0.1
0.0
−0.1
−0.2
10 20 30 40 50 60 70
Angle of Incidence (degrees)

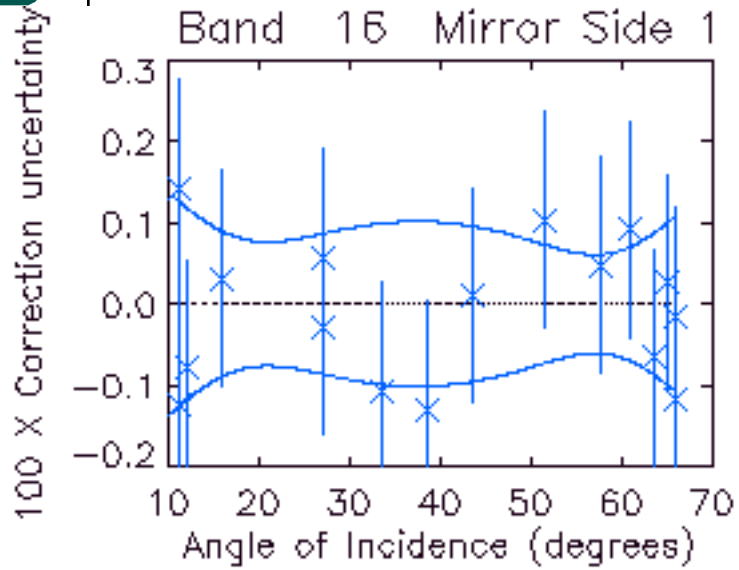
Band 16 Mirror Side 1
100 X Correction uncertainty
0.3
0.2
0.1
0.0
−0.1
−0.2
10 20 30 40 50 60 70
Angle of Incidence (degrees)

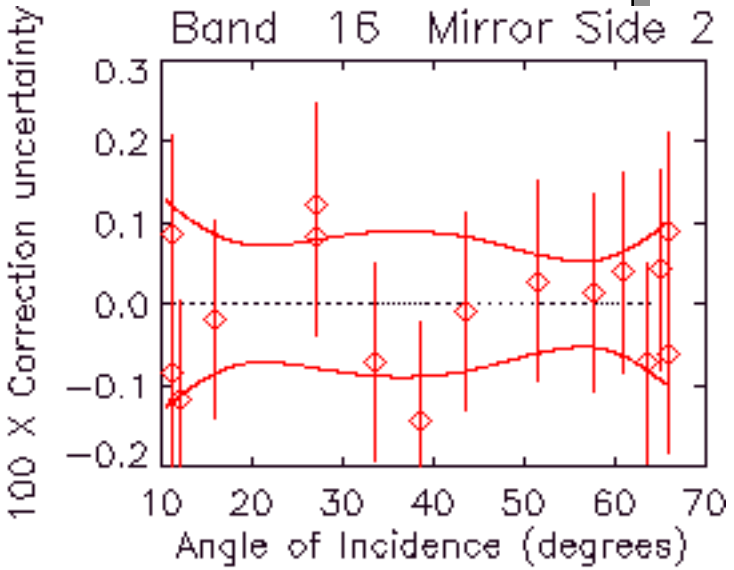
Band 16 Mirror Side 2
100 X Correction uncertainty
0.3
0.2
0.1
0.0
−0.1
−0.2
10 20 30 40 50 60 70
Angle of Incidence (degrees)

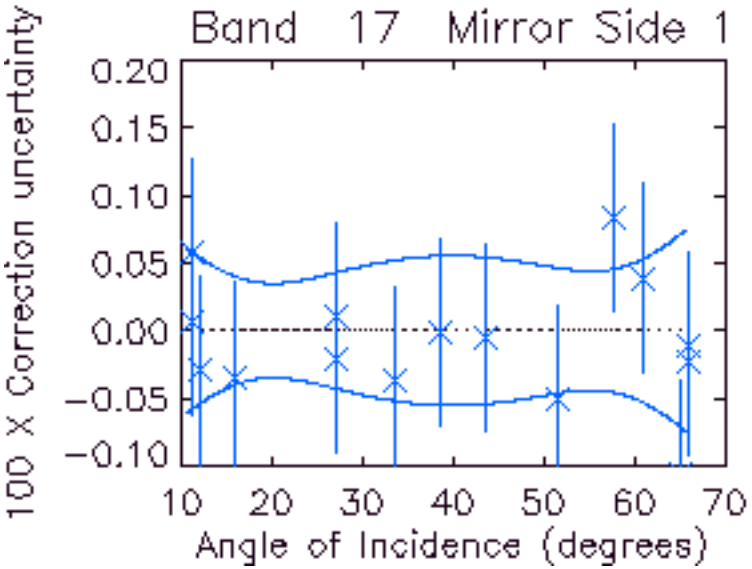
Band 17 Mirror Side 1
100 X Correction uncertainty
0.20
0.15
0.10
0.05
0.00
−0.05
−0.10
10 20 30 40 50 60 70
Angle of Incidence (degrees)

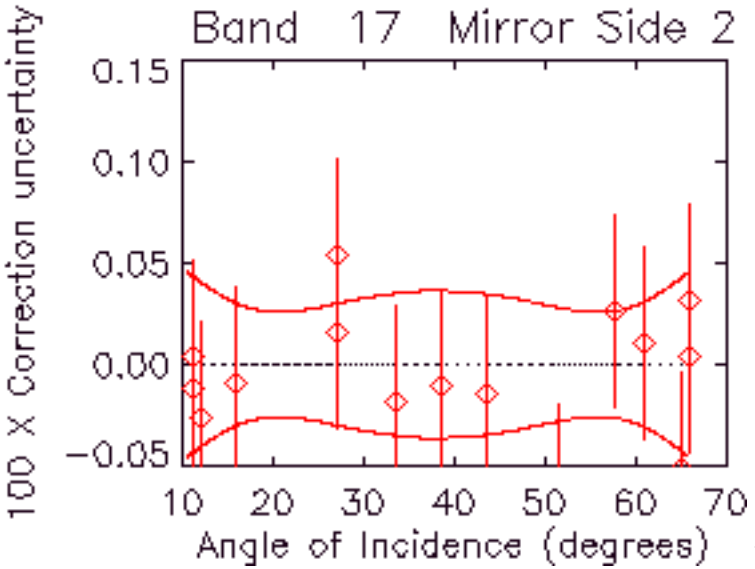
Band 17 Mirror Side 2
100 X Correction uncertainty
0.15
0.10
0.05
0.00
−0.05
10 20 30 40 50 60 70
Angle of Incidence (degrees)

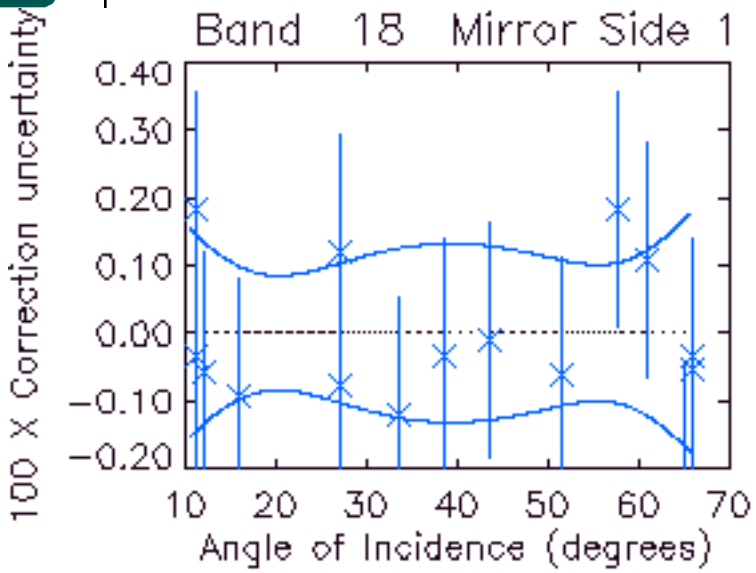
Band 18 Mirror Side 1
100 X Correction uncertainty
0.40
0.30
0.20
0.10
0.00
−0.10
−0.20
10 20 30 40 50 60 70
Angle of Incidence (degrees)

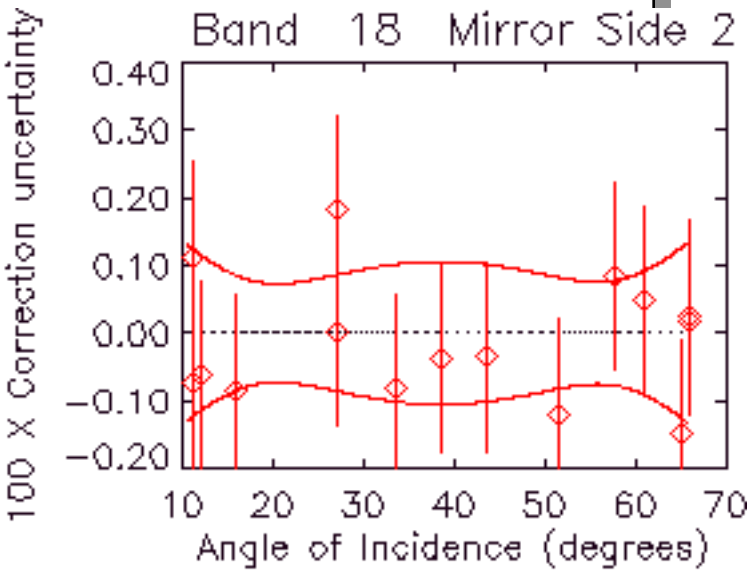
Band 18 Mirror Side 2
100 X Correction uncertainty
0.40
0.30
0.20
0.10
0.00
−0.10
−0.20
10 20 30 40 50 60 70
Angle of Incidence (degrees)

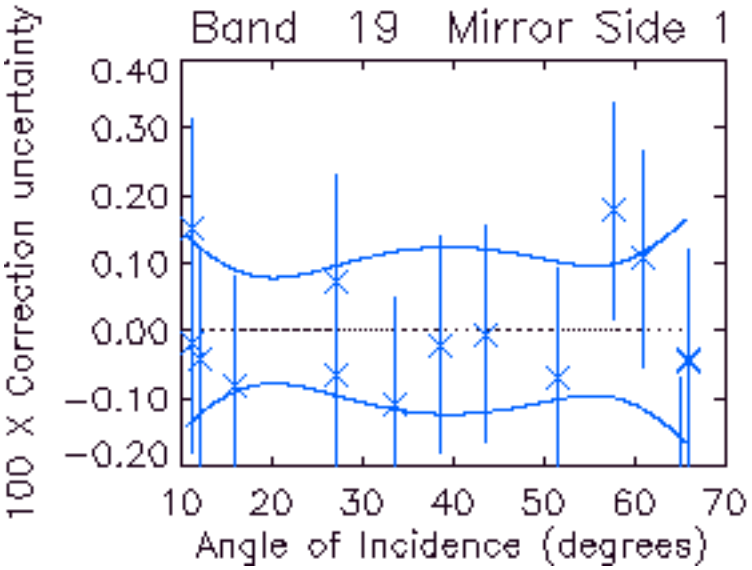
Band 19 Mirror Side 1
100 X Correction uncertainty
0.40
0.30
0.20
0.10
0.00
−0.10
−0.20
10 20 30 40 50 60 70
Angle of Incidence (degrees)

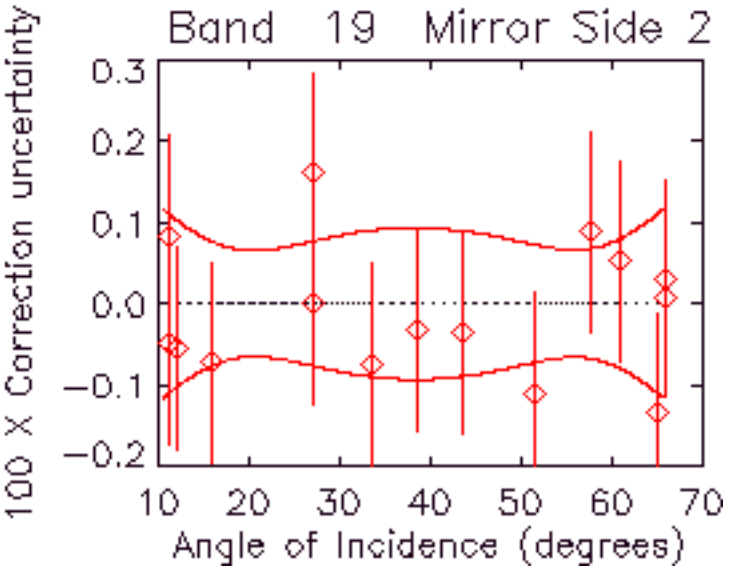
Band 19 Mirror Side 2
100 X Correction uncertainty
0.3
0.2
0.1
0.0
−0.1
−0.2
10 20 30 40 50 60 70
Angle of Incidence (degrees)

At a fixed AOI, dn versus detector (SBRS order)

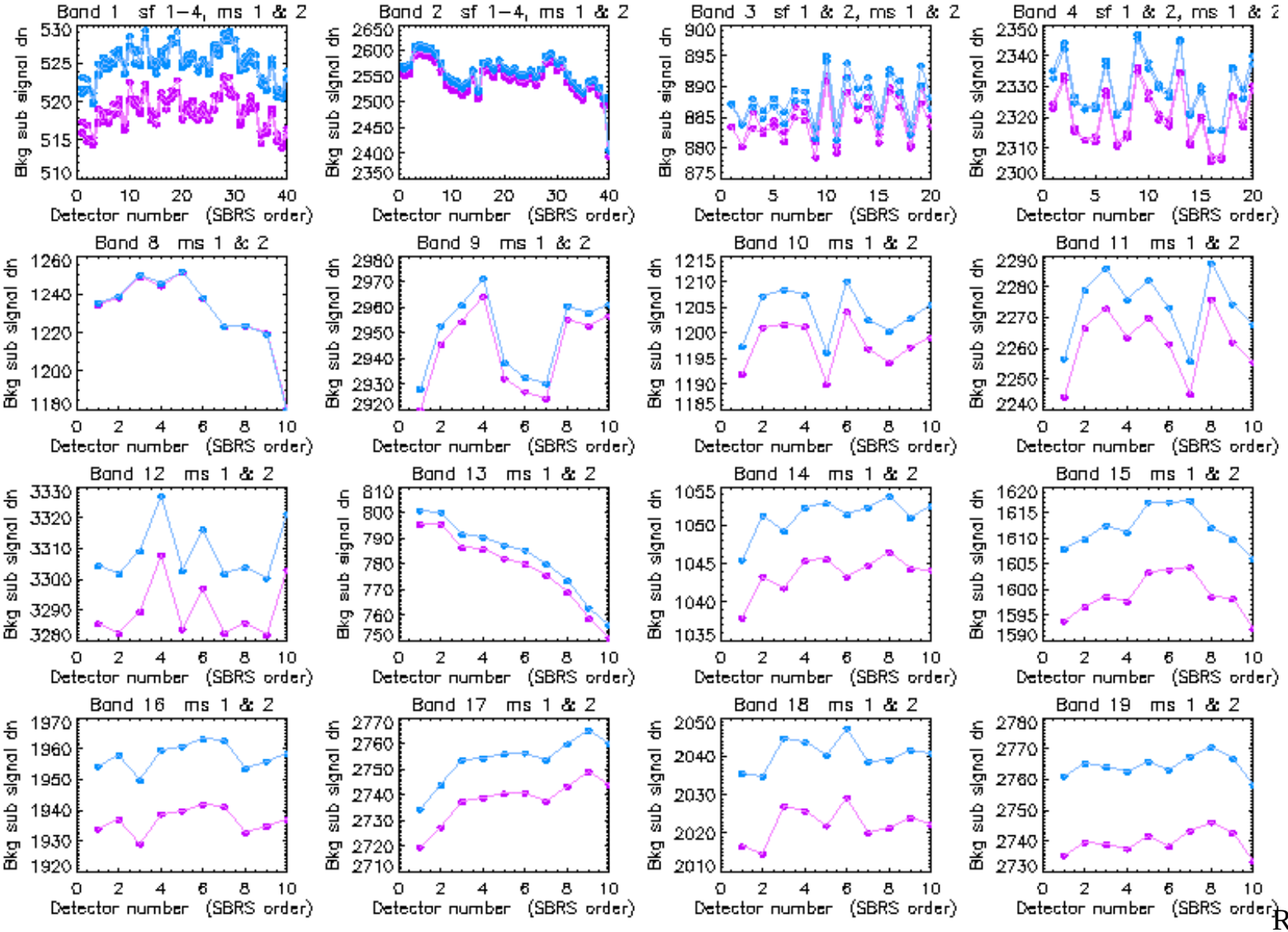

At fixed AOI, m1*dn versus detector number (SBRS order)

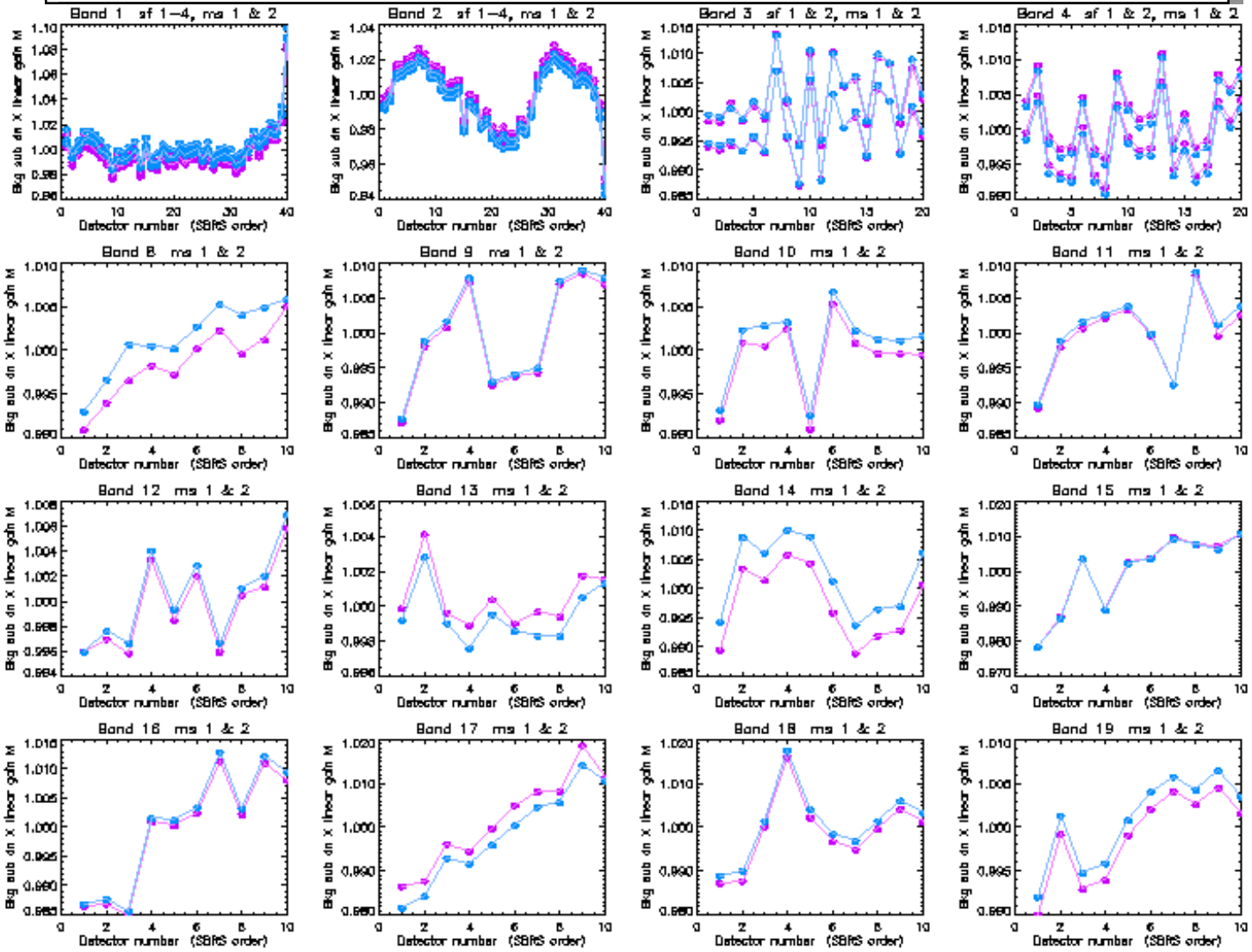

RSB RVS Summary

- Further on-orbit calibration will be carried out in light of the observed striping and the unphysical results of bands 8 and 9.
- Some of the pre-launch RVS data using SIS (100) as calibration source will be revisited, especially bands 8 and 9.
- Scene polarization effect will be discussed later.

MODIS TEB Response Versus Scan Angle (RVS) Status Report

MODIS Calibration Support Team,
June, 2000

TEB RVS Status Report

- Brief summary of Miami workshop, Feb. 1999
- What is new post-Miami
  - Physics test
  - Anomalous detector variation
  - Final pre-launch LUT for RVS
  - Nadir door scan results
  - Space view maneuver attempt

Summary of Miami Workshop

- RVS are believed to depend on Band and Mirror side only and no detector variance is expected on physical ground.
- NPL reflectance data for both polarization directions are available for both PFM and FM1.
- Only FM1 has usable high bay RVS system level measurements while PFM does not.
- Using theoretical result relating RVS to scan mirror reflectances and the fixed optics polarization parameter, an “identical twin strategy” was employed to combine PFM NPL data with FM1 fixed optics parameter to obtain PFM RVS.
- Scenes are assumed unpolarized throughout.
- Three sets of FM1 high bay RVS data were analyzed and all three sets were argued to have equal validity in determining RVS.
- Significant difference between averaged reflectance and system level RVS were observed for LWIR bands (29-31, in particular.)

Fixed optics parameter obtained by fitting RVS to $\frac{\rho_s + \rho_p}{2} + c_{fix} \frac{\rho_s - \rho_p}{2}$

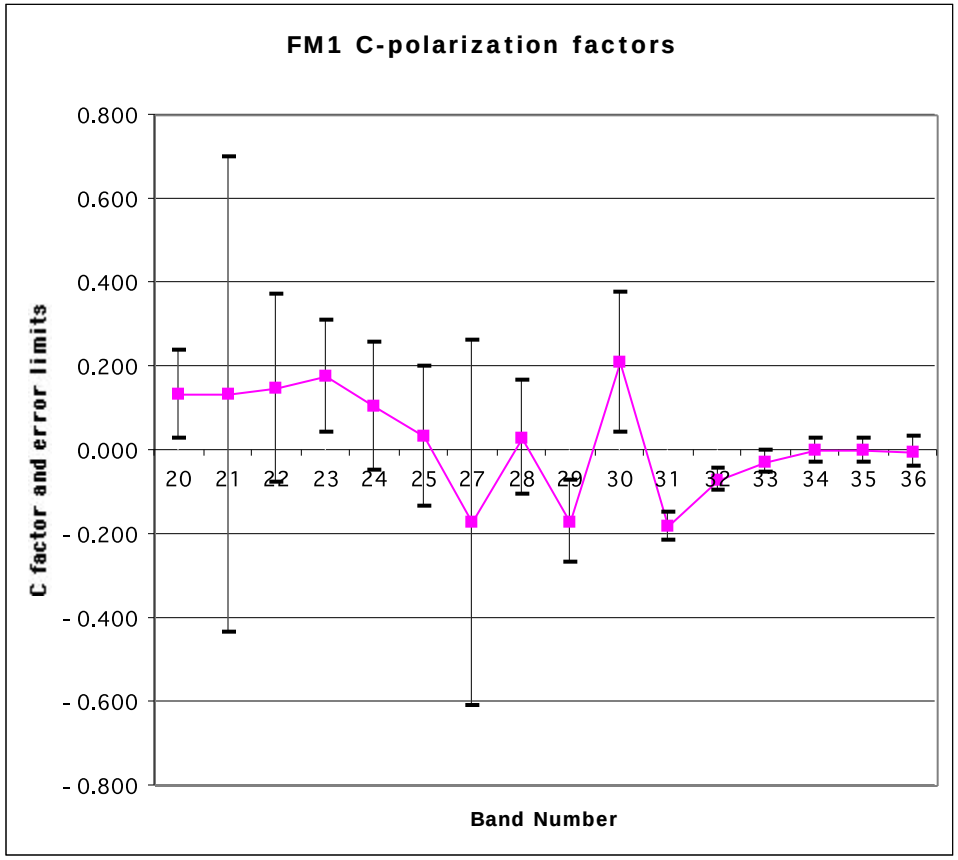

band	C_avg	c-low	c-high
20	0.134	0.028	0.240
21	0.133	-0.435	0.701
22	0.148	-0.075	0.370
23	0.177	0.044	0.311
24	0.104	-0.049	0.256
25	0.031	-0.135	0.198
27	-0.173	-0.609	0.263
28	0.030	-0.104	0.165
29	-0.170	-0.265	-0.074
30	0.209	0.044	0.375
31	-0.182	-0.215	-0.149
32	-0.069	-0.094	-0.044
33	-0.027	-0.051	-0.002
34	0.001	-0.027	0.029
35	-0.002	-0.031	0.027
36	-0.004	-0.040	0.032

Error due to neglect of polarization by setting Cfix=0

Miami charts on these used modeled Cfix instead of measured Cfix! Here what is presented is the results using the measured ones.

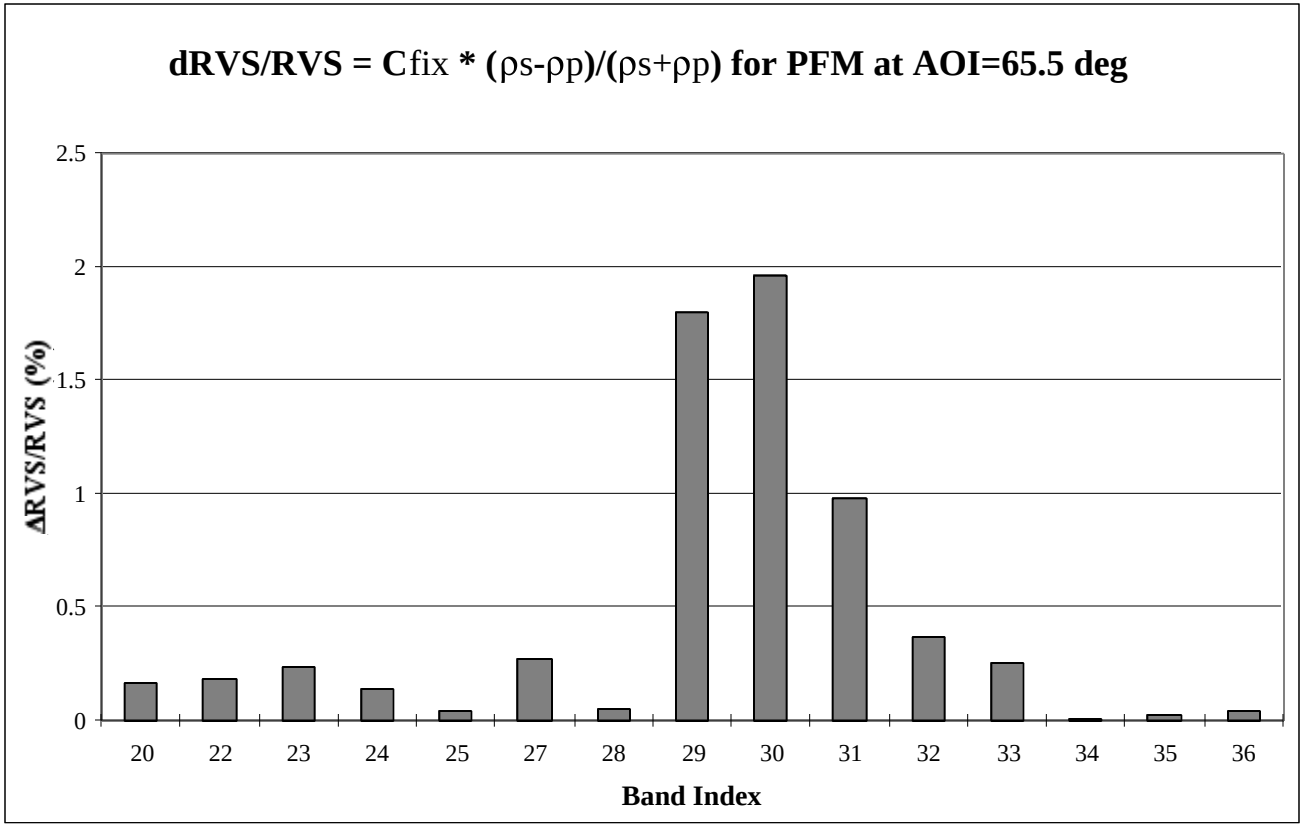

Decisions made in Miami workshop

NPL results may not provide good enough presentation for RVS due to the fixed optics polarization sensitivity and the scan mirror serving as a polarizer.

An "identical twin" strategy is used to combine the FM1 fixed optics parameter with the PFM NPL scan mirror reflectance measurement to obtain the RVS.

On-orbit RVS validation/measurement will be carried out.

What's New Since Miami

- **Insisting on getting the same dn when viewing the equivalent source led to revisiting the high bay RVS data.**
- **Atmospheric correction considered but situation was not improved. Arguments were presented to point to the inaccuracy of our estimate of atmospheric correction**
- **Anomalous detector variation were observed.**

Why test?

$$\frac{RVS_{bcs}}{RVS_{obc}} = \frac{dn_{bcs}}{dn_{obc}} \frac{t(l_{obc})L_{obc} - t(l_{svs})L_{svs}}{t(l_{bcs})L_{bcs} - t(l_{svs})L_{svs}}$$

Reminder:
Three blackbodies (BB) were used, one at earth view (EV) port denoted By bcs, one at space view port (SV) denoted by svs, and the on-board BB denoted by obc.
$t(l)$ are transmittance of light passing through a distance of l.
In thermal vacuum, t=1, we get back to our familiar equation

Using MODTRAN, t(l) calculated as in the following table:

Table for transmittance used

Band	$t(l_{obc}=0.754m)$	$t(l_{bcs}=1.77m)$	$t(l_{svs}=1.94m)$
20	1.000	1.000	1.000
21	1.000	1.000	1.000
22	1.000	1.000	1.000
23	1.000	1.000	1.000
24	0.997	0.994	0.993
25	0.999	0.999	0.999
27	0.805	0.691	0.677
28	0.949	0.907	0.902
29	1.000	0.999	0.999
30	1.000	1.000	1.000
31	1.000	1.000	1.000
32	1.000	1.000	1.000
33	0.998	0.996	0.996
34	0.998	0.995	0.994
35	0.995	0.989	0.988
36	0.987	0.971	0.968

RVS at AOI=26.5 degree should equal to RVS at -26.5 degree--physics test

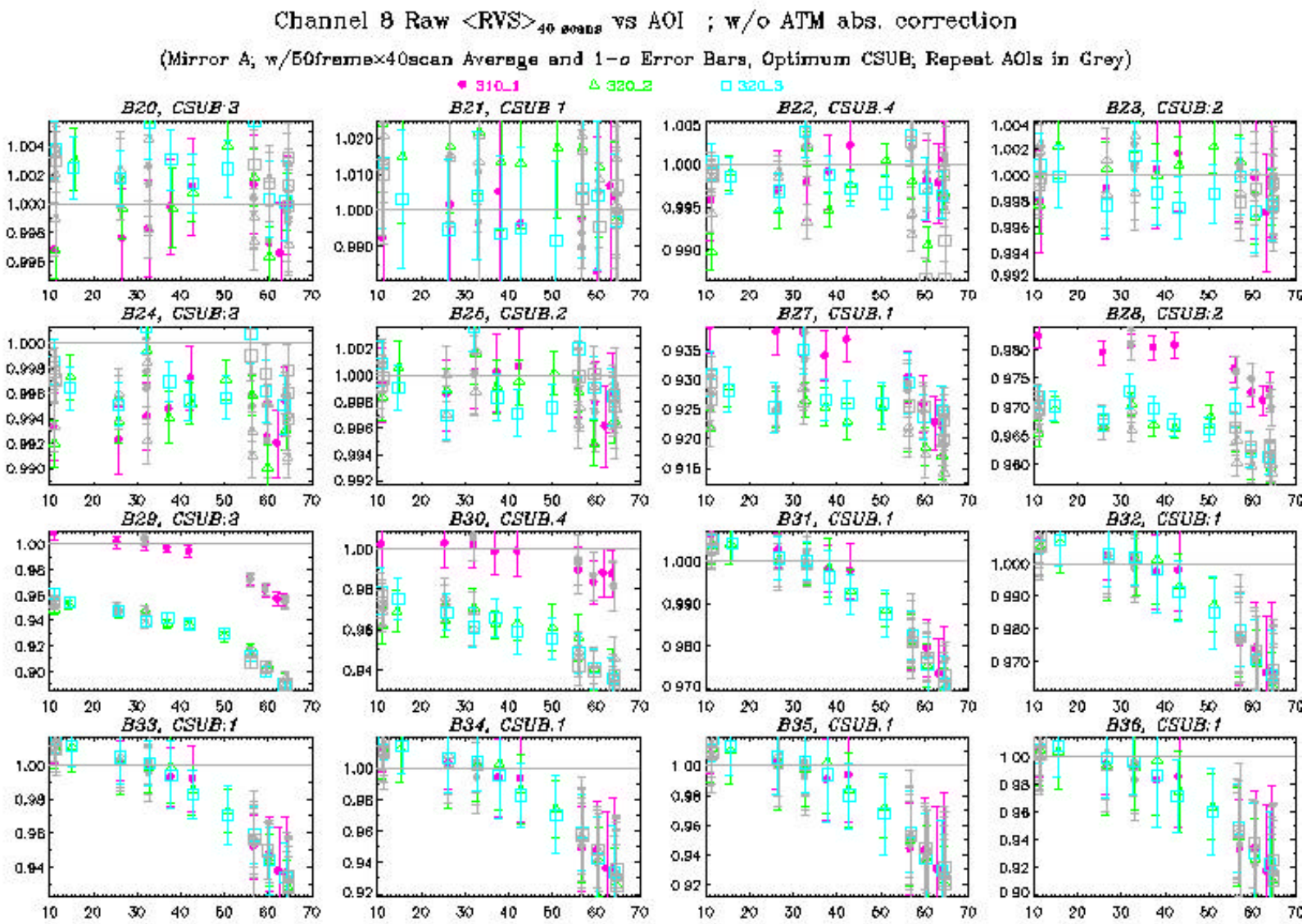

With atmospheric correction, things didn't improve

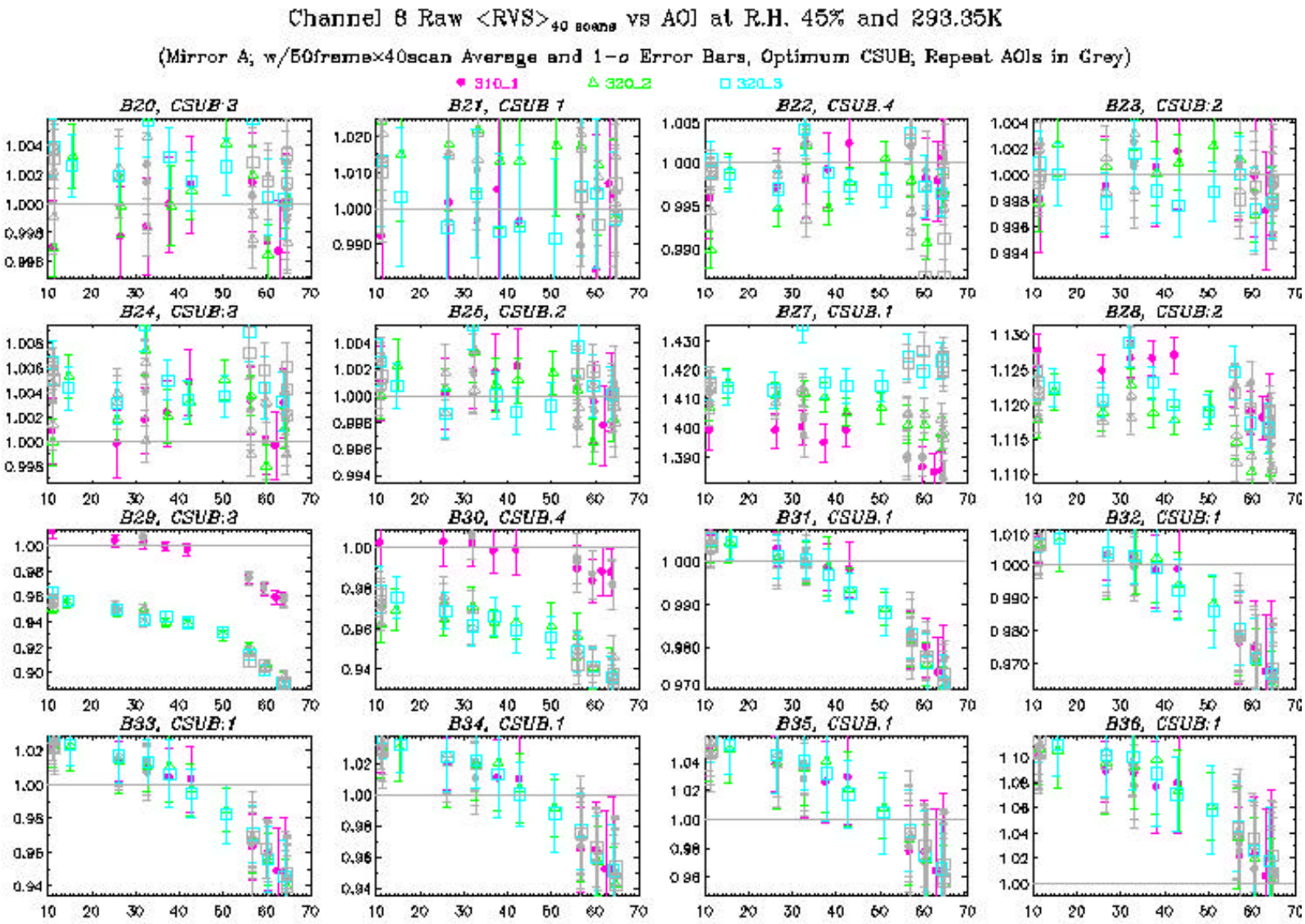

Anomalous detector variation in FM1 without atmospheric correction

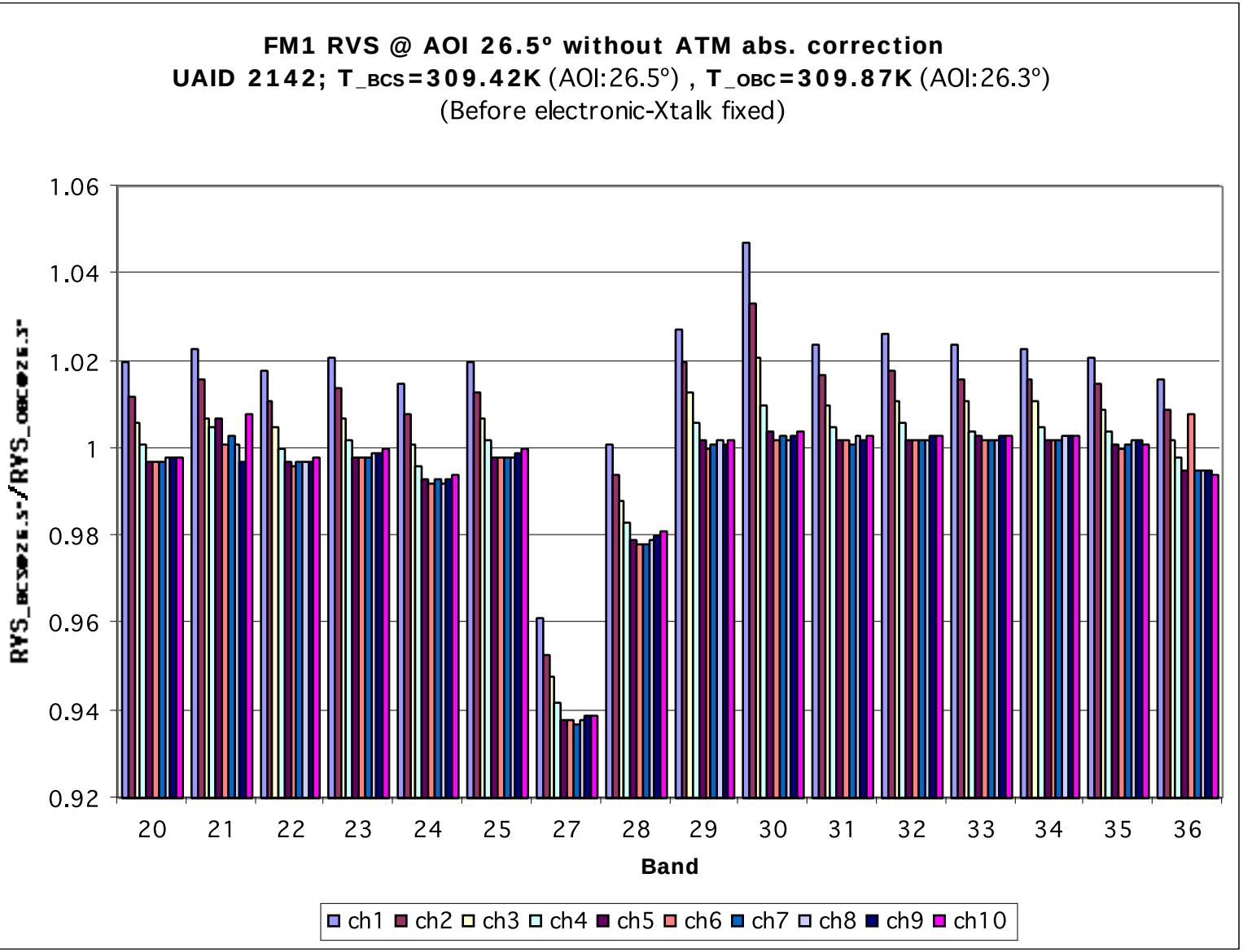

Anomalous detector variation in FM1 with atmospheric correction

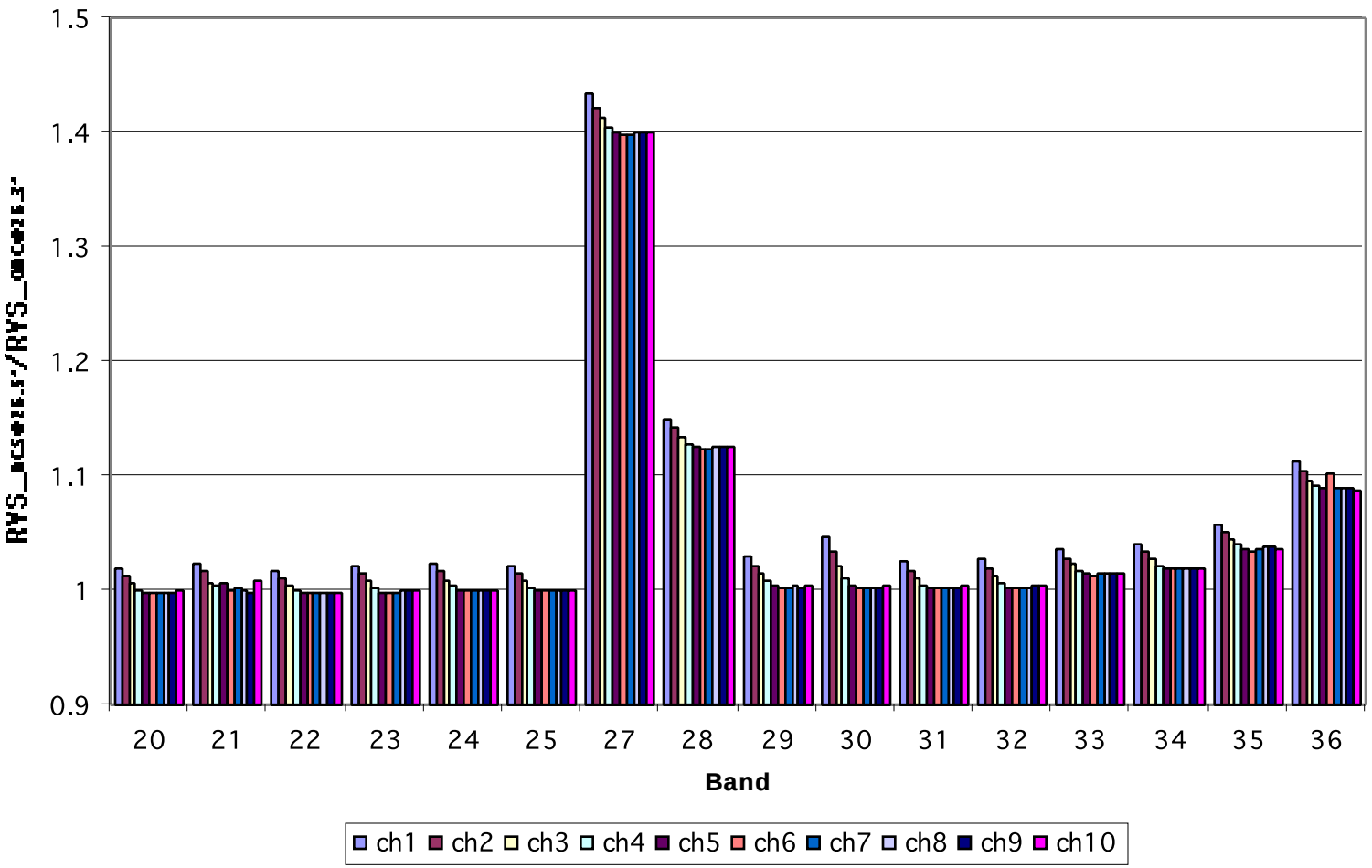

Decision made: for Band 27-30, use NPL data for both PFM and FM1

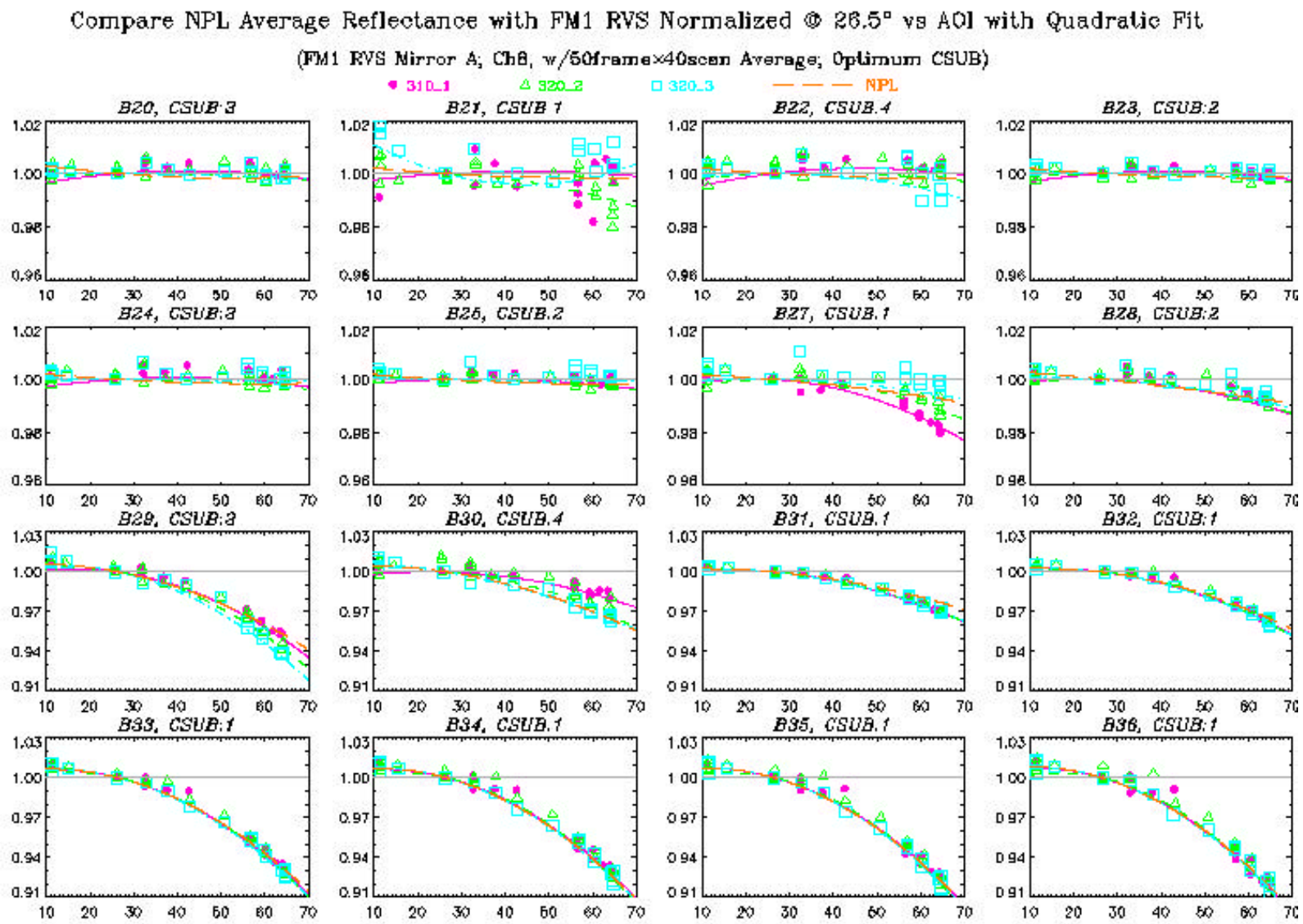

PFM pre-launch status summary

- For bands 27-30, NPL reflectance results on PFM scan mirror witness samples are used for RVS.
- For the rest of the thermal bands, RVS are obtained combining NPL results for PFM and the fixed optics parameters from FM1 high bay measurements. **NO** mirror side difference present.
- Some anomalous results showing up in FM1 high bay measurements are unresolved.
- **On-orbit RVS calibration strongly recommended**.

PFM RVS (TEB) On-Orbit Study

- Data Select and Temperature Retrieval
- RVS Equations
- RVS Mirror-side and Detector Differences
- Test the New Relative RVS
- Existing Problems

Data Select and Temperature Retrieval

- L1A granule before the Nadir door opened
  - L1A: A2000049.1610
  - Itwk/Vdet = 79/190 (at-launch configuration)
  - CFPA temperature: T_{SMIR} = 83.5K; T_{LWIR} = 83.0K
  - OBC BB temperature: 290K
- Brightness temperature of the EV Nadir door
  - T_{door} variation among TEB
  - T_{door} difference between mirror sides

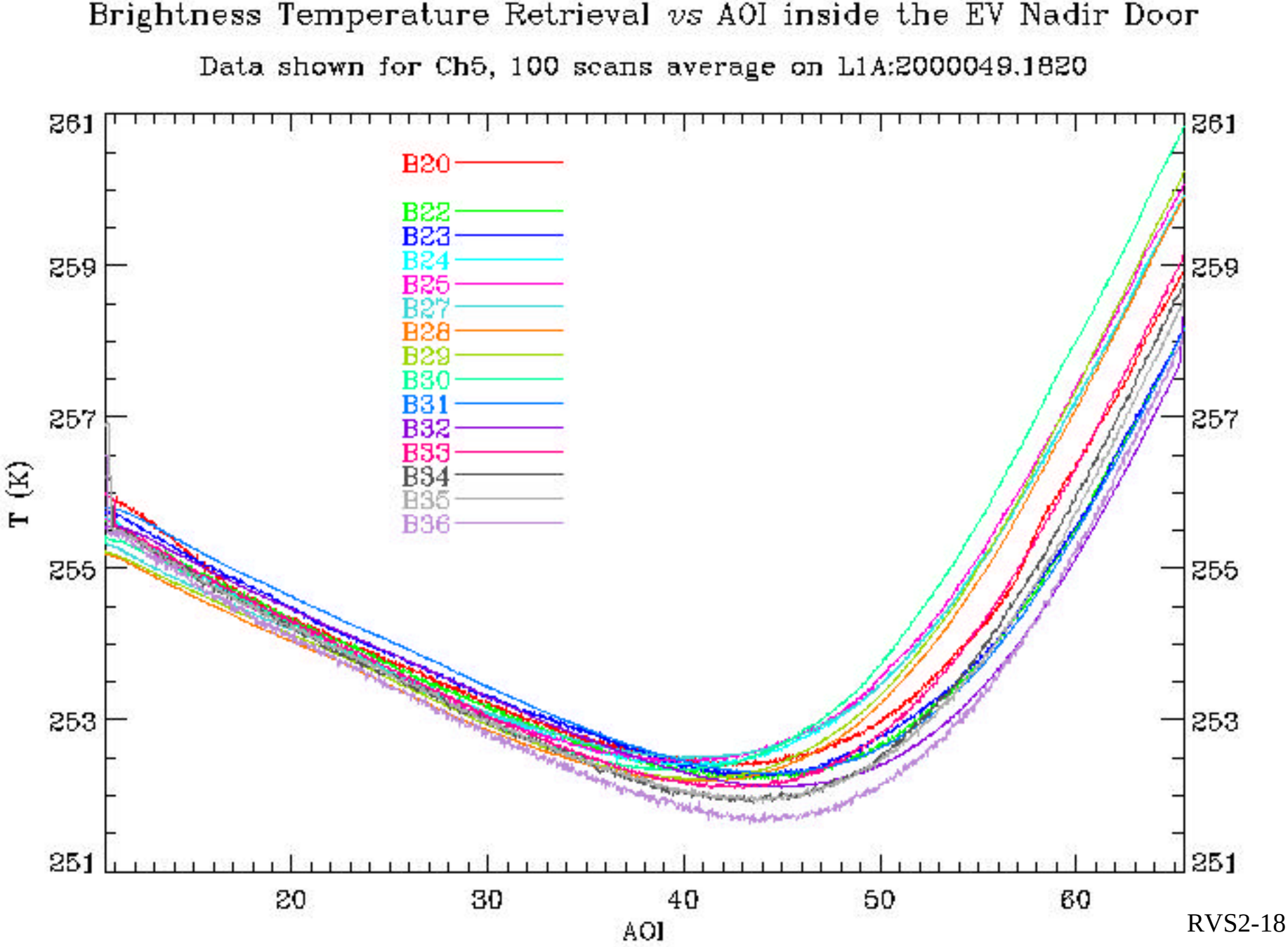
Brightness Temperature Retrieval vs AOI inside the EV Nadir Door
Data shown for Ch5, 100 scans average on L1A:2000049.1820
B20
B22
B23
B24
B25
B27
B28
B29
B30
B31
B32
B33
B34
B35
B36
T (K)
261
259
257
255
253
251
20
30
40
50
60
AOI

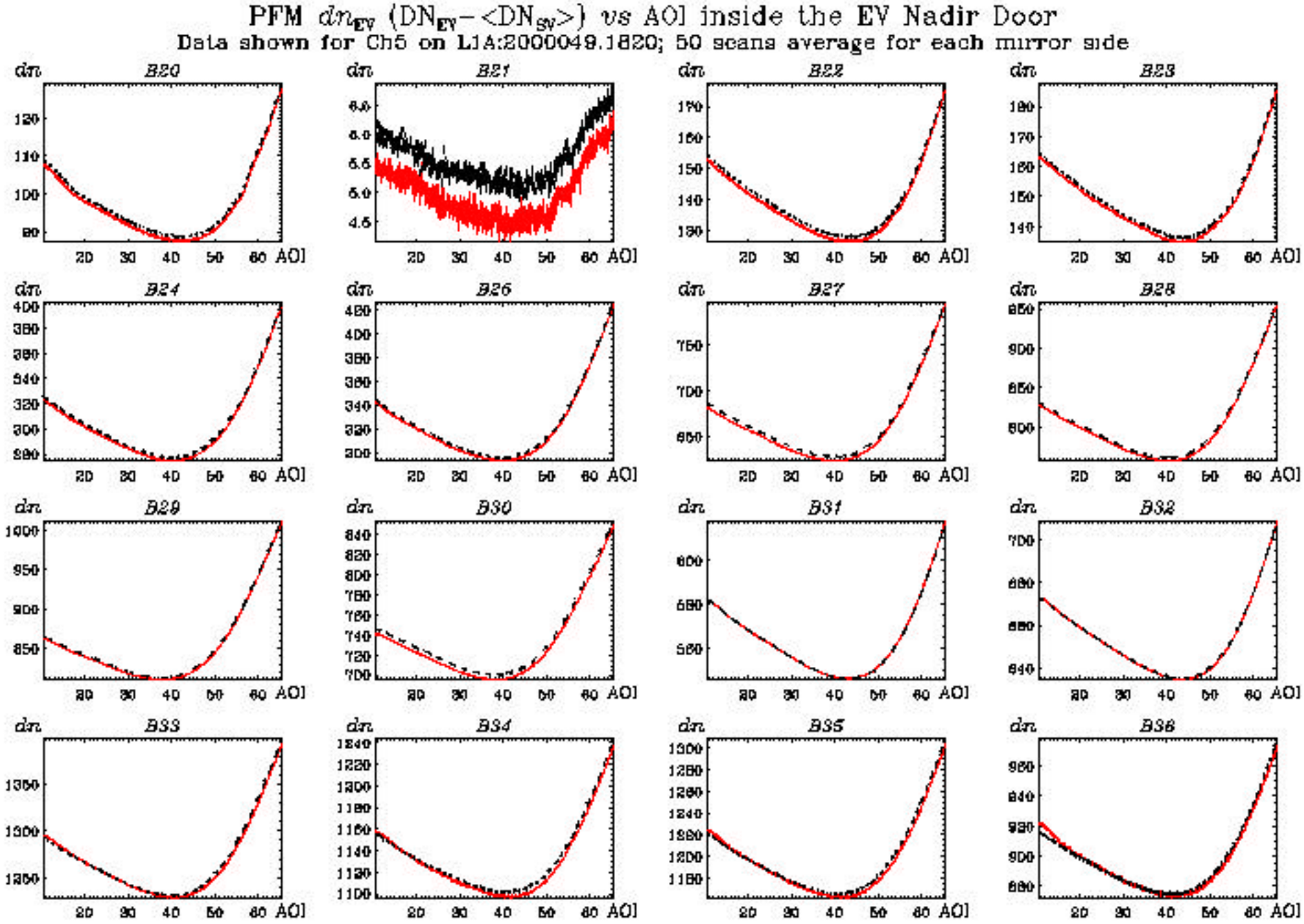
PFM dn_{EV} (DN_{EV} − <DN_{SV}>) vs AOI inside the EV Nadir Door
Data shown for Ch5 on L1A:2000049.1820; 50 scans average for each mirror side
dn
B20
B21
B22
B23
B24
B26
B27
B28
B29
B30
B31
B32
B33
B34
B35
B36
AOI
Mirror side 1
Mirror side 2

Brightness Temperature Retrieval *vs* AOI inside the EV Nadir Door

Data shown for Ch5 on L1A:2000049.1820; 50 scans average for each mirror side

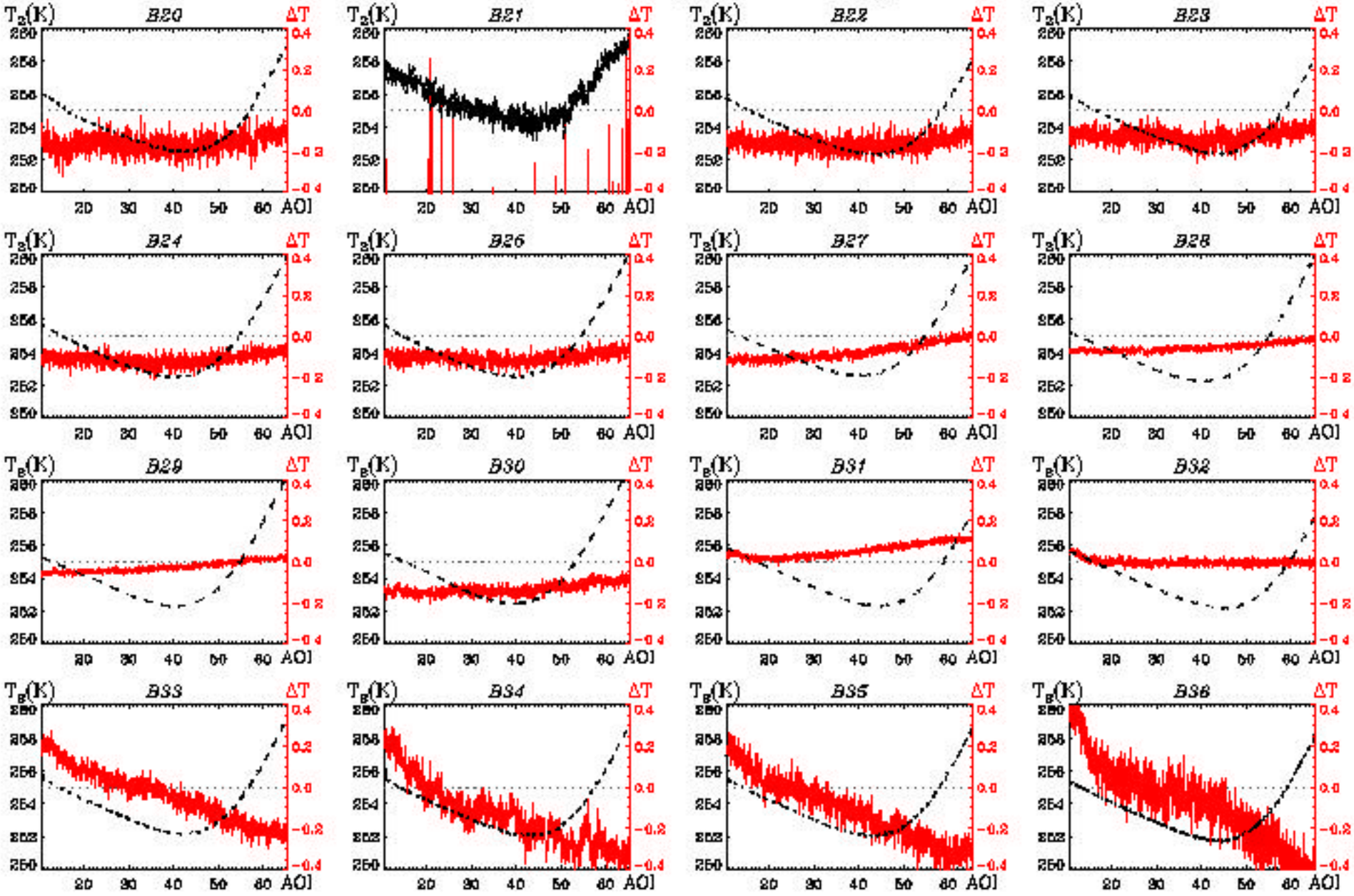

RVS Equations

The EV TEB radiance retrieval is band(B), detector(D), and mirror(M) dependent:

$$L_{EV}(\theta) = \frac{1}{RVS_{EV}(\theta)} \left\{ \left[a_0 + b_1 \ dn_{EV}(\theta) + a_2 \ dn_{EV}^2(\theta) \right] - \left[RVS_{SV} - RVS_{EV}(\theta) \right] \ L_{SM} \right\}$$

For every scan mirror rotation, let $L_{side1}(\theta) = L_{side2}(\theta)$. The mirror side 1 RVS relative to side 2 can be retrieved for each detector:

$$RVS_{EV}(\theta)_{side1} = \frac{a_0 + b_1 \ dn_{EV}(\theta) + a_2 \ dn_{EV}^2(\theta) - RVS_{SV} \ L_{SM}}{L_{EV}(\theta)_{side2} - L_{SM}}$$

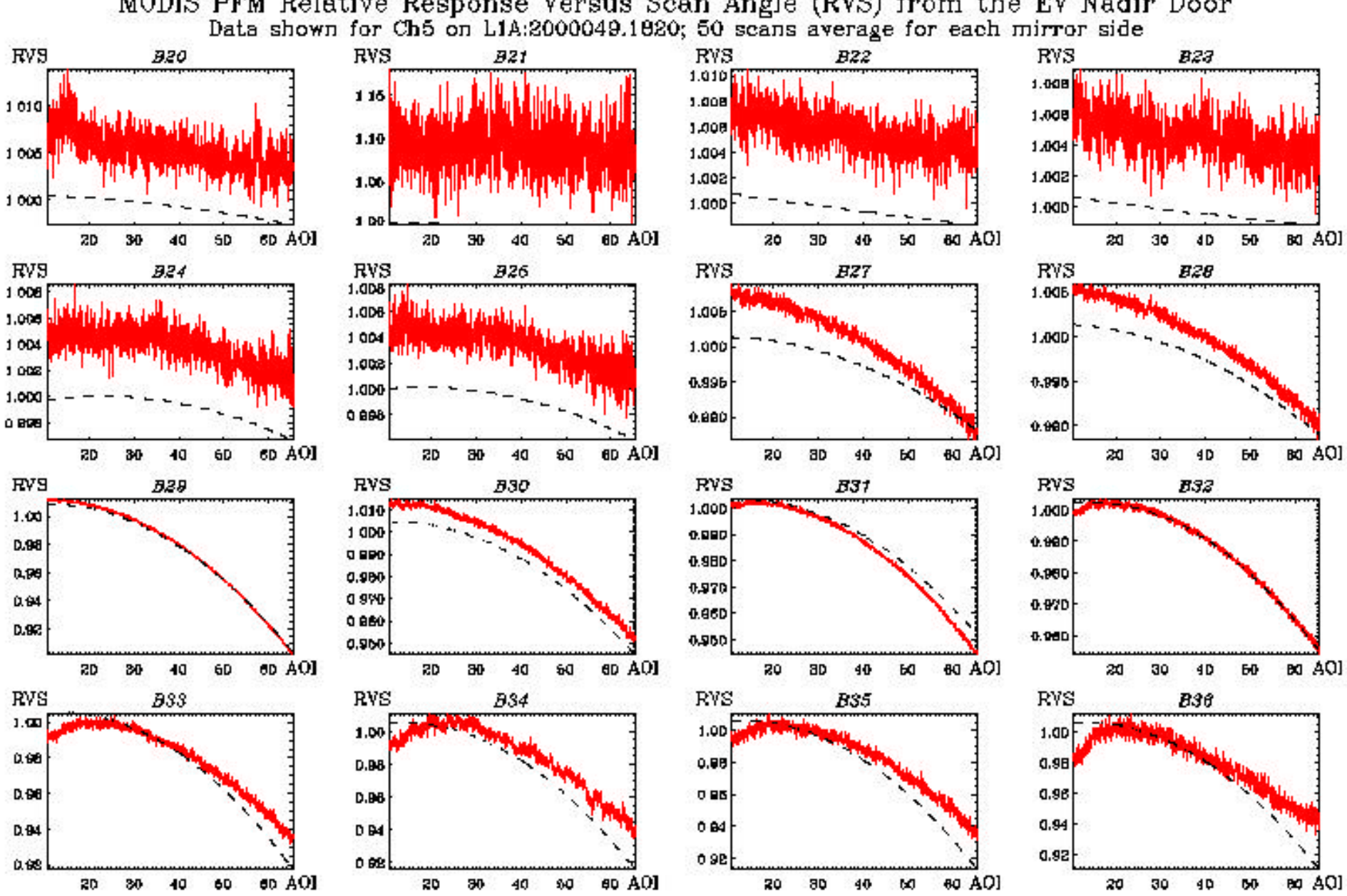
MODIS PFM Relative Response Versus Scan Angle (RVS) from the EV Nadir Door
Data shown for Ch5 on L1A:2000049.1920; 50 scans average for each mirror side
RVS
B20
B21
B22
B23
B24
B26
B27
B28
B29
B30
B31
B32
B33
B34
B35
B36
AOI
Mirror side 1
Mirror side 2

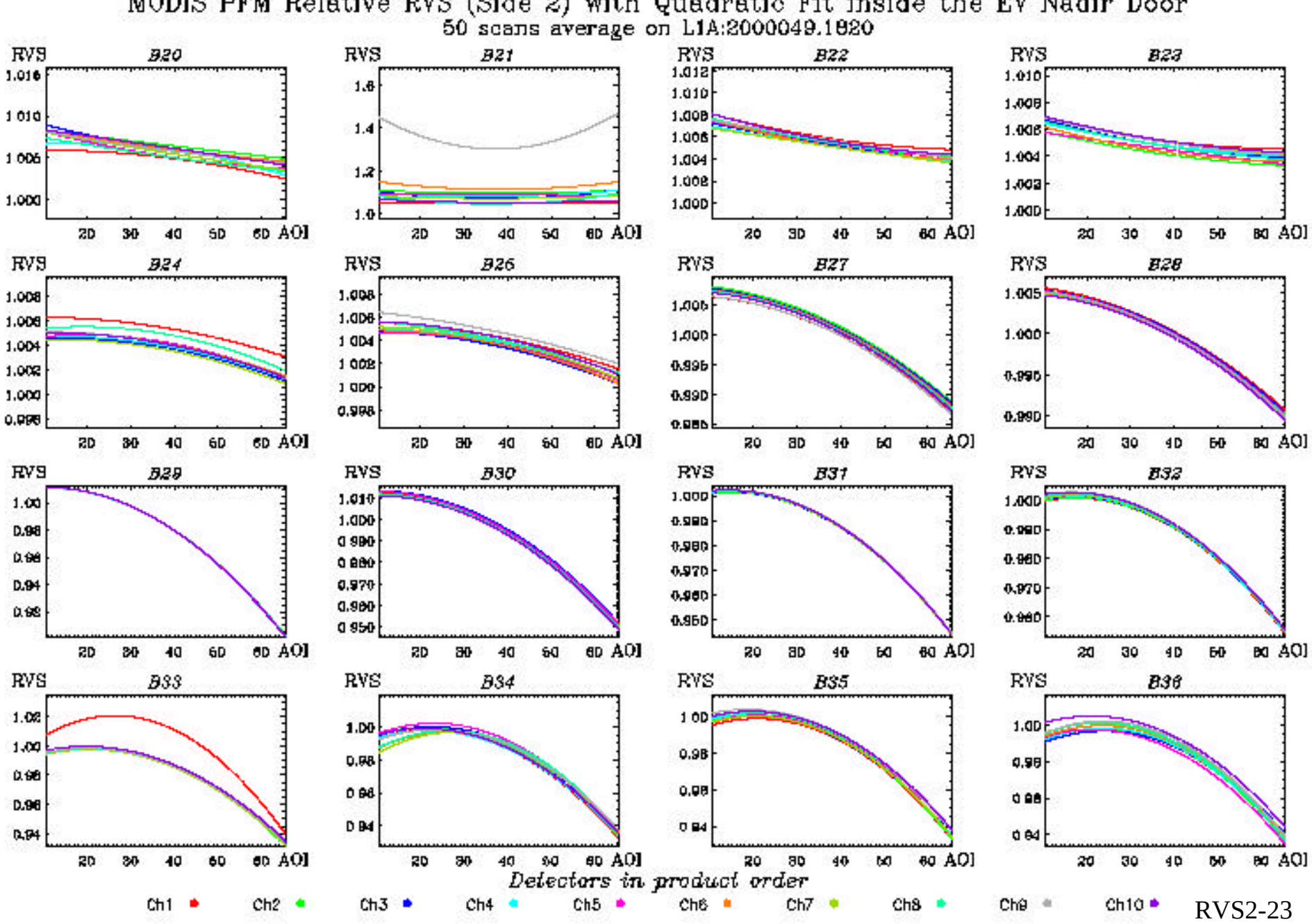
MODIS PFM Relative RVS (Side 2) with Quadratic Fit inside the EV Nadir Door
50 scans average on L1A:2000049.1920
RVS
B20
B21
B22
B23
B24
B26
B27
B28
B29
B30
B31
B32
B33
B34
B35
B36
AOI
Detectors in product order
Ch1
Ch2
Ch3
Ch4
Ch5
Ch6
Ch7
Ch8
Ch9
Ch10

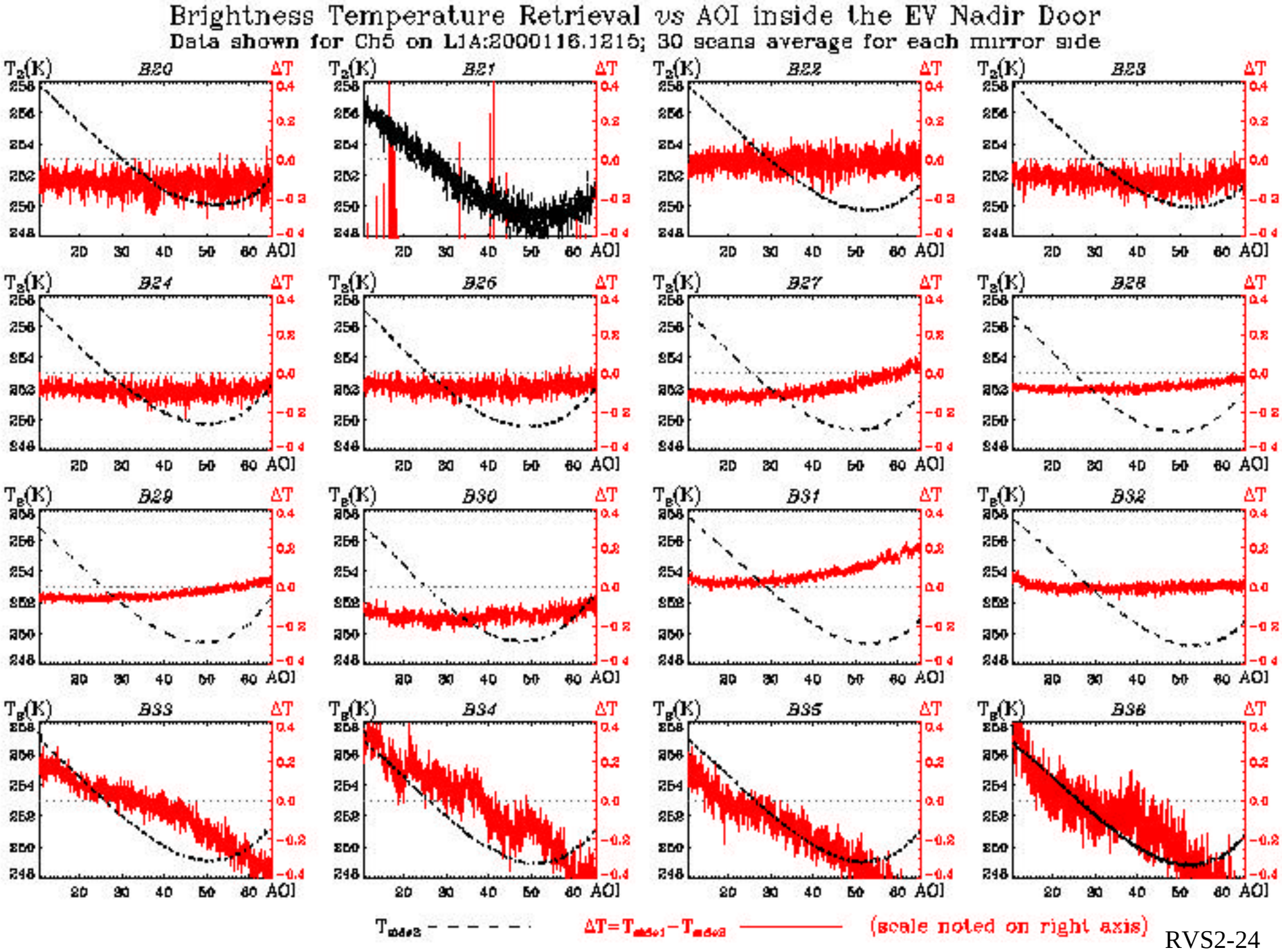
Brightness Temperature Retrieval vs AOI inside the EV Nadir Door
Data shown for Ch5 on L1A:2000116.1215; 30 scans average for each mirror side
B20
B21
B22
B23
B24
B26
B27
B28
B29
B30
B31
B32
B33
B34
B35
B36
T_B(K)
ΔT
AOI
T_side2
ΔT=T_side1−T_side2
(scale noted on right axis)

Existing Problems

- Only relative mirror side RVS
- Limited information on the spectral emissivity
- Unknown mirror side behavior near BOS
- Deep Space Maneuver Needed

Deep Space Maneuver, methodology

$$RVS(\theta_{ev}) = 1 - \left(\frac{L_{bb}}{P(T_{sm})}\right)\left(\frac{dn_{ev} - dn_{ev@bb}}{dn_{bb} - dn_{ev@bb}}\right)$$

This is the final normalized RVS retrieval equation for the entire EV sector, where the variables in the equation is summarized below:

- L_{bb} – the radiance from the OBC BB
- $P(T_{sm})$ – the Planck function at scan mirror temperature
- dn_{ev} – the Earth view sector digital number when viewing cold space, and $dn_{ev@bb}$ is the dn_{ev} when scan angle equals to the OBC BB viewing angle.
- dn_{bb} – the digital number when MODIS viewing the OBC BB.

Error due to NEdN

$$\frac{\delta RVS}{RVS}(\theta_{ev}) = \frac{\left(\frac{L_{bb}}{P(T_{sm})}\right)\frac{2NEdN}{|dn_{bb} - dn_{ev@bb}|}\sqrt{1+\left(\frac{dn_{ev} - dn_{ev@bb}}{dn_{bb} - dn_{ev@bb}}\right)^2}}{1 - \left(\frac{L_{bb}}{P(T_{sm})}\right)\frac{dn_{ev} - dn_{ev@bb}}{dn_{bb} - dn_{ev@bb}}}$$

$$\approx \frac{\left(\frac{L_{bb}}{P(T_{sm})}\right)\frac{2NEdN}{|dn_{bb} - dn_{ev@bb}|}}{1 - \left(\frac{L_{bb}}{P(T_{sm})}\right)\frac{dn_{ev} - dn_{ev@bb}}{dn_{bb} - dn_{ev@bb}}}$$

This may NOT be a large number! $\approx \frac{2NEdN}{|dn_{bb} - dn_{ev@bb}|}$ when $T_{bb}=T_{sm}$

Deep space maneuver summary

- Relative error bar is estimated to be

$$\approx \frac{2\,NEdN}{\left|dn_{bb} - dn_{ev@bb}\right|}$$

- Theoretical estimate of error bar only considers detector noise.
- Theoretical results rely strongly on the ansatz that RVS(-AOI)=RVS(AOI).

Issues related to striping

- When scene is polarized, there will be an error in RVS in all AOI. This so far is not captured in our calibration algorithm. The following assessment assume that scene is un-polarized.
- If RVS indeed is detector independent, as is expected on physical ground, the error in RVS **alone** will not cause striping. *(It is possible that we missed something in our calibration algorithm due to lack of understanding of the instrument physics, that RVS in fact is detector dependent and RVS(-26.5) is different from RVS(26.5).)*
- If there is error in RVS, the error will be minimum at the normalization angle (AOI=AOI of BB for TEB and AOI=AOI of SD for RSB).
- Combining RVS error with **un-calibrated** variations in detector gains **will result in striping** which generally increase as AOI increases.
- On-orbit data support our pre-launch conclusion that RVS need to be further calibrated.

Earth Remote Sensor Polarization Effects on Calibration Accuracy

Modis Calibration Support Team

June, 2000

Outline

- Introduction
- Polarization Formalism
- Polarized Response Versus Scan Angle (RVS) for parallel scanners like MODIS.
- Parametric studies for parallel scanners for protected silver coated scan mirror sensors.
- Polarization data (PC08) analysis report.
- Summary

Polarization of SiO_x Protected Silver-coated Scan Mirrors

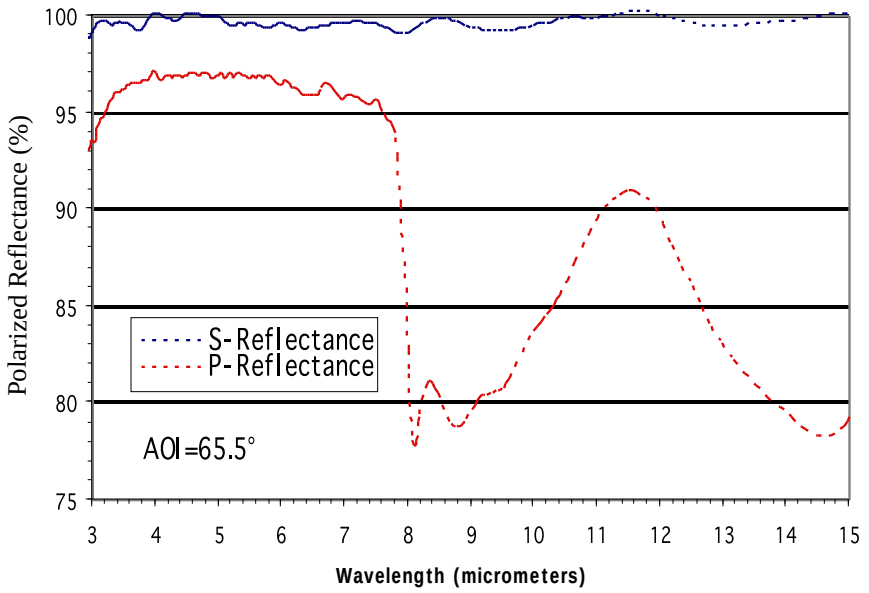

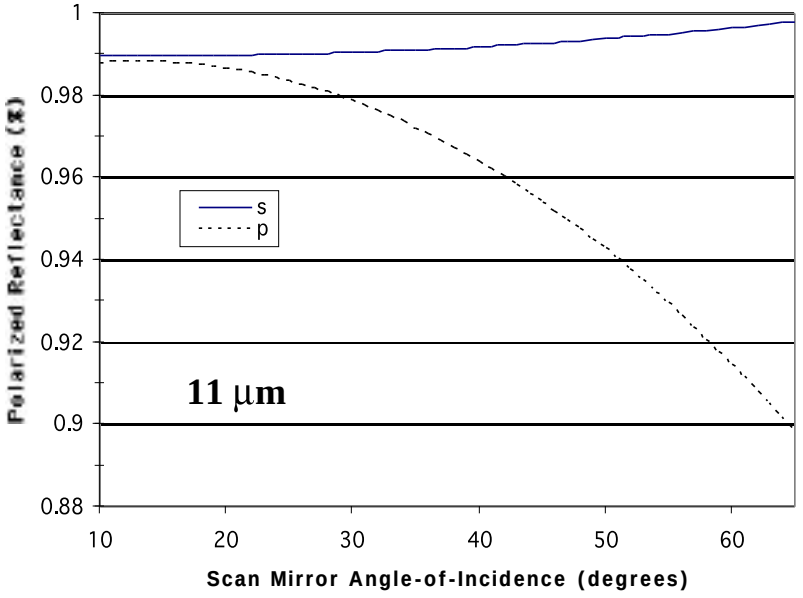

Polarized reflectances at 65.5 degree angle-of-incidence for the MODIS ProtoFlight Model silver coated scan mirror protected with SiO_x coating produced by Denton Inc. Measurements courtesy of British National Physical Laboratories.

General Formalism for Single Optical Element Relay of Polarized Light

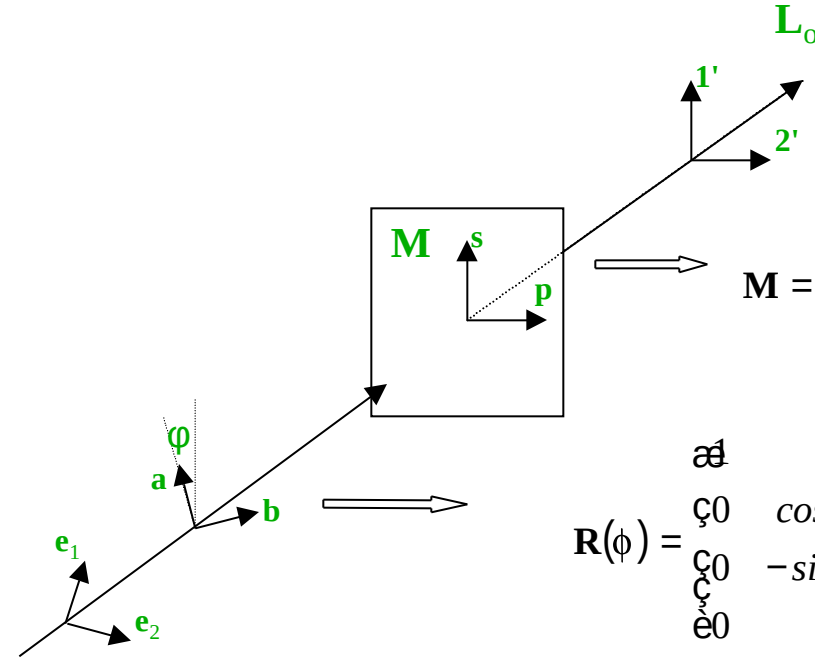

$$\mathbf{L}_{out}(\mathbf{s},\mathbf{p}) = \mathbf{M}\ \mathbf{R}(\phi)\ \mathbf{L}_{in}(\mathbf{a},\mathbf{b})$$

$$\mathbf{M} = \frac{1}{2}\begin{pmatrix} q+r & q-r & 0 & 0 \\ q-r & q+r & 0 & 0 \\ 0 & 0 & \pm 2\sqrt{qr} & 0 \\ 0 & 0 & 0 & \pm 2\sqrt{qr} \end{pmatrix}$$

Optical element Mueller Matrix
(+ sign for transmittance;
- sign for reflectance)

$$\mathbf{R}(\phi) = \begin{pmatrix} 1 & 0 & 0 & 0 \\ 0 & \cos(2\phi) & \sin(2\phi) & 0 \\ 0 & -\sin(2\phi) & \cos(2\phi) & 0 \\ 0 & 0 & 0 & 1 \end{pmatrix}$$

Rotation Matrix to rotate
the incident ray (**a**,**b**) into
the optical element coordinate (**s**,**p**)

$$\mathbf{L}_{in} = \begin{pmatrix} L_1 + L_2 \\ L_1 - L_2 \\ 2\sqrt{L_1 L_2}\cos(\delta_2 - \delta_1) \\ 2\sqrt{L_1 L_2}\sin(\delta_2 - \delta_1) \end{pmatrix} \Rightarrow \mathbf{L}_{in} = \begin{pmatrix} L_a + L_b \\ L_a - L_b \\ 0 \\ L_3 \end{pmatrix}$$

$$f = \frac{L_a - L_b}{L_a + L_b}$$

Incoming polarized light ray represented by a Stokes vector in an arbitrary coordinate System ($\mathbf{e}_1$,$\mathbf{e}_2$)

Same Incoming polarized light ray represented by a Stokes vector in the scene preferred coordinate system **(a,b)**

Polarization factor:
define the degree of polarization of the scene

Polarization Formalism Applied to a Multiple Optical Element System

$$\mathbf{L}_D = \left[(\mathbf{M}_n \ \mathbf{R}_n)\cdots(\mathbf{M}_2 \ \mathbf{R}_2)\right] \ \mathbf{R}_{sm}(\psi) \left[\mathbf{M}_{sm}(\rho_s,\rho_p) \ \mathbf{R}_{sm}(\phi)\right] \ \mathbf{L}_{in}$$

$$\equiv \mathbf{A} \ \mathbf{R}_{sm}(\psi) \left[\mathbf{M}_{sm}(\rho_s,\rho_p) \ \mathbf{R}_{sm}(\phi)\right] \mathbf{L}_{in}$$

where,

$$\mathbf{A} = \left[(\mathbf{M}_n \ \mathbf{R}_n)\cdots(\mathbf{M}_2 \ \mathbf{R}_2)\right]$$

is the fixed optics Mueller matrix, and $\mathbf{R}_{sm}(\psi)$ is required to rotate the **s** and **p** directions of the scan mirror into a set of fixed coordinates, such that the fixed optics Mueller matrices are scan angle independent. The final at-detector signal is

$$S = \mathbf{D}^T \ \mathbf{L}_D = \mathbf{D}^T \ \mathbf{A} \ \mathbf{R}_{sm}(\psi) \left[\mathbf{M}_{sm} \ \mathbf{R}_{sm}(\phi)\right] \mathbf{L}_{in}$$

where $\mathbf{D}^T$ is the transposed detector vector. By defining the system level *R*esponse *V*ersus *S*can-angle (RVS) vector as

$$\mathbf{RVS}(\theta,\phi) = \mathbf{D}^T \ \mathbf{A} \ \mathbf{R}_{sm}(\psi) \ \mathbf{M}_{sm} \ \mathbf{R}_{sm}(\phi)$$

Then, the at-detector signal becomes

$$S = \mathbf{RVS}(\theta,\phi) \ \mathbf{L}_{in}(\mathbf{a},\mathbf{b})$$

$$= RVS_0(\theta,\phi) \ (L_a + L_b) + RVS_1(\theta,\phi) \ (L_a - L_b)$$

$$= RVS_{eff}(\theta,\phi) \ (L_a + L_b)$$

$$\equiv RVS_{eff}(\theta,\phi) \ L$$

L = total scene radiance
RVS_{eff} = effective RVS

where $RVS_{eff}(\theta,\phi) = RVS_0(\theta,\phi) + RVS_1(\theta,\phi) \ f$ and $f = (L_a - L_b)/(L_a + L_b)$

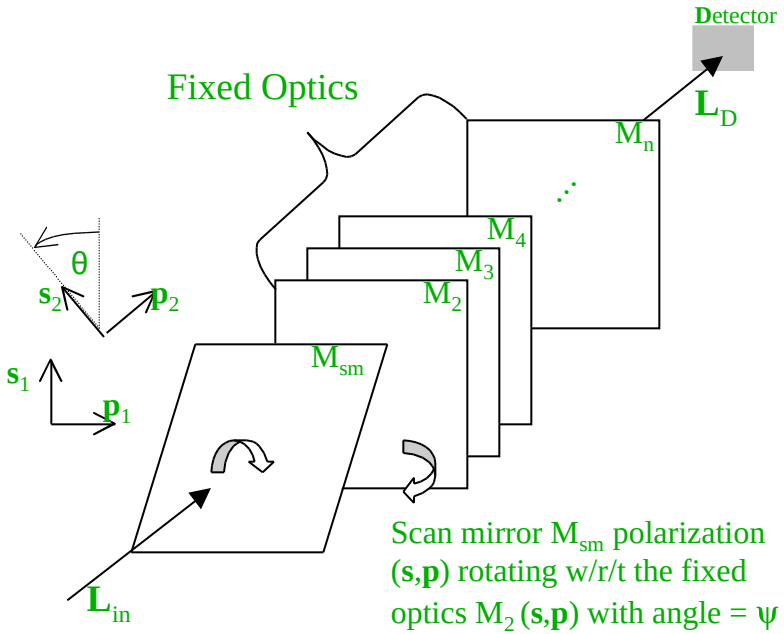

Scan mirror M_{sm} polarization (**s**,**p**) rotating w/r/t the fixed optics M_2 (**s**,**p**) with angle = ψ

M_{sm} is a rotating Scan Mirror with rotational angle =θ.

RVS Formalism for Parallel Scanner (1)

For a parallel scanner: $\mathbf{R}_{sm}(\psi = 0) = \mathbf{I}$,

thus $\mathbf{RVS}_{para}(\theta) = \mathbf{D}^{T}\ \mathbf{A}\ \mathbf{M}_{sm}\left(\rho_s(\theta), \rho_p(\theta)\right)\ \mathbf{R}(\phi)$

and

$$RVS^{0}_{para}(\theta,\phi) = \tau\ \frac{\rho_s(\theta) + \rho_p(\theta)}{2} + \eta\ \frac{\rho_s(\theta) - \rho_p(\theta)}{2}$$

$$RVS^{1}_{para}(\theta,\phi) = \left[\tau\ \frac{\rho_s(\theta) - \rho_p(\theta)}{2} + \eta\ \frac{\rho_s(\theta) + \rho_p(\theta)}{2}\right] \cos(2\phi) + \sigma\sqrt{\rho_s(\theta)\rho_p(\theta)}\sin(2\phi)$$

where $\tau = D_i\ A_{i0}$ is the fixed-optics total throughput (or optical efficiency)

and $\eta = D_i\ A_{i1}$, $\sigma = D_i\ A_{i2}$ are fixed-optics polarization parameter

and $\rho_s(\theta)$, $\rho_p(\theta)$ are the scan mirror s and p reflectivity components

and $RVS_{eff}(\theta,\phi) = RVS^{0}_{para}(\theta,\phi) + RVS^{1}_{para}(\theta,\phi)\ \ f$ is the final effective system RVS

RVS Formalism for a Parallel Scanner (2)

Parallel Scanner:

Scan swath plane || incident plane

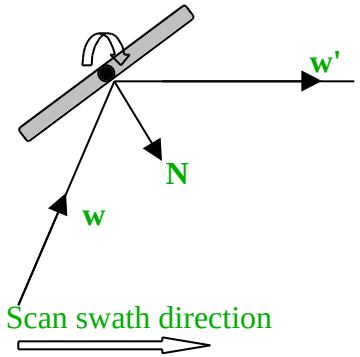

For a parallel scanner: $\phi = 0$, $\mathbf{R}_{sm}(\phi = 0) = \mathbf{I}$

thus $\mathbf{RVS}_{para}(\theta) = \mathbf{D}^{T}\ \mathbf{A}\ \mathbf{M}_{sm}(\rho_s(\theta), \rho_p(\theta))$

and

$$RVS^{0}_{para}(\theta) = \tau\ \frac{\rho_s(\theta) + \rho_p(\theta)}{2} + \eta\ \frac{\rho_s(\theta) - \rho_p(\theta)}{2}$$

$$RVS^{1}_{para}(\theta) = \tau\ \frac{\rho_s(\theta) - \rho_p(\theta)}{2} + \eta\ \frac{\rho_s(\theta) + \rho_p(\theta)}{2}$$

$$RVS_{eff}(\theta) = RVS^{0}_{para}(\theta) + RVS^{1}_{para}(\theta)\ \ f$$

Conclusion: The parallel scanner RVS depends on the scan angle θ through the scan mirror polarized reflectivities ($\rho_s(\theta)$, $\rho_p(\theta)$). For an unpolarized scene (i.e., f=0), the fixed-optics polarization (i.e., $\eta \neq 0$) contributes to the system RVS for a polarized scan mirror (i.e., $\rho_s \neq \rho_p$), but does not for an unpolarized scan mirror (i.e., $\rho_s = \rho_p$), Therefore, the sensor RVS function cannot be determined by simply measuring the scan mirror average reflectivity, unless the fixed-optics polarization is near zero (i.e., $\eta = 0$), or the scan mirror is unpolarized. For a polarized scene (i.e., $f \neq 0$), fixed-optics polarization contributes to the system RVS for both unpolarized and polarized scan mirror.

At-detector Signal due to Scene (*S*)

- **Unpolarized Scene** $f = 0$, $RVS_{eff} = RVS_0$, $S = RVS_0 \; L$

Parallel Scanner: $$S = RVS^0_{\text{para}}(\theta) \; L = \left[\frac{\rho_s(\theta) + \rho_p(\theta)}{2} + \eta \; \frac{\rho_s(\theta) - \rho_p(\theta)}{2} \right] L$$

- **Polarized Scene** $f \neq 0$, $RVS_{eff} = RVS_0 + f \; RVS_1$, $S = RVS_{eff} \; L$

Parallel Scanner: $$S = RVS_{eff}(\theta) \; L = \left[RVS^0_{\text{para}}(\theta) + RVS^1_{\text{para}}(\theta) \; f \right] L$$

Conclusion: For unpolarized scenes , fixed-optics polarization will contribute to the RVS when the scan mirror is polarized(i.e., $\rho_s \neq \rho_p$). For polarized scenes , fixed-optics polarization will contribute to the RVS for both polarized and unpolarized scan mirrors, such that, **sensors calibrated to an unpolarized source, with identical scan mirrors and different fixed-optics polarization characteristics, will not agree when viewing a polarized scene.**

Parametric Study for a Parallel Scanner Remote Sensor

Quantitative results are presented for parallel scanners operating in the thermal emissive wavelength region, covering a realistic range of scan mirror, fixed-optics and scene polarization parameters. These are:

- Scan mirror polarization (2 cases)
  1) a silver-coated scan mirror (similar to the MODIS scan mirror)
  2) a gold-coated scan mirror (a near perfect unpolarized mirror with $r_s=r_p=(r_s+r_p)/2$)
- Fixed-optics polarization (3 cases)
  1) zero fixed optics polarization
  2) 5% fixed-optics polarization (typical of a filter type spectroradiometer, e.g., MODIS)
  3) 70% fixed-optics polarization (typical of a grating type spectroradiometer)
- Scene polarization (2 cases)
  1) an unpolarized scene
  2) 5% polarized scene

Response versus Scan Angle for a Silver-coated Scan Mirror Sensor Viewing an Unpolarized Scene

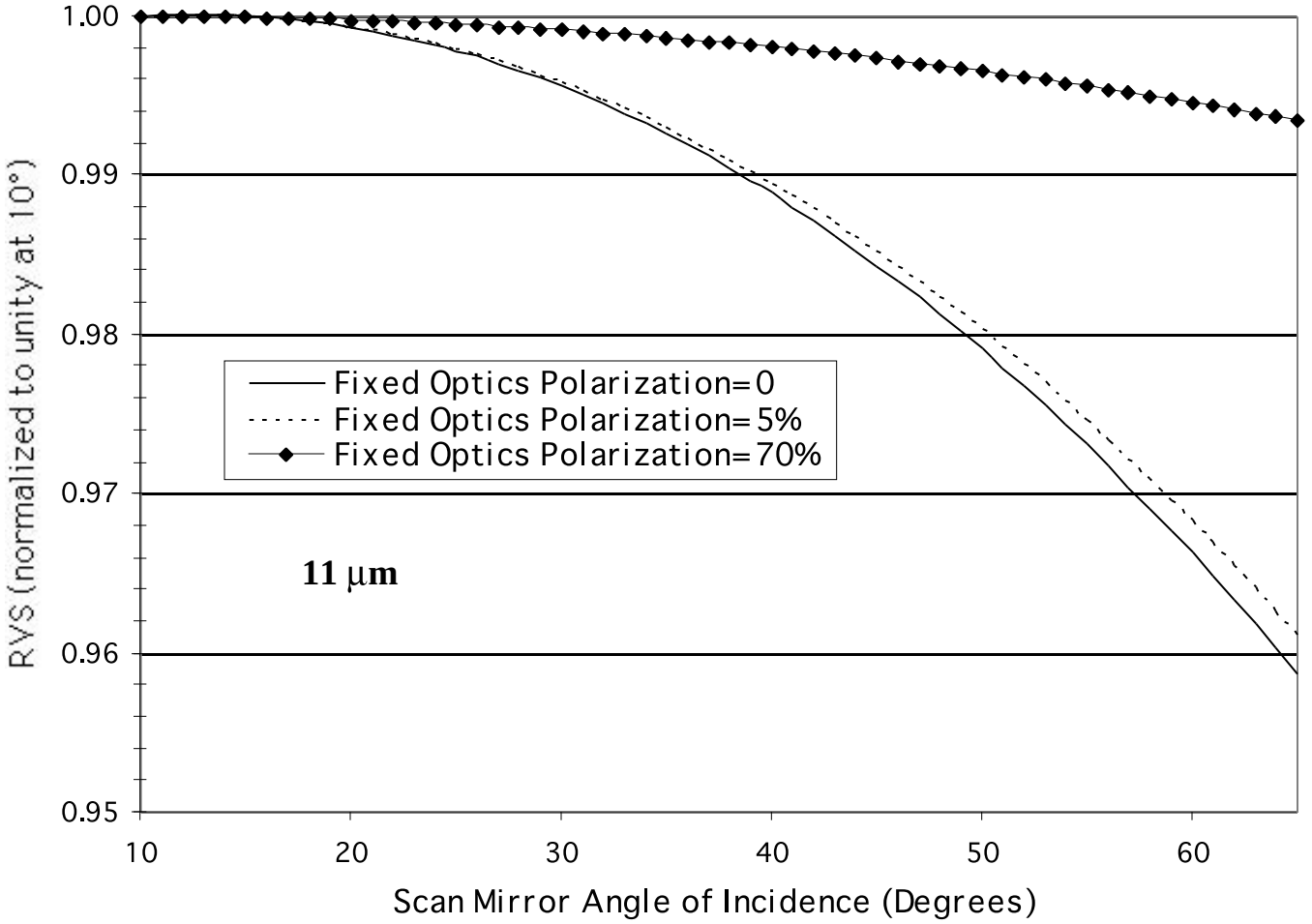

Effective Response versus Scan Angle for a Silver-coated Scan Mirror Sensor Viewing a 5% Polarized Scene

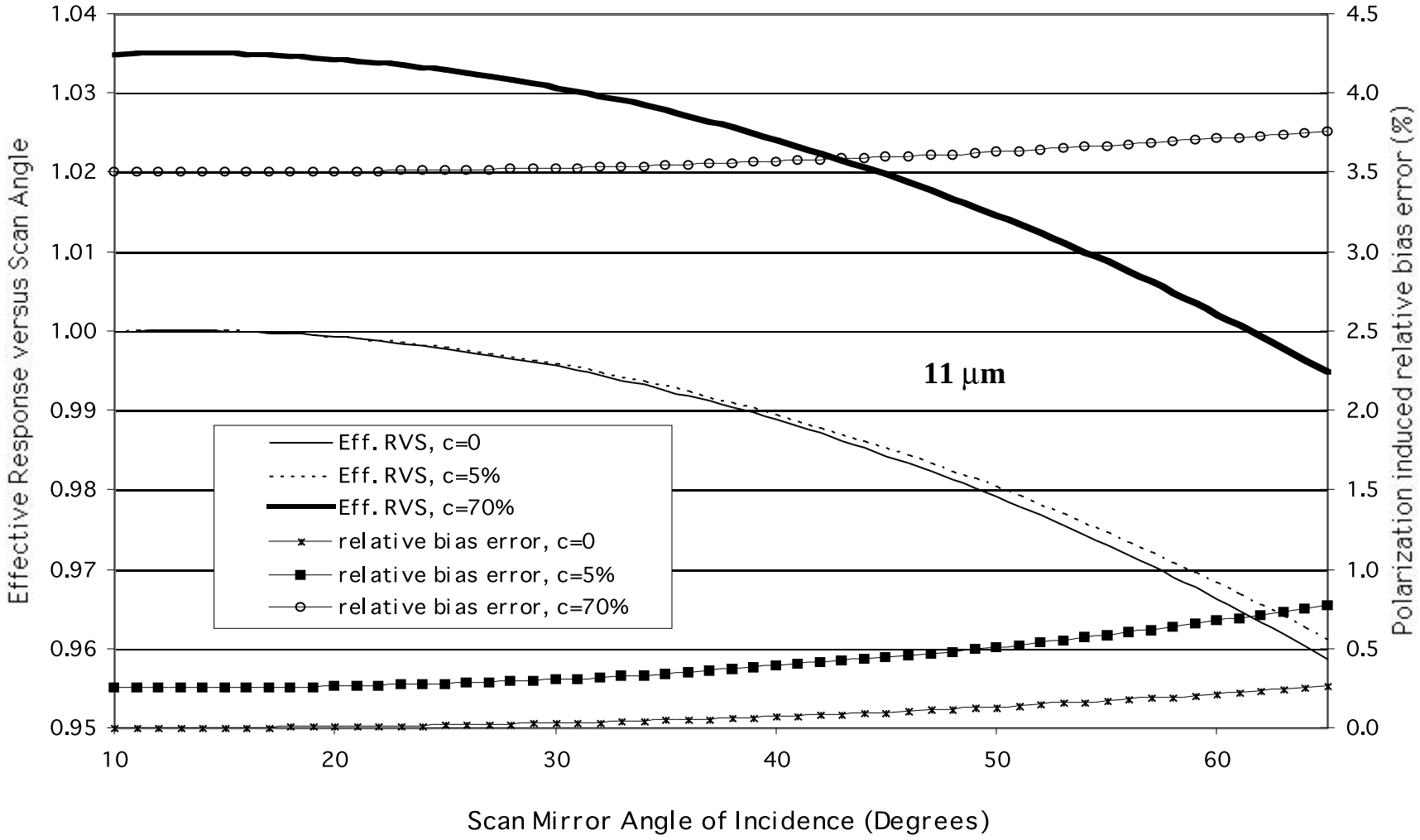

PC08 data analysis

For a general linear sensor, the system response to a polarized scene can be expressed as

$$S = RVS_0(\theta)\left[1 + f\ a(\theta)\cos\left(2\phi + \delta(\theta)\right)\right]$$

where S is the at detector signal, RVS_0 is the response versus scan angle for un-polarized scene, θ is the scan angle or angle of incidence (AOI), f is the scene polarization factor, $a(\theta)$ is the amplitude of the system polarization response, $\delta(\theta)$ is the phase angle of the system polarization response, and ϕ is the scene polarization direction angle measured with respect to the MODIS scan mirror plane of incidence, namely when the polarization direction is in this plane, ϕ=0, and when it is perpendicular to this plane ϕ=90. This reference plane, determined by the nadir direction and the scan mirror normal direction, remains the same for each scan.

Band 13 and 13high

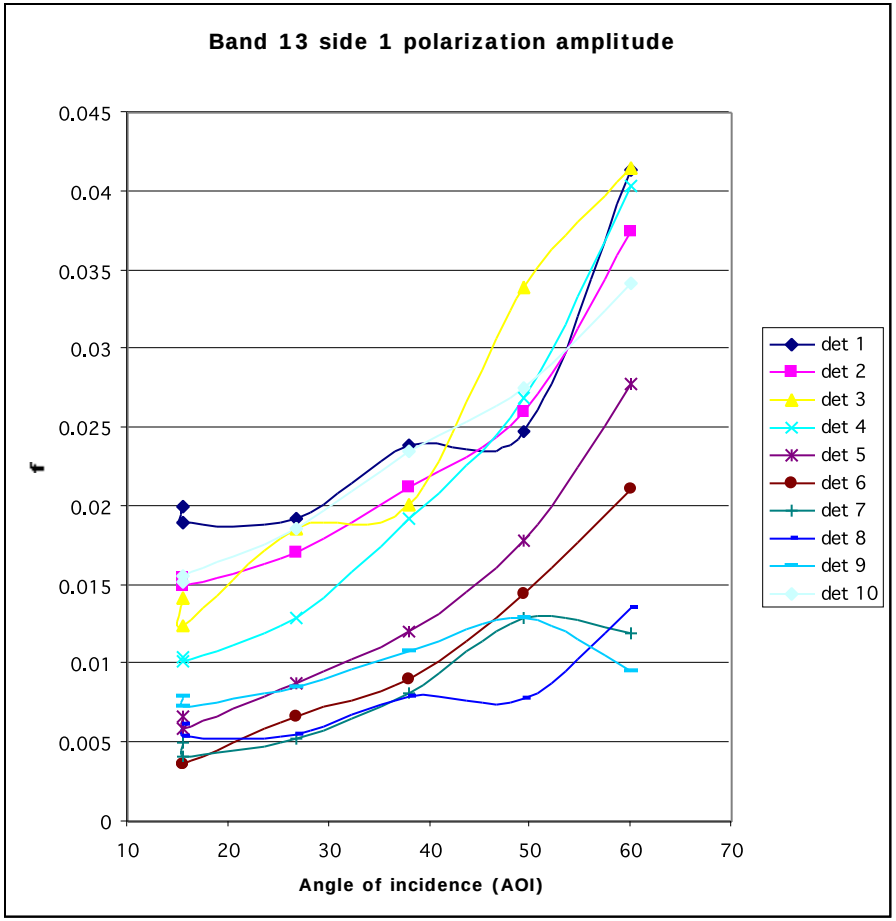

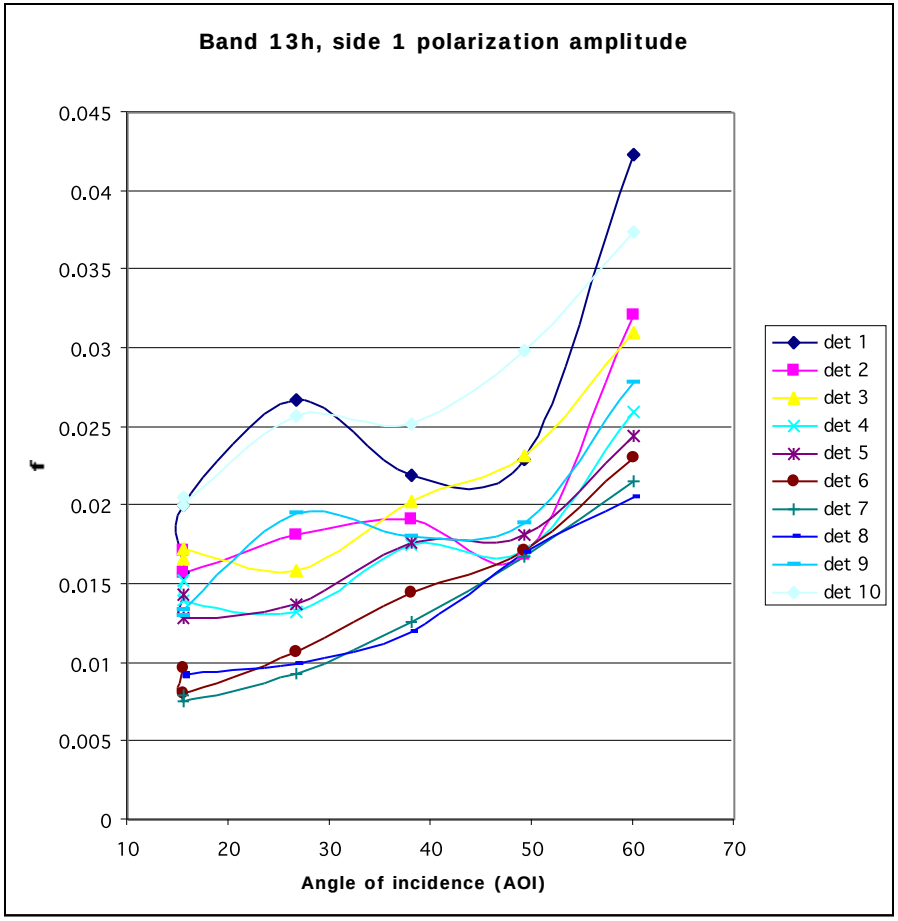

Band 14 and 14high

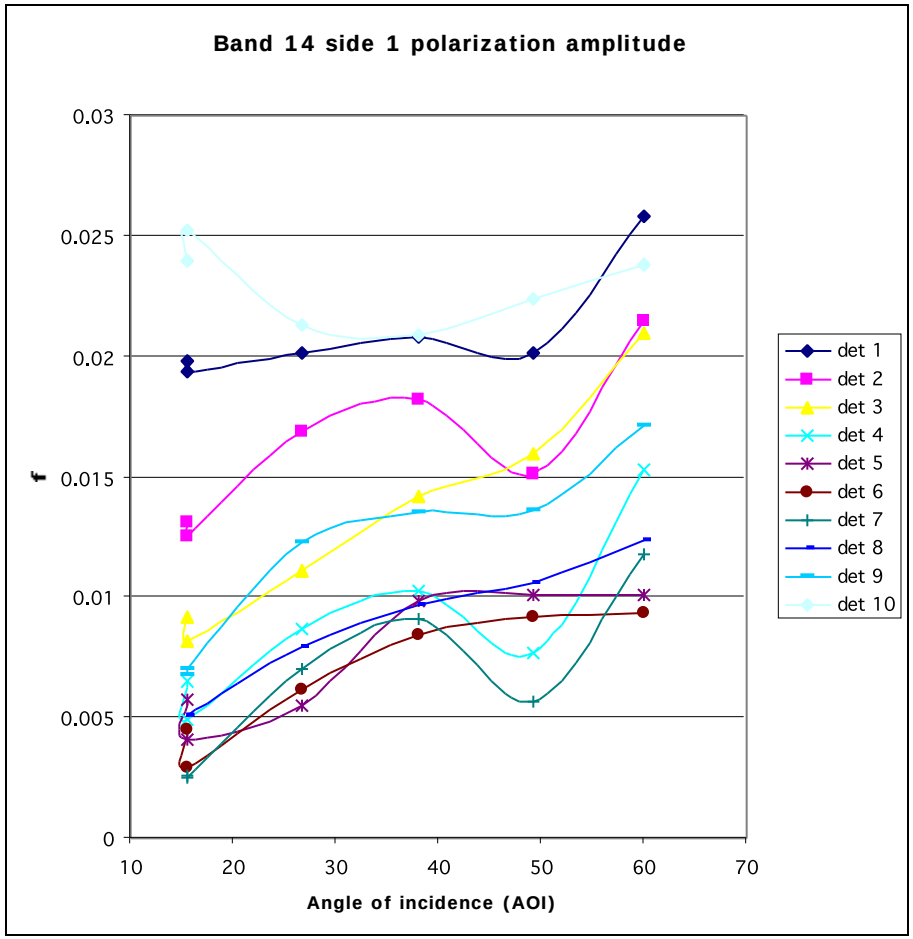

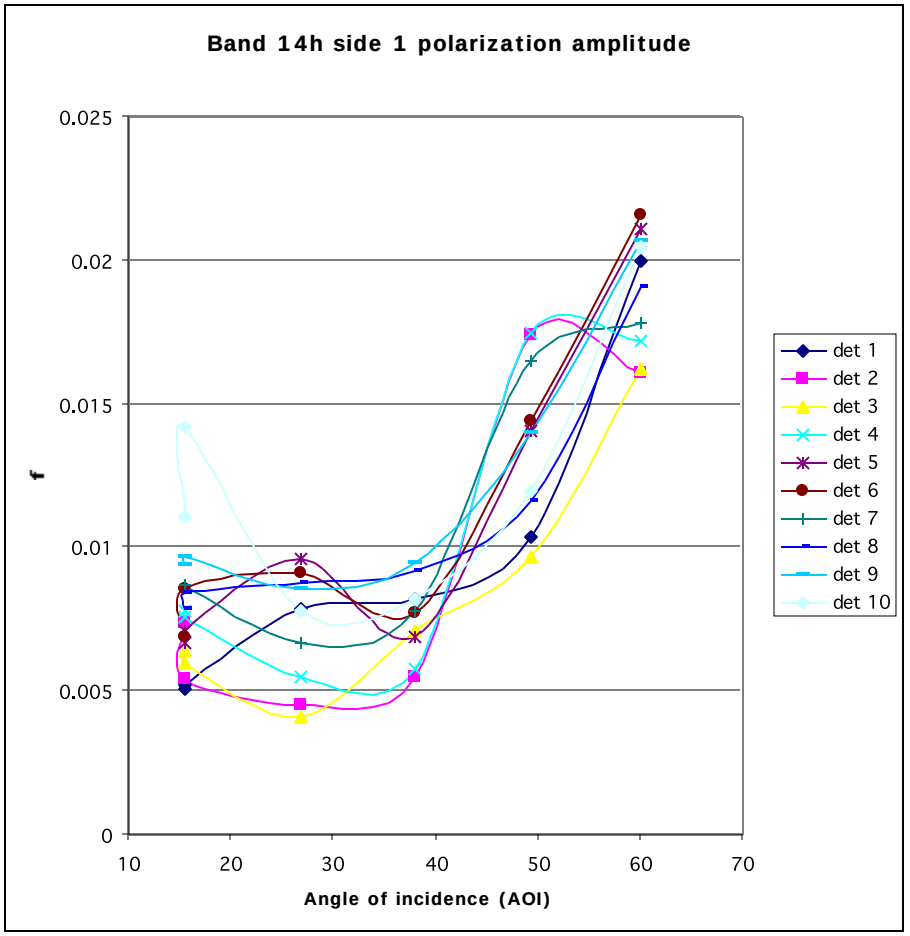

Compare for det 5 and mirror side 1

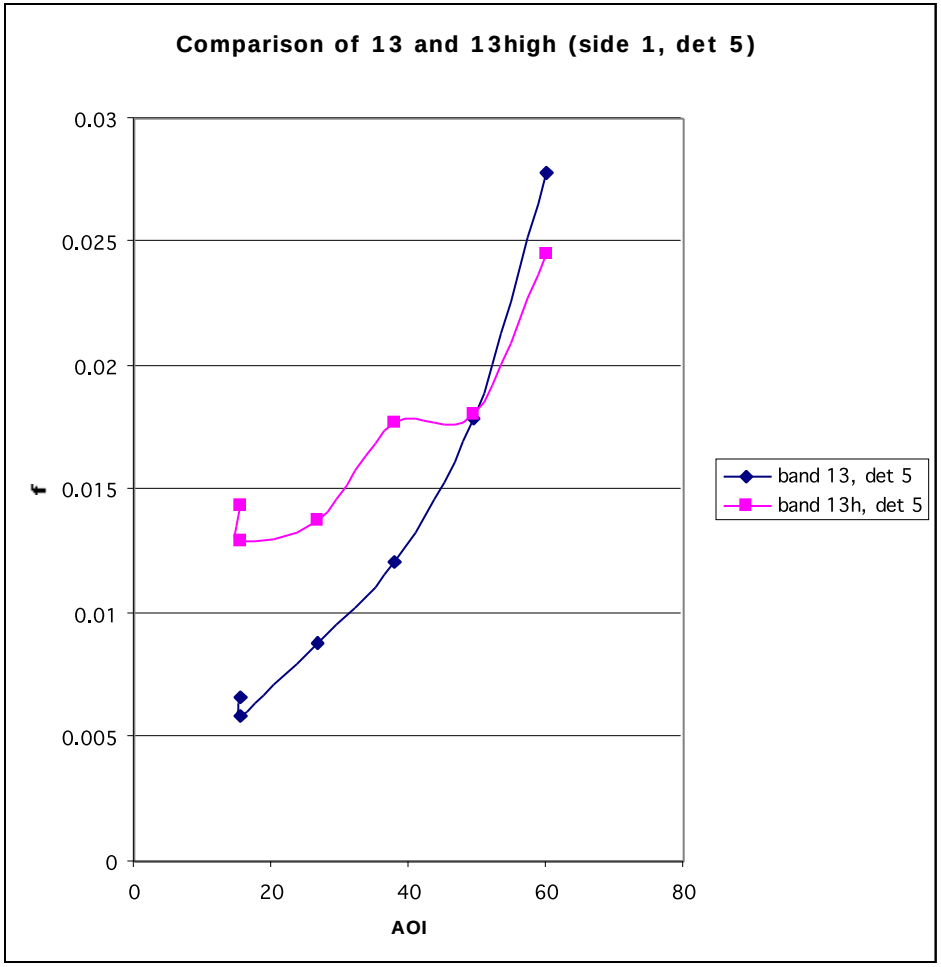

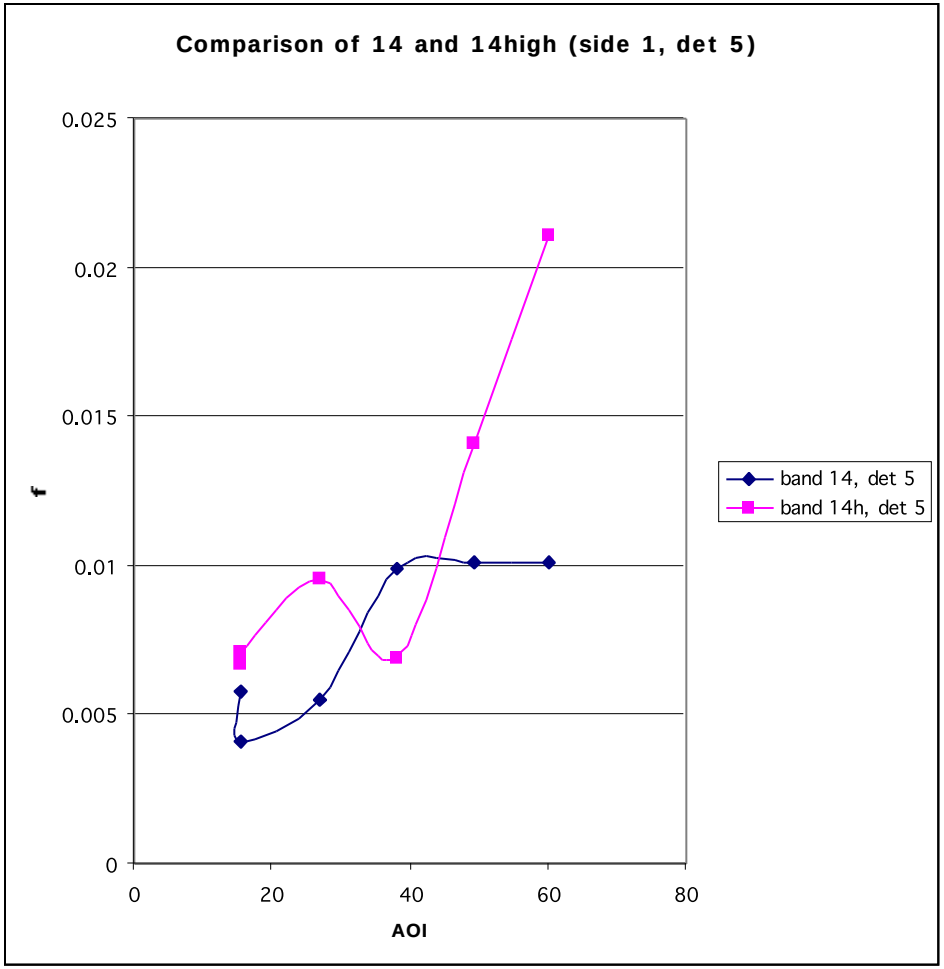

Summary

- PC 08 data generally give the uncertainty of the amplitude determination on the order of 0.01.
- Detector to detector variation is also on the scale of 0.01. Unless the detector gains are polarization sensitive, this size of variation should be regarded as the size of uncertainty.
- Differences between 13 and 13h, and 14 and 14h also on the scale of 0.01.

Appendix: amplitude tables (phase angle tables are not given here. For those interested, EXCEL workbooks on both amplitude and phase angle are available.

Band 1 Mirror side 1, amplitude

Det	15.5	15.5	26.75	38	49.25	60
1	0.0042	0.0025	0.0031	0.0025	0.0035	0.0064
2	0.0042	0.0034	0.0062	0.0028	0.0022	0.0074
3	0.0045	0.0019	0.0048	0.0045	0.0031	0.0077
4	0.0025	0.0017	0.0029	0.0037	0.0021	0.0089
5	0.0037	0.0026	0.0034	0.0026	0.0022	0.0075
6	0.0036	0.0029	0.0043	0.0042	0.003	0.0083
7	0.0029	0.0036	0.0028	0.0036	0.0015	0.0082
8	0.0031	0.0034	0.0024	0.0027	0.0022	0.0089
9	0.0022	0.003	0.0036	0.0036	0.0023	0.0075
10	0.0028	0.0023	0.0032	0.0023	0.0006	0.0086
11	0.0047	0.003	0.0023	0.0034	0.0027	0.0098
12	0.0027	0.0017	0.0024	0.0024	0.0021	0.0095
13	0.0022	0.0025	0.0028	0.0032	0.0027	0.0099
14	0.0017	0.0023	0.0023	0.0027	0.0021	0.0098
15	0.0035	0.0021	0.0021	0.0031	0.0015	0.0079
16	0.0026	0.0029	0.0028	0.0026	0.0013	0.0076
17	0.0022	0.0021	0.003	0.0038	0.0015	0.0096
18	0.0034	0.0028	0.0039	0.0023	0.0012	0.0079
19	0.003	0.0037	0.003	0.0032	0.0015	0.0098
20	0.0033	0.0027	0.0036	0.0021	0.0008	0.007
21	0.0029	0.0042	0.0035	0.0032	0.0013	0.0084
22	0.0033	0.0052	0.0033	0.0026	0.0012	0.0069
23	0.0033	0.003	0.0031	0.0024	0.0019	0.0109
24	0.0043	0.0045	0.0025	0.0013	0.0013	0.0074
25	0.0022	0.0021	0.0022	0.0019	0.0021	0.0098
26	0.003	0.003	0.0026	0.0021	0.0028	0.0093
27	0.0035	0.0033	0.0035	0.0027	0.0022	0.0093
28	0.0033	0.0029	0.0038	0.0037	0.0019	0.0087
29	0.004	0.0024	0.0035	0.0025	0.0016	0.0078
30	0.0038	0.0031	0.0044	0.0025	0.0029	0.0081
31	0.0037	0.0038	0.0045	0.0027	0.0017	0.0122
32	0.0029	0.0032	0.0033	0.0042	0.0023	0.0119
33	0.0026	0.0023	0.0035	0.0032	0.0028	0.0107
34	0.0042	0.0028	0.0027	0.0024	0.0019	0.0076
35	0.003	0.0035	0.0027	0.0021	0.0034	0.0087
36	0.0034	0.0036	0.0032	0.003	0.0019	0.009
37	0.0043	0.003	0.0034	0.0023	0.0007	0.0041
38	0.0042	0.0029	0.0039	0.0029	0.0015	0.0027
39	0.0069	0.005	0.0044	0.0027	0.0012	0.003
40	0.0091	0.0085	0.0108	0.0086	0.0073	0.0098

Band 1, mirror side 2, amplitude

Det	15.5	15.5	26.75	38	49.25	60
1	0.0064	0.0018	0.0044	0.0021	0.0028	0.0016
2	0.0038	0.0048	0.0048	0.0081	0.0058	0.0024
3	0.0039	0.0041	0.0045	0.0056	0.0045	0.0013
4	0.0016	0.0025	0.0034	0.0037	0.0027	0.0016
5	0.0037	0.0023	0.0045	0.0046	0.0028	0.0015
6	0.0026	0.0031	0.0036	0.0059	0.0043	0.0024
7	0.0036	0.0028	0.0042	0.004	0.0031	0.0014
8	0.0041	0.0024	0.0043	0.0047	0.0033	0.0013
9	0.0019	0.0027	0.0037	0.0043	0.0043	0.0021
10	0.0016	0.0042	0.0032	0.0038	0.0039	0.0024
11	0.004	0.0031	0.0051	0.0044	0.0042	0.0013
12	0.0021	0.0018	0.0031	0.0036	0.0033	0.0011
13	0.0019	0.0024	0.0032	0.0041	0.0037	0.0012
14	0.0024	0.0021	0.0021	0.0032	0.0022	0.0011
15	0.0037	0.0023	0.0049	0.0031	0.0029	0.0005
16	0.0028	0.0031	0.003	0.0042	0.0038	0.0007
17	0.0028	0.0027	0.0031	0.0049	0.0031	0.0007
18	0.0033	0.0031	0.0043	0.0047	0.0039	0.0013
19	0.0032	0.0028	0.0033	0.0044	0.0035	0.0005
20	0.0039	0.0037	0.004	0.0036	0.003	0.0009
21	0.0035	0.0039	0.0046	0.0044	0.0034	0.0008
22	0.004	0.0036	0.0042	0.0067	0.0043	0.0014
23	0.0031	0.0028	0.0042	0.0039	0.0028	0.0017
24	0.0037	0.0038	0.0042	0.0036	0.0034	0.0021
25	0.0022	0.0024	0.0027	0.004	0.0024	0.0024
26	0.0042	0.003	0.0031	0.0035	0.0037	0.0014
27	0.0033	0.0029	0.005	0.0056	0.0042	0.0012
28	0.0035	0.0034	0.0029	0.0045	0.0035	0.0013
29	0.0042	0.0021	0.0053	0.0046	0.0038	0.0013
30	0.0027	0.0027	0.0044	0.0049	0.0041	0.0018
31	0.0033	0.0038	0.0045	0.0043	0.0024	0.0019
32	0.0028	0.0027	0.0039	0.0062	0.0046	0.0023
33	0.003	0.0025	0.0032	0.0038	0.0027	0.0021
34	0.004	0.0029	0.0046	0.0042	0.0038	0.0016
35	0.0031	0.0031	0.0038	0.0039	0.0033	0.0012
36	0.0023	0.0031	0.004	0.0044	0.0022	0.0022
37	0.0048	0.0019	0.0036	0.0054	0.0045	0.0014
38	0.0041	0.003	0.0037	0.0056	0.0048	0.0018
39	0.0041	0.0073	0.0091	0.0091	0.0065	0.0034
40	0.0053	0.0101	0.0147	0.0116	0.0052	0.0101

Band 2, mirror side 1, amplitude

Det	15.5	15.5	26.75	38	49.25	60
1	0.0085	0.0106	0.018	0.0108	0.0212	0.0346
2	0.01	0.0114	0.01	0.0124	0.0205	0.0256
3	0.0094	0.0103	0.0082	0.0079	0.0158	0.0218
4	0.0098	0.0087	0.0128	0.0179	0.0216	0.0265
5	0.0091	0.0095	0.0059	0.0128	0.0184	0.0236
6	0.0087	0.0077	0.0041	0.0047	0.0154	0.0162
7	0.0063	0.0063	0.0128	0.0088	0.014	0.0188
8	0.0063	0.0071	0.0045	0.0088	0.0119	0.0167
9	0.0116	0.0036	0.0023	0.0034	0.0053	0.0107
10	0.0063	0.0057	0.0046	0.0052	0.0084	0.0146
11	0.0043	0.0037	0.0045	0.0052	0.0104	0.0149
12	0.002	0.0015	0.0022	0.0071	0.0108	0.0156
13	0.0028	0.0038	0.0033	0.0058	0.0108	0.0173
14	0.0039	0.0039	0.0029	0.0056	0.0095	0.0161
15	0.0023	0.004	0.0038	0.0024	0.0046	0.0117
16	0.0029	0.0039	0.0045	0.0032	0.0101	0.0144
17	0.005	0.0047	0.003	0.0034	0.0091	0.0126
18	0.0042	0.0061	0.0029	0.0038	0.0062	0.0159
19	0.0053	0.0059	0.0023	0.0031	0.0068	0.0126
20	0.0065	0.0075	0.0042	0.0017	0.006	0.0137
21	0.0062	0.0057	0.0047	0.0047	0.0036	0.0123
22	0.0052	0.0053	0.0038	0.0024	0.0079	0.0146
23	0.0073	0.0036	0.002	0.0117	0.0124	0.0129
24	0.0058	0.0048	0.0047	0.0045	0.0092	0.0155
25	0.0053	0.0107	0.003	0.0018	0.0045	0.0073
26	0.0067	0.0072	0.0048	0.0052	0.0101	0.0152
27	0.0053	0.006	0.005	0.005	0.0079	0.0142
28	0.0044	0.0053	0.0028	0.0042	0.0124	0.0176
29	0.0116	0.004	0.0026	0.0062	0.0035	0.0131
30	0.0046	0.0053	0.0044	0.0057	0.0107	0.0168
31	0.0059	0.0058	0.0052	0.0068	0.0101	0.0156
32	0.0054	0.0059	0.0054	0.0087	0.0114	0.0179
33	0.0051	0.0028	0.003	0.007	0.0078	0.0135
34	0.0076	0.0071	0.0069	0.0067	0.0131	0.0188
35	0.0091	0.0049	0.0075	0.0088	0.0145	0.0176
36	0.0027	0.0067	0.0056	0.0107	0.0171	0.0171
37	0.0081	0.0085	0.0096	0.0137	0.019	0.0239
38	0.0079	0.0079	0.0103	0.0138	0.0182	0.0234
39	0.004	0.0032	0.0118	0.0167	0.0236	0.032
40	0.0111	0.0107	0.0194	0.0201	0.0222	0.0364

Band 2, mirror side 2, amplitude

Det	15.5	15.5	26.75	38	49.25	60
1	0.0126	0.0104	0.018	0.0164	0.0196	0.0334
2	0.0106	0.0114	0.0088	0.0102	0.019	0.0232
3	0.0148	0.0052	0.0081	0.0061	0.009	0.0194
4	0.0083	0.0105	0.0108	0.0161	0.0196	0.0265
5	0.0099	0.0067	0.0099	0.0093	0.0155	0.0216
6	0.0072	0.0057	0.0108	0.0061	0.0016	0.0128
7	0.0061	0.006	0.0058	0.013	0.0163	0.0194
8	0.0069	0.0054	0.0063	0.0075	0.0099	0.0169
9	0.0052	0.0027	0.0018	0.0058	0.0053	0.0085
10	0.0069	0.0047	0.0046	0.006	0.01	0.0121
11	0.0047	0.0033	0.0035	0.0042	0.0101	0.0164
12	0.0042	0.0067	0.0017	0.003	0.006	0.0106
13	0.0035	0.004	0.0028	0.0042	0.0099	0.0172
14	0.004	0.0037	0.0032	0.0039	0.0083	0.0143
15	0.0025	0.0021	0.0014	0.0007	0.0067	0.0085
16	0.0036	0.0044	0.0033	0.0047	0.0083	0.0147
17	0.0049	0.0054	0.0025	0.0054	0.0076	0.0133
18	0.0055	0.0061	0.004	0.0022	0.0093	0.0129
19	0.0063	0.0062	0.0037	0.003	0.007	0.0134
20	0.0056	0.0066	0.0053	0.0027	0.0052	0.0104
21	0.007	0.0068	0.0045	0.0028	0.008	0.0109
22	0.0055	0.0057	0.0026	0.0027	0.0069	0.0158
23	0.0065	0.0043	0.0016	0.0099	0.0292	0.0149
24	0.0054	0.0055	0.0051	0.0045	0.0071	0.0142
25	0.0059	0.0071	0.0052	0.0035	0.0054	0.0065
26	0.0069	0.006	0.0049	0.0046	0.0086	0.0137
27	0.0055	0.007	0.0038	0.007	0.0117	0.0157
28	0.0058	0.0054	0.0029	0.0039	0.0055	0.0165
29	0.0046	0.0034	0.0028	0.0024	0.0097	0.0254
30	0.0045	0.0048	0.0024	0.0059	0.0092	0.0183
31	0.0053	0.0053	0.0037	0.0066	0.0107	0.0167
32	0.0055	0.006	0.0063	0.0068	0.0107	0.0175
33	0.0066	0.012	0.0065	0.0038	0.0044	0.0107
34	0.0069	0.0056	0.0073	0.0076	0.0116	0.0177
35	0.0073	0.0085	0.0074	0.0101	0.0134	0.0166
36	0.0034	0.0048	0.0073	0.0073	0.0107	0.0172
37	0.009	0.0087	0.009	0.0119	0.016	0.0218
38	0.0077	0.0088	0.0089	0.0114	0.016	0.0222
39	0.0042	0.0144	0.0044	0.0138	0.0208	0.0243
40	0.0099	0.011	0.0198	0.018	0.0216	0.0263

Band 3, mirror side 1, amplitude

Det	15.5	15.5	26.75	38	49.25	60
1	0.0122	0.009	0.0145	0.0142	0.0237	0.033
2	0.0085	0.007	0.011	0.0154	0.0214	0.0301
3	0.0068	0.0065	0.0076	0.012	0.0186	0.0282
4	0.0018	0.0029	0.0057	0.0091	0.0201	0.0256
5	0.0036	0.0014	0.0059	0.011	0.017	0.026
6	0.0045	0.003	0.007	0.0105	0.0179	0.0283
7	0.0029	0.0044	0.0075	0.0112	0.0197	0.0279
8	0.0019	0.0034	0.0077	0.0101	0.0171	0.027
9	0.0036	0.0016	0.006	0.0088	0.0184	0.0273
10	0.0029	0.0051	0.0086	0.0116	0.0175	0.0281
11	0.0028	0.0028	0.007	0.0101	0.0155	0.0252
12	0.0035	0.0029	0.0053	0.0103	0.0154	0.0241
13	0.0038	0.0041	0.0072	0.011	0.0167	0.0265
14	0.0042	0.0034	0.0066	0.0094	0.0158	0.0268
15	0.0025	0.0034	0.0069	0.0106	0.0182	0.0275
16	0.0041	0.0056	0.0054	0.011	0.0203	0.029
17	0.0045	0.0039	0.0081	0.0144	0.0221	0.0293
18	0.0067	0.007	0.0105	0.0145	0.0217	0.0316
19	0.0064	0.0057	0.0123	0.0139	0.0221	0.0289
20	0.0102	0.0125	0.0128	0.0174	0.0293	0.0326

Band 3, mirror side 2, amplitude

Det	15.5	15.5	26.75	38	49.25	60
1	0.013	0.0157	0.0146	0.0148	0.0213	0.0302
2	0.0072	0.0057	0.0107	0.0155	0.0215	0.0267
3	0.0028	0.0057	0.0079	0.0113	0.0171	0.0249
4	0.0065	0.0024	0.0056	0.0117	0.0168	0.0237
5	0.0019	0.0018	0.0031	0.0092	0.0148	0.0219
6	0.004	0.003	0.0061	0.0109	0.0177	0.0244
7	0.0017	0.0059	0.0055	0.0099	0.0168	0.0236
8	0.0026	0.0039	0.0044	0.0087	0.0144	0.0213
9	0.0026	0.0028	0.0048	0.0094	0.0144	0.0223
10	0.0025	0.004	0.0065	0.009	0.0153	0.0227
11	0.003	0.003	0.0047	0.0098	0.0138	0.0214
12	0.0037	0.0032	0.0037	0.0111	0.0148	0.0198
13	0.0064	0.0038	0.0064	0.011	0.0157	0.0226
14	0.0034	0.0051	0.0049	0.0089	0.0156	0.0225
15	0.0026	0.0058	0.0052	0.0117	0.0168	0.0247
16	0.0038	0.0048	0.0055	0.0104	0.0188	0.0235
17	0.0044	0.0051	0.009	0.0138	0.0194	0.0265
18	0.0045	0.0078	0.0087	0.0134	0.0202	0.0289
19	0.0062	0.0053	0.0107	0.011	0.0194	0.0269
20	0.0125	0.0103	0.0142	0.0144	0.0283	0.0286

Band 4, mirror side 1, amplitude

Det	15.5	15.5	26.75	38	49.25	60
1	0.0128	0.0092	0.0087	0.0113	0.0135	0.0213
2	0.0105	0.0118	0.0081	0.0092	0.0132	0.0213
3	0.0075	0.0071	0.0061	0.0078	0.0116	0.0191
4	0.009	0.0077	0.0063	0.0064	0.0095	0.0164
5	0.0093	0.0088	0.0066	0.0057	0.0069	0.0163
6	0.0096	0.0097	0.0075	0.0053	0.006	0.0141
7	0.0097	0.0119	0.0106	0.0093	0.0058	0.0108
8	0.0126	0.0134	0.0074	0.0055	0.0036	0.0106
9	0.01	0.0113	0.0073	0.0057	0.0037	0.0114
10	0.0114	0.0119	0.0097	0.0073	0.0042	0.0111
11	0.0132	0.0127	0.0111	0.0072	0.0059	0.0108
12	0.0123	0.0123	0.0092	0.0073	0.0046	0.0109
13	0.0123	0.0114	0.0094	0.0068	0.0054	0.0107
14	0.0129	0.0109	0.0087	0.0075	0.0068	0.0117
15	0.0136	0.0119	0.0083	0.0061	0.0063	0.0123
16	0.0119	0.0105	0.0072	0.0059	0.0083	0.0148
17	0.0111	0.0104	0.0086	0.0086	0.0111	0.0174
18	0.0094	0.0078	0.0075	0.0076	0.0116	0.0186
19	0.0077	0.008	0.0076	0.008	0.0115	0.0219
20	0.0081	0.0058	0.01	0.0144	0.0184	0.0213

Band 4, mirror side 2, amplitude

Det	15.5	15.5	26.75	38	49.25	60
1	0.0122	0.0082	0.0093	0.0112	0.0115	0.0227
2	0.0079	0.0109	0.0085	0.0089	0.0131	0.0196
3	0.0083	0.008	0.0082	0.0077	0.0107	0.0168
4	0.0083	0.0071	0.0079	0.0068	0.0086	0.0144
5	0.0105	0.0105	0.0076	0.0058	0.006	0.014
6	0.0097	0.0095	0.0081	0.0054	0.0047	0.01
7	0.0102	0.0113	0.0106	0.0084	0.0071	0.0109
8	0.0137	0.0135	0.0096	0.0058	0.0032	0.0082
9	0.0121	0.0116	0.0085	0.005	0.0031	0.0085
10	0.011	0.0127	0.0105	0.0067	0.0043	0.0079
11	0.0126	0.0132	0.013	0.0084	0.0051	0.0082
12	0.0125	0.0127	0.0109	0.0074	0.0044	0.0084
13	0.0115	0.0126	0.0104	0.0064	0.005	0.0088
14	0.0124	0.0124	0.0114	0.0073	0.0061	0.0102
15	0.0126	0.0123	0.0105	0.0068	0.0054	0.0106
16	0.0114	0.0109	0.0089	0.006	0.0065	0.0125
17	0.0108	0.0093	0.009	0.0074	0.01	0.016
18	0.0082	0.0076	0.0082	0.0075	0.0099	0.0168
19	0.0084	0.0078	0.0087	0.0107	0.0113	0.0168
20	0.0112	0.0061	0.0075	0.0105	0.0182	0.023

Band 8, amplitude

side =1						
Det	15.5	15.5	26.75	38	49.25	60
1	0.0434	0.0421	0.0453	0.0596	0.0561	0.0633
2	0.0316	0.03	0.0447	0.0543	0.0572	0.0641
3	0.0359	0.0364	0.0461	0.0477	0.0566	0.065
4	0.0368	0.0399	0.0472	0.0512	0.057	0.0654
5	0.0457	0.0445	0.0509	0.0551	0.0601	0.0672
6	0.0346	0.0352	0.043	0.049	0.0564	0.0633
7	0.032	0.0351	0.041	0.0445	0.0517	0.0616
8	0.0313	0.0309	0.039	0.0406	0.0485	0.0563
9	0.0281	0.0291	0.041	0.0443	0.0455	0.0607
10	0.0318	0.0282	0.0368	0.052	0.0593	0.0649
side=2						
Det	15.5	15.5	26.75	38	49.25	60
1	0.042	0.0414	0.0376	0.0531	0.0488	0.047
2	0.0299	0.0266	0.0443	0.045	0.0535	0.0579
3	0.0364	0.0336	0.0464	0.0448	0.0532	0.0576
4	0.0383	0.0407	0.0456	0.0505	0.0535	0.0576
5	0.0425	0.0446	0.0483	0.0551	0.0566	0.0609
6	0.0375	0.0355	0.0426	0.0499	0.0515	0.0573
7	0.0316	0.0354	0.0388	0.0453	0.0483	0.0538
8	0.0325	0.0338	0.0365	0.0416	0.0437	0.049
9	0.0261	0.034	0.0419	0.045	0.0443	0.0532
10	0.025	0.019	0.0421	0.0482	0.0555	0.0523

Band 9, amplitude

band=9	side=1					
Det	15.5	15.5	26.75	38	49.25	60
1	0.019	0.0174	0.0143	0.033	0.0307	0.0358
2	0.0151	0.0114	0.0201	0.0253	0.0327	0.0405
3	0.0129	0.0133	0.0216	0.0218	0.03	0.0413
4	0.0144	0.0169	0.0242	0.024	0.0294	0.0433
5	0.0197	0.0196	0.0231	0.0275	0.0336	0.0417
6	0.018	0.0188	0.0232	0.0271	0.0336	0.0417
7	0.0168	0.0184	0.0208	0.025	0.0332	0.0414
8	0.0151	0.0152	0.0204	0.0242	0.0312	0.0409
9	0.015	0.0191	0.0198	0.0225	0.0315	0.0414
10	0.0152	0.0105	0.0256	0.0288	0.0356	0.042
band=9	side=2					
Det	15.5	15.5	26.75	38	49.25	60
1	0.0187	0.0177	0.0141	0.0321	0.0283	0.0315
2	0.0078	0.01	0.0191	0.0175	0.0309	0.0355
3	0.0115	0.0095	0.0211	0.0207	0.0278	0.0362
4	0.0152	0.0164	0.0233	0.0232	0.0273	0.0374
5	0.0198	0.0197	0.0229	0.0268	0.0312	0.0374
6	0.0185	0.0179	0.0219	0.028	0.0314	0.0351
7	0.0177	0.0181	0.0218	0.025	0.0299	0.0383
8	0.0152	0.0183	0.0185	0.0238	0.0289	0.0364
9	0.019	0.0198	0.0191	0.0212	0.0302	0.0369
10	0.0121	0.0133	0.0238	0.0278	0.0335	0.0364

Band 10, amplitude

band=10	side=1					
Det	15.5	15.5	26.75	38	49.25	60
1	0.0069	0.0069	0.002	0.0125	0.0144	0.02
2	0.0066	0.0071	0.0024	0.0057	0.0132	0.0224
3	0.0084	0.0083	0.0023	0.0019	0.0082	0.0203
4	0.0082	0.0085	0.0038	0.0005	0.0033	0.0182
5	0.0079	0.0084	0.0051	0.0034	0.0072	0.0173
6	0.0085	0.0085	0.0056	0.0048	0.0077	0.0173
7	0.0079	0.0083	0.0044	0.0047	0.0091	0.0198
8	0.0077	0.0083	0.0044	0.0049	0.0092	0.0213
9	0.0064	0.0073	0.0031	0.005	0.0139	0.0253
10	0.0038	0.004	0.0073	0.0102	0.0168	0.024
band=10	side=2					
Det	15.5	15.5	26.75	38	49.25	60
1	0.0093	0.0057	0.0037	0.008	0.0126	0.0158
2	0.0081	0.008	0.0038	0.0053	0.0112	0.0193
3	0.0086	0.0082	0.0027	0.0019	0.0063	0.0163
4	0.0084	0.0085	0.0053	0.0009	0.0019	0.0141
5	0.0082	0.0084	0.0073	0.0043	0.0057	0.0143
6	0.0084	0.0087	0.0059	0.0055	0.0064	0.0148
7	0.0082	0.0079	0.006	0.0046	0.0073	0.014
8	0.0082	0.0081	0.006	0.005	0.0078	0.0144
9	0.0067	0.0067	0.0021	0.0066	0.0129	0.0194
10	0.0011	0.0033	0.0059	0.0111	0.0154	0.0204

Band 11, amplitude

band=11	side=1					
Det	15.5	15.5	26.75	38	49.25	60
1	0.0095	0.0073	0.0089	0.0151	0.0226	0.0253
2	0.0059	0.0052	0.0106	0.0146	0.0188	0.0295
3	0.0029	0.0011	0.0062	0.0097	0.0124	0.0256
4	0.0029	0.0038	0.0043	0.0093	0.0123	0.0215
5	0.003	0.0045	0.0056	0.0097	0.0123	0.0206
6	0.0013	0.0034	0.0032	0.006	0.0117	0.0161
7	0.0033	0.004	0.0022	0.0064	0.0129	0.0167
8	0.0026	0.0024	0.0032	0.0073	0.0118	0.0191
9	0.0015	0.0026	0.0025	0.0063	0.0166	0.0204
10	0.0084	0.0074	0.0101	0.0143	0.0217	0.0287
band=11	side=2					
Det	15.5	15.5	26.75	38	49.25	60
1	0.0126	0.0063	0.0088	0.0114	0.0209	0.0264
2	0.0042	0.0045	0.0092	0.0136	0.0169	0.0265
3	0.0042	0.0029	0.0057	0.0094	0.0108	0.0218
4	0.0019	0.0028	0.0049	0.0086	0.0111	0.0185
5	0.0039	0.0043	0.0068	0.008	0.0108	0.0191
6	0.0021	0.0037	0.0029	0.0071	0.0099	0.0136
7	0.0042	0.0043	0.0023	0.006	0.0102	0.014
8	0.0019	0.0028	0.0033	0.0072	0.0103	0.0173
9	0.0023	0.0029	0.0011	0.0063	0.0169	0.018
10	0.0084	0.0092	0.0097	0.0151	0.0194	0.0259

Band 12, amplitude

band=12	side=1					
Det	15.5	15.5	26.75	38	49.25	60
1	0.0012	0.0033	0.0088	0.0125	0.0162	0.0271
2	0.0021	0.001	0.0032	0.0082	0.0115	0.0205
3	0.0035	0.0054	0.0037	0.003	0.0057	0.0162
4	0.0075	0.0082	0.008	0.0011	0.0024	0.0114
5	0.0067	0.0073	0.0093	0.0017	0.002	0.0085
6	0.0085	0.0081	0.0108	0.0008	0.0025	0.0081
7	0.01	0.0087	0.0105	0.0036	0.0062	0.0105
8	0.0097	0.01	0.0049	0.0032	0.0067	0.0134
9	0.0059	0.0055	0.0084	0.0065	0.0136	0.0176
10	0.0137	0.0041	0.0057	0.0096	0.0161	0.0232
band=12	side=2					
Det	15.5	15.5	26.75	38	49.25	60
1	0.0036	0.0031	0.0082	0.0096	0.0145	0.0236
2	0.0018	0.0039	0.0029	0.0066	0.008	0.0171
3	0.0038	0.0057	0.0032	0.0022	0.0045	0.014
4	0.0078	0.0084	0.0059	0.0009	0.0012	0.0084
5	0.0067	0.0074	0.01	0.0025	0.0017	0.006
6	0.0083	0.0086	0.0111	0.0021	0.0028	0.0057
7	0.0095	0.0085	0.01	0.0037	0.0041	0.0074
8	0.0098	0.0093	0.0063	0.0032	0.0048	0.011
9	0.0064	0.0068	0.0068	0.0056	0.0126	0.0149
10	0.0139	0.0042	0.0056	0.0102	0.0135	0.0204

Band 13, amplitude

band=13	side=1					
Det	15.5	15.5	26.75	38	49.25	60
1	0.02	0.019	0.0192	0.0239	0.0248	0.0413
2	0.0154	0.015	0.0171	0.0213	0.026	0.0375
3	0.0142	0.0124	0.0186	0.0201	0.0339	0.0415
4	0.0104	0.0102	0.0129	0.0192	0.0269	0.0404
5	0.0066	0.0059	0.0088	0.0121	0.0179	0.0278
6	0.0037	0.0036	0.0067	0.009	0.0145	0.0211
7	0.005	0.0041	0.0053	0.0082	0.0129	0.012
8	0.0061	0.0054	0.0055	0.0079	0.0078	0.0136
9	0.0079	0.0073	0.0086	0.0108	0.013	0.0096
10	0.0152	0.0156	0.0186	0.0235	0.0275	0.0342
band=13	side=2					
Det	15.5	15.5	26.75	38	49.25	60
1	0.0219	0.018	0.0172	0.0225	0.024	0.04
2	0.0157	0.0155	0.0156	0.0204	0.0249	0.041
3	0.0127	0.0122	0.0176	0.0181	0.0323	0.0429
4	0.0107	0.0079	0.0126	0.0175	0.0247	0.0398
5	0.0065	0.0058	0.0085	0.0113	0.0166	0.0264
6	0.0038	0.0032	0.006	0.0085	0.0131	0.0193
7	0.0046	0.0037	0.0052	0.008	0.0122	0.0127
8	0.006	0.0052	0.0057	0.0075	0.008	0.0114
9	0.0064	0.0072	0.0084	0.0111	0.0157	0.0128
10	0.0126	0.0157	0.0198	0.0225	0.0255	0.0336

Band 13 high, amplitude

band=13h side=1

Det	15.5	15.5	26.75	38	49.25	60
1	0.0157	0.0201	0.0267	0.0219	0.0229	0.0423
2	0.0171	0.0157	0.0181	0.0192	0.0169	0.0321
3	0.0167	0.0173	0.0159	0.0203	0.0232	0.031
4	0.0152	0.014	0.0132	0.0175	0.0171	0.026
5	0.0144	0.0129	0.0138	0.0177	0.0181	0.0245
6	0.0097	0.0081	0.0107	0.0145	0.0172	0.0231
7	0.0079	0.0076	0.0093	0.0126	0.0168	0.0215
8	0.0091	0.0093	0.0099	0.012	0.017	0.0205
9	0.013	0.0133	0.0195	0.018	0.0189	0.0279
10	0.0205	0.02	0.0257	0.0252	0.0299	0.0374

band=13h side=2

Det	15.5	15.5	26.75	38	49.25	60
1	0.0213	0.0202	0.0272	0.0209	0.022	0.042
2	0.0176	0.0159	0.0179	0.0205	0.0158	0.0322
3	0.0172	0.0181	0.0138	0.02	0.022	0.0273
4	0.0161	0.0106	0.0131	0.0169	0.0168	0.0248
5	0.0155	0.0122	0.0138	0.0136	0.0175	0.0247
6	0.0092	0.0079	0.0105	0.0139	0.0166	0.0233
7	0.0082	0.008	0.0101	0.0114	0.0162	0.0215
8	0.0088	0.0089	0.0099	0.0114	0.0164	0.0214
9	0.0149	0.0124	0.019	0.0175	0.0202	0.0301
10	0.0207	0.0201	0.0277	0.0252	0.0294	0.0385

Band 14, amplitude

band=14	side=1					
Det	15.5	15.5	26.75	38	49.25	60
1	0.0198	0.0194	0.0201	0.0208	0.0201	0.0258
2	0.0131	0.0125	0.0169	0.0182	0.0151	0.0215
3	0.0092	0.0082	0.0111	0.0142	0.016	0.021
4	0.0065	0.0049	0.0087	0.0103	0.0077	0.0153
5	0.0058	0.0041	0.0055	0.0099	0.0101	0.0101
6	0.0045	0.0029	0.0062	0.0084	0.0092	0.0094
7	0.0026	0.0025	0.007	0.0091	0.0057	0.0118
8	0.0051	0.0051	0.0079	0.0097	0.0106	0.0124
9	0.0068	0.007	0.0123	0.0135	0.0136	0.0171
10	0.024	0.0252	0.0213	0.0209	0.0224	0.0238
band=14	side=2					
Det	15.5	15.5	26.75	38	49.25	60
1	0.02	0.0206	0.0185	0.0196	0.0212	0.0285
2	0.0134	0.0126	0.0153	0.018	0.0163	0.0273
3	0.0094	0.0088	0.0111	0.0146	0.0173	0.0215
4	0.0049	0.0044	0.0089	0.0109	0.009	0.0185
5	0.0042	0.0032	0.0068	0.0082	0.0114	0.0156
6	0.0028	0.0027	0.008	0.0086	0.0105	0.0152
7	0.0027	0.0023	0.0072	0.0094	0.007	0.0154
8	0.0052	0.0049	0.0084	0.0092	0.012	0.0163
9	0.0071	0.007	0.0115	0.0131	0.0159	0.0198
10	0.0164	0.0176	0.0194	0.0204	0.0242	0.0255

Band 14 high, amplitude

band=14h side=1

Det	15.5	15.5	26.75	38	49.25	60
1	0.0051	0.0052	0.0079	0.0082	0.0104	0.02
2	0.0074	0.0054	0.0045	0.0055	0.0174	0.0161
3	0.0064	0.006	0.0041	0.0071	0.0097	0.0162
4	0.0078	0.0076	0.0055	0.0058	0.0175	0.0172
5	0.0067	0.0071	0.0096	0.0069	0.0141	0.0211
6	0.0069	0.0086	0.0091	0.0077	0.0144	0.0216
7	0.0087	0.0087	0.0067	0.0078	0.0165	0.0178
8	0.0079	0.0084	0.0088	0.0092	0.0116	0.0191
9	0.0094	0.0097	0.0086	0.0095	0.014	0.0207
10	0.0111	0.0142	0.0078	0.0082	0.012	0.0205

band=14h side=2

Det	15.5	15.5	26.75	38	49.25	60
1	0.005	0.0047	0.0067	0.0039	0.0068	0.0101
2	0.0061	0.0069	0.0044	0.0037	0.0122	0.0066
3	0.006	0.0059	0.0038	0.006	0.0052	0.0064
4	0.0072	0.0074	0.0048	0.0048	0.0133	0.0068
5	0.0067	0.008	0.0064	0.0055	0.0076	0.0107
6	0.0082	0.0082	0.0058	0.0068	0.0081	0.0107
7	0.0083	0.009	0.0082	0.0066	0.0116	0.0086
8	0.0086	0.0085	0.0079	0.0071	0.0094	0.0113
9	0.0101	0.009	0.0085	0.0077	0.009	0.0109
10	0.0123	0.0148	0.0072	0.0063	0.0101	0.0091

Band 15, amplitude

band=15	side=1					
Det	15.5	15.5	26.75	38	49.25	60
1	0.0077	0.0023	0.0058	0.0043	0.0112	0.0256
2	0.0034	0.002	0.0037	0.005	0.0144	0.0241
3	0.0018	0.0053	0.002	0.006	0.0095	0.0228
4	0.0076	0.0053	0.0024	0.0035	0.0181	0.0211
5	0.0024	0.0033	0.0058	0.0067	0.0154	0.0247
6	0.0056	0.0033	0.0076	0.0058	0.0156	0.0276
7	0.0055	0.0061	0.0047	0.0072	0.0161	0.0214
8	0.0062	0.0057	0.0095	0.0069	0.0106	0.0256
9	0.0057	0.005	0.0063	0.0069	0.0142	0.0253
10	0.0074	0.0109	0.0086	0.0064	0.0133	0.0223
band=15	side=2					
Det	15.5	15.5	26.75	38	49.25	60
1	0.0062	0.0042	0.0035	0.0045	0.0061	0.0137
2	0.0033	0.0028	0.0038	0.0034	0.0115	0.0137
3	0.0015	0.0003	0.0022	0.0014	0.0052	0.0117
4	0.0044	0.0031	0.0014	0.0007	0.014	0.0112
5	0.0013	0.0037	0.0037	0.0026	0.0081	0.016
6	0.0047	0.0031	0.006	0.0027	0.0086	0.0178
7	0.0053	0.0047	0.0042	0.0042	0.0132	0.0117
8	0.0048	0.0057	0.0051	0.0076	0.0071	0.0161
9	0.0055	0.0061	0.0049	0.0049	0.0095	0.0154
10	0.0071	0.0104	0.0044	0.0027	0.0098	0.0113

Band 16, amplitude

band=16	side=1					
Det	15.5	15.5	26.75	38	49.25	60
1	0.0067	0.0091	0.0139	0.0107	0.0212	0.033
2	0.0156	0.0127	0.0117	0.0146	0.0189	0.0326
3	0.012	0.0173	0.0106	0.0134	0.0201	0.0317
4	0.0105	0.0118	0.0142	0.0217	0.0246	0.0338
5	0.0118	0.0083	0.0074	0.0131	0.019	0.0326
6	0.0125	0.015	0.0137	0.0165	0.0208	0.0367
7	0.0106	0.0098	0.0158	0.0198	0.0222	0.0325
8	0.007	0.0145	0.0104	0.019	0.0232	0.0332
9	0.0079	0.0092	0.0094	0.0141	0.0198	0.0319
10	0.0111	0.008	0.0109	0.011	0.0118	0.0261
band=16	side=2					
Det	15.5	15.5	26.75	38	49.25	60
1	0.0081	0.0075	0.0102	0.01	0.0168	0.0276
2	0.0097	0.0123	0.0093	0.0125	0.0165	0.0254
3	0.0146	0.0159	0.011	0.0122	0.0166	0.0271
4	0.0119	0.0127	0.0065	0.0177	0.0218	0.0265
5	0.0165	0.0092	0.0106	0.0089	0.0159	0.0295
6	0.0115	0.0123	0.01	0.0187	0.0194	0.0289
7	0.0052	0.0126	0.0082	0.0134	0.0176	0.0233
8	0.0068	0.0148	0.0055	0.0114	0.0153	0.0237
9	0.0076	0.0145	0.0041	0.0106	0.0111	0.0223
10	0.0116	0.0089	0.0062	0.0114	0.0114	0.0172

Band 17, amplitude

band=17	side=1					
Det	15.5	15.5	26.75	38	49.25	60
1	0.003	0.0061	0.0039	0.0062	0.0119	0.0258
2	0.0057	0.0059	0.0066	0.0082	0.0164	0.0273
3	0.0079	0.0069	0.0066	0.0086	0.0149	0.0279
4	0.0052	0.0073	0.0063	0.0082	0.0146	0.0272
5	0.0089	0.0053	0.0067	0.0083	0.0139	0.029
6	0.0042	0.0063	0.0058	0.0084	0.013	0.0265
7	0.0023	0.0066	0.0047	0.0097	0.0143	0.0246
8	0.004	0.0075	0.0069	0.0096	0.0142	0.025
9	0.0064	0.0068	0.0074	0.009	0.0143	0.0259
10	0.0072	0.0146	0.003	0.0044	0.0059	0.0217
band=17	side=2					
Det	15.5	15.5	26.75	38	49.25	60
1	0.0041	0.0024	0.0051	0.003	0.0083	0.019
2	0.0035	0.0067	0.0036	0.0057	0.0107	0.0192
3	0.0067	0.0057	0.005	0.0063	0.0098	0.0196
4	0.0078	0.0059	0.0053	0.0068	0.0104	0.0205
5	0.0041	0.0044	0.0061	0.0062	0.0108	0.0189
6	0.0072	0.0068	0.0027	0.0045	0.008	0.0187
7	0.0056	0.0071	0.0018	0.0038	0.0082	0.0178
8	0.0064	0.0065	0.0034	0.0054	0.0101	0.0177
9	0.0068	0.0061	0.0045	0.0055	0.0126	0.0171
10	0.008	0.0017	0.0048	0.0047	0.0029	0.0107

Band 18, amplitude

band=18	side=1					
Det	15.5	15.5	26.75	38	49.25	60
1	0.4696	0.2968	0.2911	0.4639	0.4394	0.4975
2	0.1397	0.3679	0.2139	0.1194	0.3712	0.3806
3	0.2641	0.8415	0.758	0.1381	0.1436	0.399
4	0.1964	0.3002	1.0284	0.2904	0.242	0.0421
5	0.0236	0.1658	0.6688	0.4969	0.5966	0.3645
6	0.165	0.7418	0.4146	0.3736	0.8446	1.175
7	0.271	0.2558	0.2431	0.3029	0.429	0.2093
8	0.1963	0.3848	0.1942	0.0663	0.1779	0.3613
9	0.1609	0.3077	0.498	0.1125	0.2063	0.301
10	0.2509	0.2144	0.2419	0.3096	0.538	0.2744
band=18	side=2					
Det	15.5	15.5	26.75	38	49.25	60
1	0.3886	0.1561	0.5657	0.4683	0.1842	0.0482
2	0.0672	0.1728	0.0406	0.179	0.0551	0.0861
3	0.714	0.1839	0.2472	0.1536	0.1663	0.1327
4	0.3765	0.0448	0.0693	0.1784	0.0621	0.2461
5	0.7624	0.0783	0.0862	0.2274	0.0875	0.0824
6	0.4768	0.1539	0.1474	0.392	0.265	0.0607
7	0.3404	0.0994	0.2722	0.0514	0.0579	0.2411
8	1.59	0.0669	0.1116	0.1582	0.2082	0.3456
9	0.5677	0.1406	0.0694	0.1866	0.2074	0.2654
10	0.3695	0.1625	0.1605	0.1711	0.1683	0.2476

Band 19, amplitude

band=19	side=1					
Det	15.5	15.5	26.75	38	49.25	60
1	0.021	0.0195	0.0194	0.0232	0.0256	0.0419
2	0.0159	0.0155	0.0172	0.0211	0.026	0.0376
3	0.0142	0.0128	0.0193	0.0197	0.0343	0.0427
4	0.0105	0.0104	0.0133	0.0194	0.0262	0.041
5	0.0062	0.0061	0.009	0.0124	0.0175	0.0277
6	0.0039	0.0036	0.0068	0.0089	0.0144	0.0222
7	0.0049	0.0041	0.0054	0.0086	0.0132	0.0128
8	0.0063	0.0056	0.0056	0.0079	0.0077	0.0141
9	0.0083	0.008	0.0089	0.0107	0.0165	0.0106
10	0.0152	0.0155	0.0184	0.0234	0.0276	0.0341
band=19	side=2					
Det	15.5	15.5	26.75	38	49.25	60
1	0.021	0.0191	0.0177	0.0223	0.0241	0.0405
2	0.015	0.0154	0.0165	0.0212	0.0251	0.0403
3	0.0129	0.0121	0.0176	0.0175	0.0322	0.043
4	0.0107	0.0078	0.0121	0.0174	0.0248	0.0399
5	0.0065	0.0058	0.0083	0.0115	0.0168	0.027
6	0.004	0.0032	0.006	0.0084	0.0133	0.0201
7	0.0049	0.0037	0.0054	0.0079	0.0121	0.0137
8	0.0064	0.0055	0.0058	0.008	0.008	0.0116
9	0.0075	0.0074	0.0083	0.0106	0.0156	0.0122
10	0.0123	0.0161	0.0195	0.0225	0.0257	0.0337

B21 Calibration (Preliminary)

- B21 Calibration Information
  - Specified Lmax = 86.0 Watts/m^2/sr/μm (Tmax = 500K)
  - BCS at 340K produces radiance = 2.9 Watts/m^2/sr/μm
  - Band 21 specified radiance uncertainty at Lmax = ±10%

- B21 Pre-launch Calibration Summary
  - Different approaches for T_{SAT} evaluation

- B21 Initial On-orbit Calibration
  - Evaluate changes from pre-launch to on-orbit using OBC BB
  - New coefficients derived due to Itwk/Vdet setting change
  - New T_{SAT}
  - Moon in space view port (M-SV)

B21 Calibration (pre-launch)

- Three methods used to determine B21 fixed gain **at prelauch**:
  - Pagano method: extrapolation of detector voltage
    - Tsat = 471K
  - Young
    - Tsat = 464K
  - Chiang method: SpMA RSR response for Bands 20-23
    - B20 --> Tsat = 456K
    - B22 --> Tsat = 470K
    - B23 --> Tsat = 464K
  - Xiong's linear extrapolation of linear gain from BCS@340K
    - Tsat = 475K
- L1B uses LUT with fixed b1 determined from TV RC02
  - Each detector treated independently (no mirror side difference)

B21 On-orbit Calibration (Preliminary)

- **OBC BB (maximum of 315K on-orbit)**
  - **New LUT proposed due to Itwk/Vdet setting change**
  - **Responses variation of ±4% from time to time**

- **B21 calibration via views of Moon through SVP (in process)**
  - **Use unsaturated band 31, need lunar emissivity information**

On-orbit B21 Calibration from OBC BB

- New coefficients
- New T_{SAT}

Detetor	<b1>	T_sat (K)
1	0.01131	455
2	0.01595	476
3	0.01663	478
4	0.01587	475
5	0.01613	476
6	0.01613	476
7	0.01612	476
8	0.01633	477
9	NA	NA
10	0.01660	478

- Responses variation

On-orbit B21 Responses Variation

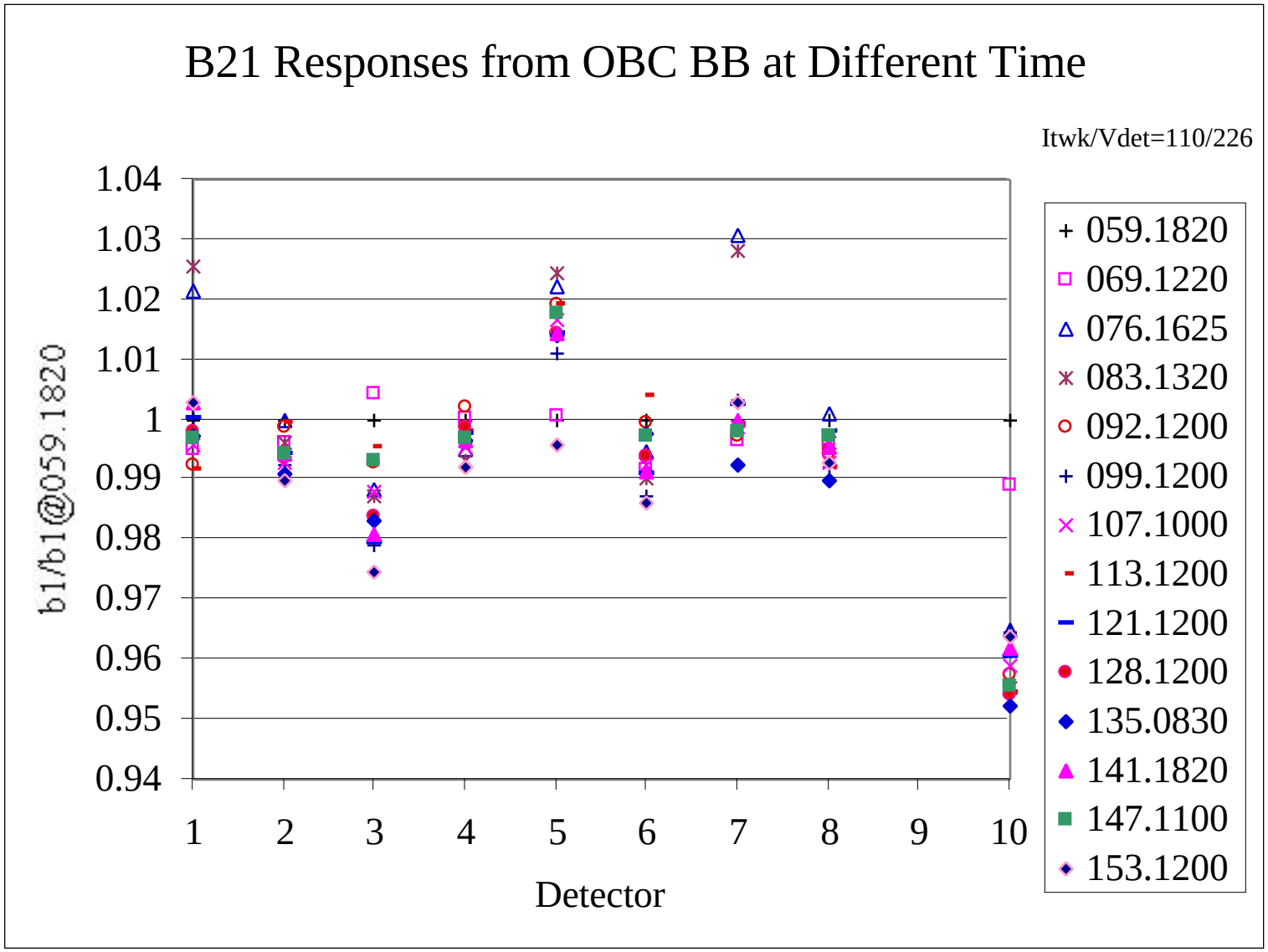

B21 Calibration using M-SV (in process)

Band 31 and 21 (Channel 5 Procuct Order) During 84/20:20 Moon View Event

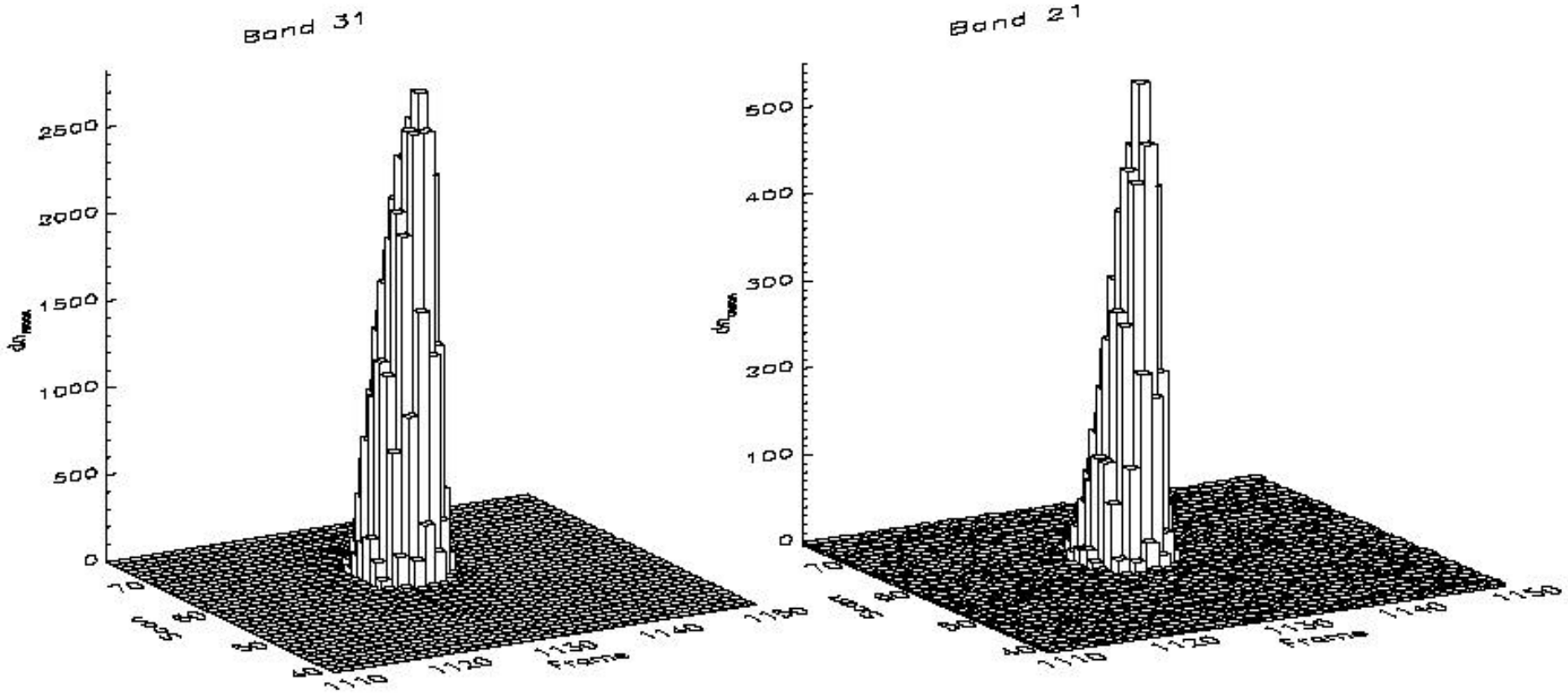

Co-Registration

- MCST Results
  - Using moon in space view port (M-SV)
  - SRCA
- SDST Results

Co-Registration Using Moon in Space View Port (M-SV)

- Track frame number (and signal) of each detector as moon sweeps across focal plane
- Uses purely geometrical approach
- Primary error sources
  - Detector noise
  - Circular (non-rectangular) shape of moon
  - Non-uniform source distribution across lunar surface

Algorithm Concept

Each band (or detector) responds to the lunar signal differently; normalization between detectors achieved from adjacent fully illuminated pixels

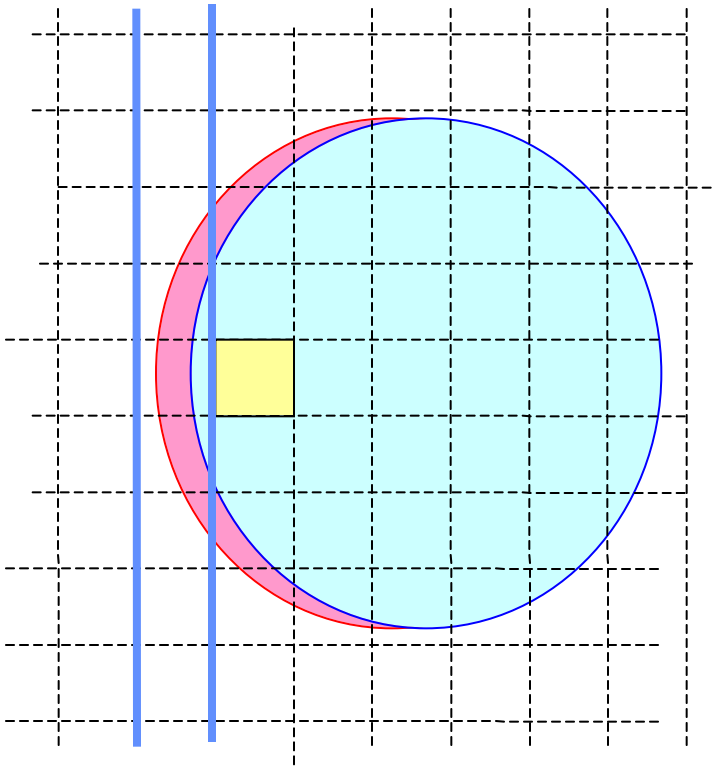

Results from the March Lunar view

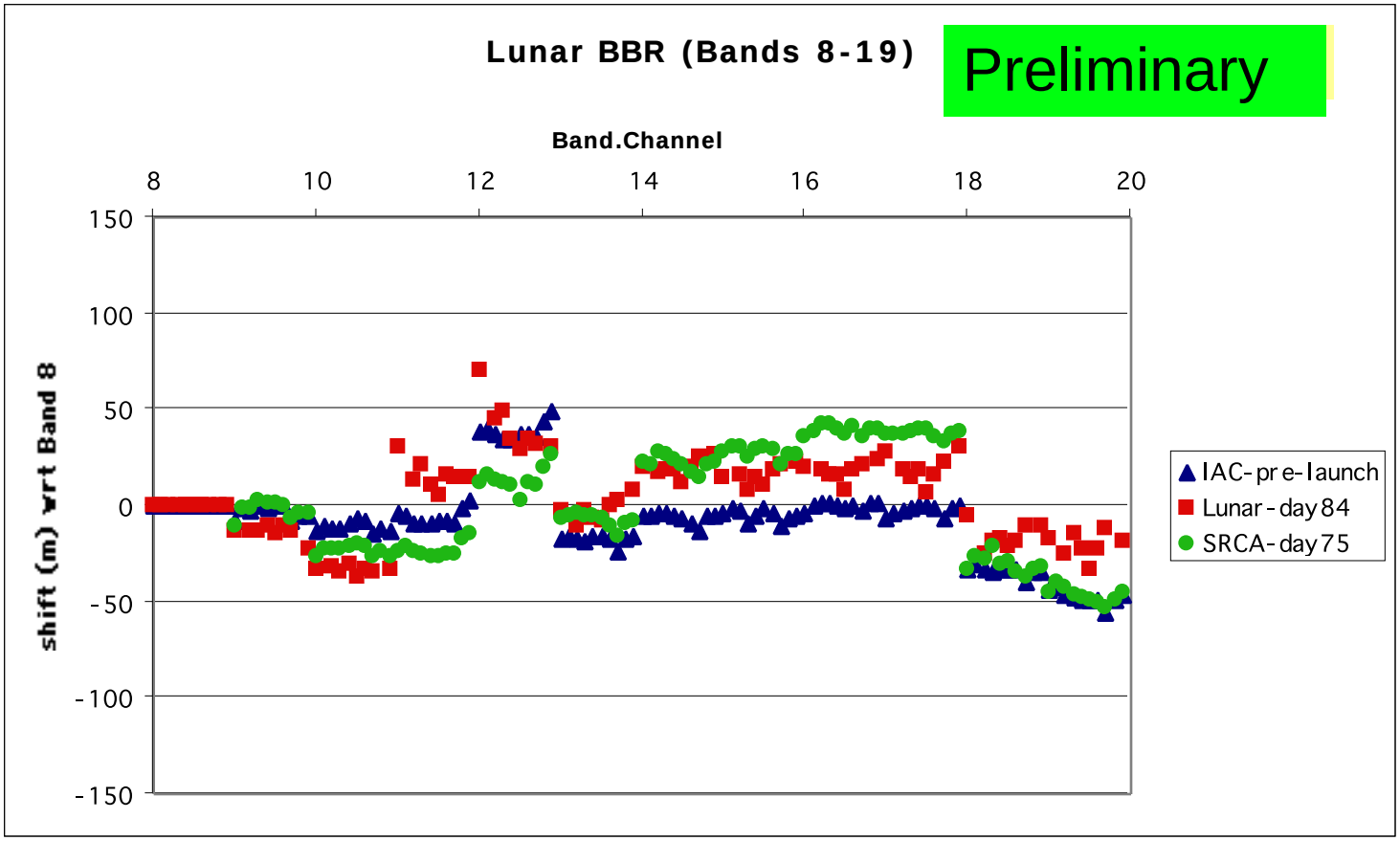

Additional Results - Similar Approach, Different Implementation

band	8	9	10	11	12	13
collect_1	0	-0.009	-0.019	0.008	0.033	0.004
collect_2	0	-0.014	-0.019	0.003	0.025	0.003

band	14	15	16	17	18	19
collect_1	0.023	0.027	0.025	0.029	-0.009	-0.011
collect_2	0.027	0.028	0.028	0.036	0.001	-0.022

band	20	21	22	23	24	25
collect_1	-0.135	-0.145	-0.107	-0.152	-0.111	-0.125
collect_2	-0.115	-0.141	-0.076	-0.131	-0.085	-0.099

band	26	27	28	29	30	
collect_1	0.083	-0.172	-0.121	-0.099	-0.136	
collect_2	0.162	-0.11	-0.083	-0.066	-0.123	

band	31	32	33	34	35	36
collect_1	-0.039	-0.014	-0.024	0.004	0.001	0.006
collect_2	-0.009	0.043	0	0.041	0.039	0.053

This implementation less dependent on sharp lunar edge across focal plane and is able to obtain registration for TEB as well.

Preliminary Results for Band−to−Band Registration from Image Correlation Method

K. Yang, R. Wolfe, M. Nishihama, A. Fleig

Determination of Shifts

Image correlation is used to find the location of the best match of the images of two bands. The pixel shifts in scan and track are at the maximum correlation value.

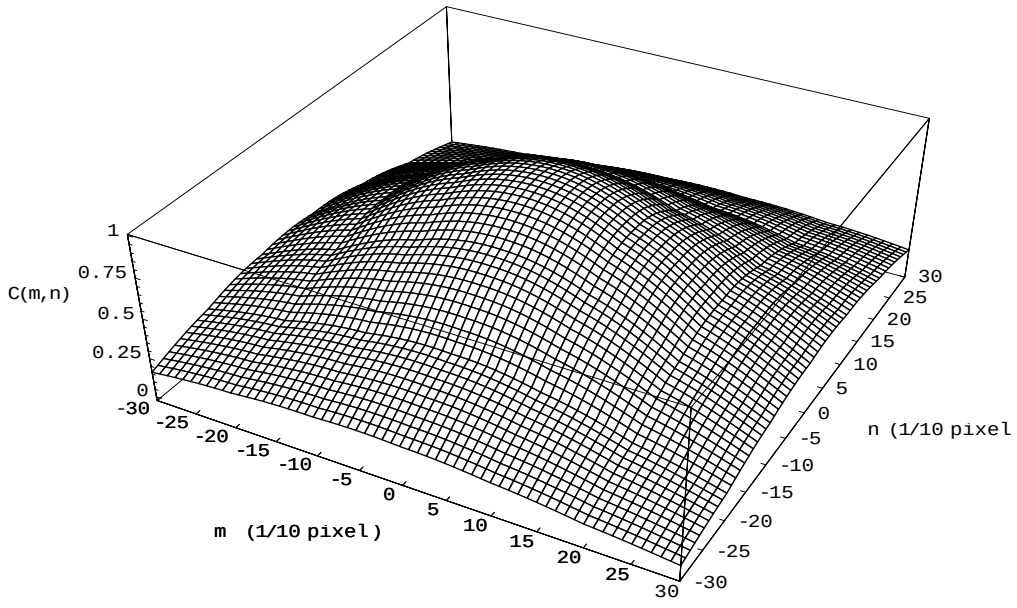

About 1440 image correlations are done in a day for a pair of bands. Results that satisfy certain criteria are include in the calculations of average and standard deviatons of the shifts.

Defination of Shifts

Same pixel (line, sample), but different ground location for different spectral bands.

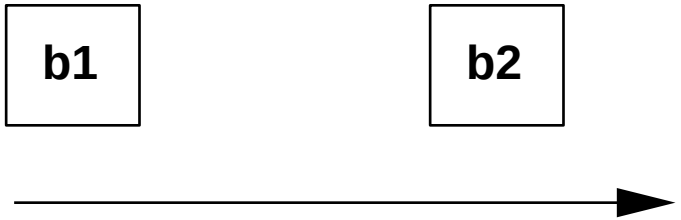

a. Positive shift for b2 relative to b1 in scan.

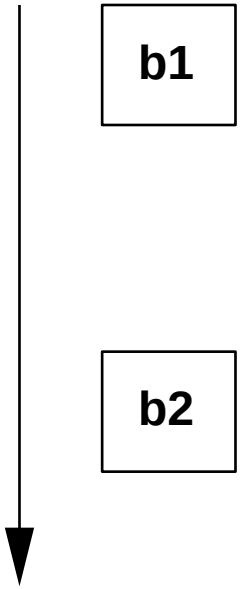

b. Positive shift for b2 relative to b1 in track.

Results

One day results (day 103)

1. **Average shifts in scan and track for bands 1−20 relative to bands 1 and 2.**

2. **Average shifts in scan and track for bands 29−36 among themselves.**

Ten day results (days 86 − 95)

1. **Average shifts and their standard deviations.**

Scan Shift (meters), Day 103

	1	2	3	4	5	6	7	8
1	-	-2.6	-21.3	-18.2	-8.6	-4.7	-12.8	-22.9
2	-	-	-19.3	-15.9	-5.5	0.7	- 8.6	-24.7

	9	10	11	12	13	14	15	16
1	-24.7	-45.8	-7.6	15.9	-22.0	15.0	8.5	22.7
2	-23.9	-40.1	-4.4	22.2	-20.0	14.7	15.3	25.5

	17	18	19	20
1	25.5	-14.5	-28.3	-97.6
2	31.5	-10.6	-24.0	-87.9

Track Shift (meters), Day 103

	1	2	3	4	5	6	7	8
1	-	1.3	9.0	7.5	45.9	39.4	40.3	27.5
2	-	-	8.8	6.4	47.9	40.8	40.8	22.2

	9	10	11	12	13	14	15	16
1	22.2	15.2	20.8	17.3	2.7	2.6	-2.8	8.6
2	22.2	13.7	19.5	10.3	-1.1	-5.9	-12.4	4.0

	17	18	19	20
1	5.0	5.3	1.8	20.7
2	5.2	3.8	1.4	25.9

Scan Shift (meters), Day 103

	29	30	31	32	33	34	35	36*
29	-	-33.7	-19.7	-92.6	23.0	57.2	91.0	302.0
30	-	-	-50.5	-128.0	61.2	98.3	153.0	343.0
31	-	-	-	-67.7	-2.3	28.2	68.6	278.0
32	-	-	-	-	-83.9	-67.4	-17.5	208.0
33	-	-	-	-	-	-25.9	62.1	303.0
34	-	-	-	-	-	-	36.1	282.0
35	-	-	-	-	-	-	-	282.0
36	-	-	-	-	-	-	-	-

* Large relative shifts seen in band 36 may be due to factors such as ghosting or cross talk.

Track Shift (meters), Day 103

	29	30	31	32	33	34	35	36
29	-	-7.5	28.6	32.3	-35.6	-47.2	-72.9	-67.7
30	-	-	18.0	23.5	-13.7	-28.4	3.3	4.3
31	-	-	-	-2.8	5.0	-4.9	-4.5	-10.9
32	-	-	-	-	7.7	-0.3	1.9	-0.3
33	-	-	-	-	-	7.6	-24.5	-19.5
34	-	-	-	-	-	-	0.5	-3.4
35	-	-	-	-	-	-	-	-16.6
36	-	-	-	-	-	-	-	-

Day 103

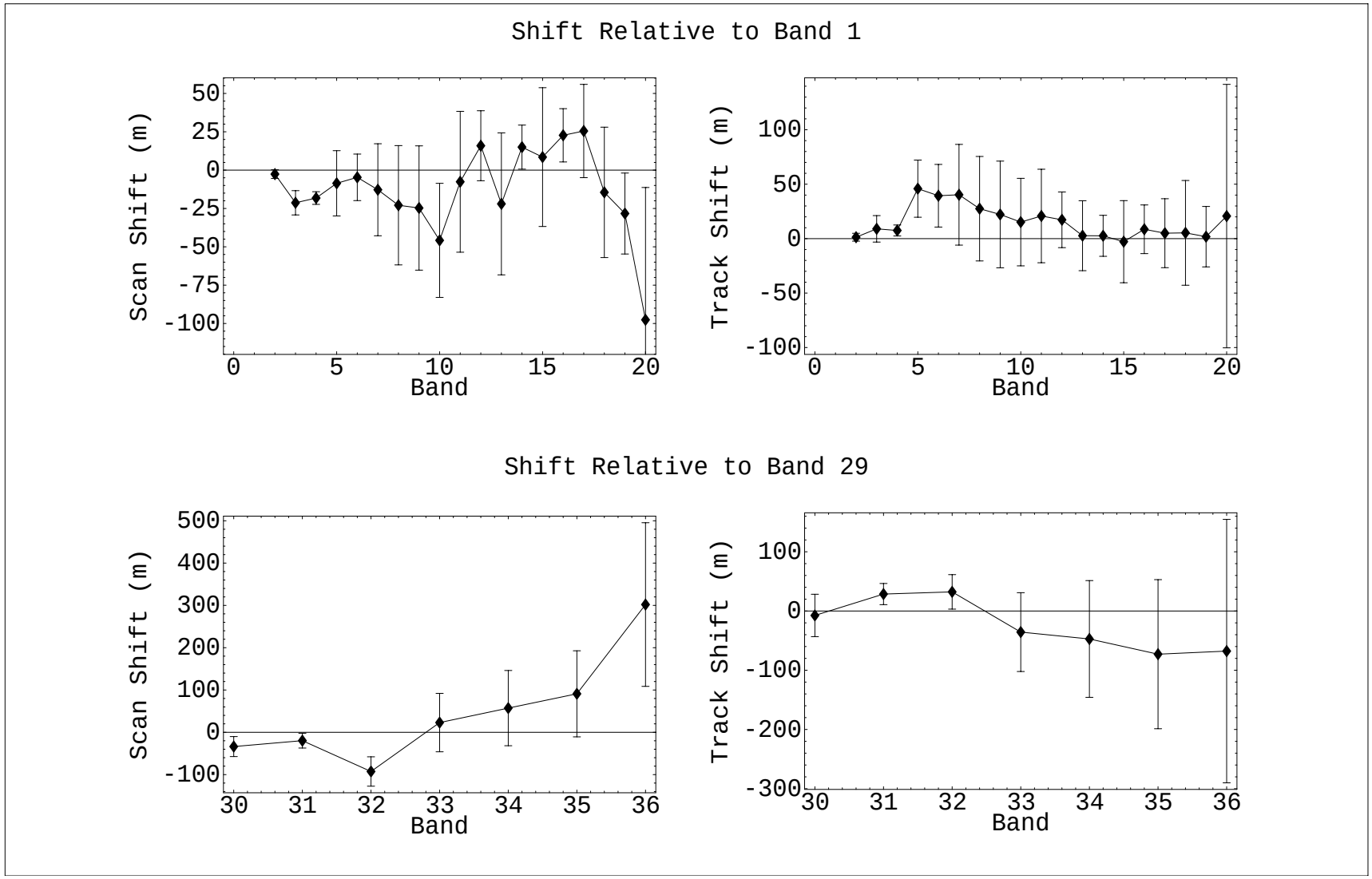
Shift Relative to Band 1
Scan Shift (m)
50
25
0
-25
-50
-75
-100
0
5
10
15
20
Band
Track Shift (m)
100
50
0
-50
-100
0
5
10
15
20
Band
Shift Relative to Band 29
Scan Shift (m)
500
400
300
200
100
0
-100
30
31
32
33
34
35
36
Band
Track Shift (m)
100
0
-100
-200
-300
30
31
32
33
34
35
36
Band

10-day Average Shifts and Standard Deviations

Bands 2 & 1

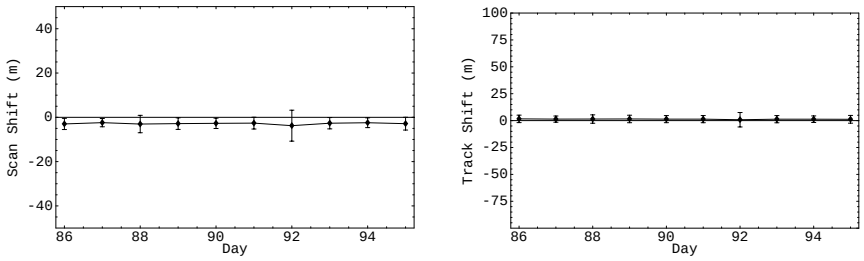

Bands 3 & 1

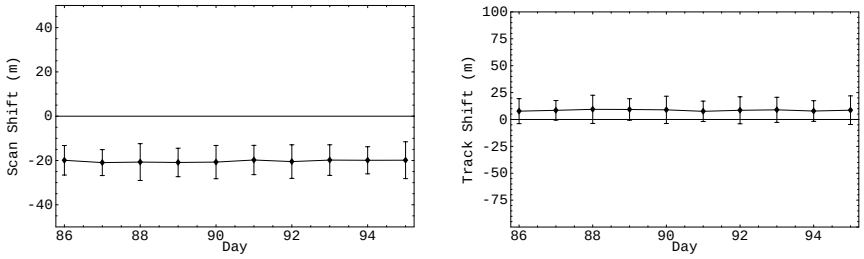

Bands 4 & 1

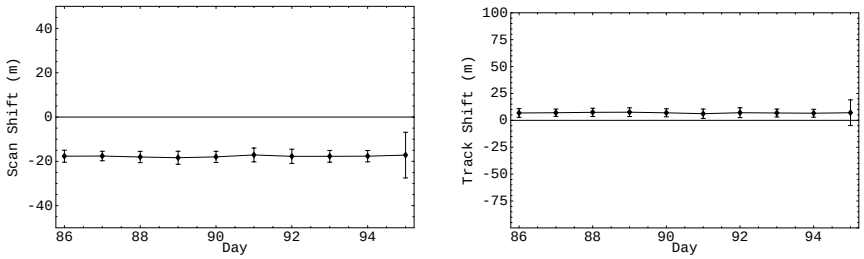

Bands 5 & 1

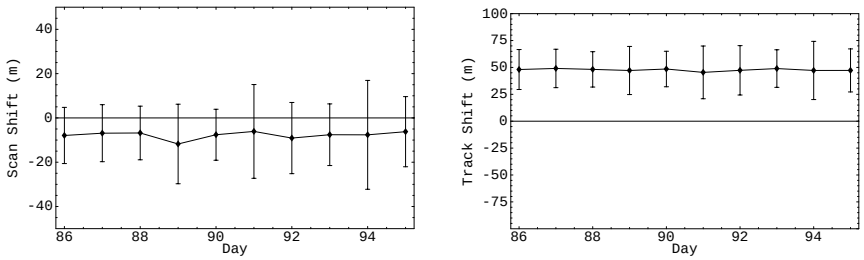

Bands 6 & 1

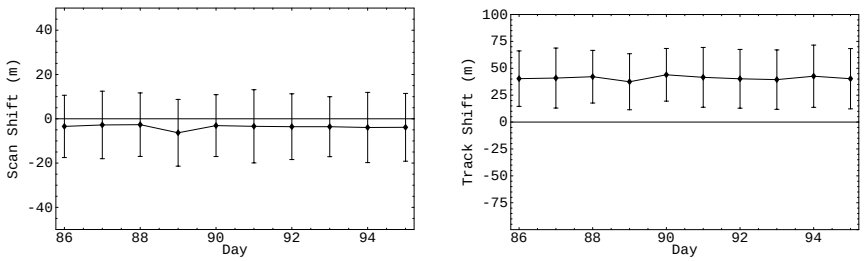

Bands 7 & 1

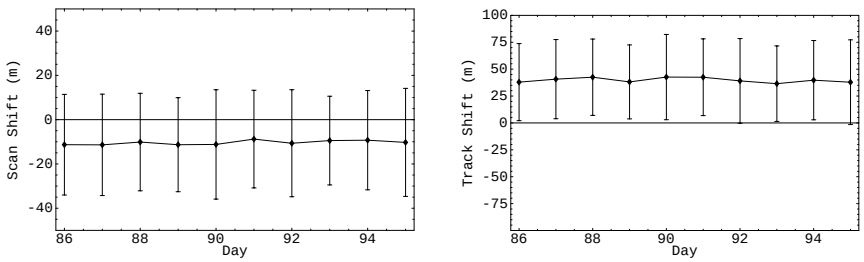

Summary

1. **Bands 1 and 2 are well aligned to within a few meters.**

2. **Bands 3 to 7 shifts less than 50m (both scan and track) relative to bands 1 and 2.**

3. **Bands 8−20 shifts less than 100m or 0.1 pixel relative to bands 1 and 2.**

4. **Relative shifts are stable over a 10−day period. More results (not shown here) indicates that these shifts are stable over a much longer period.**

5. **Bands 29−35 are in general well aligned to within 100m or 0.1 pixel. Some exceed the 100m, and in particular, large shifts (about 300m) in scan for band 36 relative to other bands. These shifts may not be actual detectors shifts on the focal plane but due to other factors such as ghosting, cross talk, etc..**

6. **No results shown for bands 21−26 .**

Band-to-band co-registration using the SRCA spatial mode

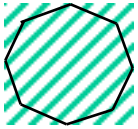

Reticles and CARFs of SRCA in spatial mode

Along-scan

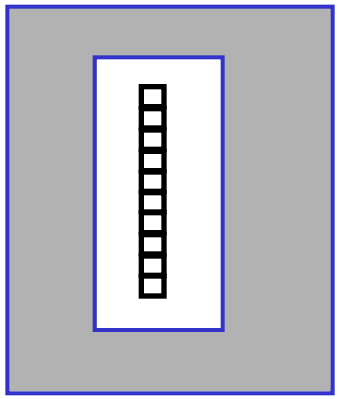

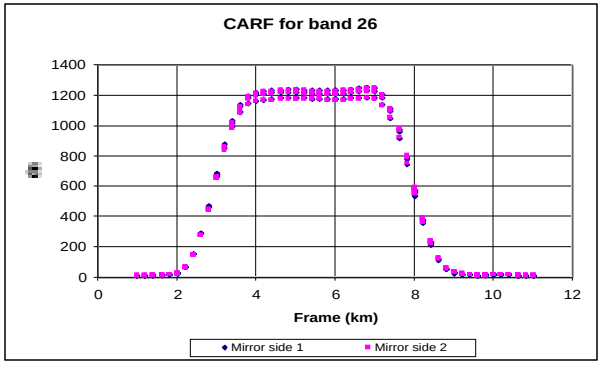

CARF -- Combined Aperture Response Function

Along-track

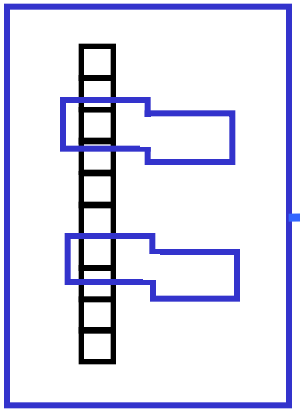

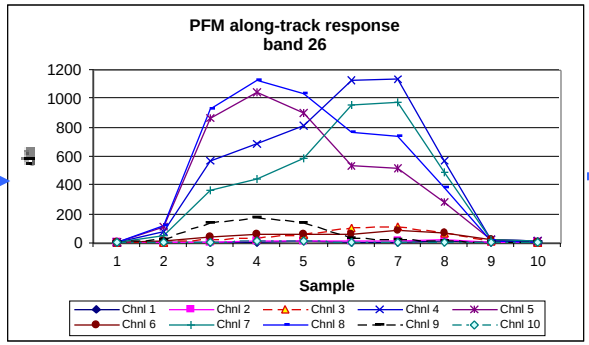

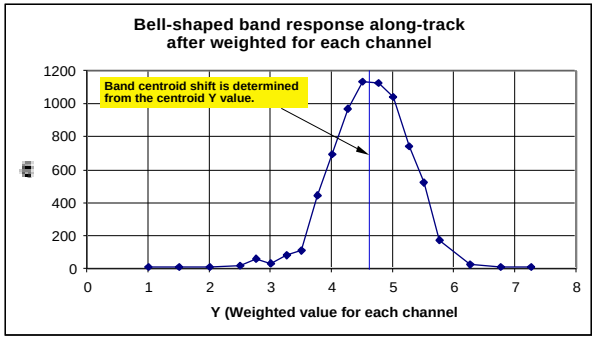

Along-scan direction

Summary -- general

- **Ninety four** percent of the detectors meet the co-registration specification.
- The SRCA spatial signal pattern remains the same or is better than pre-launch quality.
- The SRCA spatial calibration is successful. The calibration results are consistent with prelaunch in TV.
- The repeatability of the four tests on-orbit is ±10m for both along-scan and along-track.

Summary -- on-orbit shift

- The range of channel/band shifts relative to Nominal for each FPA is summarized as follows (Average±variation range) in meters:

	FPA	Day#060	Day#075	Day #089	Day #096
Along-scan	VIS	16±15	15±12	1±6	-2±6
	NIR	0±8	-1±8	0±8	1±8
	SMWIR	21±53	20±53	9±55	12±55
	LWIR	-11±40	-7±36	-17±40	-13±38
Along-track	VIS	48±19	42±14	34±13	35±14
	NIR	-9±9	-8±8	-8±8	-8±8
	SMWIR	-45±15	-45±15	-42±19	-45±16
	LWIR	-61±20	-55±18	-55±17	-52±16

Summary -- channel/band co-registration

- The co-registration on-orbit is 48m worse than at pre-launch Nominal plateau (along-scan) and is 12m better than at pre-launch Nominal plateau (along-track) on average.

- The channel shift along-track is based on the IAC test results at prelaunch. The SRCA measures only the band centroid shift.

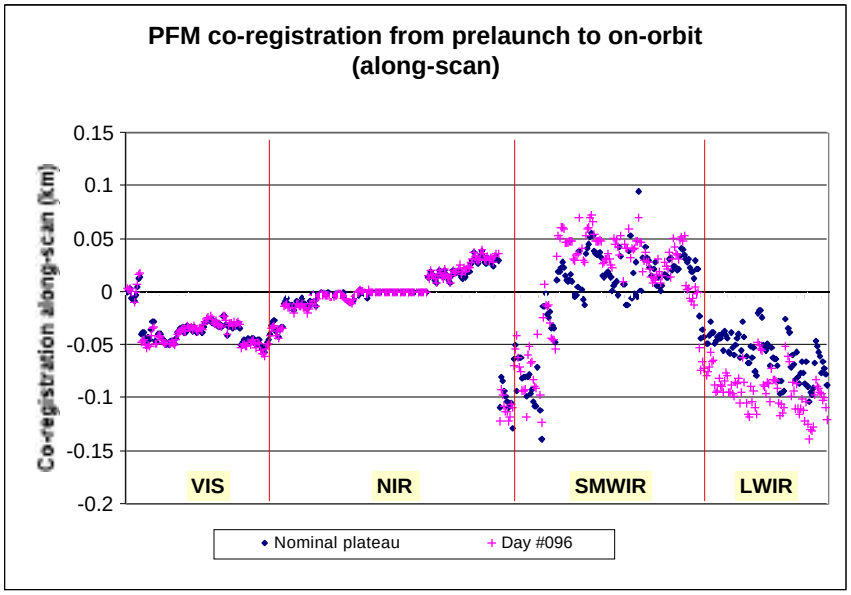

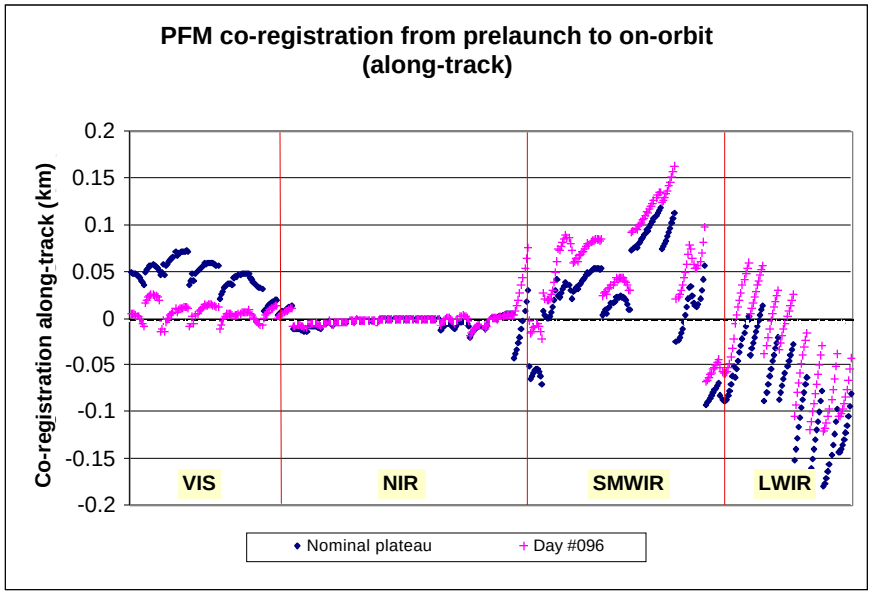

Summary -- FPA co-registration

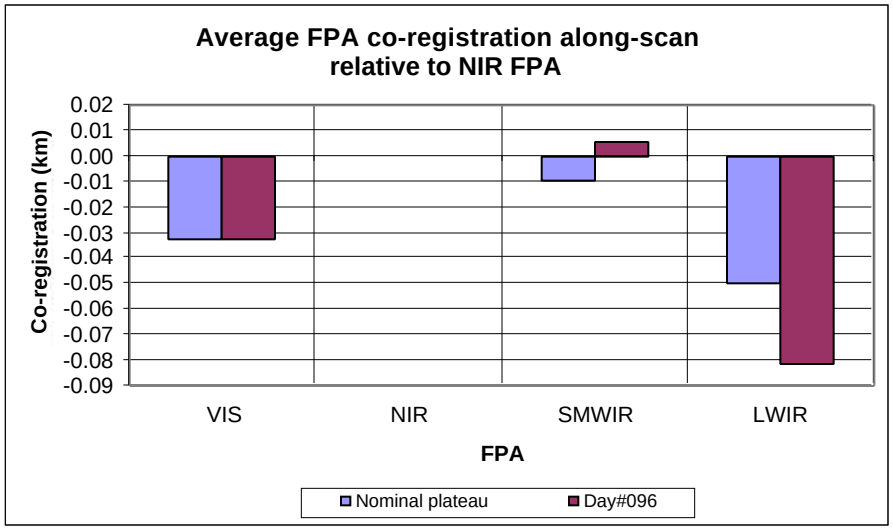

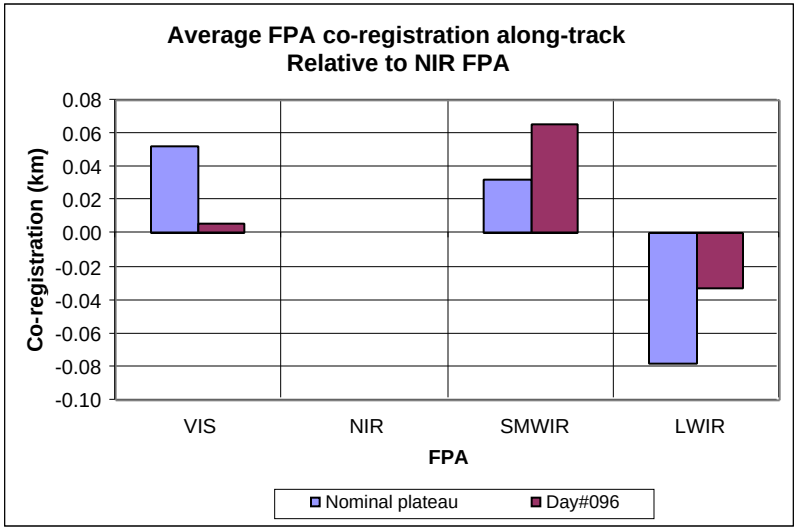

Definition

- Shift: Position measured relative to band 1 for the same channel without IAC bias correction.

- Co-registration: Position measured relative to band 1 for the same channel with SRCA bias correction based on IAC data.

- Band-to-band relative co-registration: Position of band i relative to band j for the same channel with SRCA bias correction based on the IAC.

SRCA limitation

- Both shifts along-scan and along-track are relative to band 1 to exclude possible misalignment between the SRCA and MODIS.
- The SRCA determines channel shift along-scan and band centroid shift along-track.

SRCA spatial mode results -- Co-registration between bands/channels

- Ninety-four percent of the detectors meet the co-registration specification (red square of ±0.1km frame).
- Edge channel (channel 10 for 1km bands)for bands 7, 21, and 30 has unreasonable shift values for all four tests. Their shift values are interpolated from their neighbor channels.
- The shift along-track for bands 6, 7, and 22 are interpolated due to the presence of inoperable channels.

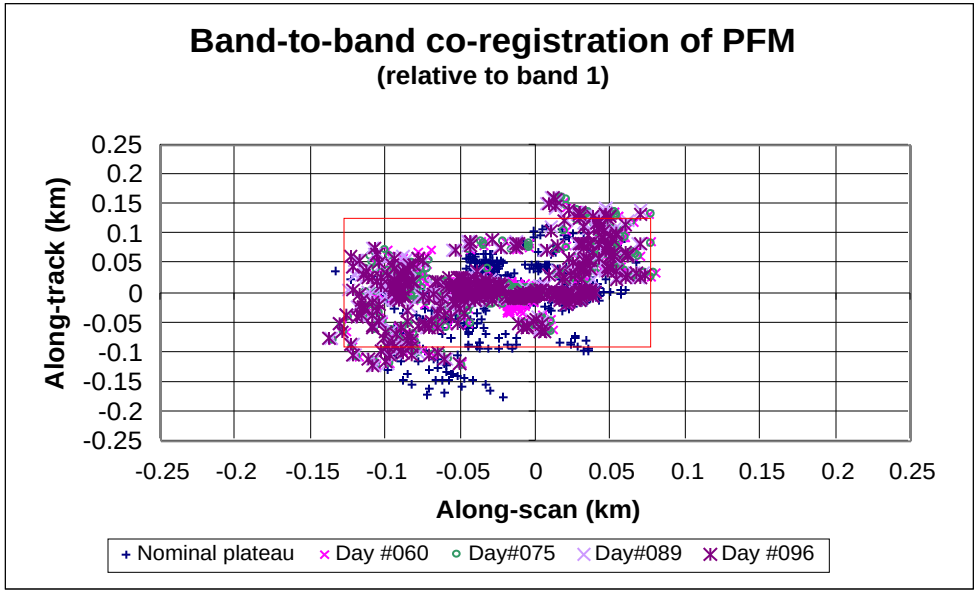

SRCA spatial mode results -- Shift along-scan comparison between Nominal and orbit (1)

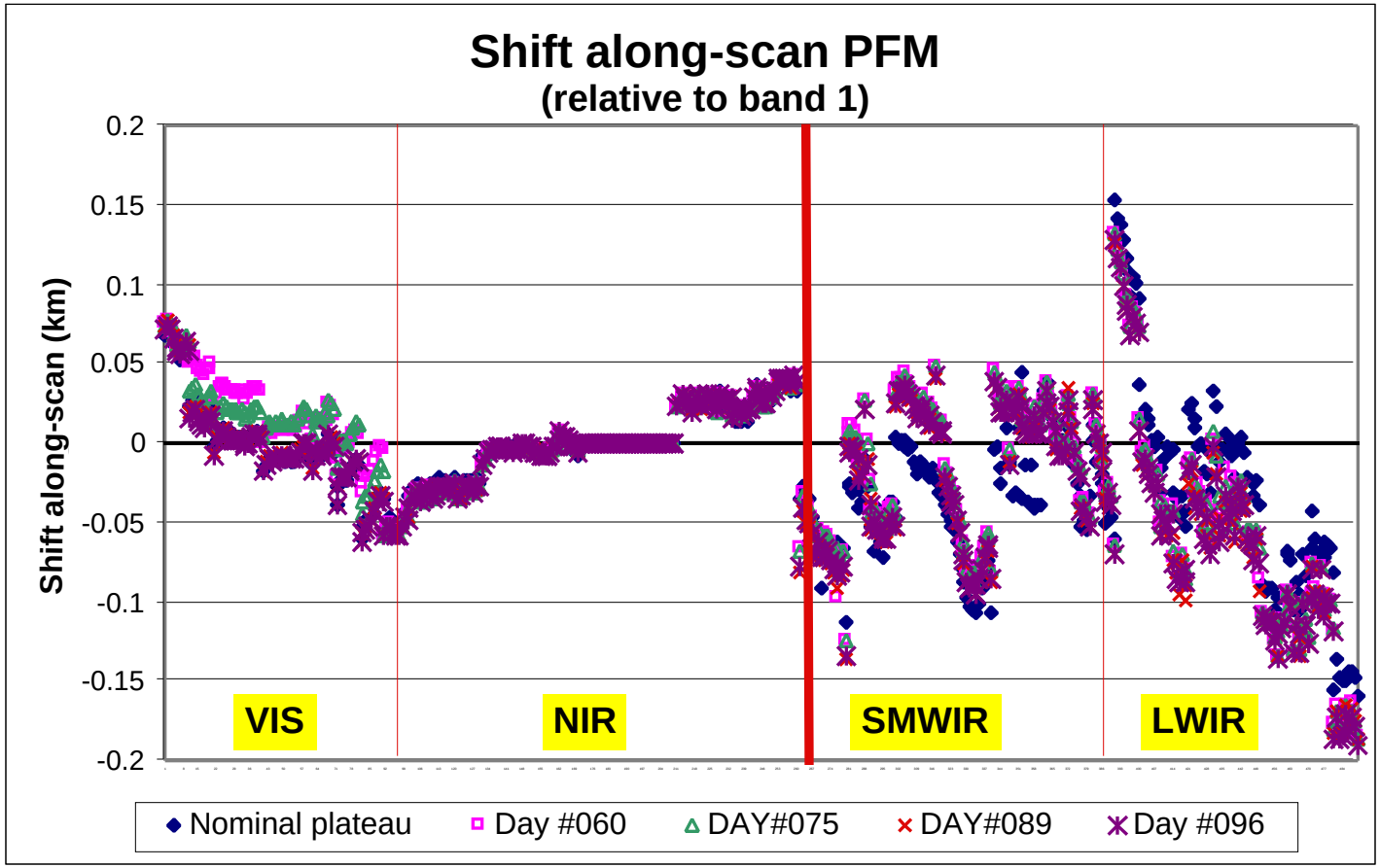

SRCA spatial mode results -- Shift along-scan from Nominal to orbit (2)

- Comparing to Nominal, the shift along-scan is more scattered for SMWIR and LWIR FPAs.

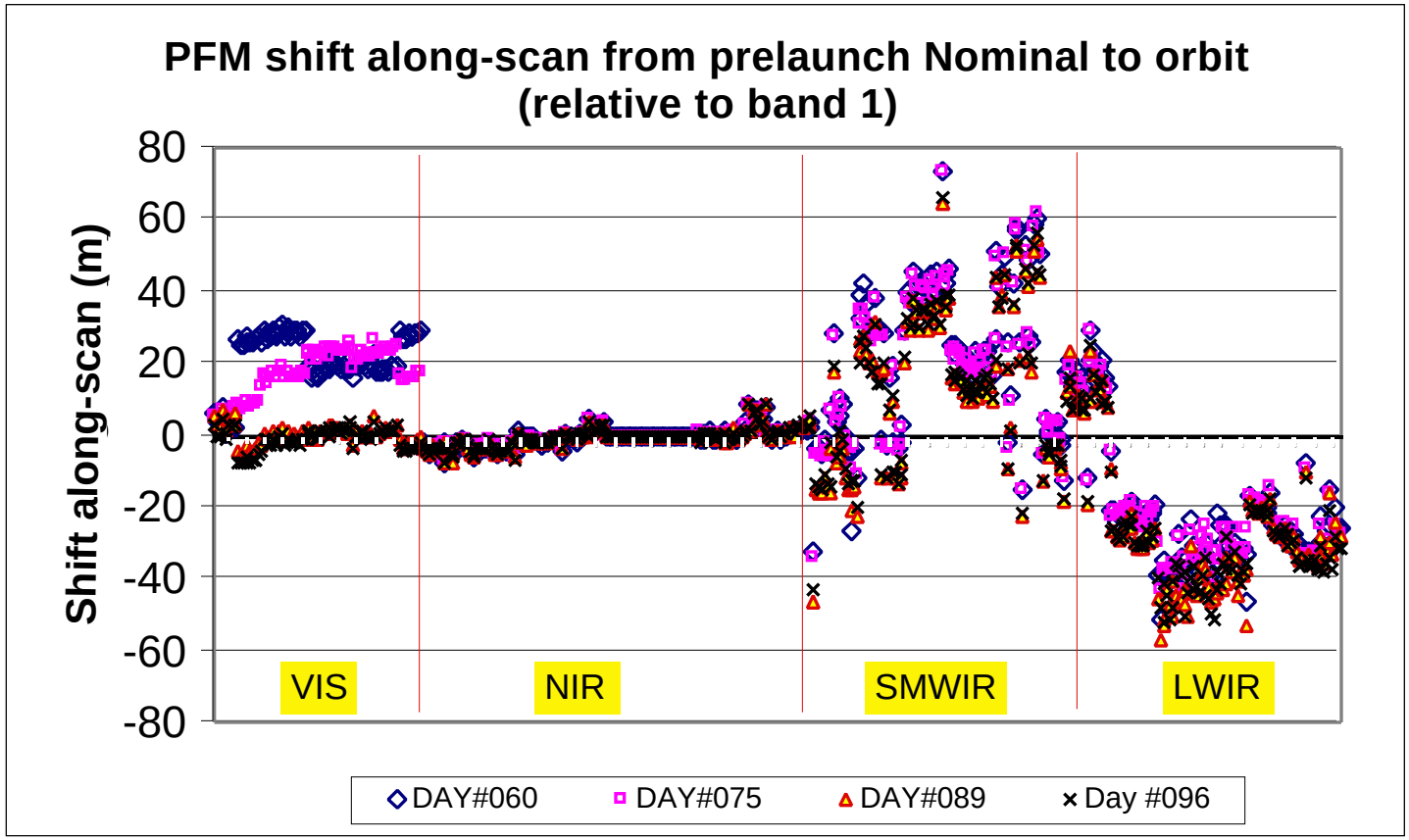

SRCA spatial mode results -- Shift along-scan stability on-orbit

- The band location in the figure is in the same sequence as band location in the FPA.
- For VIS FPA, Day#060 has inconsistent shifts within FPA. It is caused by the phase-delay problem for bands 3, 8, and 9 (20m shift in the figure).
- Day#089 is almost the same as Day#096. Day#060 and Day#075 have nearly the same shifts (less than 10m) for SMWIR and LWIR FPAs.

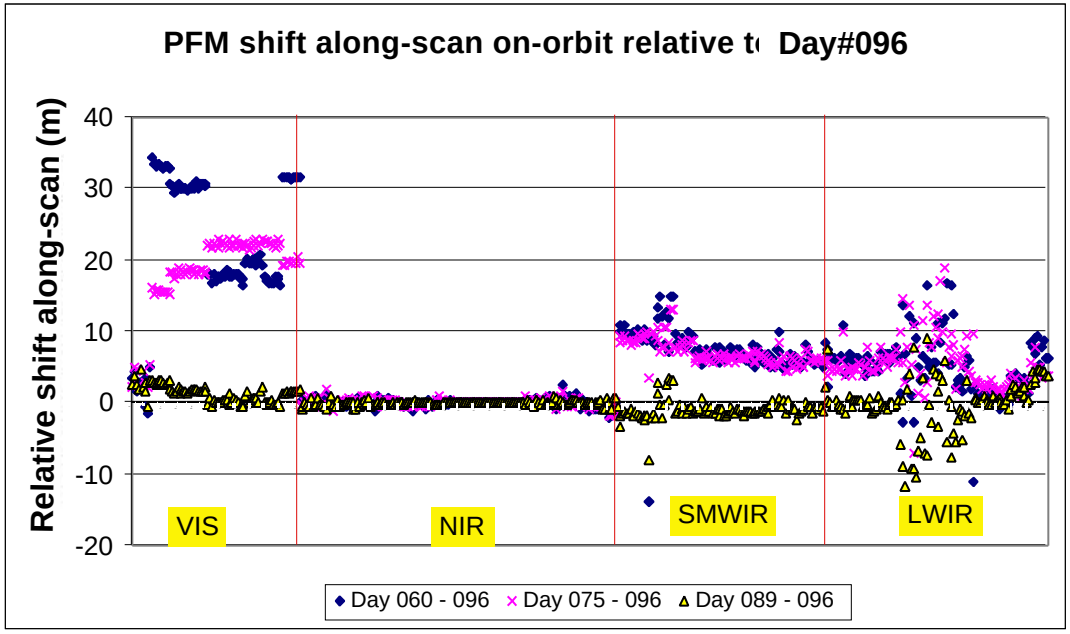

SRCA spatial mode results -- Shift along-scan vs. channel from Nominal to orbit

- The pattern of shift along-scan from prelaunch Nominal to orbit has minimum change.

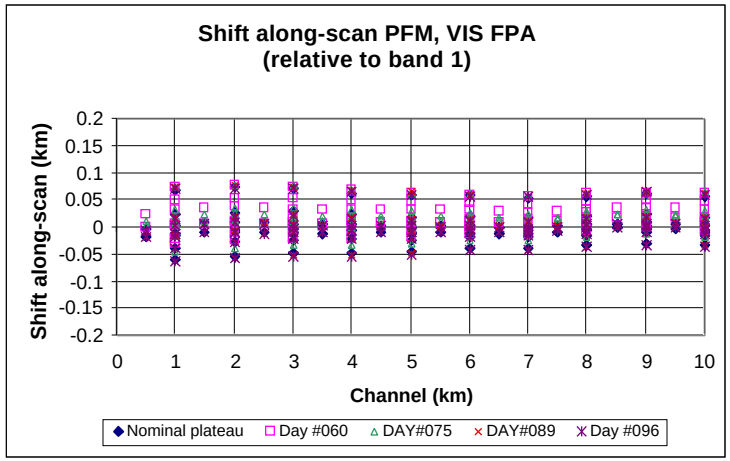

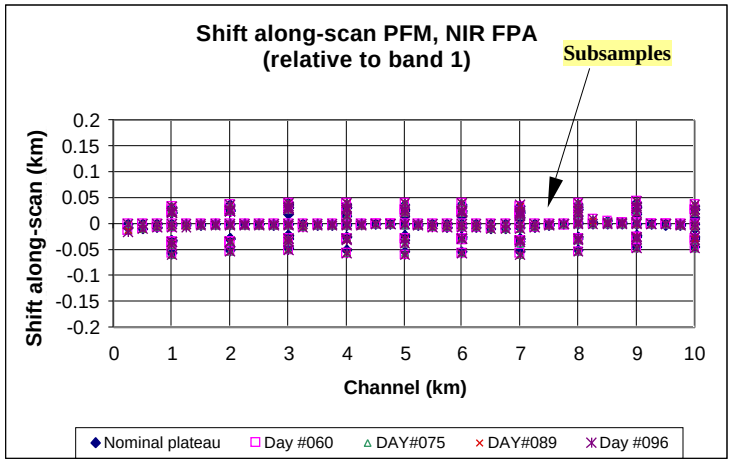

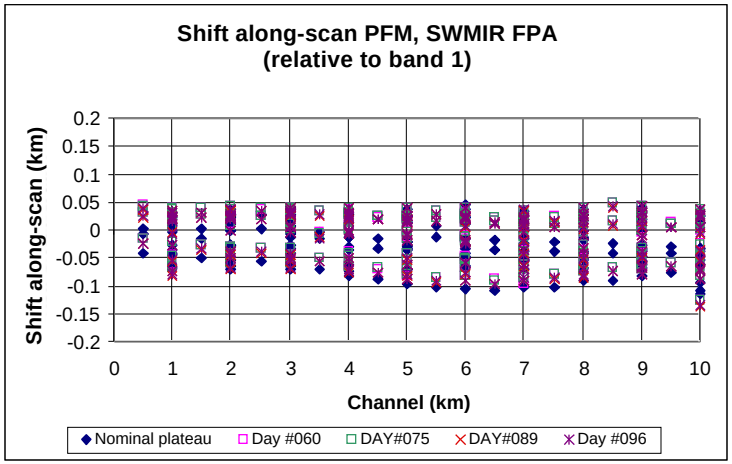

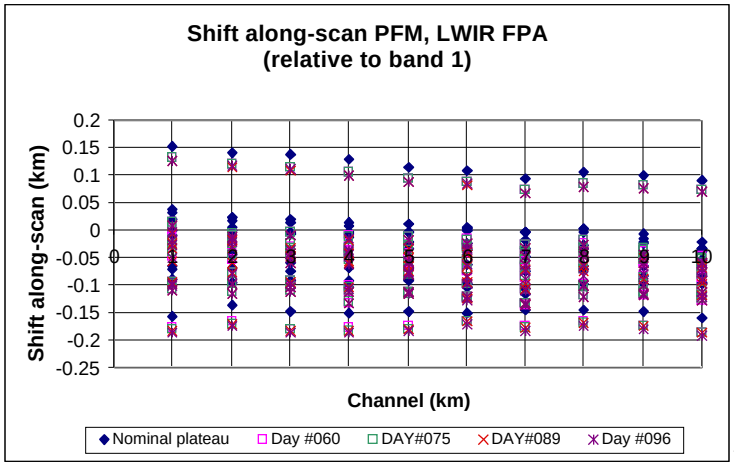

SRCA spatial mode results -- Shift along-track from Nominal to orbit

- Data points in each FPA are in the same sequence as band location in the FPA.
- FPAs have no extra-rotation.

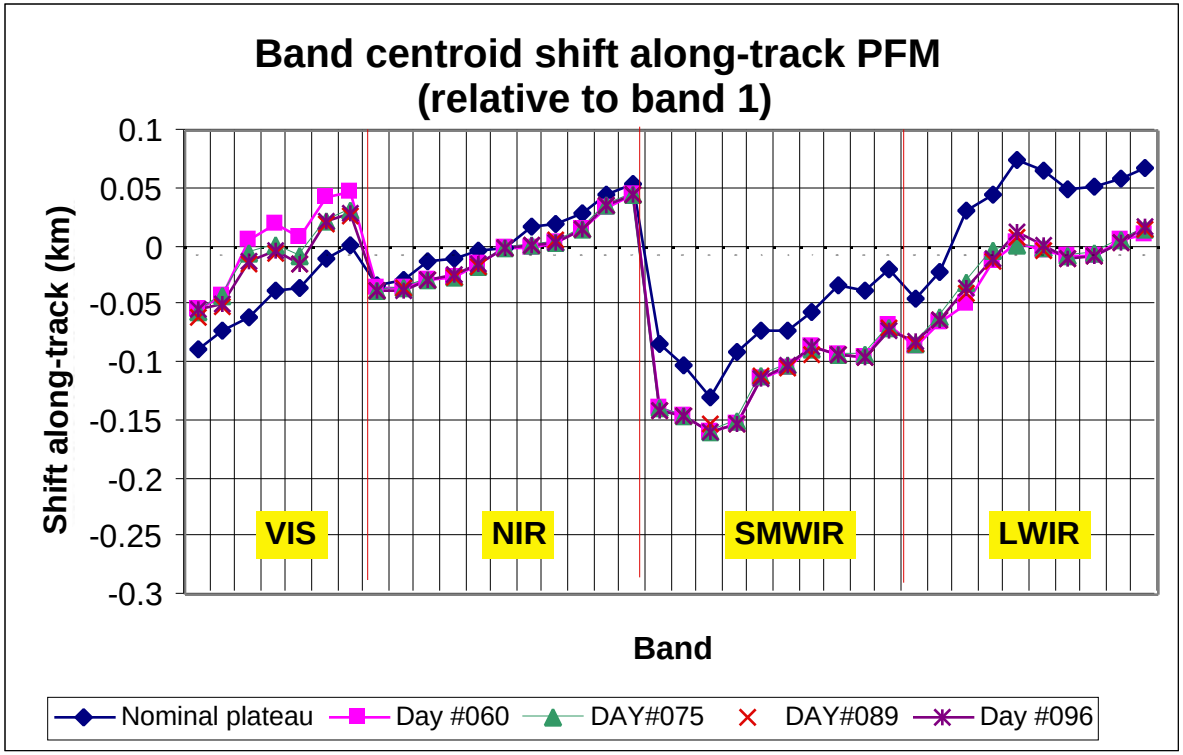

SRCA spatial mode results -- Shift along-track relative to Nominal plateau

- The shift pattern of bands in a FPA has minimum change except VIS FPA where Day#060 shows bias.
- Data points in each FPA is in sequence of band location in the FPA.

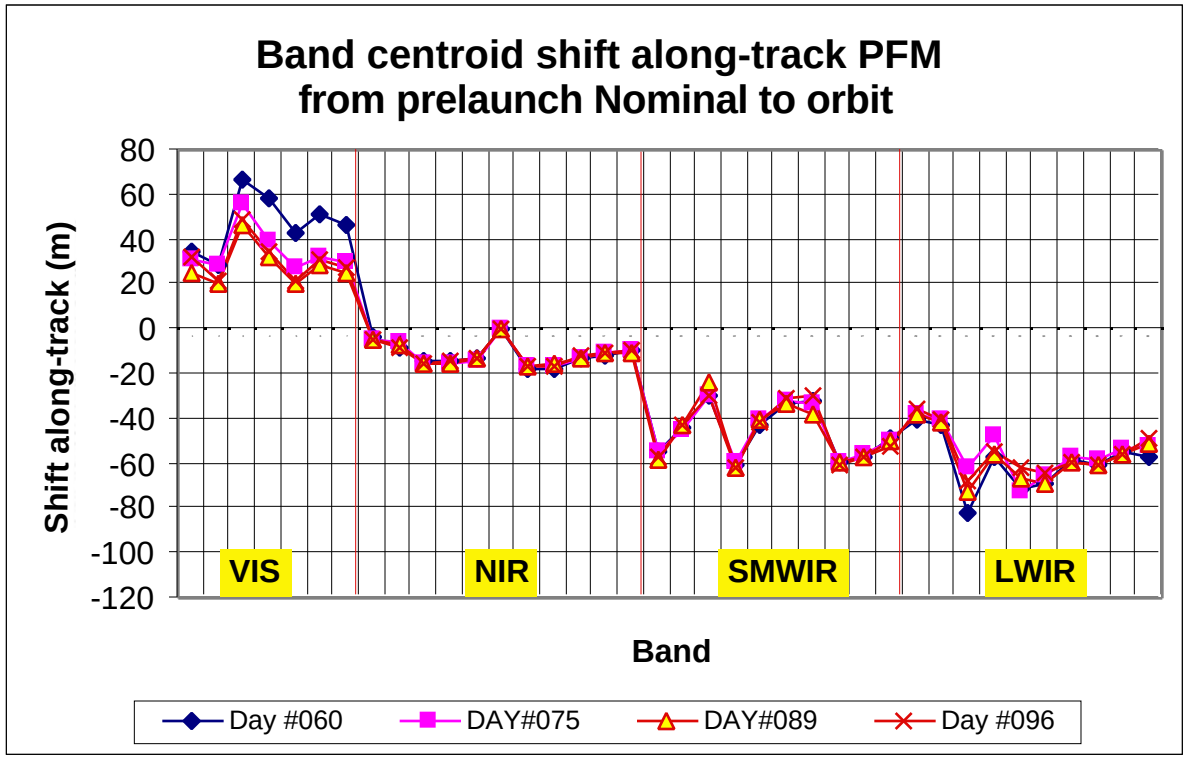

SRCA spatial mode results -- Shift along-track stability on-orbit

- The FPA shift along-track is stable except Day#060 VIS FPA. High repeatability is observed between Day#089 and Day#096.

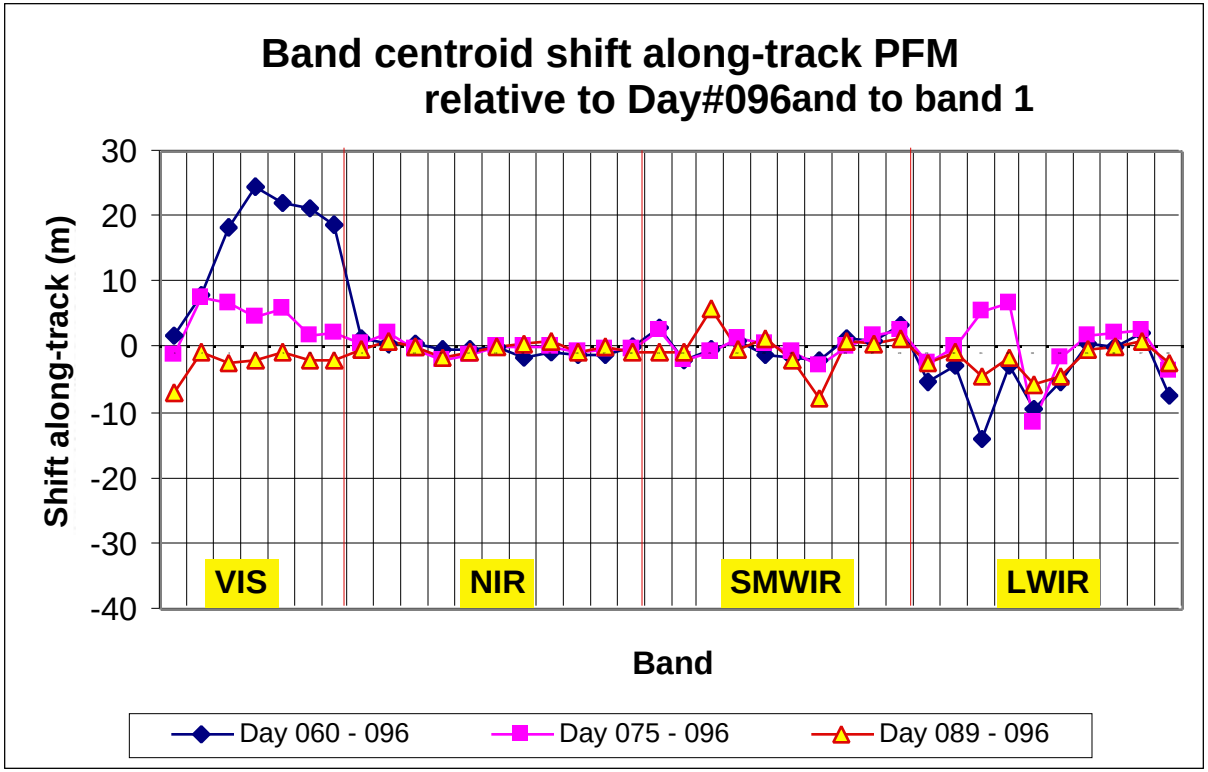

SRCA spatial mode results -- Comparison of shift along-track between Nominal and orbit

- Shifts along-track on-orbit for bands 6, 7, 21, 22 are interpolated values.
- Data points in each FPA are in sequence of band location in the FPA.
- Figures show that the band shift patterns for the four FPAs are retained.

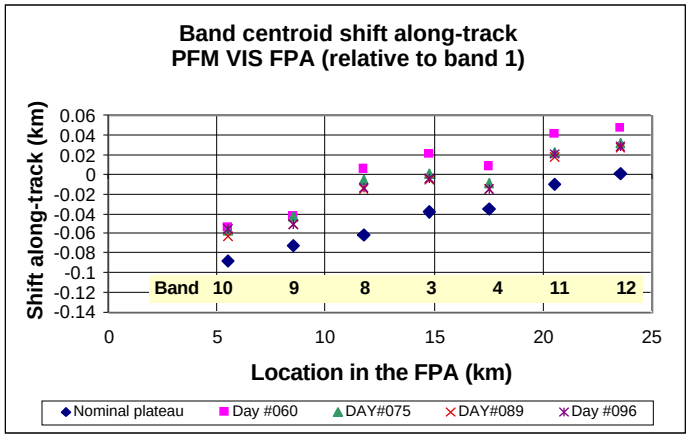

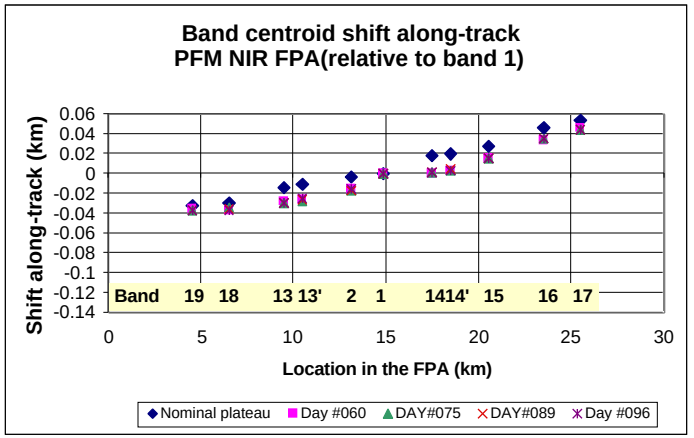

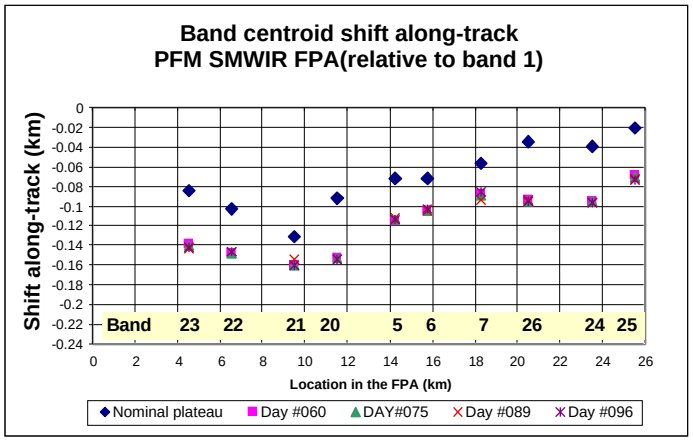

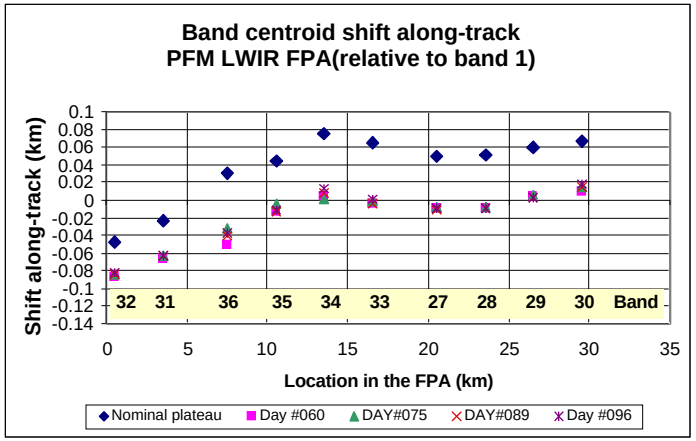

SRCA spatial mode results -- co-registration (1)

- The co-registration tables are the average of Day#089 and #096.
- The values in the tables should be interpreted as:

	B1	B2	B3	B4	B5	B6	B7	B8	B9	B10
B1	**0**	**SA**								
B2		**0**								

- If SA is a positive value, then B2(column)B1(row) value means that B2 is shifted by a amount of SA in along-scan (along-track) direction relative to B1; or B1(column)B2(row) means B1 is shifted a negative SA relative to B2.

SRCA spatial results -- band-to band relative co-registration (2)

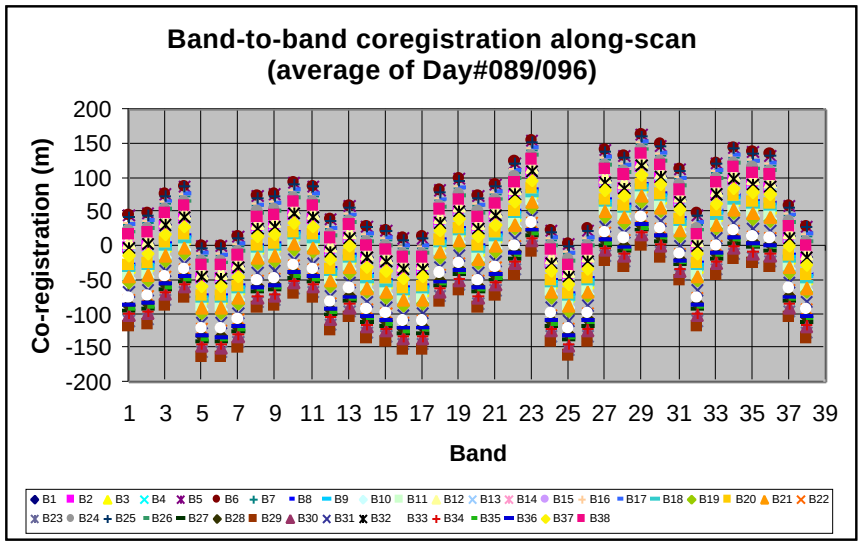

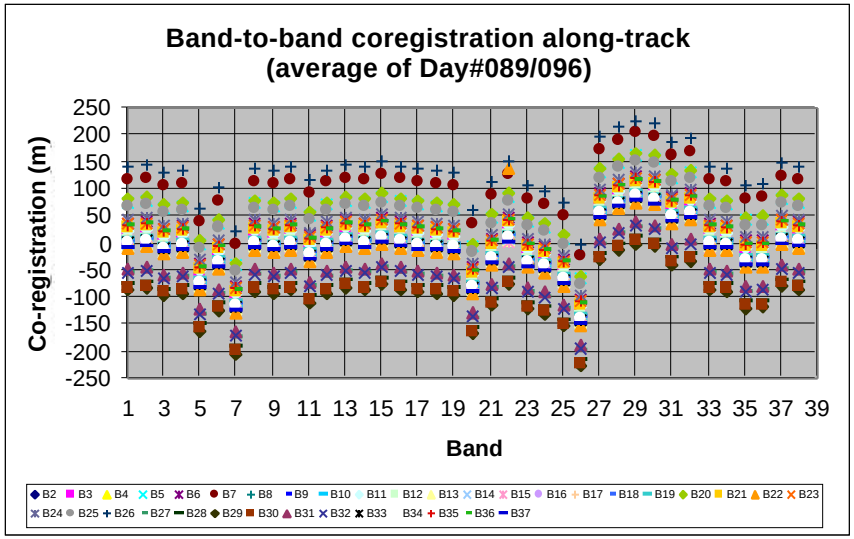

SRCA spatial results -- band-to band relative co-registration along-scan on-orbit (m)

CO-REGISTRATION ALONG-SCAN (DAY#089/#096)

	B1	B2	B3	B4	B5	B6	B7	B8	B9	B10	B11	B12	B13	B14	B15	B16	B17	B18	B19	B20	B21	B22	B23	B24	B25	B26	B27	B28	B29	B30	B31	B32	B33	B34	B35	B36	B37	B38
B1	0	-3	-32	-43	45	45	45	-28	-31	-48	-43	6	-14	16	22	34	32	-36	-53	-27	-16	-78	-110	22	43	21	-96	-87	-119	-96	-67	-2	-77	-100	-93	-89	-14	16
B2		0	-28	-40	48	49	48	-24	-27	-45	-40	9	-11	19	25	37	36	-33	-50	-24	-12	-74	-107	26	46	24	-93	-84	-116	-92	-64	2	-74	-96	-89	-85	-11	19
B3			0	-11	76	77	76	4	1	-17	-12	37	18	47	53	65	64	-5	-21	4	16	-46	-79	54	75	53	-64	-56	-87	-64	-36	30	-46	-68	-61	-57	18	47
B4				0	88	88	88	15	12	-5	0	49	29	59	65	77	75	7	-10	16	27	-35	-67	65	86	64	-53	-44	-76	-53	-24	41	-34	-57	-50	-46	29	59
B5					0	1	0	-72	-75	-93	-88	-39	-59	-29	-23	-11	-12	-81	-98	-72	-60	-122	-155	-22	-2	-24	-141	-132	-164	-141	-112	-46	-122	-144	-137	-133	-59	-29
B6						0	-1	-73	-76	-93	-88	-40	-59	-30	-24	-12	-13	-82	-98	-73	-61	-123	-156	-23	-2	-24	-141	-133	-164	-141	-112	-47	-122	-145	-138	-134	-59	-30
B7							0	18	22	16	39	18	11	17	6	14	20	23	26	97	78	-270	52	60	84	158	-39	-58	-70	-58	-31	-39	15	16	49	46	9	15
B8								0	-3	-21	-16	33	14	44	49	61	60	-9	-25	0	12	-50	-83	50	71	49	-68	-60	-91	-68	-40	26	-49	-72	-65	-61	14	43
B9									0	-18	-13	36	17	46	52	64	63	-6	-22	3	15	-47	-80	53	74	52	-65	-57	-88	-65	-37	29	-47	-69	-62	-58	17	46
B10										0	5	54	34	64	70	82	81	12	-5	21	33	-30	-62	71	91	69	-48	-39	-71	-48	-19	47	-29	-52	-44	-40	34	64
B11											0	49	29	59	65	77	76	7	-10	16	28	-35	-67	66	86	64	-53	-44	-76	-53	-24	42	-34	-57	-49	-45	29	59
B12												0	-19	10	16	28	27	-42	-59	-33	-21	-83	-116	17	37	15	-102	-93	-124	-101	-73	-7	-83	-105	-98	-94	-19	10
B13													0	30	36	47	46	-23	-39	-14	-2	-64	-97	36	57	35	-82	-73	-105	-82	-53	12	-63	-86	-79	-75	0	30
B14														0	6	18	17	-52	-69	-43	-31	-94	-126	7	27	5	-112	-103	-135	-112	-83	-17	-93	-116	-108	-104	-30	0
B15															0	12	11	-58	-75	-49	-37	-99	-132	1	21	-1	-118	-109	-140	-117	-89	-23	-99	-121	-114	-110	-36	-6
B16																0	-1	-70	-87	-61	-49	-111	-144	-11	9	-13	-130	-121	-152	-129	-101	-35	-111	-133	-126	-122	-47	-18
B17																	0	-69	-85	-60	-48	-110	-143	-10	11	-11	-128	-120	-151	-128	-100	-34	-109	-132	-125	-121	-46	-17
B18																		0	-17	9	21	-41	-74	59	79	58	-60	-51	-82	-59	-31	35	-41	-63	-56	-52	23	52
B19																			0	26	37	-25	-57	75	96	74	-43	-34	-66	-43	-14	51	-24	-47	-40	-36	39	69
B20																				0	12	-50	-83	50	70	48	-69	-60	-92	-68	-40	26	-50	-72	-65	-61	14	43
B21																					0	-16	-49	84	105	83	-34	-26	-57	-34	-6	60	-16	-38	-31	-27	48	77
B22																						0	-33	100	121	99	-18	-10	-41	-18	11	76	1	-22	-15	-11	64	93
B23																							0	133	153	132	14	23	-8	15	43	109	33	11	18	22	97	126
B24																								0	21	-1	-118	-110	-141	-118	-90	-24	-100	-122	-115	-111	-36	-7
B25																									0	-22	-139	-130	-162	-139	-110	-45	-120	-143	-136	-132	-57	-27
B26																										0	-117	-108	-140	-117	-88	-23	-98	-121	-114	-110	-35	-5
B27																											0	9	-23	0	29	94	19	-4	3	7	82	112
B28																												0	-32	-8	20	86	10	-12	-5	-1	73	103
B29																													0	23	52	117	42	19	26	30	105	135
B30																														0	43	108	33	10	17	21	96	126
B31																															0	66	-10	-33	-25	-21	53	83
B32																																0	-75	-98	-91	-87	-12	17
B33																																	0	-23	-15	-12	63	93
B34																																		0	7	11	86	115
B35																																			0	4	79	108
B36																																				0	75	104
B37																																					0	30
B38																																						0

SRCA spatial results -- band-to band relative co-registration along-track on-orbit (m)

CO-REGISTRATION ALONG-TRACK (DAY#089/#096)																																								
	B1	B2	B3	B4	B5	B6	B7	B8	B9	B10	B11	B12	B13	B14	B15	B16	B17	B18	B19	B20	B21	B22	B23	B24	B25	B26	B27	B28	B29	B30	B31	B32	B33	B34	B35	B36	B37	B38
B1	0	-3	10	5	75	37	116	1	6	0	23	4	-5	0	-10	-3	4	6	9	81	28	-10	35	44	67	140	-56	-74	-87	-81	-47	-55	0	2	33	32	-8	-2
B2		0	13	9	78	40	120	5	9	4	26	8	-2	3	-7	1	7	9	12	84	32	-7	38	47	70	144	-52	-71	-84	-77	-44	-52	4	5	36	35	-5	2
B3			0	-4	65	27	107	-8	-3	-9	13	-5	-15	-10	-20	-12	-6	-4	-1	71	19	-20	26	34	57	131	-65	-84	-96	-90	-57	-64	-9	-7	23	22	-17	-11
B4				0	69	32	111	-4	1	-5	17	-1	-11	-6	-15	-8	-2	1	4	76	23	-16	30	38	61	135	-61	-80	-92	-86	-53	-60	-5	-3	27	27	-13	-7
B5					0	-38	42	-74	-69	-74	-52	-70	-80	-75	-85	-77	-71	-69	-66	6	-46	-85	-40	-31	-8	66	-130	-149	-162	-156	-122	-130	-74	-73	-42	-43	-83	-77
B6						0	79	-36	-31	-37	-14	-33	-42	-37	-47	-40	-34	-31	-28	44	-9	-47	-2	6	30	103	-93	-111	-124	-118	-84	-92	-37	-35	-4	-5	-45	-39
B7							0	-115	-110	-116	-94	-112	-122	-117	-126	-119	-113	-110	-107	-35	-88	-127	-81	-73	-50	24	-172	-191	-203	-197	-164	-171	-116	-114	-84	-85	-124	-118
B8								0	5	-1	22	3	-6	-1	-11	-4	2	5	8	80	27	-12	34	42	66	139	-57	-76	-88	-82	-49	-56	-1	1	32	31	-9	-3
B9									0	-6	17	-2	-11	-6	-16	-9	-3	0	3	75	22	-16	29	37	61	134	-62	-81	-93	-87	-53	-61	-6	-4	27	26	-14	-8
B10										0	22	4	-6	-1	-10	-3	3	6	9	81	28	-11	35	43	67	140	-56	-75	-87	-81	-48	-55	0	2	32	32	-8	-2
B11											0	-18	-28	-23	-33	-26	-19	-17	-14	58	6	-33	12	21	44	118	-78	-97	-110	-104	-70	-78	-23	-21	10	9	-31	-25
B12												0	-10	-5	-14	-7	-1	2	5	77	24	-15	31	39	63	136	-60	-79	-91	-85	-52	-59	-4	-2	28	28	-12	-6
B13													0	5	-5	3	9	11	14	86	34	-5	40	49	72	146	-50	-69	-82	-76	-42	-50	6	7	38	37	-3	4
B14														0	-10	-2	4	6	9	81	29	-10	35	44	67	141	-55	-74	-87	-80	-47	-55	1	2	33	32	-8	-1
B15															0	7	14	16	19	91	38	0	45	54	77	150	-45	-64	-77	-71	-37	-45	10	12	43	42	2	8
B16																0	6	9	12	84	31	-8	38	46	70	143	-53	-72	-84	-78	-45	-52	3	5	36	35	-5	1
B17																	0	2	6	77	25	-14	32	40	63	137	-59	-78	-90	-84	-51	-58	-3	-1	29	28	-11	-5
B18																		0	3	75	22	-16	29	38	61	134	-61	-80	-93	-87	-53	-61	-6	-4	27	26	-14	-8
B19																			0	72	19	-19	26	34	58	131	-65	-83	-96	-90	-56	-64	-9	-7	24	23	-17	-11
B20																				0	-53	-91	-46	-37	-14	60	-136	-155	-168	-162	-128	-136	-81	-79	-48	-49	-89	-83
B21																					0	-39	7	15	38	112	-84	-103	-115	-109	-76	-83	-28	-26	4	4	-36	-30
B22																						0	45	54	77	151	-45	-64	-77	-70	-37	-45	11	12	43	42	3	9
B23																							0	8	32	105	-91	-110	-122	-116	-82	-90	-35	-33	-2	-3	-43	-37
B24																								0	23	97	-99	-118	-130	-124	-91	-98	-43	-41	-11	-12	-51	-45
B25																									0	74	-122	-141	-154	-148	-114	-122	-67	-65	-34	-35	-75	-69
B26																										0	-196	-215	-227	-221	-188	-195	-140	-138	-108	-109	-148	-142
B27																											0	-19	-31	-25	8	1	56	58	88	87	48	54
B28																												0	-12	-6	27	20	75	77	107	106	67	73
B29																													0	6	40	32	87	89	120	119	79	85
B30																														0	33	26	81	83	114	113	73	79
B31																															0	-8	48	49	80	79	40	46
B32																																0	55	57	88	87	47	53
B33																																	0	2	32	32	-8	-2
B34																																		0	31	30	-10	-4
B35																																			0	-1	-41	-35
B36																																				0	-40	-34
B37																																					0	6
B38																																						0

Determination of band center wavelength shift using the SRCA spectral mode

Summary

- The operation of the SRCA spectral calibration on-orbit is successful. The current center wavelength and the shift from prelaunch are provided.
- Operation of the spectral calibration during space dark retains the reference SiPD noise at prelaunch level.
- The SRCA monochromator parameters are very stable.
- The band center wavelength shift from prelaunch Nominal plateau to orbit is less than 0.4nm for wavelengths less than 1 μm.
- Some changes of band response profiles are observed.

SRCA monochromator parameters are normal

- The monochromator parameters determine the wavelength scale and are used to convert grating step number into wavelength.
- The two key parameters are stable at different conditions. The monochromator parameters tested on-orbit on Days #049 and #061 show that the monochromator is operating normally.

Test case	β	θ_off
SBRS_cold.10W	15.059	0.005
SBRS_hot.10W	15.024	0.001
SBRS_nom.30W	15.082	0.005
SBRS_nom.10W	15	0.001
VF_cold.30W	15.035	0.004
VF_cold.10W	15.072	0.006
VF_hot.30W	15.05	0.004
VF_hot.10W	15.051	0.004
Day#049, 30W	**14.996**	**0.001**
Day#049, 10W	**15.033**	**0.003**
Day#061, 30W	**15.049**	**0.003**
Day#061, 10W	**15.146**	**0.006**

Average center wavelength and shift from Nominal to orbit (1)

- The averaged band center wavelength shifts from prelaunch Nominal plateau are less than 0.4nm for $\lambda<1\mu m$. The current center wavelengths, corrected for the SpMA and SRCA differences, and the center wavelength shift from prelaunch Nominal plateau are listed below. The SWIR band shifts are not normalized by the SRCA source profile.

	Current center wavelength	Center wavelength shift from prelaunch(nm)	
Band	mean value (um)	Day#061	Day#049
8	0.4119	-0.20	0.15
9	0.4420	-0.23	-0.20
3	0.4659	0.02	0.14
10	0.4868	-0.12	-0.16
11	0.5297	-0.02	-0.07
12	0.5470	0.17	0.11
4	0.5539	0.05	0.20
1	0.6466	0.09	0.16
13	0.6655	-0.19	-0.20
14	0.6772	0.16	0.21
15	0.7466	0.01	0.02
2	0.8583	0.31	0.33
16	0.8663	-0.10	-0.03
17	0.9044	0.00	0.19
18	0.9354	-0.18	-0.36
19	0.9359	-0.37	-0.34
5	1.2424	0.39	0.23
26	1.3822	0.05	-0.10
6	1.6297	0.22	0.54
7	2.1151	-0.19	0.38

center wavelength shift from Nominal to orbit (2)

- The center wavelength shift variations over channels are as shown. The band sequence of wavelength is listed on the previous sheet.

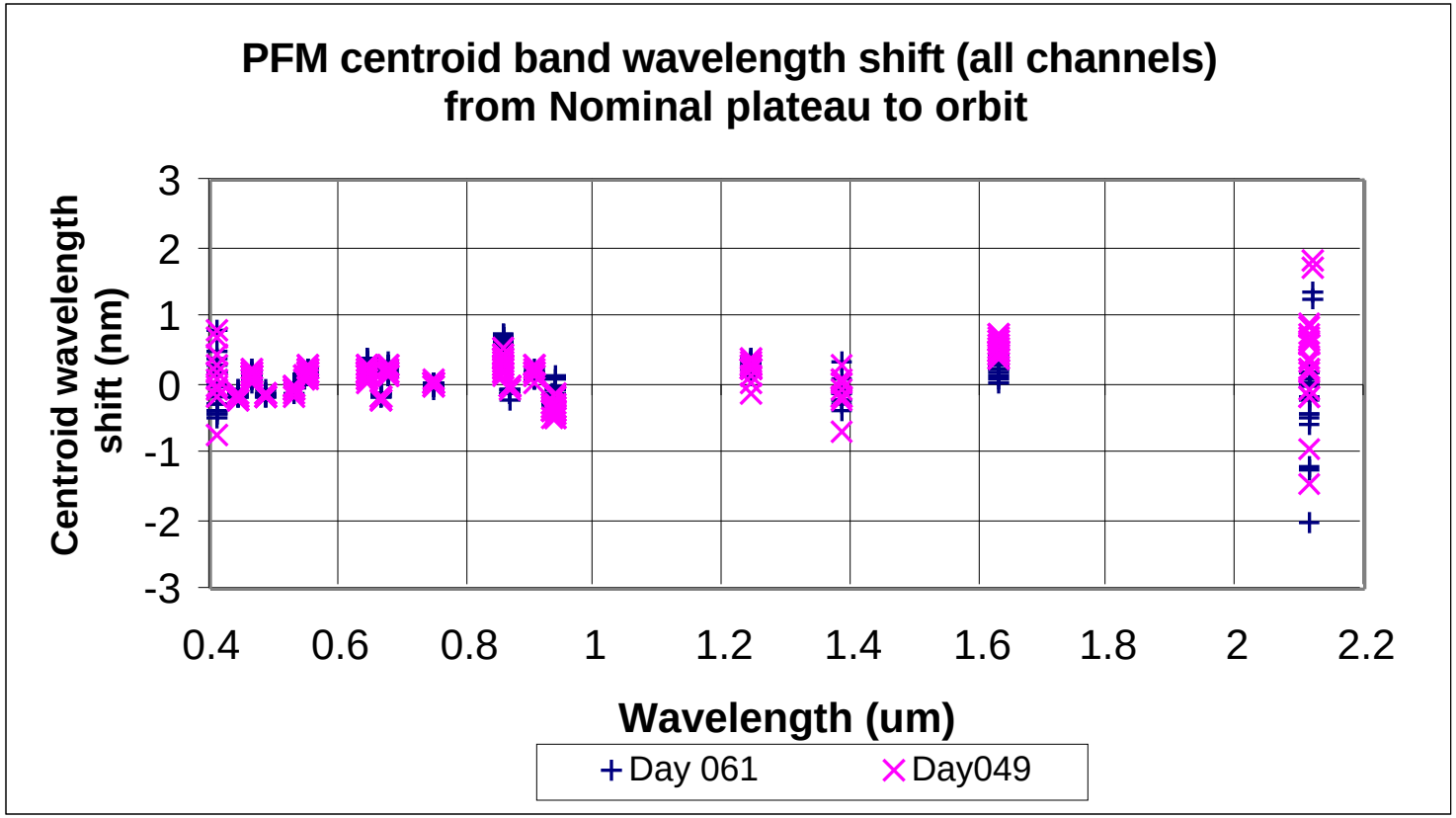

Center wavelength shift variation over channels
Comparison between prelaunch to orbit (1)

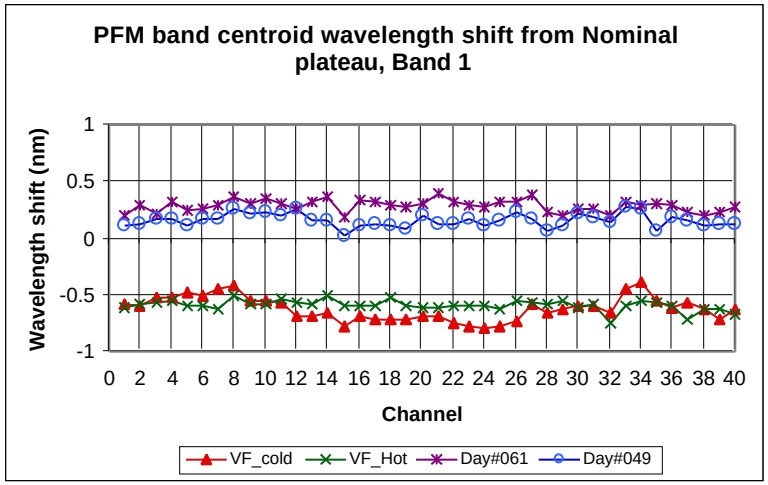

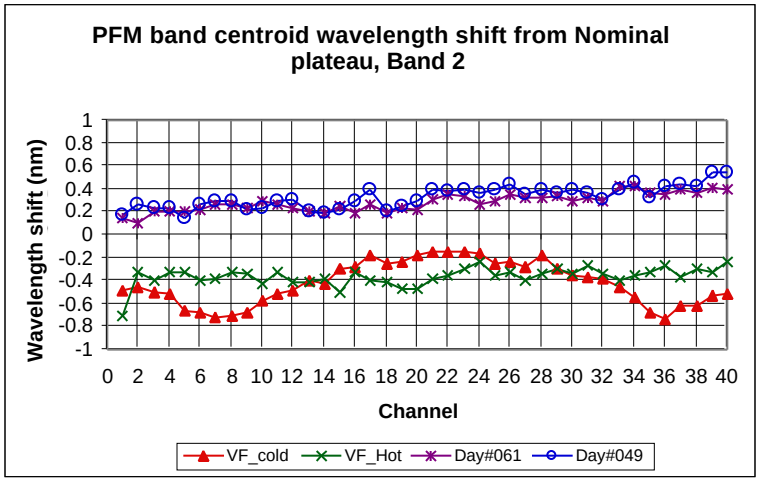

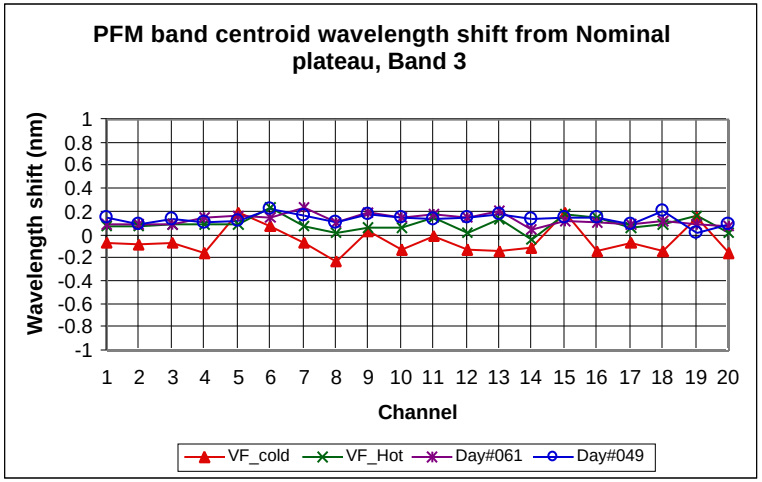

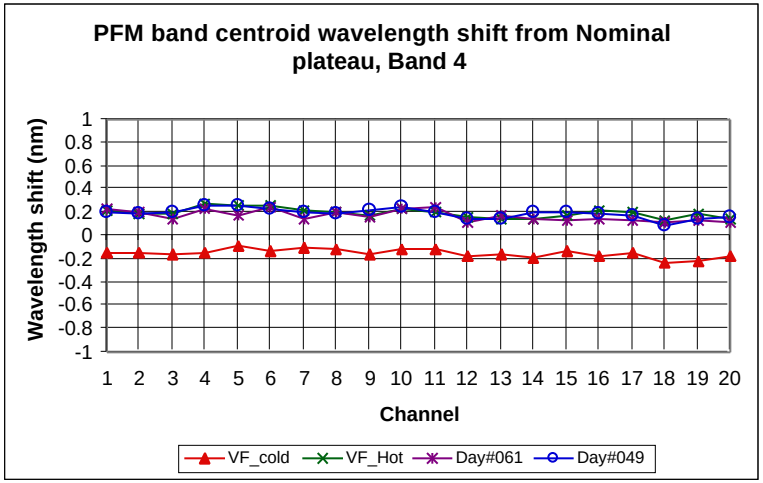

Center wavelength shift variation over channels
Comparison between prelaunch to orbit (2)

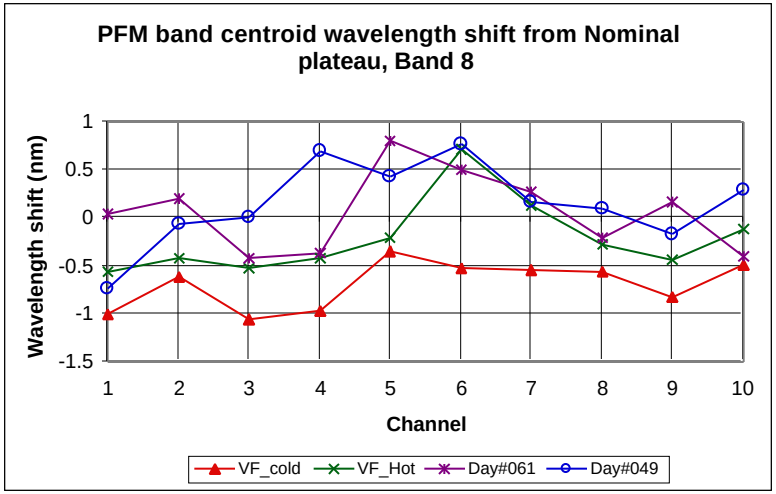

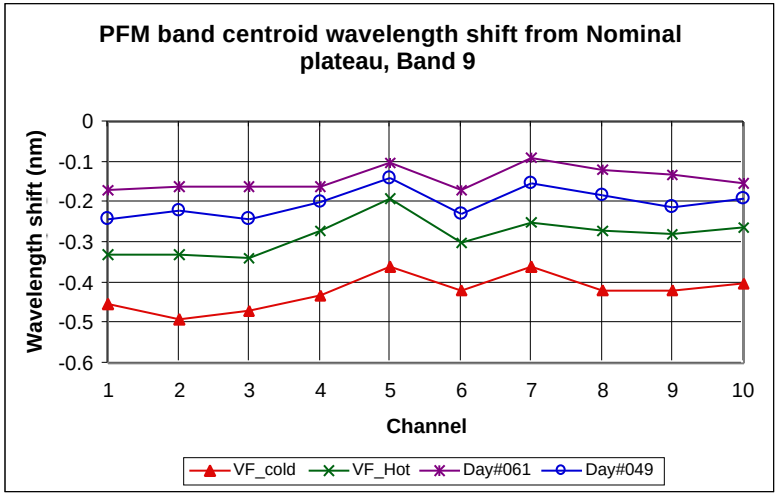

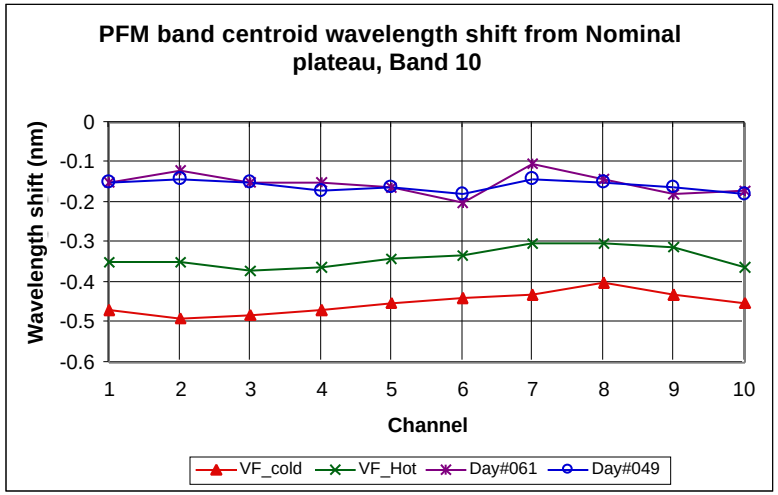

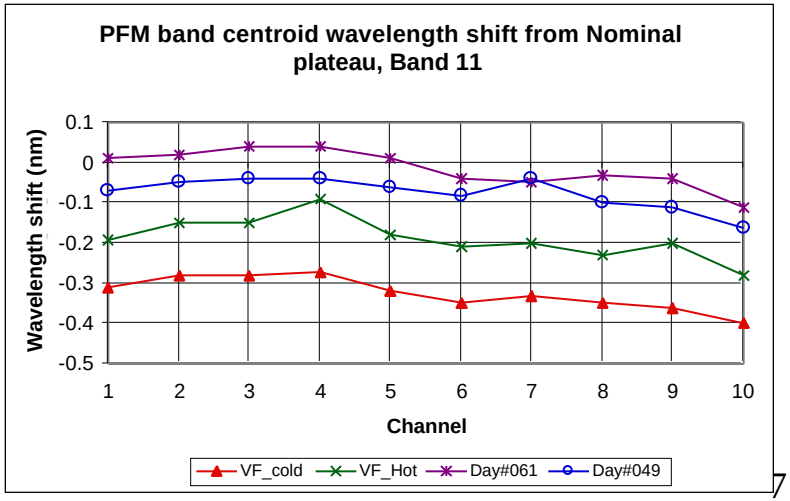

Center wavelength shift variation over channels
Comparison between prelaunch to orbit (3)

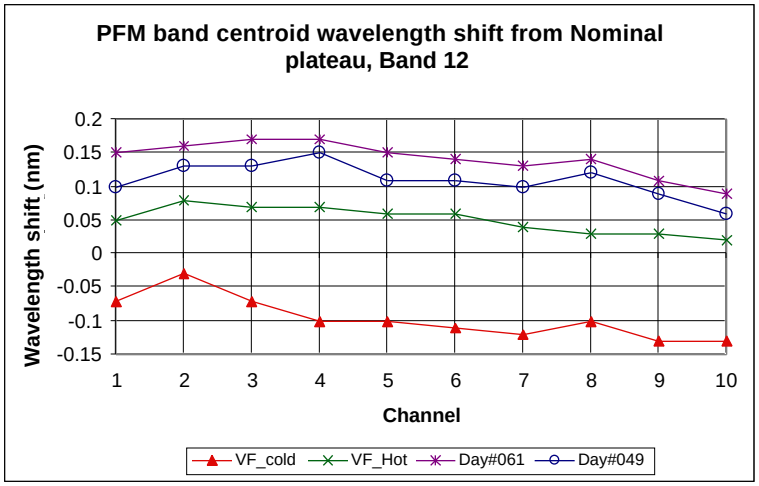

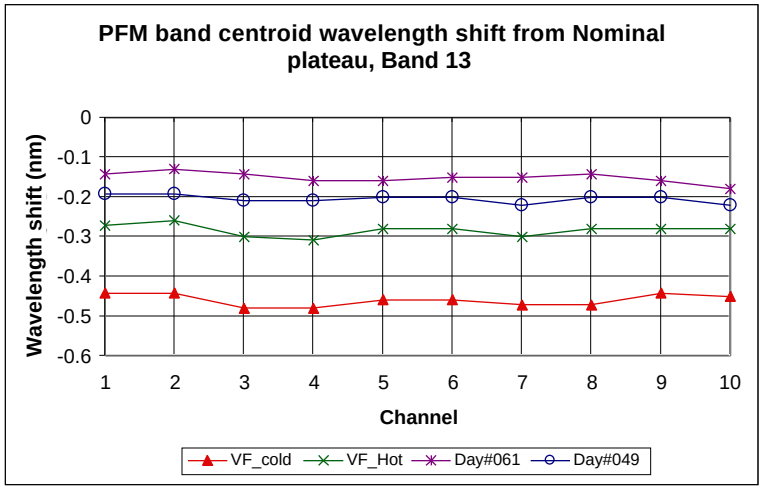

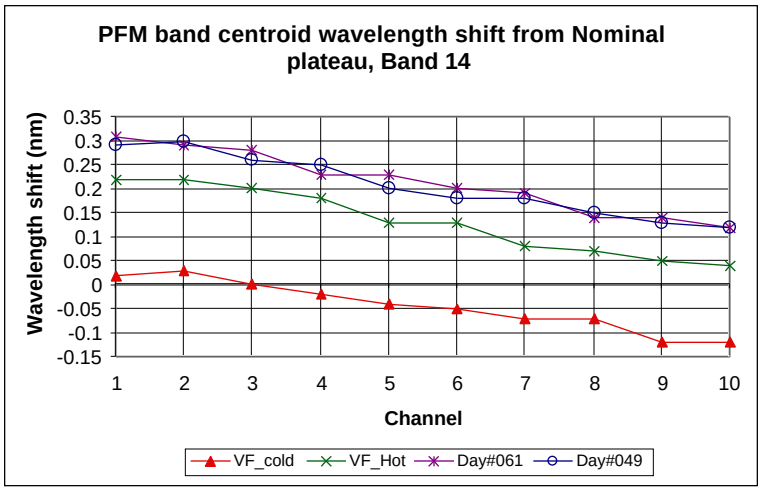

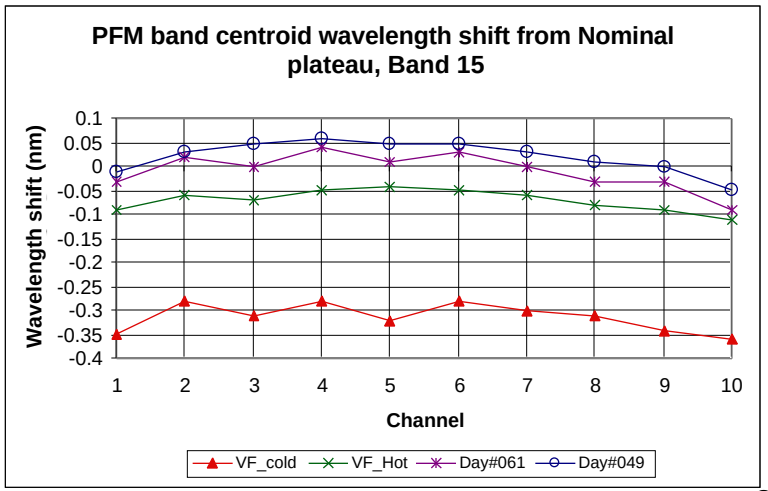

Center wavelength shift variation over channels
Comparison between prelaunch to orbit (4)

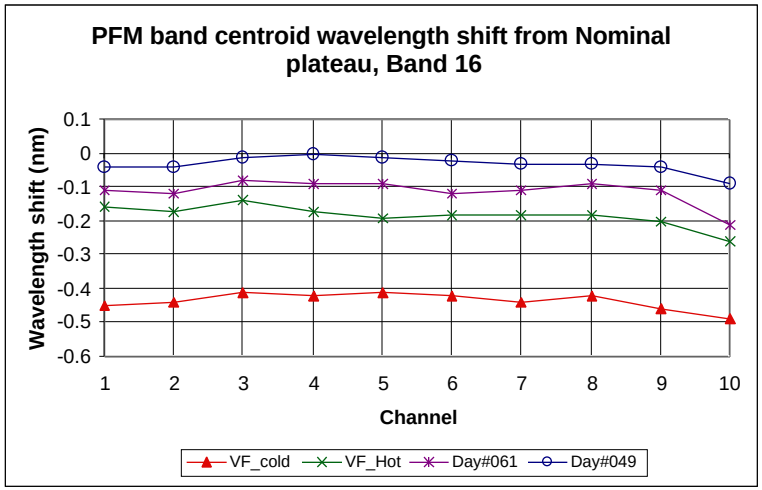

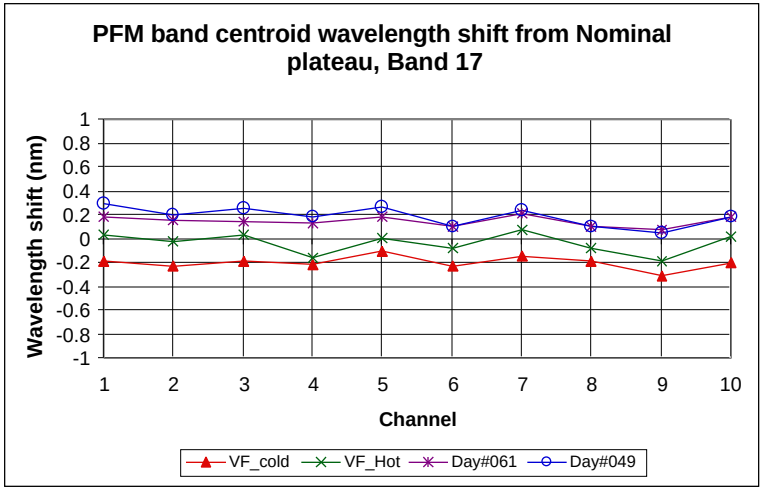

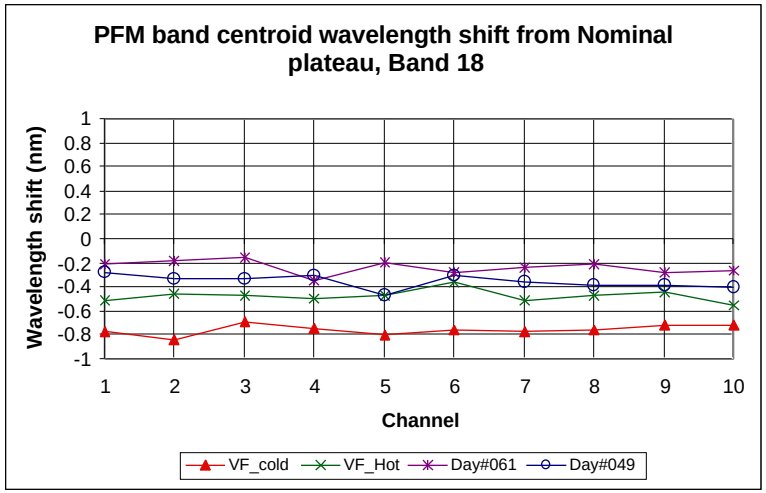

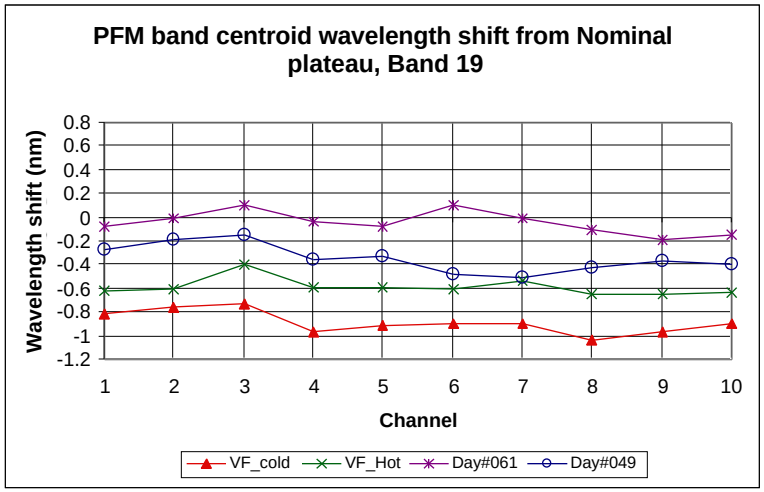

Center wavelength shift variation over channels
Comparison between prelaunch to orbit (5)

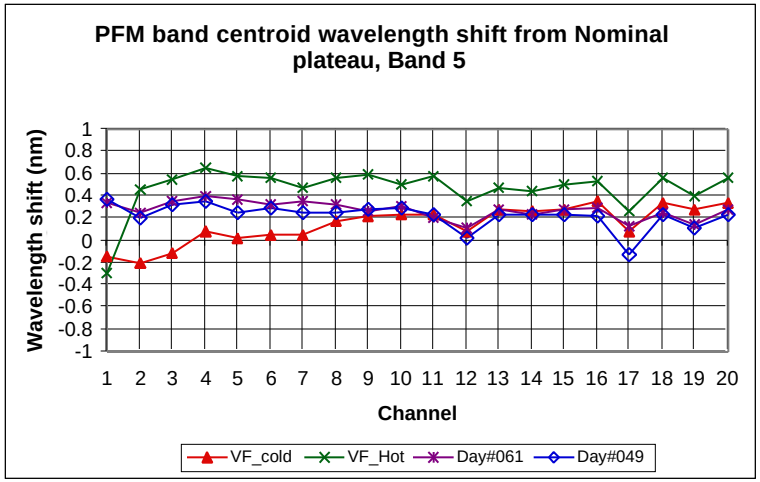

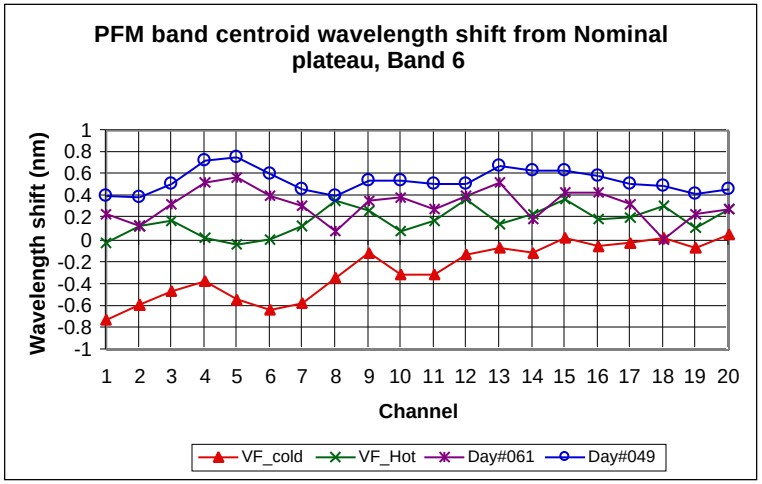

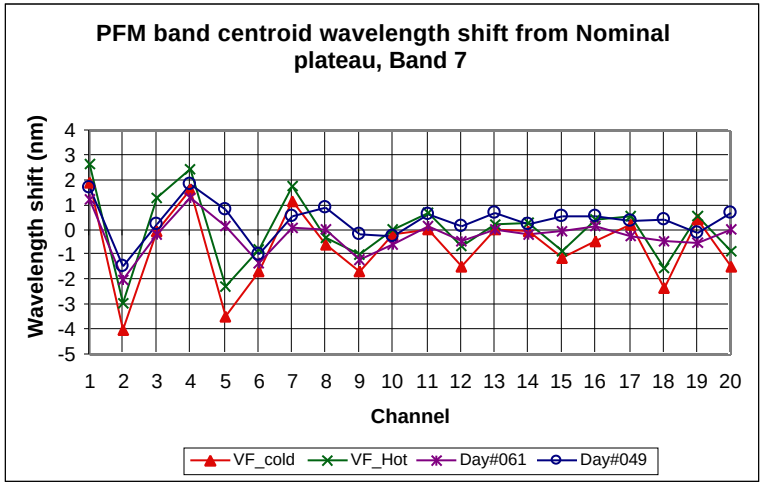

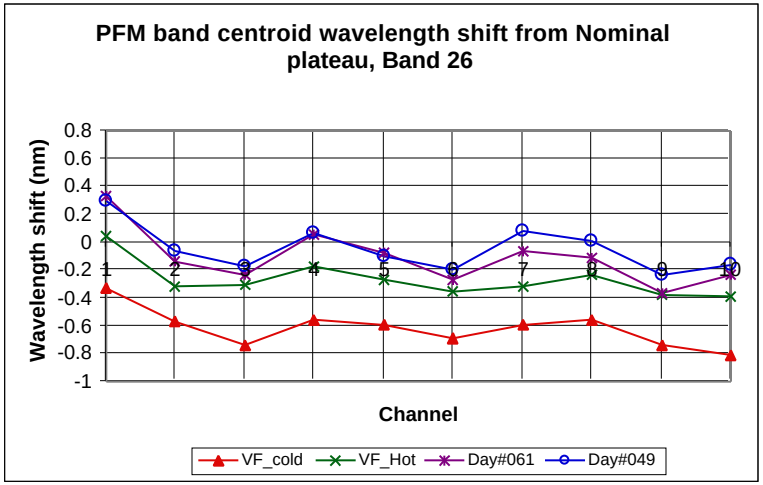

Center wavelength shift variation over channels Comparison between prelaunch to orbit (6)

- For the majority of the bands, the center wavelength shift pattern from prelaunch Nominal plateau is normal. The shift for the two tests on-orbit basically are consistent.
- Band 8 does not have good repeatability due to low SNR.
- Bands 7 has a large variation.

MODIS PFM band response recovery on-orbit (1)

- The stable SRCA monochromator parameters help in reconstruction of MODIS band response on-orbit from the SRCA measurements.
- Short wavelength band response is liable to change.
- A Fourier Transform technique is applied to recover band responses assuming that the slit function of the SRCA monochromator has not changed.
- The recovered band response is limited to the wavelength range that the SRCA measures and is compared with that MODIS band response measured by the Spectral Measurements Assembly (SpMA) for wavelength <1μm.
- The reconstruction is not given for band 2 due to the change of slit function by using grating order of one instead of two (prelaunch).
- Band profiles are changed on-orbit for bands 8, 12, 14, and 18 (next sheet). Negligible change is detected for the other bands. One sub-peak of band 8 is flattened which may be related to the polarization change.

MODIS PFM band response recovery on-orbit (2)

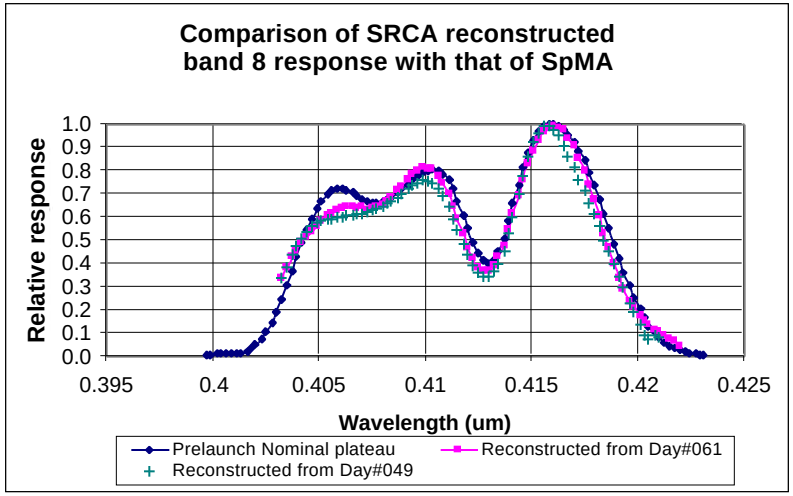

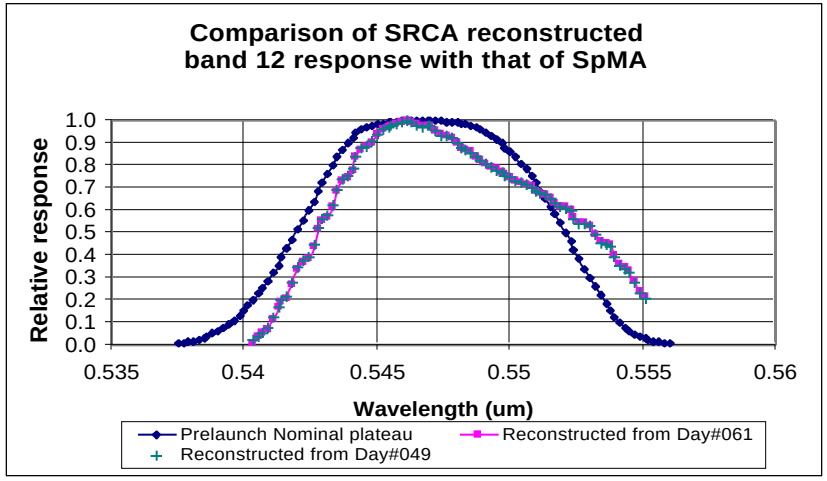

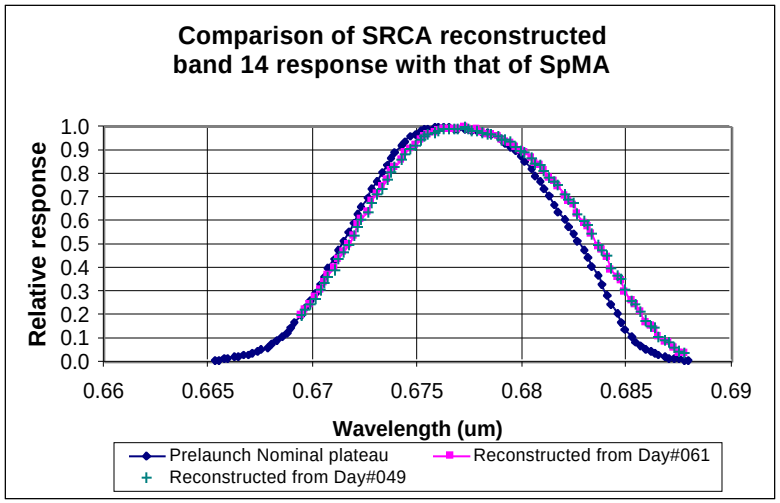

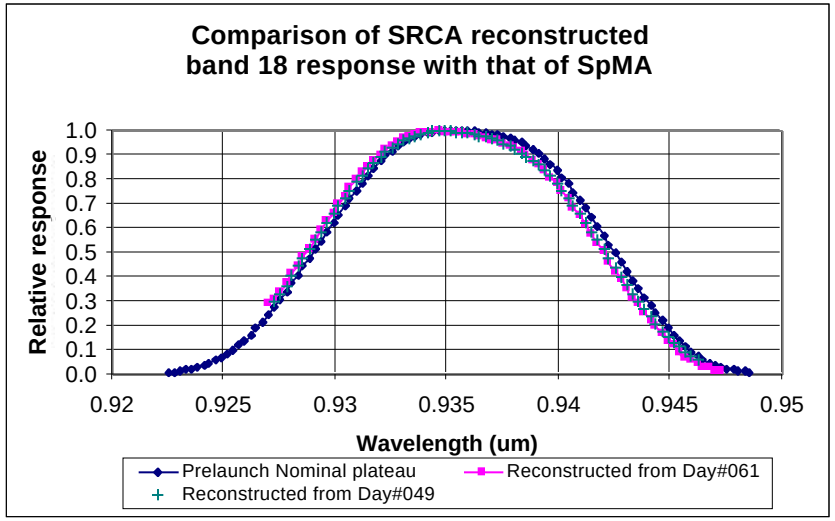

FM1 Issues

- Remaining FM1 Testing Objectives